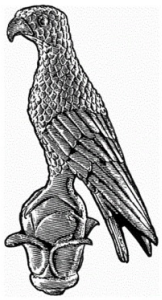

ΠΑΝΕΠΙΣΤΗΜΙΟ ΙΩΑΝΝΙΝΩΝ
ΣΧΟΛΗ ΘΕΤΙΚΩΝ ΕΠΙΣΤΗΜΩΝ
ΤΜΗΜΑ ΦΥΣΙΚΗΣ

Κατασκευή και Φαινομενολογική Ανάλυση Μεγαλοενοποιημένων Συμμετριών Βαθμίδας από τις Θεωρίες των Υπερχορδών και Πολύ-Μεμβρανών

Αθανάσιος Καρόζας

Διδακτορική διατριβή

ΙΩΑΝΝΙΝΑ 2019

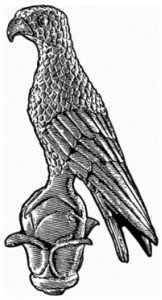

UNIVERSITY OF IOANNINA
SCHOOL OF NATURAL SCIENCES
DEPARTMENT OF PHYSICS

Construction and Phenomenological Analysis of GUTs in Superstring and D-brane Theories

Athanasios Karozas

Ph.D. Thesis

IOANNINA 2019

Three-member advisory committee:

- Georgios Leontaris (Supervisor), Professor, Department of Physics, University of Ioannina, Greece
- Ioannis Rizos, Professor, Department of Physics, University of Ioannina, Greece
- Kyriakos Tamvakis, Emeritus Professor, Department of Physics, University of Ioannina, Greece

Seven-member Assessment Committee:

- Ignatios Antoniadis, Professor, Laboratory of Theoretical Physics and High Energies-LPTHE, Sorbonne University, France
- Nikolaos Vlachos, Professor, Department of Physics, Aristotle University of Thessaloniki, Greece
- Panagiota Kanti, Professor, Department of Physics, University of Ioannina, Greece
- Georgios Leontaris, Professor, Department of Physics, University of Ioannina, Greece (Thesis Supervisor)
- Ioannis Rizos, Professor, Department of Physics, University of Ioannina, Greece
- Kyriakos Tamvakis, Emeritus Professor, Department of Physics, University of Ioannina, Greece
- Nikolaos Tracas, Professor, School of Applied Mathematical & Physical Scienes, National Technical University of Athens, Greece

Acknowledgements

First of all, I would like to express my deep gratitude to my supervisor, Professor George Leontaris, for his continuous academic and moral support and all guidance and motivation he has given me throughout these years during my graduate studies.

I am specially thankful to Professor Kyriakos Tamvakis for the financial support through the program "THALIS" during the first years of my PhD research studies.

All these years I had the opportunity to met and collaborate with great people in theoretical physics *society*. I am deeply grateful to Stephen F. King, Andrew K. Meadowcroft and Miguel Crispim Romão for the collaboration in various projects and with whom we had countless of *online* meetings and discussions which led to a very productive collaboration. I would like to acknowledge them for their important contributions on various parts of this work. I am also thankful to Professor Qaisar Shafi for the collaboration and his contributions on the final project of the present thesis. I would like also to thank Waqas Ahmed for the great collaboration we had on a parallel project and for sharing his passion for physics with me.

A special thank to all my childhood friends and all those I have met in Ioannina, who are too many to be named individually. Thank you for all the great times we had together and for making my life better every day.

To all my family, specially my parents, Kostas and Eleni, my sister Machie, my uncles Christos and Eleni and my cousin Despina – thank you for your support and encouragement and for always being there for me. Without your support I could not have reached this stage.

At the end, I would like to thank my Sevasti, for being my companion and for always believing in me.

Co-financed by Greece and the European Union

Parts of the research presented in this thesis has been co-financed by the European Union (European Social Fund - ESF) and Greek national funds through the Operational Program "Education and Lifelong Learning" of the National Strategic Reference Framework (NSRF) - Research Funding Program: "THALIS". Investing in the society of knowledge through the European Social Fund.

Μέρος της έρευνας που παρουσιάζεται στην παρούσα διδακτορική διατριβή έχει συγχρηματοδοτηθεί από την Ευρωπαϊκή Ένωση (Ευρωπαϊκό Κοινωνικό Ταμείο–ΕΚΤ) και από εθνικούς πόρους μέσω του Επιχειρησιακού Προγράμματος «Εκπαίδευση και Δια Βίου Μάθηση» του Εθνικού Στρατηγικού Πλαισίου Αναφοράς (ΕΣΠΑ) – Ερευνητικό Χρηματοδοτούμενο Έργο: ΘΑΛΗΣ. Επένδυση στην κοινωνία της γνώσης μέσω του Ευρωπαϊκού Κοινωνικού Ταμείου, MIS:375734

.....dedicated to my family

Abstract

In this thesis, we present string theory models and we study their phenomenological consequences. We focus on the non-perturbative version of type *IIB* superstring theory, known as *F-theory*, where non-Abelian gauge symmetries are linked to the singularities of the elliptically fibred compactification manifold. These singularities are of the ADE type and as a result the E_8 exceptional group is the highest one. Hence, popular grand unified theories (GUTs) based on the groups E_6, $SO(10)$ and $SU(5)$, can be naturally realised as effective F-theory models. Within this framework we derive and study the low energy implications of several models. Firstly, an F-theory supersymmetric $SU(5)$ model accompanied by V_4 Klein monodromy and a Z_2 geometric parity is derived. At low energies, the model leads to the MSSM spectrum extended by two right-handed neutrinos seesaw mechanism. Next,a model based on $SU(5)$, together with the non-Abelian family symmetry D_4 plus an Abelian family symmetry is presented. The model produces a realistic low energy spectrum and is capable to explain the neutrino mixing effects predicted by neutrino oscillation experiments. Due to a Z_2 geometric parity the model is shown to exhibit baryon violating processes, without proton decay. A systematic study on R-parity violation (RPV) effects in semi-local and local F-theory constructions follows, where we have shown that RPV is a generic feature, but may occur without proton decay, due to flux effects. The values of RPV Yukawa couplings are also computed in an F-theory local background and compared with their corresponding values from field theory results. Next, we explore the low-energy implications of F-theory inspired E_6 models, in which a light Z' neutral gauge boson survives at low energies. The breaking to $SO(10)$ and then to $SU(5)$ is performed with the help of Abelian fluxes. The low-energy spectrum is then chosen to be part of this high-energy spectrum and consists of MSSM plus some vectorlike exotics. A renormalisation group analysis at two-loop level for gauge and Yukawa couplings is performed and it is shown to be compatible with the high-energy predictions coming from the computation of Yukawa couplings in F-theory. We also identify points in the parameter space of the flux densities where the top, bottom and tau Yukawa couplings unify.

Εκτεταμένη Περίληψη

(Extended Summary in Greek)

Η αλματώδης ανάπτυξη της σύγχρονης θεωρητικής φυσικής υψηλών ενεργειών οδήγησε στη θεμελίωση μιας ενιαίας και επιτυχούς περιγραφής των αλληλεπιδράσεων και ιδιοτήτων των στοιχειωδών σωματιδίων. Η κβαντική θεωρία πεδίου που περιγράφει τα φαινόμενα αυτά ονομάζεται "*Καθιερωμένο Πρότυπο*" (ΚΠ) και βασίζεται στην ομάδα συμμετρίας βαθμίδας $SU(3)_C \times SU(2)_L \times U(1)_Y$ η οποία ενοποιεί τις τρεις μη-βαρυτικές θεμελιώδεις αλληλεπιδράσεις της φύσης. Η πρόσφατη ανακάλυψη του μποζονίου Higgs στο Μεγάλο Επιταχυντή Αδρονίων (Large Hadron Collider, LHC) στο Ευρωπαϊκό Πυρηνικό Κέντρο Ερευνών (CERN), ήταν καταλυτική για την οριστική επιβεβαίωση της ορθότητας του ΚΠ. Όμως, παρ'όλο που η επιτυχία του ΚΠ στην ενεργειακή περιοχή ισχύος του είναι πλέον δεδομένη, πολλά σημαντικά ερωτήματα παραμένουν αναπάντητα. Μεταξύ άλλων, ορισμένα προβλήματα και ερωτήματα που δεν απαντώνται στο πλαίσιο του ΚΠ είναι α) η κβάντωση του φορτίου, β) η μη ενοποίηση των τριών συζεύξεων βαθμίδας, γ) προβλήματα *ιεραρχίας* και η κατανόηση της μάζας του μποζονίου Higgs, δ) οι μάζες των τριών νετρίνων, ε) η φύση της σκοτεινής ύλης του σύμπαντος και οι συναφείς κοσμολογικές επιπτώσεις, ζ) η δυνατότητα ενοποίησης της τέταρτης γνωστής δύναμης, δηλαδή της βαρύτητας.

Τα παραπάνω προβλήματα καταδεικνύουν ότι το ΚΠ δεν αποτελεί μία πλήρης περιγραφή της φυσικής των στοιχειωδών σωματιδίων για όλο το φάσμα ενεργειών. Για να απαντήσουμε σε όσο το δυνατόν περισσότερα απο τα παραπάνω ερωτήματα θα πρέπει να αναζητήσουμε *Θεωρίες Πέρα από το ΚΠ* οι οποίες στηρίζονται σε πιο θεμελιώδη θεωρητικά και μαθηματικά πρότυπα. Τέτοια πρότυπα αποτελούν η *Υπερσυμμετρία* (Supersymmetry, SUSY) καθώς και θεωρίες που βασίζονται σε *Μεγαλοενοποιημένες Συμμετρίες Βαθμίδας* (Grand Unified Theories, GUTs). Για παράδειγμα, στην *Ελάχιστη Υπερσυμμετρική Επέκταση του ΚΠ* (Minimal Supersymmetric SM, MSSM), υπό συγκεκριμένες συνθήκες, η ενοποίηση των τριών συντελεστών σύζευξης βαθμίδας είναι εφικτή και επιτυγχάνεται σε ενέργειες της τάξης $\sim 10^{16}$ GeV. Το ιδιαίτερο αυτό αποτέλεσμα, οδηγεί στην ιδέα πως το ΚΠ αποτελεί την χαμηλοενεργειακή έκφανση ενός υπερσυμμετρικού μοντέλου το οποίο θα βασίζεται σε μια μεγαλύτερη ομάδα συμμετρίας. Μερικές από τις πιο γνωστές μεγαλοενοποιημένες συμμετρίες βαθμίδας είναι η $SU(5)$, $SO(10)$ και η ειδική ομάδα (exceptional group) E_6.

Τα πρότυπα μεγάλης ενοποίησης παρουσιάζουν κάποια ενδιαφέροντα χαρακτηριστικά και μπορούν να δώσουν λύσεις σε μερικά από τα προβλήματα του ΚΠ. Για παράδειγμα, εξηγούν τις τιμές των φορτίων που έχουν τα πεδία στο ΚΠ, προβλέπουν την ενοποίηση των συντελεστών σύζευξης και εμπεριέχουν επιπλέον αναπαραστάσεις οι οποίες μπορούν να ταυτιστούν με βαρυά *Majorana*

νετρίνα τα οποία μέσω του *μηχανισμού της αιώρας* (seesaw mechanism) μπορούν να ερμηνεύσουν τη μικρή μάζα των νετρίνων. Ωστόσο, στην απλούστερη τους μορφή, οι μεγαλοενοποιημένες θεωρίες παρουσιάζουν κάποια σημαντικά προβλήματα. Τέτοια είναι τα φαινόμενα διάσπασης του πρωτονίου, ο διαχωρισμός διπλέτας-τριπλέτας (doublet-triplet splitting problem) καθώς και ασυνεπής σχέσεις (κυρίως για τις ελαφρύτερες γενιές) μεταξύ των συντελεστών σύζευξης Yukawa για ενέργειες κοντά στην κλίμακα ενοποίησης. Τα προβλήματα αυτά μπορούν να ρυθμιστούν επεκτείνωντας τη συμμετρία μεγάλης ενοποίησης με επιπλέον $U(1)$ ή/και διακριτές συμμετρίες. Στην περίπτωση αυτή, γίνεται κατανοητή η ανάγκη εύρεσης ενός πιο γενικού θεωρητικού πλαισίου, το οποίο θα ερμηνεύει την προέλευση των συμμετριών αυτών. Τέτοια πρότυπα είναι οι *Θεωρίες των Υπερχορδών*, στο πλαίσιο των οποίων δίνεται η δυνατότητα ενσωμάτωσης και της βαρύτητας σε ενέργειες συγκρίσημες με την κλίμακα του Planck ($M_{Pl} \simeq 2.4 \times 10^{18}$ GeV).

Στις θεωρίες των υπερχορδών, τα θεμελιώδη δομικά συστατικά δεν είναι σημειακά σωμάτια, αλλά εκτεταμένα μονοδιάστατα αντικείμενα τα οποία ονομάζονται *χορδές*. Αυτές διακρίνονται σε ανοιχτές και κλειστές χορδές, με τις τελευταίες να σχετίζοντα με τον τομέα βαρύτητας της θεωρίας. Μία μαθηματικά συνεπής περιγραφή της φυσικής των χορδών προϋποθέτει την ύπαρξη επιπλέον διαστάσεων πέρα από τις (3+1) γνωστές διαστάσεις του ΚΠ. Οι επιπλέον διαστάσεις θεωρούνται *μικρές* και *συμπαγοποιημένες* (compactified). Μία ακόμη σημαντική πρόβλεψη της θεωρίας χορδών είναι η υπερσυμμετρία η οποία εξασφαλίζει την ένταξη φερμιονικών βαθμών ελευθερίας στη θεωρία. Επιπλέον, η μελέτη της θεωρίας πέρα από τις χορδές προβλέπει την ύπαρξη και άλλων εκτεταμένων αντικειμένων που ονομάζονται *πολυ-μεμβράνες* ή *Dp-Βράνες* (*Dp-Branes*), όπου το p χαρακτηρίζει τις χωρικές διαστάσεις της βράνης. Οι πολυ-μεμβράνες είναι δυναμικά αντικείμενα και μπορούν να συσχετιστούν με $U(1)$ πεδία βαθμίδας. Κατ'επέκταση, μία συστοιχία από N Dp-Βράνες (stack of branes) θα χαρακτηρίζεται από μια $U(N)$ συμμετρία βαθμίδας, ένω $SU(N)$ συμμετρίες προκύπτουν από συστήματα τεμνόμενων βρανών (intersecting branes).

Σήμερα υπάρχουν 5 διαφορετικές θεωρίες υπερχορδών. Αυτές είναι γνωστές ως τύπου-I, τύπου-IIA και τύπου-IIB, καθώς και δύο θεωρίες *ετεροτικών χορδών* (Heterotic strings) που βασίζονται στις ομάδες συμμετρίας $SO(32)$ και $E_8 \times E_8$. Είναι σημαντικό το γεγονός ότι, οι παραπάνω θεωρίες χορδών σχετίζονται μεταξύ τους μέσω μετασχηματισμών *δυϊκότητας* (Dualities). Η ιδιότητα αυτή καταδυκνείει ότι οι διαφορετικές τύπου θεωρίες αποτελούν μέρος μίας μεγαλύτερης και πιο ενιαιάς θεωρίας. Αξίζει να σημειωθεί ότι η θεωρία τύπου-IIB είναι έτερη προς τον εαυτό της (self dual) μέσω μετασχηματισμών S-δυϊκότητας, ιδιότητα που οδηγεί στη 12-διάστατη γεωμετρική εκδοχή της, γνωστή ως *Θεωρία-F* (F-theory) και η οποία αποτελεί το βασικό αντικείμενο μελέτης της παρούσας διπλωματικής εργασίας.

Η θεωρία-F εισήχθει για να περιγράψει τα μη-διαταρακτικά φαινόμενα που προκύπτουν από την παρουσία D7-βρανών στην θεωρία IIB. Ο εσωτερικός συμπαγοποιημένος χώρος της θεωρίας-F περιγράφεται ως μία *ελλειπτική ίνωση* (elliptic fibration) και αποτελεί ένα *Calabi-Yau τετράπτυχο* (Calabi-Yau fourfold). Ένα σημαντικό πλεονέκτημα της θεωρίας-F σε σχέση με τα συμβατικά συστήματα τεμνόμενων βρανών αποτελεί το γεγονός ότι, οι μη-Αβελιανές μεγαλοενοποιημένες συμμετρίες βαθμίδας συνδέονται με τις ανωμαλίες της ελλειπτικής ίνωσης. Αυτές οι ανωμαλίες ταξινομούνται σε ομάδες συμμετρίας ADE τύπου και κατά συνέπεια η ειδική ομάδα E_8 αποτελεί την ανώτερη συμετρία ή οποία μπορεί να συσχετιστεί με τη θεωρία. Κατά συνέπεια,

γνωστές μεγαλοενοποιημένες θεωρίες μπορούν να προκύψουν ως ενεργά μοντέλα της θεωρίας-F, καθώς η E_8 αποτελεί *πατρική* ομάδα των συμμετριών αυτών: $E_8 = G_{GUT} \times SU(N)_\perp$, με $G_{GUT} = SU(5)$, $SO(10)$, E_6 για $N = 5, 4, 3$ αντίστοιχα.

Στην ημι-τοπική προσέγγιση της θεωρίας-F, θεωρούμε ότι οι μεγαλοενοποιημένες συμμετρίες G_{GUT} προέρχονται από την ομάδα E_8 ενώ σημαντικό ρόλο παίζει η συμπληρωματική ομάδα $SU(N)_\perp$ η οποία συνοδεύει την GUT συμμετρία. Τα παραπάνω περιγράφονται με κομψό τρόπο μέσω της πολυωνυμικής εξίσωσης *spectral cover* (SC). Οι συντελεστές του πολυωνύμου SC εμπεριέχουν αρκετές από τις τοπολογικές ιδιότητες του εσωτερικού χώρου ενώ οι ρίζες του ταυτίζονται με τα βάρη της άλγεβρας Cartan της $SU(N)_\perp$ συμμετρίας. Η αναπαραστάσεις ύλης του GUT μοντέλου περιγράφονται από εξισώσεις των ριζών αυτών και κατά συνέπεια μπορούν να εκφραστούν ως συναρτήσεις των συντελεστών του πολυωνύμου SC. Επιπλέον, σημαντικό ρόλο στην κατασκευή ρεαλιστικών μοντέλων διαδραματίζουν σχέσεις συμμετρίας (*monodromies*) μεταξύ των ριζών του SC πολυωνύμου. Συγκεκριμένα, μελετώντας τις ιδιότητες και τους τρόπους παραγωντοποίησης του SC πολυωνύμου δύναται η συσχέτιση του $SU(N)_\perp$ με διακριτές συμμετρίες όπως η ομάδα των πιθανών μεταθέσεων N στοιχείων S_N καθώς και υποομάδες αυτής.

Με βάση τα παραπάνω, η παρούσα διατριβή διαπραγματεύεται την κατασκευή και μελέτη των χαμηλοενεργειακών επιπτώσεων διάφορων μοντέλων που προκύπτουν από το πλαίσιο της θεωρίας-F. Αρχικά, παρουσιάζεται ένα υπερσυμμετρικό μοντέλο $SU(5)$ το οποίο συνοδεύεται από μία Klein V_4 monodromy καθώς μία Z_2 parity γεωμετρικής προέλευσης. Στις χαμηλές ενέργειες, το σωματιδιακό φάσμα του μοντέλου ταυτίζεται με αυτό του MSSM εκτετάμενο από δύο δεξιόστροφα νετρίνο. Στη συνέχεια, μελετάτε ένα $SU(5)$ μοντέλο το οποίο αυτή τη φορά συνοδεύεται από την μη-Αβελιανή διακριτή συμμετρία D_4 και έναν Αβελιανό παράγοντα $U(1)$. Στις χαμηλές ενέργειες το μοντέλο προβλέπει ένα ρεαλιστικό φάσμα σωματιδιακών καταστάσεων και είναι ικανό να ερμηνεύσει τα φαινόμενα ανάμιξης των νετρίνων όπως αυτά προκύπτουν από τα πειραματικά δεδομένα. Επιπλέον, λόγω της ύπαρξης μίας γεωμετρικής Z_2 parity, το μοντέλο προβλέπει διαδικασίες παραβίασης του βαρυονικού αριθμού όπως ταλαντώσεις νετρονίου-αντινετρονίου, ενώ ταυτόχρονα απουσιάζουν φαινόμενα διάσπασης του πρωτονίου. Ακολουθεί μία συστηματική μελέτη φαινομένων παραβίασης της R-parity στην ημι-τοπική και τοπική προσέγγιση της θεωρίας-F, από την οποία προκύπτει ότι τα φαινόμενα αυτά αποτελούν γενικό χαρακτηριστικό της θεωρίας, μπορούν όμως να υπάρχουν χωρίς φαινόμενα διάσπασης του πρωτονίου λόγω της ύπαρξης μαγνητικών ροών. Επιπλέον, οι τιμές των συντελεστών σύζευξης Yukawa των όρων παραβίασης της R-parity υπολογίζονται στην τοπική προσέγγιση της θεωρίας-F και συγκρίνονται με τις αντίστοιχες τιμές που προκύπτουν από την θεωρία πεδίου. Τέλος, γίνεται μελέτη E_6 μοντέλων από τη θεωρία-F, τα οποία προβλέπουν την ύπαρξη ενός ελαφριού μποζονίου βαθμίδας Z' στις χαμηλές ενέργειες. Η ρήξη της συμμετρίας E_6 στην $SO(10)$ και έπειτα στην $SU(5)$ επιτυγχάνεται μέσω Αβελιανών μαγνητικών ροών. Το σωματιδιακό φάσμα των μοντέλων αποτελείται από το MSSM και επιπλέον διανυσματικού τύπου εξωτικές καταστάσεις. Πραγματοποιείται ανάλυση της ομάδας εξισώσεων ανακανονικοποίησης σε επίπεδο δύο-βρόγχων για τους συντελεστές σύζευξης βαθμίδας και Yukawa και δείχνεται ότι στις υψηλές ενέργειες τα αποτελέσματα είναι συγκρίσιμα με τις προβλέψεις που προέρχονται από τον υπολογισμό συντελεστών σύζευξης Yukawa στην θεωρία-F. Τέλος, προσδιορίζονται σημεία του παραμετρικού χώρου της θεωρίας όπου οι συντελεστές Yukawa των φερμιονίων top, bottom και tau ενοποιούνται.

List of Publications

- *Within the context of my PhD studies:*

[1]. *Discrete Family Symmetry from F-Theory GUTs*,
A. Karozas, S. F. King, G. K. Leontaris, A. Meadowcroft,
JHEP 1409 (2014) 107

[2]. *Phenomenological implications of a minimal F-theory GUT with discrete symmetry*,
A. Karozas, S. F. King, G. K. Leontaris, A. Meadowcroft,
JHEP 1510 (2015) 041

[3]. *MSSM from F-theory $SU(5)$ with Klein Monodromy*,
M. C. Romao, A. Karozas, S. F. King, G. K. Leontaris, A. Meadowcroft,
Phys.Rev. D93 (2016) no.12, 126007

[4]. *R-Parity violation in F-Theory*,
M. C. Romao, A. Karozas, S. F. King, G. K. Leontaris, A. Meadowcroft,
JHEP 1611 (2016) 081

[5]. *Vectorlike particles, Z' and Yukawa unification in F-theory inspired E_6*,
A. Karozas, G. K. Leontaris and Q. Shafi,
Phys.Lett. B778 (2018) 213-220

- *I also worked in parallel on the following two articles:*

[6]. *750 GeV diphoton excess from E_6 in F-theory GUTs*,
A. Karozas, S. F. King, G. K. Leontaris, A. Meadowcroft,
Phys.Lett. B757 (2016) 73-78

[7]. *Inflation from a no-scale supersymmetric $SU(4)_C \times SU(2)_L \times SU(2)_R$ model*,
W. Ahmed and A. Karozas,
Phys.Rev. D98 (2018) no.2, 023538

Contents

List of Figures

List of Tables

Chapter 1

Theories Beyond the Standard Model

In this introductory chapter, we present theories beyond the Standard Model (SM) of particle physics, such as Supersymmetry (SUSY) and Grand Unified Theories (GUTs). Next, we give a basic introduction in F-theory, which is a geometric version of II-B superstring theory and we present how GUT models can be realized in this framework. Since any supersymmetric GUT model at low energies must be consistent with the successful predictions of SM, we present a short overview of its features first.

1.1 Overview of the Standard Model

The Standard Model of particle physics has been tested experimentally in many different ways and to high precision during the last decades. It turned out that this elegant theory provides a very good description of particle physics at low energies. This successful theory describes the properties and the interactions of particles based on only a few simple symmetry principles [8, 9, 10]. The framework behind it is a quantum field theory in which the fundamental interactions are represented by gauge symmetries and the force carriers are the corresponding gauge bosons. The particles are described by fields transforming non-trivially under the representations of these symmetries. The SM describes only the non-gravitational fundamental forces, which are the electromagnetic, the weak and the strong force; there is so far no theory of gravity compatible with a gauged quantum field theory.

SM gauge group and field content

The various particles observed in nature show very similar properties thus suggesting the existence of symmetries in the *world* of elementary particles. Modern particle physics is strongly related with symmetry principles. The basic principle which guides the construction of models of particle physics is that of local gauge invariance. The full gauge symmetry group of the SM

Name	Particles	SM reps
Gauge Bosons	G	$(\mathbf{8},\mathbf{1})_0$
	W	$(\mathbf{1},\mathbf{3})_0$
	B	$(\mathbf{1},\mathbf{1})_0$
Quarks	$\begin{pmatrix} u \\ d \end{pmatrix}_L, \begin{pmatrix} c \\ s \end{pmatrix}_L, \begin{pmatrix} t \\ b \end{pmatrix}_L$	$(\mathbf{3},\mathbf{2})_{1/6}$
	$u_R^\dagger,\ c_R^\dagger,\ t_R^\dagger$	$(\overline{\mathbf{3}},\mathbf{1})_{-2/3}$
	$d_R^\dagger,\ s_R^\dagger,\ b_R^\dagger$	$(\overline{\mathbf{3}},\mathbf{1})_{1/3}$
Leptons	$\begin{pmatrix} \nu_e \\ e \end{pmatrix}_L, \begin{pmatrix} \nu_\mu \\ \mu \end{pmatrix}_L, \begin{pmatrix} \nu_\tau \\ \tau \end{pmatrix}_L$	$(\mathbf{1},\mathbf{2})_{-1/2}$
	$e_R^\dagger,\ \mu_R^\dagger,\ \tau_R^\dagger$	$(\mathbf{1},\mathbf{1})_1$
Higgs field	H	$(\mathbf{1},\mathbf{2})_{1/2}$

Table 1.1: Field content of the SM. The last column shows the representations under the SM gauge group which is given in the order $(SU(3)_C, SU(2)_L)_{U(1)_Y}$.

is the direct product of three simple groups:

$$\mathcal{G}_{SM} = SU(3)_C \times SU(2)_L \times U(1)_Y. \tag{1.1}$$

The strong interaction is described by the unbroken color gauge group $SU(3)_C$. This group acts on the quarks which are the elementary constituents of matter and the interaction force is mediated by the gluons G^A which are embedded in the (adjoint) octet representation of the group. The quarks and the gluons are colored fields.

The remaining part of the SM gauge group, $SU(2)_L \times U(1)_Y$, is the gauge group of the unified weak and electromagnetic interactions. More analytical, $SU(2)_L$ is the weak isospin group, acting on left-handed fermions, and $U(1)_Y$ is the hypercharge group. At low energies the $SU(2)_L \times U(1)_Y$ symmetry is spontaneously broken and the residual group is $U(1)_{EM}$ whose generator is a linear combination of the $U(1)_Y$ hypercharge generator and a generator of $SU(2)_L$. This generator corresponds to a massless gauge boson, the photon.

Every particle of the SM can be embedded in a representation with certain symmetry properties under $SU(3)_C$, $SU(2)_L$ and $U(1)_Y$ transformations. The fermions of the SM can be separated in two classes, the quarks and the leptons. Quarks transform in the triplet representation under the strong interaction whereas the leptons do not carry a color charge, so they are singlets under the strong interaction. The charged leptons and quarks come in pairs of left- and right- handed fermions. An exception holds for the neutral leptons, the neutrinos, which are purely left-handed, theres is no right-handed neutrinos in the SM. In Table 1.1 we classify

the fields according to the dimension of their representation of $SU(3)_C$ and $SU(2)_L$ and their hypercharge which gives the transformation properties under the $U(1)_Y$ group. In addition the table shows that the fermions (quarks and leptons) appear in each case in three copies, the so-called families or generations. In the next sections of this thesis we will use the following notation for the fermion fields:

$$Q_{iL} = \begin{pmatrix} u_{iL} \\ d_{iL} \end{pmatrix} \quad , \quad L_{iL} = \begin{pmatrix} \nu_{iL} \\ e_{iL} \end{pmatrix}$$

$$u_{iR} \quad , \quad d_{iR} \quad , \quad e_{iR}$$

where $i = 1, 2, 3$ denotes the generations and we have labeled with Q_{iL} (L_{iL}) any left-handed quark (lepton) doublet and with u_{iR} (d_{iR}) the right-handed up(down)-type quark singlet. Finally e_{iR} represents the right-handed charged lepton singlets.

The SM Lagrangian

For a proper definition of the SM Lagrangian density it is necessary to introduce a few more objects. One of these objects is the covariant derivative which is given by:

$$D_\mu \equiv \partial_\mu + ig_1 Y B_\mu + ig_2 W_\mu S^I + ig_3 G^A_\mu T^A. \tag{1.2}$$

Here, S^I (with $I = 1, 2, 3$) and T^A (with $A = 1...8$) are the fundamental representations generators of the $SU(2)$ and $SU(3)$ groups respectively and Y is the hypercharge of the corresponding field where the covariant derivative acts.

In addition we define the field-strength tensors of the SM gauge fields as:

$$SU(3): \qquad G^A_{\mu\nu} = \partial_\mu G^A_\nu - \partial_\nu G^A_\mu - g_3 f^{ABC} G^B_\mu G^C_\nu \tag{1.3}$$

$$SU(2): \qquad W^I_{\mu\nu} = \partial_\mu W^I_\nu - \partial_\nu W^I_\mu - g_2 \epsilon^{IJK} W^J_\mu W^K_\nu \tag{1.4}$$

$$U(1): \qquad B_{\mu\nu} = \partial_\mu B_\nu - \partial_\nu B_\mu. \tag{1.5}$$

Introducing also the *isodoublet* of the Higgs doublet as $\tilde{H} = i\sigma_2 H^*$, we have all the necessary ingredients in order to write down the SM Lagrangian density:

$$\begin{aligned} \mathcal{L}_{SM} = & -\frac{1}{4} G^A_{\mu\nu} G^{A\mu\nu} - \frac{1}{4} W^I_{\mu\nu} W^{I\mu\nu} - \frac{1}{4} B_{\mu\nu} B^{\mu\nu} \\ & + i(\overline{L} \not{D} L + \overline{e}_R \not{D} e_R + \overline{Q} \not{D} Q + \overline{u}_R \not{D} u_R + \overline{d}_R \not{D} d_R) \\ & + (D_\mu H)^\dagger (D^\mu H) - V(H) \\ & - [(\overline{L} \mathbf{Y_e} e_R) H + (\overline{Q} \mathbf{Y_u} u_R) \tilde{H} + (\overline{Q} \mathbf{Y_d} d_R) H + h.c]. \end{aligned} \tag{1.6}$$

In this shorthand version of the SM Lagrangian the first and second lines contain kinetic terms for the gauge bosons and fermion fields respectively. The first term on the third line is the kinetic term of the Higgs-boson field while $V(H)$ is the Higgs scalar potential which we will analyse next. Finally the last line is the Yukawa sector of the Lagrangian and as we will describe next the fermion masses originate from these terms.

Spontaneous EW Symmetry Breaking

The SM Lagrangian introduced above describes all the gauge bosons and fermion fields as massless particles. Writing down explicit mass terms in the Lagrangian spoils the gauge invariance, and is the gauge symmetry that ensures renormalisabililty. This is not a problem for massless particles, like the photon and the gluons. On the other hand, $W^{\pm}$ and Z bosons for the weak interaction, are among the heaviest elementary particles in nature. Giving masses to these gauge bosons was one of the main reasons to introduce the concept of *Spontaneous Symmetry Breaking* (SSB) in particle physics which triggers what is known as the *Higgs* mechanism [11, 12, 13, 14]. A symmetry is broken when the Lagrangian of a theory respects the symmetry but the vacuum of the theory is not invariant. In the SM, the Higgs field (a complex-valued $SU(2)$ doubled), adds the scalar potential $V(H)$ in (1.6) which has the following form:

$$V(H) = \mu^2 H^{\dagger} H + \lambda (H^{\dagger} H)^2. \tag{1.7}$$

The potential is invariant under $SU(2)_L \times U(1)_Y$ transformations, however its ground state is not. The shape of the potential depends on the sign of the parameters μ^2 and λ. For $\mu^2 < 0$ and $\lambda > 0$ the potential have a set of minima. However, if we select one of the minima, the symmetry will be broken. More precisely, the neutral component of the Higgs doublet will develop a *vacuum expectation value* (VEV):

$$< 0|H|0 >= \frac{1}{\sqrt{2}} \begin{pmatrix} 0 \\ \upsilon \end{pmatrix} \tag{1.8}$$

where υ can be computed to be : $\upsilon = \sqrt{-\mu^2/\lambda}$. In addition, the scalar potential is still invariant under a change of the phase of the scalar field H. As a result, the vacuum state spontaneously breaks the EW symmetry down to $U(1)_{EM}$ which is still a good symmetry of the theory. The physical Higgs field h^0, arises as an expansion around the VEV. We can expand the Higgs doublet as:

$$H = \frac{1}{\sqrt{2}} \begin{pmatrix} G^+ \\ \upsilon + h^0 + iG^0 \end{pmatrix} \tag{1.9}$$

where h^0 is the physical Higgs field, a real scalar field with zero spin. Here G^+ and G^0 are Goldstone modes [15], [16] which absorbed on the definition of the W^+ and Z^0 bosons respectively.

By consider the four massless fields W^I_{μ} and B_{μ} and their interaction with H, after substituting the VEV from (1.8) ones finds the tree-level masses

$$M_{W^{\pm}} = \frac{\upsilon g_1}{2}, \quad M_Z = \frac{\upsilon \sqrt{g_1^2 + g_2^2}}{2}, \quad M_A = 0. \tag{1.10}$$

where Z_{μ} and A_{μ} are the mass eigenstates of W^3_{μ} and B_{μ}. The new field A_{μ} will be massless, corresponding to the photon, while the Z_{μ} field will be a neutral, massive boson mediating neutral current processes of the weak interaction. As we can see, the mass of the Z boson is different from the mass of the $W^{\pm}$ gauge bosons. This inequality of the weak boson masses can

be parametrised using the weak mixing angle (or Weinberg angle) between W^3_μ and B_μ and the physical mass eigenstates:

$$\cos\theta_W = \frac{M_W}{M_Z} \tag{1.11}$$

or in terms of the gauge couplings, $\tan\theta_W = g_1/g_2$. Similarly, the mass of the physical Higgs boson (h^0) at tree-level is given by $m_{h^0} = 2v^2\lambda$ and strongly depends on λ and quantum corrections. The measured values of the weak force gauge boson masses and the gauge couplings imply that $v \approx 246$ GeV.

Fermion masses and mixing

Up to now, we have discussed only the generation of gauge boson masses. In fact, not only the $W^\pm$ and Z^0 bosons acquire mass via the Higgs mechanism. Also the fermion mass terms originate from their Yukawa interaction with H. To illustrate the point, let us study for example the charged lepton Yukawa term:

$$Y_e^{ij}\overline{L}_i H e_{jR} \longrightarrow \frac{1}{\sqrt{2}}Y_e^{ij}\begin{pmatrix}\overline{\nu}_{iL} & \overline{e}_{iL}\end{pmatrix}\begin{pmatrix}0\\ v+h^0\end{pmatrix}e_{jR} = \frac{Y_e^{ij}v}{\sqrt{2}}\overline{e}_{iL}e_{jR} + \frac{Y_e^{ij}}{\sqrt{2}}h^0\overline{e}_{iL}e_{jR} \tag{1.12}$$

Observing the first term it is clear that when the Higgs field receives a VEV, the Yukawa term in the Lagrangian generates a fermion mass term. We obtain similar results for the up- and down-type quarks and collectively we can write: $m_f^{ij} = Y_f^{ij}v/\sqrt{2}$, whith $f = u, d, e$. Because of the 3 generations described in the SM, $m_{u,d,e}$ are 3×3 matrices and as a result there is a mixing between generations. Since these mass matrices are not diagonal in generation space, one has to rotate the fermion felds to the mass eigenbasis using unitary matrices as follows

$$\psi_f \to V_f\psi_f, \quad \psi_{f^c} \to V_{f^c}\psi_{f^c} \tag{1.13}$$

where the matrices V_f and V_{f^c} satisfy,

$$V_u^T Y_u V_{u^c} = \text{diagonal and positive.} \tag{1.14}$$

Since now V_u and V_d are not required to be the same, they will in general not cancel out in the weak interaction changing vertex of $W^\pm$ vector bosons to fermions. This implies that the mentioned vertices will transform under eq. (1.13) as

$$g u_i^\dagger d_j W^+ + h.c \longrightarrow g u_i^\dagger (V_u^\dagger V_d)_{ij} d_j W^+ + h.c. \tag{1.15}$$

The unitary matrix formed in the parenthesis of the above relation is called the Cabibbo-Kobayashi-Maskawa (CKM) mixing matrix [17],

$$V_{CKM} = V_u^\dagger V_d.$$

This 3×3 matrix parametrises the mixing between the three generations in each interaction vertex of fermions with the weak charged bosons.

In general, V_{CKM} has nine degrees of freedom consisting by three mixing angles and six phases. However, since V_{u^c} and V_{d^c} are not physical, one can reduce the number of parameters from nine to four. That way we receive the standard parametrisation of V_{CKM} which is given by

$$V_{CKM} = \begin{pmatrix} c_{12}c_{13} & s_{12}c_{13} & s_{13}e^{-i\delta} \\ -s_{12}c_{23} - c_{12}s_{23}s_{13}e^{i\delta} & c_{12}c_{23} - s_{12}s_{23}s_{13}e^{i\delta} & s_{23}c_{13} \\ s_{12}s_{23} - c_{12}c_{23}s_{13}e^{i\delta} & -c_{12}s_{23} - s_{12}c_{23}s_{13}e^{i\delta} & c_{23}c_{13} \end{pmatrix} \tag{1.16}$$

where $\delta = \delta^{CKM}$, $c_{ij} = \cos\theta_{ij}^{CKM}$ and $s_{ij} = \sin\theta_{ij}^{CKM}$. The angle θ_{12}^{CKM} is also known as the Cabibbo mixing angle θ_C. Of course, at this stage, there is no analogue to V_{CKM} matrix for the lepton sector since the SM describe the neutrinos as massless particles. This changes if we introduce right-handed neutrino fields ν_i^c as we will see next in this chapter.

Regarding the second term in (1.12) describes the coupling between the Higgs field and the left- and right-handed charged fermions. These type of interactions are important because can be tested experimentally. However, since $Y_{u,d,e}^{ij} = m_{u,d,e}^{ij}\sqrt{2}/\upsilon$, the coupling is small for the lighter generations. On the other hand, the heaviest generations (top, bottom, tau) and especially the top quark (the heaviest of all fermions in the SM with mass about $m_t \simeq 173.3$ GeV) couples strongly to the Higgs boson [18], [19].

Anomaly cancellation

It is well known that when a classical Lagrangian is invariant under a gauge symmetry, a direct consequence is the existence of a conserved current. While a current may be conserved at tree-level, when we include high order loop corrections due to quantum effects, it is possible that that current may no longer be conserved. Generically, this occurs if the action of a theory is invariant under a symmetry, but the measure of the path integral, is not. In gauge field theory, this type of inconsistencies are known as gauge anomalies. The consequence of this would be that observable quantities depend on the gauge, and therefore the theory makes no sense. Thus, such anomalies should not occur.

In a chiral gauge theory like the SM, gauge anomalies appear. In terms of Feynman diagrams the existence of an anomaly can be calculated by evaluating the triangle diagram like the one presented in Fig. 1.1. For a general gauge group G of a 4-dimensional theory the final result [1] is proportional to a group theoretical factor

$$\mathcal{A}_{abc}^{\mathcal{R}} = \mathrm{tr}[t_a^{\mathcal{R}}\{t_b^{\mathcal{R}}, t_c^{\mathcal{R}}\}], \tag{1.17}$$

where the $t_{a,b,c}^{\mathcal{R}}$ are the group generators correspond to the external currents in the triangle diagram and $\mathcal{R}$ denotes the representation under which the fermions contributing to the anomaly, transforms. Equation (1.17) is the anomaly cancellation condition that we have to check when we build a new model. However, since the existence of an anomaly clearly depends on a pure group theory factor, some general model independent conclusions can be extracted. More precisely,

[1] For a complete analysis on the subject see [20] and references there in.

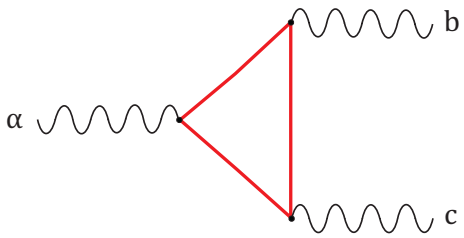

Figure 1.1: Triangle Feynman diagram leading to gauge anomalies. Here, each external leg may be any gauge boson of the theory, while the internal propagators are due to all fermionic fields to which those bosons couple.

one can show that if a group G has only real or pseudoreal representations, its $\mathcal{A}^{\mathcal{R}}_{abc}$ all vanish and there cannot be any anomalies for a gauge theory with such a gauge group G. This implies that all the $SO(2n+1)$ groups with $n \geq 1$ (including $SU(2) \simeq SO(3)$) and $SO(4n)$ with $n \geq 2$ have $\mathcal{A}_{abc} = 0$.

In the case of the SM the gauge group is $SU(3) \times SU(2) \times U(1)$ and according to the above discussion we have contributions to $\mathcal{A}_{abc}$ for the following different anomalies:
$SU(3) - SU(3) - SU(3)$, $SU(3) - SU(3) - U(1)$, $SU(2) - SU(2) - U(1)$ and $U(1) - U(1) - U(1)$.

In order to illustrate the point, we will study in some detail the "$U(1)^3_Y$" anomaly. In this particular example the three external legs of the diagram correspond to $U(1)_Y$ currents. The condition leads to a polynomial like equation involves the hypercharge of all the SM fermions that can couple with the $U(1)_Y$ gauge boson. Then, using Table 1.1 the condition reads:

$$(U(1)_Y)^3: \quad \mathcal{A} \sim \left\{2 \times (\frac{1}{6})^3 + 1 \times (-\frac{2}{3})^3 + 1 \times (\frac{1}{3})^3\right\} \times n_c + \left\{2 \times (-\frac{1}{2})^3 + (1)^3\right\}$$

where n_c is the number of quark colors. Performing the computation ones find that $\mathcal{A} \sim \frac{3}{4}(1 - \frac{n_c}{3})$. Clearly, for $n_c = 3$ we find that, $\mathcal{A} = 0$, as we wanted. The interesting point here is that cancellation of the anomalies seems to support the concept of colour in the SM as well as the fact that we have complete number of generations, since for $n_c \neq 3$ or for an incomplete fermion family, the result is different than zero. Similarly, we can show that the anomaly factor in (1.17) vanishes for all the other cases in the SM.

In summary, we see that in the SM the anomaly $\mathcal{A}_{abc}$ vanishes as it should be to keep the gauge symmetries unbroken. However, we have to clarify that this happens only due to the fact that the anomalies from all the loop contributions with quarks and leptons cancel. This is a surprising result and seems to be connected with the problem of charge quantization in the SM. Charge quantization is just one of a long list of SM open questions and limitations that we will discuss in some detail in what follows.

1.2 Troubles with the SM

The SM is an extremely successful theory to explain most of elementary particle properties and interactions. Masses of the $W^{\pm}$ and Z weak gauge bosons as predicted by the SM theory are very close to those suggested by the experiments. In addition, SM also predicted the existence of the charm quark [21] from the requirement to suppress flavour changing neutral currents (FCNC) before it was actually discovered in 1974. In a similar fashion the SM also predicted the mass of the heavy top quark in the right region before its discovery. In 2012 the success of the SM was established with the discovery of the Higgs particle by ATLAS [22, 23] and CMS [24, 25] experiments at CERN's *Large Hadron Collider* (LHC). Up today the Higgs particle is the only experimentally observed elementary scalar field.

Despite all the successes of the SM, there are experimental and theoretical reasons to consider models beyond the Standard Model (BSM). Most of these issues motivate us to think the SM as the low energy remmant of a theory based on a higher symmetry group. In the following we briefly discuss some of these problems.

Charge Quantization

It is well known that the electric charge of the proton it is equal with the absolute value of the charge of the electron, $Q_p = -Q_e = e$. In addition, the proton (uud) and the (neutral) neutron (udd) are composite particles of up and down type quarks. With this information in mind one can easily find fractional charges $Q_d = \frac{-1}{3}e$ and $Q_u = \frac{+2}{3}e$ for the down and up quarks respectively. Lets define the smallest charge as $\tilde{e} \equiv e/3$, then for the absolute values of the up and down quark charges we see that: $|Q_d| = \tilde{e}$, $|Q_u| = 2\tilde{e}$ and $|Q_e| = 3\tilde{e}$. It is clear that a charge assignment like this must have a deeper theoretical explanation, but in the SM chosen that way in order to match with the experimental observations. However, most GUTs do provide an explanation for this issue as they embed the $U(1)_Y$ into a larger non-Abelian group.

Gauge coupling (non) Unification

It is a well known feature of quantum field theories that the coupling constants and the masses depend on the energy scale of interaction. This dependency on the energy scale of the theory can be described in the framework of *renormalisation*. The evolution of gauge, scalar and Yukawa couplings in the SM is described by the *Renormalisation Group* (RG) equations. The one-loop RG equations for the SM gauge couplings g_1, g_2, g_3 are

$$\beta_{g_a} \equiv \frac{d}{dt} g_a = \frac{1}{16\pi^2} b_a g_a^3, \quad \text{with} \quad a = 1, 2, 3 \tag{1.18}$$

where $t = \ln Q/Q_0$, with Q_0 the input scale and Q the RG scale. The b's coefficients depend on the gauge group and the field content of the model. In the case of the SM these coefficients are: $(b_1, b_2, b_3)_{SM} = (41/10, -19/6, -7)$. In terms of the quantities $\alpha_a = g_a^2/4\pi$, the RG equations (1.18) receive an elegant, linear form:

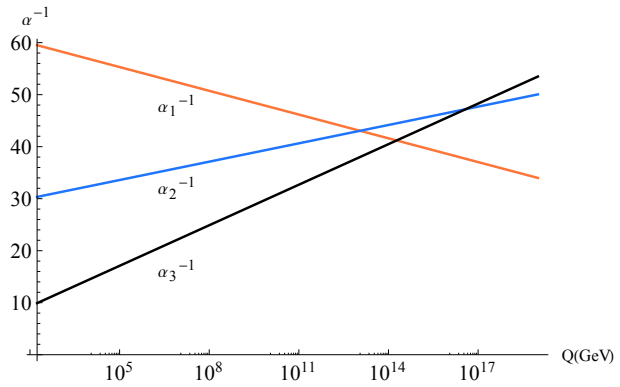

Figure 1.2: Running of the inverse gauge couplings $\alpha_a^{-1}(Q)$ on one-loop level in the SM. As input scale we took $Q_0 = m_{top} \simeq 173.4$ GeV while the input values of the gauge couplings at this scale was received from [26].

$$\frac{d}{dt}\alpha_a^{-1} = -\frac{b_a}{2\pi}. \tag{1.19}$$

The one-loop RG evolution of these quantities is presented in Figure 1.2. As we can see, the three gauge couplings approach each other with increasing energy. They nearly meet at high energies, close to the *Planck scale* ($\sim 10^{19}$ GeV), which motivate us to unify the gauge symmetries at this scale. Actually unification of gauge couplings can be realised in the framework of Supersymmetry. More precisely, in the minimal supesymmetric extension of the SM the gauge couplings actually meet at the so-called *GUT scale* $M_{GUT} \sim 10^{16}$ GeV.

Hierarchy Problems

In the SM, the Higgs boson mass is not protected by any symmetry. Thus, there is no natural scale for the Higgs boson mass, m_h, in the theory. Consequently, when radiative corrections are taken into account, there is nothing to stopped Higgs boson from receiving a mass as large as the the Planck scale. This is the so called *gauge hierarchy problem*. The most significant contribution to the Higgs boson mass arises from one-loop interactions of the Higgs boson with fermions, like the one presented in Figure 1.3. From the diagram it is clear that the contribution from the fermion loop is proportional to the squared Yukawa couplings (y_f^2). As a result these contributions became important when heavy quarks (like the top) are running in the loop.

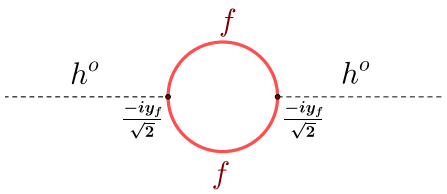

Figure 1.3: One-loop radiative corrections to the Higgs boson mass from interactions with fermions.

Suppose the theory of the SM is valid up to the Planck scale and the cut-off scale Λ lies there, then the correction to the Higgs boson mass is proportional to that scale[2]

$$\delta m_{h^0}^2 \approx -\frac{y_f^2}{8\pi^2}\Lambda^2. \tag{1.20}$$

The renormalized Higgs boson squared mass is then given by

$$\tilde{m}_{h^0}^2 = m_{h^0,bare}^2 + \delta m_{h^0}^2 \tag{1.21}$$

and looking at eq. (1.20) the requirement of *fine tuning* for a EW scale Higgs mass is necessary, since the scales of $\tilde{m}_{h^0}$ and Λ differ by many orders of magnitude.

Another type of hierarchy problem, arises from the Yukawa sector of the SM and is known as the *Fermion mass hierarchy problem*. There are large hierarchies between the fermion masses. For example, the top quark mass is approximately 174 GeV while the mass of the lightest quark (up), lies in the range of few MeV's. This translates in hierarchies between the Yukawa couplings and are as large as $\sim 10^6$.

Neutrino masses

According to the SM, neutrinos should be massless. But they aren't. Various types of experiments have provided clear evidence of a phenomenon known as *Neutrino Oscillations* [27]. Simply put it, neutrino oscillation is the phenomenon whereby a neutrino created with a specific flavor (electron, muon, or tau) can later be observed to have a different flavor. This phenomenon is only possible because neutrinos are not massless after all. Hence, a modification to the SM of particle physics is required. This is the first direct experimental evidence of physics BSM so far [28].

In terms of quantum field theory, the lepton flavor $\nu_{e,\mu,\tau}$ eigenstates of neutrinos are the linear combinations of the mass eigenstates of neutrinos $\nu_{1,2,3}$:

$$\nu_{lL}(x) = \sum_{j=1}^{3} U_{lj}\nu_{jL}(x) \tag{1.22}$$

where $l = e, \mu, \tau$. Here U is the 3×3 unitary neutrino mixing matrix, commonly known as Pontecorvo-Maki-Nakagawa-Sakata (PMNS) matrix and is the analogue of the CKM matrix describing the mixing on the quark sector. Similar, this matrix can be parameterized by 3 angles, and, depending on whether the massive neutrinos ν_j are Dirac or Majorana particles, by 1 or 3 CP violation phases.

$$U = \begin{pmatrix} c_{12}c_{13} & s_{12}c_{13} & s_{13}e^{-i\delta} \\ -s_{12}c_{23} - c_{12}s_{23}s_{13}e^{i\delta} & c_{12}c_{23} - s_{12}s_{23}s_{13}e^{i\delta} & s_{23}c_{13} \\ s_{12}s_{23} - c_{12}c_{23}s_{13}e^{i\delta} & -c_{12}s_{23} - s_{12}c_{23}s_{13}e^{i\delta} & c_{23}c_{13} \end{pmatrix} \times diag(1, e^{i\frac{a_{21}}{2}}, e^{i\frac{a_{31}}{2}}) \tag{1.23}$$

where $c_{ij} = \cos\theta_{ij}$, $s_{ij} = \sin\theta_{ij}$, the angles $\theta_{ij} = [0, \pi/2], \delta = [0, 2\pi]$ is the Dirac CP violation phase and a_{21}, a_{31} are two Majorana CP violation (CPV) phases.

Parameter	Best fit value ($\pm 1\sigma$)	3σ range
$\frac{\Delta m^2_{21}}{10^{-5}[eV^2]}$	$7.40^{+0.21}_{-0.20}$	$(6.80 \to 8.02)$
$\frac{\Delta m^2_{31}}{10^{-3}[eV^2]}$	$\begin{cases} 2.494^{+0.033}_{-0.031} & \text{NH} \\ -2.465^{+0.032}_{-0.031} & \text{IH} \end{cases}$	$\begin{cases} (2.399 \to 2.593) & \text{NH} \\ (-2.562 \to -2.369) & \text{IH} \end{cases}$
$\sin^2\theta_{12}$	$0.307^{+0.013}_{-0.012}$	$(0.272 \to 0.346)$
$\sin^2\theta_{23}$	$\begin{cases} 0.538^{+0.033}_{-0.069} & \text{NH} \\ 0.554^{+0.023}_{-0.033} & \text{IH} \end{cases}$	$\begin{cases} (0.418 \to 0.613) & \text{NH} \\ (0.435 \to 0.616) & \text{IH} \end{cases}$
$\sin^2\theta_{13}$	$\begin{cases} 0.0220^{+0.00075}_{-0.00075} & \text{NH} \\ 0.0222^{+0.00074}_{-0.00074} & \text{IH} \end{cases}$	$\begin{cases} (0.01981 \to 0.02436) & \text{NH} \\ (0.0206 \to 0.02452) & \text{IH} \end{cases}$

Table 1.2: The best-fit values and allowed ranges of the neutrino oscillation parameters, derived from a global fit of the current neutrino oscillation data [29]. Here $\Delta m^2_{ij} = m^2_i - m^2_j$. There are two types of possible mass hierarchy: normal hierarchy ($m_1 < m_2 < m_3$) and inverted hierarchy ($m_3 < m_1 < m_2$).

In most of the cases, the parameters that we are more interested when we construct a model for the description of the neutrinos, are the 3 mixing angles $\theta_{12}, \theta_{13}, \theta_{23}$ and the neutrino masses m_1, m_2, m_3. The best-fit values and ranges of these parameters, derived from a global fit analysis of the neutrino oscillation data are given in Table 1.2. Notice that the experiments are sensitive only on the mass squared differences $\Delta m^2_{ij} = m^2_i - m^2_j$ of the 3-neutrino states. There are only two independent neutrino mass squared differences, say $\Delta m^2_{21} > 0$ and $\Delta m^2_{31} \neq 0$. Since the sign of the latter remains unknown there are two possibilities of mass ordering. Normal hierarchy refers to the case where $m_1 < m_2 < m_3$ and inverted hierarchy implies $m_3 < m_1 < m_2$. As we observe from the data, $|\Delta m^2_{31}|$ ($|\Delta m^2_{32}|$) and $|\Delta m^2_{21}|$, in the case of $m_1 < m_2 < m_3$ ($m_3 < m_1 < m_2$), differ by approximately a factor of ~ 34.

There are also experimental bounds coming from cosmological measurements. According to the latest results of the *Planck Collaboration* [30], the following bound for the sum of the neutrino masses was obtained:

$$\sum_i m_i < 0.12 \quad eV. \tag{1.24}$$

The origin of neutrino mass is one of the most well kept secrets of Nature. SM Lagrangian

[2]There are additional contributions from one-loop corrections that are *logarithmically divergent* but are well under control due to the behaviour of the log function.

lacks a term which can generate neutrino mass at renormalizable level. The mechanism of this mass generation is unknown. In addition since the neutrinos are the only charge neutral particle in the SM there is a possibility, that a neutrino is a Majorana particle. Thus, by introducing right-handed neutrinos ν_R in the spectrum, we can have two possible neutrino mass terms :

$$\mathcal{L} = m_D \bar{\nu}_L \nu_R + M_R \bar{\nu}_R \nu_R + h.c \tag{1.25}$$

where in general m_D and M_R are 3×3 matrices. The first term arise from a usual Dirac type operator, $(Y_\nu)_{ij} \bar{L}_i \bar{H} \nu_{Rj}$, when the Higgs field receives a VEV. In this operator the coefficient Y_ν is the Dirac neutrino Yukawa coupling and demanding a neutrino mass ~ 1 eV one gets $Y_\nu \sim 10^{-11}$. This value is extremely small compared to the electron Yukawa coupling, $Y_e \sim 10^{-6}$.

The second term in (1.25) can be generated in a general model independent way as was suggested by Weinberg [31], who noted that one can form a dimension five ($d = 5$) operator, by using the SM doublets:

$$\mathcal{L}_{d=5} = \lambda_\nu^{ij} \frac{(L_i \bar{H})(\bar{H} L_j)}{\Lambda}. \tag{1.26}$$

Here λ_ν^{ij} are coupling constant coefficients and Λ is the mass scale where new physics occurs. This turns into a Majorana neutrino mass once the electroweak symmetry breaks through the nonzero VEV of the Higgs doublet. Note that majorana mass terms violate the total lepton number by two units[3], $\Delta L = 2$. There is an elegant way to generate the $d = 5$ operator at the treelevel. This is commonly known as the *see-saw* mechanism and depending on further details is classified on three categories: Type-I [32], Type-II [33] and Type-III [34] *see-saw* mechanism.

In Type-I seesaw mechanism the right-handed neutrino fields are pure gauge singlets. Hence, they can have Majorana mass terms, M_R, themselves even before electroweak SSB. Thus the magnitude of these masses are not directly constrained and we can assume that they are large enough that the new fields can be integrated out for calculations around the EW scale. Then, equation (1.25) can be expressed by a mixing matrix between Dirac masses and Majorana masses:

$$M_\nu = \begin{pmatrix} 0 & m_D \\ m_D^T & M_R \end{pmatrix} \tag{1.27}$$

and the light neutrino mass is given by

$$m_\nu = m_D M_R^{-1} m_D^T. \tag{1.28}$$

Here M_R often corresponds to the scale of new physics mentioned in (1.26) and for $M_R \gg m_D$, the light neutrino mass is a natural outcome. By consider m_ν at eV scale and $m_D \sim m_{top} \sim 100$ GeV we can estimate that $M_R \sim 10^{14}$ GeV. For a complete review on the theory of neutrino masses and mixing see [35].

[3] On theoretical level, a similar phenomenon which violates Baryon number by two units, $\Delta B = 2$, is neutron-antineutron oscillations.

Problems of cosmological origin

Finally, there are additional problems with the SM that are of cosmological origin. One of that is the problem of dark matter. There is nothing in the SM spectrum that could take into account the observed presence of dark matter [36], [37], [38]. Despite that the current experiments searching for dark matter signals have advanced significantly, so far no clear sign of its origin has been reported. Moreover, there are several other cosmological phenomena, of both theoretical and experimental nature that are not explained by the SM, such as the mystery of baryon-antibaryon asymmetry in the universe [39], the cosmological constant problem [40] and inflation which are not discussed further in the present thesis.

Because of all these issues the SM cannot be a complete theory for the description of particle physics. One needs to search for extensions of the SM that address one or as many as possible of the problems listed above. On the other hand, the predictions of the SM are surprisingly accurate. Consequently, any model or more a generic theory attempting to extend it must make sure that it contains the SM as a low energy effective theory. Several BSM approaches have been proposed during the last decades. SUSY and GUTs together provide an attractive framework which can explain most of the above mentioned open questions. Next we discuss some aspects of these approaches.

1.3 Aspects of Supersymmetry

Supersymmetry is one of the most attractive concepts in theoretical physics. Despite the lack of experimental evidence so far, a number of theoretical arguments can be given in support of this elegant theory. For example, is the only possible extension of the Poincare algebra in four dimensions [41]-[49]. SUSY is a spacetime symmetry mapping particles of integer spin (bosons) into particles of half-integer spin (fermions) and *vice versa*. Different said, unifies matter (fermions) and forces (bosons). In addition, SUSY is one of the main predictions of String Theory. From the phenomenological point of view, SUSY under certain conditions gives an elegant solution to the hierarchy problem and predicts unification of gauge couplings. At the same time, suitable dark matter candidates can be found on the extended field content of SUSY models.

The generators $\mathcal{Q}$ of this symmetry act as:

$$\mathcal{Q}|Fermion\rangle = |Boson\rangle \quad \text{and vice versa.} \tag{1.29}$$

From this schematic definition it is obvious that this operator changes the spin of a particle. Hence, affects also its space time properties. In a SUSY framework, each particle state has (at least) one *superpartner*. Since now two different type of particles are connected, in a SUSY theory instead of single particle states, one has to deal with *supermultiplets* of particle states. In addition, one can have theories with different number of SUSY generators $\mathcal{Q}$: $\mathcal{Q}^I$ with $I = 1...\mathcal{N}$. The number of SUSY generators, however, cannot be arbitrarily large but is constrained from the spacetime dimensions and the maximal spin of the theory. For theories in the convetional

Superfields	spin 1	spin 1/2	G_{SM}
$\hat{G}_a$	G_a	$\tilde{G}_a$	**8**, **1**, 0
$\hat{W}_a$	W_a	$\tilde{W}_a$	**1**, **3**, 0
$\hat{B}$	$\tilde{B}$	B	**1**,**1**,0

Table 1.3: Vector supermultiplets of the MSSM along with their boson and fermion content. Notice that the hypercharge of the new fermions (gauginos) is zero and consequently they not contribute to gauge anomalies.

4-dim spacetime, any supermultiplet must contains particles with spin at least as large as $\mathcal{N}/4$. This implies that for local gauge theories with maximal spin 1 (like the SM), $\mathcal{N}$ can be as large as 4. For more formal aspects on the subject we refer to standard reviews [50]-[52] and textbooks [53]-[56].

1.3.1 The Minimal Supersymmetric Standard Model

The most economic ($\mathcal{N} = 1$) SUSY extension of the SM is known as *Minimal Supersymmetric Standard Model* (MSSM) [50], [52], [57]. There are two types of supermultiplets in the MSSM, chiral and vector supermultiplets. The spin-1 gauge bosons of the SM and their spin-1/2 superpartners, the gauginos (the eight gluinos $\tilde{G}_{1..8}$, three winos $\tilde{W}_a$ and the bino $\tilde{B}$) are in vector supermultiplets. More details about the vector superfield content of the MSSM are presented in Table 1.3. Notice that gauginos have zero hypercharge and hence do not introduce gauge anomalies in the theory. Concerning the fermions of the SM, left- and right-handed fields belong to chiral superfields together with their spin-0 superpartners, the squarks and sleptons. The Higgs is now interpreted as the scalar part of a chiral superfield and in the MSSM we need to introduce two Higgs chiral superfields [50], [58], $\hat{H}_u$ and $\hat{H}_d$ with opposite hypercharge, $\frac{1}{2}$ and $-\frac{1}{2}$ respectively, see Table 1.4. This way the fermionic states of the Higgs superfields, known as higgsinos, do not introduce anomalies due to the opposite hypercharge assignment. There is an additional explanation behind this extension on the Higgs sector. In the language of SUSY, interaction and mass terms for the various superfields are described by a function known as the *superpotential*. The superpotential must be an analytic function only of the superfields, and not their conjugates. As a result, we can not use the Higgs isodoublet as we have done in the SM in order to construct a gauge invariant top-Yukawa term, but instead we introduce an extra Higgs superfield.

The rich particle spectrum of SUSY models like the MSSM and its extensions, provides solutions to some of the well known SM puzzles. It seems that SUSY is the symmetry that Higgs boson desperately needs to protect its mass. More precisely, the scalar partners of the SM fermions contribute to the Higgs boson mass via one-loop diagrams like the one presented in Figure 1.4. If S is a SUSY scalar particle and λ_S is the coupling coefficient to the Higgs boson, then for $y_f^2 = -\lambda_S$ the one-loop contribution from fermion loops (1.20) cancels with the one-loop contribution from the scalar particle. Furthermore, if the mass of the scalar is equal

Superfields		spin 0	spin 1/2	G_{SM}
Quark sector	$\hat{Q}$	$(\tilde{u}_L,\ \tilde{d}_L)$	(u_L,d_L)	**3**, **2**, 1/6
	$\hat{u}^c$	$\tilde{\bar{u}}_L \sim \tilde{u}_R^\dagger$	$\bar{u}_L \sim (u_R)^c$	$\bar{\mathbf{3}}$, **1**, -2/3
	$\hat{d}^c$	$\tilde{\bar{d}}_L \sim \tilde{d}_R^\dagger$	$\bar{d}_L \sim (d_R)^c$	$\bar{\mathbf{3}}$, **1**, 1/3
Lepton sector	$\hat{L}$	$(\tilde{\nu}_{eL},\tilde{e}_L)$	(ν_{eL},e_L)	**1**, **2**, -1/2
	$\hat{e}^c$	$\tilde{\bar{e}}_L \sim \tilde{e}_R^\dagger$	$\bar{e}_L \sim (e_R)^c$	**1**, **1**, 1
Higgs sector	$\hat{H}_u$	(H_u^+,H_u^0)	$(\tilde{H}_u^+,\tilde{H}_u^0)$	**1**, **2**, 1/2
	$\hat{H}_d$	(H_d^0,H_d^-)	$(\tilde{H}_d^0,\tilde{H}_d^-)$	**1**, **2**, -1/2

Table 1.4: Chiral supermultiplet fields of the MSSM along with their spin-0 and spin-1/2 content. Phenomenological reasons and anomaly cancellation requires the existence of two Higgs supermultiplets.

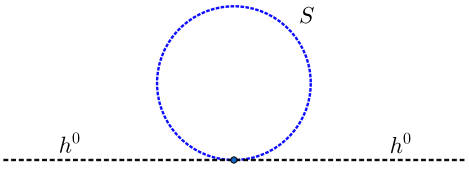

Figure 1.4: One-loop radiative corrections to the Higgs boson mass from scalar particles.

to the fermion mass ($m_f = m_S$), which means that SUSY is an exact symmetry, then even the logarithmic divergences disappear.

However, there is no experimental evidence of scalar particles having the same mass as the well-known fermions of the SM. This implies that SUSY is a broken symmetry in nature. Although many options have been discussed in the literature [59]-[64], up to now there is no an sufficient dynamical way to break SUSY. A possibility is to introduce by hand terms that break SUSY explicitly. These SUSY breaking terms must be *soft* [65, 66], which means we introduce by hand super-renormalizable breaking terms to distinquish the mass of the scalar SUSY particles. The mass of the scalars and the SUSY breaking scale must not be much heavier than the EW scale. Otherwise, the problem of naturalness is reintroduced in the theory. A more detailed analysis of the naturlness problem proves that the mass of the new SUSY particles must be around the TeV scale. At the same time, gauge coupling unification is not affected for a SUSY scale (M_{SUSY}) in the TeV range, $M_{SUSY} \sim \mathcal{O}(TeV)$. Indeed, MSSM predicts unification of the three gauge couplings at high energies. Running of the gauge couplings in the MSSM at one-loop level is described again by equations (1.18) and (1.19) where now the b coefficients have different values with: $(b_1, b_2, b_3)_{MSSM} = (33/5, 1, -3)$. In Figure 1.5 we present the evolution of the inverse gauge couplings in the MSSM. We have assume a SUSY decouple scale at $M_{SUSY} = 1$ TeV and as we observe the three gauge couplings join together

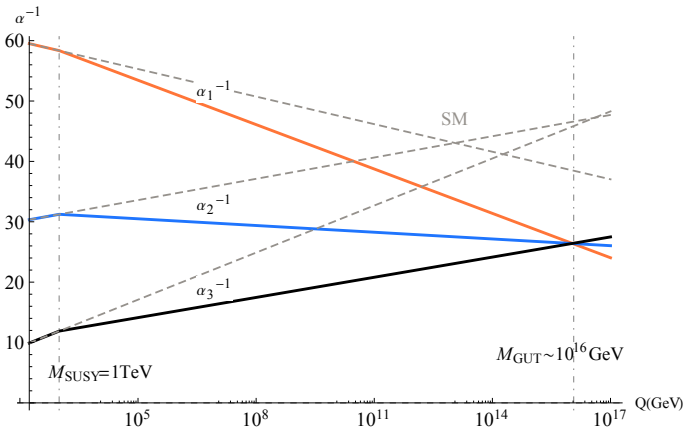

Figure 1.5: Unification of the inverse gauge couplings $\alpha_a^{-1}(Q)$ on one-loop level in the MSSM for a SUSY scale at the TeV range, $M_{SUSY} = 1$ TeV. The three gauge couplings unify at an energy scale with $M_{GUT} \sim 10^{16}$ GeV. For comparison we have also include the evolution of the gauge couplings in the case of the SM (dashed lines). As input scale we took $Q_0 = m_{top} \simeq 173.4$ GeV and the values of the gauge couplings at this scale was received from [26].

at a unification scale with $M_{GUT} \simeq 2 \times 10^{16}$ GeV. This is an astonishing result which supports the idea of a supersymmetric grand unified theory [67], [68].

The superpotential should be invariant under SUSY and gauge transformations and for a chiral superfield Φ has the general form

$$W = \frac{1}{2} M_{ij} \Phi_i \Phi_j + \frac{1}{3!} y_{ijk} \Phi_i \Phi_j \Phi_k \tag{1.30}$$

where M^{ij} is the mass matrix and y_{ijk} is the Yukawa coupling. The tree-level scalar potential is a sum of the so-called F-terms and D-terms,

$$V = F^{*i} F_i + \frac{1}{2} \sum_a D^a D_a \tag{1.31}$$

where $F_i = \frac{\partial W}{\partial \Phi_i}$ and $D^a = \sum_i g^a \Phi_i^\dagger T^a \Phi_i$ with T^a and g^a being the generators and coupling constants of the corresponding gauge groups.

In the case of MSSM the superpotential is:

$$W_{MSSM} = y_u^{ij} u_i^c Q_j \cdot H_u - y_d^{ij} d_i^c Q_j \cdot H_d - y_e^{ij} e_i^c L_j \cdot H_d + \mu H_u \cdot H_d \tag{1.32}$$

where the parameters y_u, y_d and y_e are Yukawa couplings of up type quarks, down type quarks and charged leptons respectively. The VEVs v_u and v_d of the Higgs doublets H_u and H_d provide masses for the up and down quarks/charged leptons respectively. Between the quark and lepton masses m_u, m_d, m_e and the yukawa couplings y_u, y_d, y_e we have the following relations:

$$y_u = \frac{m_u \sqrt{2}}{v \sin\beta}, \quad y_d = \frac{m_d \sqrt{2}}{v \cos\beta}, \quad y_e = \frac{m_e \sqrt{2}}{v \cos\beta} \tag{1.33}$$

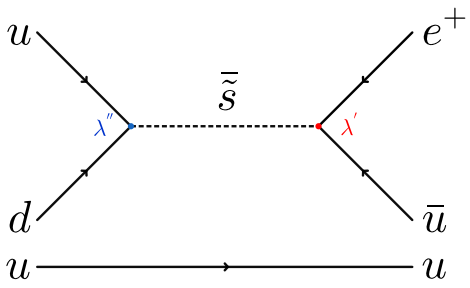

Figure 1.6: Proton decay ($p \to \pi^0 + e^+$) via λ'_{112} and λ''_{112} RPV operators.

where $v = \sqrt{v_u^2 + v_d^2}$ and $0 < \beta < \pi/2$ with $\tan\beta = v_u/v_d$. From these relations it is clear that the predictions of the model strongly depends on the value of the β angle.

The last term in superpotential (1.32) describes the mixing between the Higgs superfields and is commonly known as the *μ-term*. The parameter μ has dimensions of mass and for phenomenological reasons its value has to be of the order of the SUSY breaking scale. The question of how a SUSY mass parameter μ can assume a value of the order of M_{SUSY} is known as the *μ-problem* [69]. The term can be generated in a dynamical way by extending the MSSM spectrum with a singlet superfield[4] S in what is known as the *Next-to-Minimal Supersymmetric Standard Model* (NMSSM) [70] (see also [71]). In this model when the new scalar S receives a VEV $\langle S\rangle$, the μ-term is generated via the invariant trilinear coupling $\lambda S H_u H_d$. Since $\mu = \lambda\langle S\rangle$, by tuning the values of λ and $\langle S\rangle$ one can end up with a μ term at the desired energy scale.

1.3.2 R-parity violation

In the most popular version of MSSM described by the superpotential in (1.32), a new symmetry called R-parity [72] is assumed to be an exact symmetry. This symmetry is defined as

$$P_R = (-1)^{3(B-L)+2s} \tag{1.34}$$

where L and B are the lepton and baryon numbers and s is the spin quantum number. An alternative to P_R but with the same physical results, is known as *Matter parity*. Under the matter parity, MSSM superfields have the following assignments: $P_M = -1$ for matter superfields while $P_M = +1$ for the Higgs superfields H_u and H_d. In other words matter parity discriminates the fermion superfields (matter) from the Higgs superfields. According to matter parity, the product of P_M in a possible candidate term in the superpotential must be equal to $+1$. Thus forbids all terms with an odd power of matter fields. This has the implication that the lightest superpartner is absolutely stable and can be identified as the dark matter of the universe. This, along with other attractive properties of MSSM prompted most of the LHC searches for SUSY to focus on R-parity conserving version of the MSSM. However, in the absence of R-parity (or

[4] From now on we drop the "hat" superfield notation

any other 'protecting' symmetry) the following gauge invariant terms are exist

$$W_{RPV} = \underbrace{\mu_i H_u L_i + \frac{1}{2}\lambda_{ijk} L_i L_j e^c_k + \lambda'_{ijk} L_i Q_j d^c_k}_{\text{L-violation}} + \overbrace{\frac{1}{2}\lambda''_{ijk} u^c_i d^c_j d^c_k}^{\text{B-violation}}, \tag{1.35}$$

where the last term leads to baryon number violation while all the other terms do not respect lepton number conservation. In total, (4.2) adds 48 new couplings in the theory. As a result, the presence of R-parity violation (RPV) terms in the superpotential introduces a whole new sector of interactions in the model [73], [74]. Due to these new interactions, the lightest supersymmetric particle its no longer stable and as a result loses its precious title of *dark matter candidate*[5]. In addition, the simultaneous presence of RPV terms in the superpotential can lead to dangerous nucleon decay phenomena, like the one presented in Figure 1.6. The graph describes the decay of a proton (p) into a pion (π^0) and a positron (e^+) due to the presence of λ'_{112} and λ''_{112} RPV terms. Taking into account bounds of the proton lifetime[6] and the fact that, $\Gamma(p \to \pi^0 e^+) \sim |\lambda'_{112}\lambda''_{112}|^2 \frac{m^5_{proton}}{\tilde{m}^4_{\tilde{s}}}$, we can estimate that: $|\lambda'_{112}\lambda''_{112}| < 5 \times 10^{-27} \left(\frac{\tilde{m}_{\tilde{s}}}{1TeV}\right)^2$. This is a very strict bound suggesting that at least one of the RPV couplings is extremely small. As a result, partial conversation of R-parity (only baryon number conversation or only lepton number conversation) keeps the proton stable and at the same time allow for RPV terms in the superpotential [77].

1.4 Grand Unified Theories

We have already discussed some of the reasons why the SM is not the ultimate theory of nature. The problem of charge quantization in the SM strongly suggests that $\mathcal{G}_{SM}$ must be a subgroup of a larger gauge symmetry. Another problem of the SM is the large number of free parameters $\sim \mathcal{O}(20)$. If the SM is the low energy descent of a larger unified theory then certain relations between these parameters (for example relations between the fermion masses) can reduce this arbitrariness. In addition the explanation of the tiny but non-zero neutrino masses via the seesaw-mechanism involves heavy particles and provides some hint of high scale physics.

Historically, the first attempt for a unified theory was the *Pati-Salam model* [78] with gauge group $SU(4)_C \times SU(2)_L \times SU(2)_R$. This model has well-known attractive features (see for example the recent review [79]) and has been succesfully rederived from superstring and D-brane frameworks [80]-[84]. The Pati-Salam model unifies the fermion content of the SM in an elegant way and explains charge quantisation. However, the gauge group of the model is not simple (it is the direct product of three gauge factors) and thus it does not predict gauge coupling unification.

A first attempt to unify all the SM interactions in a single group was done by Georgi and Glashow [85] with the smallest gauge group which can embed the $\mathcal{G}_{SM}$, the Lie group $SU(5)$. The SM fermion content fits nicely in $SU(5)$ representations and the SM charges arise naturally.

[5] In this case, there is a viable escape in the form of the gravitino [75].

[6] The latest super-Kamiokande results sets the following limit on the lifetime of the proton: $\tau(p \to \pi^0 e^+) > 1.6 \times 10^{34}$ years [76].

Despite its elegance, the model in its minimal non-supersymmetric version does not lead to unification of the gauge couplings, returns inappropriate relations between the fermion masses at the GUT scale and predicts unacceptably fast proton decay effects. Some of these problems are solved with the inclusion of SUSY to the model. However, in both cases the minimal $SU(5)$ does not include RH-neutrinos in its standard fermion representations. One of the most common GUT groups which unifies all the fermions including RH-neutrinos is the $SO(10)$ group. The $SO(10)$ contains the Pati-Salam as well as $SU(5) \times U(1)$ as a maximal subgroups. Similarly, $SO(10) \times U(1)$ is a subgroup of the exceptional group E_6.

Next, we review the basic features of $SU(5)$, $SO(10)$ and E_6 GUTs. Since SUSY predicts unification of gauge couplings at a certain grand unified scale in the vicinity of the Planck scale, we will mostly concentrate on the SUSY version of these models.

1.4.1 SU(5) theory

We consider first the GUT gauge group $SU(5)$ which is rank 4, as the $\mathcal{G}_{SM}$. Any $SU(N)$ group has (N^2-1)-generators and as a result $SU(5)$ has 24 gauge bosons which transform under the maximal subgroup $SU(3) \times SU(2) \times U(1)$ as:

$$\mathbf{24} \longrightarrow \overbrace{(1,1)_0 + (8,1)_0 + (1,3)_0}^{\text{SM gauge sector}} + \underbrace{(3,2)_{-5/6} + (\bar{3},2)_{+5/6}}_{\text{New gauge bosons}}. \tag{1.36}$$

Twelve of them are identified with the SM gauge bosons while the remaining states, $((3,2)_{-5/6} + (\bar{3},2)_{+5/6})$, are new, usually named X and Y gauge bosons. Spontaneous breaking of $SU(5)$ to the $\mathcal{G}_{SM}$ can be achieved with the introduction of a Higgs field (Σ) in the **24** adjoint representation, by developing a VEV in the direction of the hypercharge generator.

Each family of lepton and quark MSSM superfields fits nicely in the $\bar{\mathbf{5}}$ and **10** multiplet of the $SU(5)$ as:

$$\bar{\mathbf{5}} \xrightarrow{SM} d^c(\bar{3},1)_{\frac{1}{3}} + L(1,2)_{-\frac{1}{2}} \tag{1.37}$$

$$\mathbf{10} \xrightarrow{SM} Q(3,2)_{\frac{1}{6}} + u^c(\bar{3},1)_{-\frac{2}{3}} + e^c(1,1)_1. \tag{1.38}$$

Regarding the Higgs sector, the H_u and H_d superfields of the MSSM descend from a pair of **5** and $\bar{\mathbf{5}}$ respectively:

$$\mathbf{5}_H \to (H_u, D), \quad \bar{\mathbf{5}}_H \to (H_d, D^c), \tag{1.39}$$

where D and D^c constitute a vector pair of exotic color triplets. The Higgs superfields are introduced to break the EW symmetry and give masses to the fermions of the model via Yukawa interaction terms, therefore we must keep these states at low energies. The invariant $SU(5)$ Yukawa terms are the following:

$$\text{up type:} \quad Y_u \mathbf{10}_i \times \mathbf{10}_j \times \mathbf{5}_H \longrightarrow Y_u Q_i u_j^c H_u, \tag{1.40}$$

$$\text{down type/charged leptons:} \quad Y_{d/e} \mathbf{10}_i \times \bar{\mathbf{5}}_j \times \bar{\mathbf{5}}_H \longrightarrow Y_{d/e}(Q_i d_j^c H_d + L_j e_i^c H_d), \tag{1.41}$$

where as we can see the down type and charged lepton Yukawa couplings arise from a common $SU(5)$ invariant operator. This implies the following relation for the Yukawa matrices:

$$\mathbf{Y}_d = \mathbf{Y}_e^T \tag{1.42}$$

meaning that the Yukawa couplings of the down type quarks and charged leptons are equal, at least at the GUT scale. Some of the predictions follow from this relation are good, especially for the heaviest generations, $Y_b = Y_\tau$ known as b-τ unification. However this same relation predicts that $m_s = m_\mu$ and $m_d = m_e$ at the GUT scale. These GUT conditions fail to reproduce the correct masses for the lightest generations at low energies

This can be corrected e.g. by adding high order ($1/M_{Pl}$) terms. An alternative solution to the problem has been suggested by Georgi and Jarlskog [86]. They pointed out that suitable relations between the Yukawa couplings at the GUT scale can be produced by extending the Higgs sector with a $\bar{\mathbf{45}}_H$ Higgs field. Then the $SU(5)$ invariant operator $\sim \mathbf{10} \times \bar{\mathbf{5}} \times (\bar{\mathbf{45}}_H)$ modifies the Yukawa matrices and leads to the well-known *Georgi-Jarlskog mass relations*

$$m_\tau = m_b \quad , \quad m_\mu = 3m_s \quad , \quad m_e = \frac{1}{3} m_d \tag{1.43}$$

at the GUT scale. Applying RG analysis it turns out that these relations are in a better agreement with the low-energy observations.

The $SU(5)$ gauge group provides a nice framework for theorists to study unification of the SM interactions. However, in its minimal (SUSY or not) form it suffers from a variety of technical issues, like the wrong GUT Yukawa relations described above. Since we put leptons and quarks in the same irreducible representation of the GUT gauge group, there must be an interaction between them which can lead to undesired interaction phenomena. As a consequence the most important problem in the construction of GUT theories is the prediction of rapid proton decay [87], [88].

In non-SUSY $SU(5)$ models the main contribution to proton decay comes from effective dimension-6 operators generated by the exchange of the extra $SU(5)$ gauge bosons X and Y. Suppression of these effects implies that the X and Y gauge bosons must be heavy with masses $\gtrsim 10^{16}$ GeV. This is intriguingly close to the predicted unification scale predicted from SUSY models. However, even with the fusion of SUSY and GUTS, fast proton decay is still there. The minimal SUSY $SU(5)$ model leads to quite fast proton decay through dimension-5 operators generated by the exotic colored triplet Higgs supermultiplets D and D^c [89, 90]. Suppresion of the effect requires these Higgs triplets to be heavy, with masses of order the GUT scale [91], [92], [93]. Since the EW Higgs doublets and the extra colored triplets descend from common $\mathbf{5}_H$ and $\bar{\mathbf{5}}_H$ representations the requirement for heavy color triplets introduces another technical problem in the theory. The question of how we keep the Higgs doublets light while the triplets are heavy, known as the *doublet-triplet splitting problem.*

Another problem of the minimal $SU(5)$ models is the absence of RH neutrinos. One has to add $SU(5)$ singlets $\mathbf{1} \equiv \nu^c$ or other suitable $SU(5)$ representations separately in order to explain the small neutrino masses (see for example [94], [95]). A single, rank-5 group which unifies all

the fermions (including RH-neutrinos) under a common representation and contains $SU(5)$ as well Pati-Salam as a subgroup, is the special orthogonal group $SO(10)$ to which we now turn.

1.4.2 SO(10) unification

In particle physics, $SO(10)$ is a popular GUT group candidate [99]. Special orthogonal groups $SO(N)$ have $N(N-1)/2$ generators and as a result $SO(10)$ GUT predicts 45 gauge bosons which transform as the **45** adjoint representation. There are two maximal subgroups of $SO(10)$. One is the Pati-Salam gauge group $\mathcal{G}_{PS}$, while the other one corresponds to the breaking pattern $SO(10) \to SU(5) \times U(1)_\chi$. Regarding the latter, symmetry breaking of $SU(5) \times U(1)_\chi$ to the $\mathcal{G}_{SM}$ can happen in two different ways. One option consists in breaking $SU(5)$ directly into $\mathcal{G}_{SM}$ as in the case of the minimal $SU(5)$ GUT. Alternatively, one can indentify the hypercharge of the SM as a linear combination of a diagonal generator of $SU(5)$ and the generator of the $U(1)_\chi$. This second option is known as the *flipped* $SU(5)$ model [96],[97], [98] which has some very interesting properties but we will not discussed it here. In order to understand the basic properties of the $SO(10)$ model we will follow the decomposition $SO(10) \supset SU(5)$.

A complete family of SM fermions fits perfectly into a single **16** spinorial representation of $SO(10)$. Indeed, 16-plet has the following decomposition under $SU(5)$:

$$\mathbf{16} \xrightarrow{SU(5)} \mathbf{10} + \bar{\mathbf{5}} + \mathbf{1}, \tag{1.44}$$

where the $\bar{\mathbf{5}}$ and **10** multiplets accommodate the full set of one generation of quarks and leptons and in addition one has the singlet field which can accommodate RH-neutrinos.

In minimal $SO(10)$ constructions, the two MSSM Higgs multiplets descend from the fundamental representation of $SO(10)$,

$$\mathbf{10}_H \xrightarrow{SU(5)} \mathbf{5}_H + \bar{\mathbf{5}}_H \tag{1.45}$$

and as we know from $SU(5)$ theory this also includes an extra pair of color triplet fields. We note that in contrast with the SU(5) models where the down Higgs H_d and L descend from the same $SU(5)$ representation, $SO(10)$ distinguishes the Higgs from matter representations.

The product of two spinor **16** representations produces the **10**, while the product $\mathbf{10} \times \mathbf{10}$ contains the singlet. That way, all the Yukawa interactions descent from the following invariant operator:

$$Y_{ij}\mathbf{16}_i \times \mathbf{16}_j \times \mathbf{10}_H \to Y_{ij}(Q_i u_j^c H_u + Q_i d_j^c H_d + L_i e_j^c H_d + L_i \nu_j^c H_u) \tag{1.46}$$

where the last term is a neutrino Dirac operator. It is clear from eq. (1.46) that SO(10) predicts unification of all Yukawa couplings at the GUT scale:

$$Y_u = Y_d = Y_e = Y_\nu. \tag{1.47}$$

Under specific conditions *Yukawa unification* can be supported for the heaviest generations (t-b-τ) in $SO(10)$ models [100]-[104]. On the other hand, this result has to be modified for the

lightest generations as in the case of the minimal $SU(5)$ model. An alternative way to deal with these flavour puzzles is to combine the GUT gauge group with a discrete flavour symmetry [105].

1.4.3 E_6 models

The next largest anomaly-free group in which we can embed $SO(10)$ is the exceptional Lie group E_6 [106], [107], [108]. Most of the appeal of E_6 models arises from the fact that String theory compactifications lead to the gauge group E_6 or its subgroups in the observable sector [109], [110]. In addition, E_6 is one of only five exceptional groups, in contrast with the infinity class of $SU(N)$ and $SO(N)$ groups. An easy way to describe the MSSM embedding into E_6 is by considering the breaking pattern $E6 \supset SU(5)$ where two abelian factors appear:

$$E_6 \to SO(10) \times U(1)_\psi \to SU(5) \times U(1)_\psi \times U(1)_\chi. \tag{1.48}$$

The SM fermions within each generation can transform under the **27** irreducible representation of E_6 which decomposes as follows under the breaking to $SO(10) \times U(1)_\psi$:

$$\mathbf{27} \longrightarrow \mathbf{16}_1 + \mathbf{10}_{-2} + \mathbf{1}_4, \tag{1.49}$$

where the index denotes the $U(1)_\psi$ charges. Further breaking of the $SO(10)$ according to (1.48) leads to the following decomposition:

$$\mathbf{27} \longrightarrow \overbrace{\mathbf{10}_{(1,-1)} + \bar{\mathbf{5}}_{(1,3)} + \mathbf{1}_{(1,-5)}}^{\mathbf{16}_1} + \underbrace{\mathbf{5}_{(-2,2)} + \bar{\mathbf{5}}_{(-2,-2)}}_{\mathbf{10}_{-2}} + \mathbf{1}_{(4,0)}, \tag{1.50}$$

where the two indices refer to the (un-normalised) charges (Q_ψ, Q_χ) under the two abelian factors $U(1)_\psi \times U(1)_\chi$, respectively.

The fermion families are accommodated in three 16-plets of $SO(10)$. The ordinary quark triplets, the RH electron and lepton doublets comprise the $10_{(1,-1)}$ and $\bar{5}_{(1,3)}$ of $SU(5)$, and in the standard description, the singlet $1_{(1,-5)}$ is identified with the RH neutrino. The pair $5_{(-2,2)} + \bar{5}_{(-2,-2)}$ consists of color triplet exotic pairs along with a pair of MSSM doublets which can be the either the Higgs doublets of the MSSM or exotic lepton doublets. In order to restore gauge coupling unification, an extra pair of exotic Higgs-like doublets must be introduced to the spectrum[7]. There are also $SO(10)$ singlets with charges $(4, 0)$ which can be used for a dynamical realization of a TeV scale μ-term. Furthermore, there are also additional E_6 multiplets, except of the fundamental **27**($\overline{\mathbf{27}}$) representations, that can be used to extend the matter or symmetry breaking sector of the theory, like the **78** adjoint representation or the two index symmetric representation $\mathbf{351'}$-$\overline{\mathbf{351'}}$ [112]. In the case that we discuss here, Yukawa couplings descent from the following E_6 invariant operator:

$$\mathbf{27} \times \mathbf{27} \times \mathbf{27}.$$

[7] It is well-known that perturbative gauge coupling unification is maintained when we extend the MSSM spectrum with vectorlike pairs that transform as complete SU(5) multiplets [111]

Of course, the same operator contains the necessary Dirac neutrino term as well as mass terms for the extra vectorlike pairs.

As we see so far, a special characteristic of the E_6 models is that they contain plethora of new states, like extra scalar singlets and exotic vectorlike pairs. All these new states have huge impact on the low energy phenomenology of the model. The precise low energy spectrum of the E_6 models strongly depend on the breaking path down to the SM gauge group that we choose and consequently on the symmetry breaking sector of the model. Among the many low energy descendants of the E_6 gauge group, $U(1)$ extensions of the MSSM (UMSSM) have very interesting consequences both at the theoretical and low energy phenomenological level [113]. Noting that $SU(5)$ in (1.48) contains the SM gauge group and the breaking of E_6 directly into $\mathcal{G}_{\mathcal{SM}} + U(1)_\chi + U(1)_\psi$ is a possible scenario [114], [115]. The extra $U(1)$ group of the UMSSM now is a linear combination of $U(1)_\chi$ and $U(1)_\psi$ parametrised by a mixing angle ϕ as

$$U(1)' = U(1)_\chi \cos\phi + U(1)_\psi \sin\phi \tag{1.51}$$

with $\phi \in [0, \frac{\pi}{2}]$. Consequently, the $U(1)'$ symmetry will be associated with a heavy Z' gauge boson that could have profound implications for particle physics and cosmology [116].

We can follow the same logic by which $\mathcal{G}_{SM}$ is a maximal subgroup of $SU(5)$, which extended with a $U(1)$ factor turns into a maximal subgroup of $SO(10)$ and so on. That way we end up to the largest exceptional group:

$$E_8 \supset E_7 \supset E_6 \supset SO(10) \supset SU(5) \supset \mathcal{G}_{SM}$$

From the group theory point of view, E_8 acts as a "parent" symmetry for all the GUT groups that we have discussed so far. However, due to the complicated structure of these large exceptional groups, it is not easy to construct a realistic 4 dimensional model at the field theory level. This is necessarily outside the 4d GUT framework and one has to look into more generic structures. Indeed, the E_8 group plays a special role in superstring compactifications, especially in heterotic string theories ($E_8 \times E_8$) and more recently in the non-perturbative version of IIB superstring theory, known as F-theory.

1.5 GUTs from F-theory

The quest for a unified theory of elementary particles has led to numerous extensions of the successful SM of electroweak and strong interactions. Supersymmetric GUTs described in the previous section provide some nice features, like charge quantization, gauge coupling unification, RH neutrino candidates and more. However, due to the presence of extra gauge bosons and exotic states, these models usually suffer from proton decay effects and other technicalities like the doublet-triplet splitting problem. These problems are in sharp conflict with the requirement for gauge coupling unification. A way to deal with these issues is realised by extending the GUT group with a suitable extra symmetry. This can be for example, a continues $U(1)$ factor (like in the case of the flipped $SU(5)$) or a discrete symmetry. Many GUT models accompanied

by continuous as well as discrete symmetries have been proposed as realistic extensions of the MSSM. Since there are plethora of choices on the construction of an extended GUT model, we need a consistent and motivated guide when constructing such models. String theories have a rich group structure embodying both continuous as well as discrete symmetries at the same time.

During the last decades, string theory has been proven to be a powerful approach to describing gravity, which also enforces restrictions on the particle physics theory. In addition GUTs may be embedded in string constructions, while supersymmetry is also incorporated in a consistent way. Although string theory does not provide a unique prediction for the precise GUT symmetry and matter content, it enables a classification of possible solutions in a well defined and organized way. Moreover, it provides computational tools for various parameters such as the Yukawa couplings and potentials which would otherwise be left unspecified in more arbitrary extensions of the SM.

1.5.1 F-theory basics

F-theory [117], was discovered about two decades ago during the *era* of the *second string revolution*. Technically, provides a more accessible description of the non-perturbative aspects originating from the type II-B superstring theory. In what follows we present some of the generic features of F-theory following mainly the works of [118, 119] and [120, 121]. See also the reviews [122]-[128].

F-theory is a 12-dimensional theory which arises from the *geometrization* of the type II-B string theory. So we discuss some properties of type II-B superstring theory first.

The effective theory is described by the type II-B supergravity whose bosonic field spectrum splits in two sectors. From the nature of the stringy origin of these two sectors, are referred to as Ramond-Ramond (R-R fields) and Neveu-Schwarz (NS-NS fields) [129]:

$$NS-NS: \quad g_{MN} \quad \text{(metric)}, \quad \phi \quad \text{(dilaton)}, \quad B_2 \quad \text{(a 2-form potential)}$$

$$R-R: \quad C_p \quad \text{with} \quad p=0,2,4$$

where the 2-form potential on the NS-NS sector gives rise to the field-strength, $H_3 = dB_2$. Similar, from the exterior derivatives of the p-form potentials, C_p, we will have also the corresponding field strengths $F_{p+1} = dC_p$. In particular, the 5-form F_5 has to respect the self-duality condition $F_5 = *F_5$ where $*$ denotes the Hodge star operation. Furthermore, the fields C_0 and ϕ are combined together into the following complex modulus

$$\tau = C_0 + ie^{-\phi} \equiv C_0 + \frac{i}{g_s} \tag{1.52}$$

which is known as the complex *axion-dilaton* and has a central role on the definition of F-theory. In addition, it is also useful to introduce the following field combinations

$$G_3 = F_3 - \tau H_3 \tag{1.53}$$
$$\tilde{F}_5 = F_5 - \frac{1}{2} G_2 \wedge H_3 - \frac{1}{2} B_2 \wedge F_3 \tag{1.54}$$

and by definition the 5-form $\tilde{F}_5$ has also to fulfill the self-duality condition. We are now well equipped to write down the bosonic part of the type II-B supergravity action [122], [129]:

$$\begin{aligned} S_{IIB} \propto & \int d^{10}x\sqrt{-g}\, R \\ & - \frac{1}{2}\int \frac{1}{(\mathrm{Im}\tau)^2} d\tau \wedge *d\bar{\tau} + \frac{1}{\mathrm{Im}\tau} G_3 \wedge *\overline{G}_3 + \frac{1}{2}\tilde{F}_5 \wedge *\tilde{F}_5 + C_4 \wedge H_3 \wedge F_3 \end{aligned} \tag{1.55}$$

where we set the string length l_s, which is related with slope parameter α' equal to unity, $l_s = 2\pi\sqrt{\alpha'} \equiv 1$. The type II-B supergravity action is invariant under a SL(2,R) symmetry group, which is reduced to $SL(2,Z)$ in the quantum level [130]. Indeed, the action is invariant under the following $SL(2,Z)$ transformations:

$$\tau \to \frac{a\tau + b}{c\tau + d} \quad , \quad \begin{pmatrix} H_3 \\ F_3 \end{pmatrix} \to \mathcal{M} \begin{pmatrix} H_3 \\ F_3 \end{pmatrix} \quad \text{with} \quad \mathcal{M} = \begin{pmatrix} d & c \\ b & a \end{pmatrix} \in SL(2,Z) \tag{1.56}$$
$$\tilde{F}_5 \to \tilde{F}_5 \quad , \quad g_{MN} \to g_{MN}. \tag{1.57}$$

In the sense of mathematics, the transformation (1.56) of the axion-dilaton field τ under an $SL(2,Z)$ duality transformation is identical to the behaviour of the complex structure of an elliptic curve, say E_τ, under a modular transformation. The idea now is to use the value of the string coupling-related axion-dilaton τ to describe the shape of a torus [117]. An interpretation like this, converts the 10 dimensional space-time of type IIB theory into a 12 dimensional elliptically fibered total space which leads in what is known as F-theory.

In F-theory τ is interpreted as the complex structure modulus of an elliptic curve generating a complex fourfold which constitutes the elliptic fibration over the Calabi-Yau (CY) threefold. Since the fibration relies on the $\tau = C_0 + \imath/g_s$, this means that the gauge coupling is not a constant and the resulting compactification is not perturbative. In addition, for N = 1 supersymmetry to be conserved, the elliptic fibration has to be Calabi-Yau. Hence, according to the above discussion, the total space of F-theory is defined on a background $R^{3,1} \times \mathcal{X}$ with $R^{3,1}$ our usual space-time and $\mathcal{X}$ an elliptically fibered Calabi-Yau fourfold with a section over a complex three-fold base B_3. This graphically is illustrated in Figure 1.7.

Consider now three complex coordinates (x, y, z) corresponding to the three spatial dimensions of the base space B_3. Then the elliptic fibration is described mathematically by the *Weierstraß equation*,

$$y^2 = x^3 + f(z)x + g(z) \tag{1.58}$$

where $f(z)$ and $g(z)$ are eighth and twelfth degree polynomials in z. For each point of the base B_3, the equation describes a torus labeled by the coordinate z.

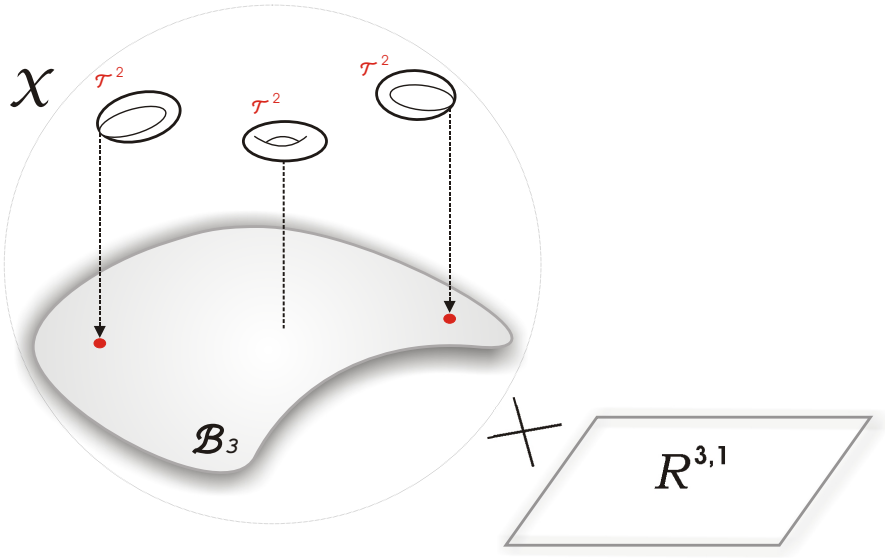

Figure 1.7: Schematic representation of the total space ($R^{3,1} \times \mathcal{X}$) in F-theory. The top/left part of the figure represents a Calabi-Yau foufold ($\mathcal{X}$) constituting an elliptic fibration over a threefold base, B_3. Every point in the base is represented with a 2-torus (fibre), as shown. The modular parameter of the torus at each point is related to the axion-dilaton profile, $\tau = C_0 + i/g_s$.

There are two important quantities characterising the elliptic fibration : the discriminant Δ of Equation (1.58) and the *j-invariant* modular function.

The discriminant classifies the singularities of the elliptic curve and is given by the formula,

$$\Delta(z) = 4\, f(z)^3 + 27\, g(z)^2\,. \tag{1.59}$$

For $\Delta \neq 0$, the curve described by (1.58) is non-singular. On the other hand, at the zeroes of the discriminant ($\Delta = 0$) the elliptic curve becomes singular with one cycle shrinking to zero size and the fiber degenerates. There are 24-roots z_i of the discriminant which corresponds to 24 7-branes located at z_i with $i = 1, ..., 24$. We can see this by study the j-invariant function.

The $SL(2, Z)$ modular invariant function $j(\tau)$ relates the modular of the torus (τ) with the discriminant,

$$j(\tau) = \frac{4(24f)^3}{\Delta} = \frac{4(24f)^3}{4f^3 + 27g^2} \tag{1.60}$$

where $j(\tau) = e^{-2\pi i\tau} + 744 + \mathcal{O}(e^{2\pi i\tau})$.

In the vicinity of a singular point-z_i, using (1.60) one can write [131]

$$j(\tau(z)) \sim \frac{1}{z - z_i} \longrightarrow \tau(z) \approx \frac{1}{2\pi i} \ln(z - z_i) \tag{1.61}$$

up to $SL(2, Z)$ transformations. Further, since $\ln(z - z_i) = \ln|z - z_i| + i\,\theta$, as one encircle the position z_i, τ undergoes a monodromy $\tau \to \tau + 1$, or in terms of C_0

$$C_0 \to C_0 + 1, \longrightarrow \oint_{z_i} F_1 = \oint_{z_i} dC_0 = 1$$

Since C_0 is sensitive on the dynamics of the brane, this implies the existence of a 7-brane at z_i, while totally there are 24 such branes in the compact transverse space.

In summary, the idea of F-theory states that the physics of Type II-B compacitifications with 7-branes on a complex threefold B_3 is encoded in the geometry of a fourfold $\mathcal{X}$ which is elliptically fibered over B_3. The elliptic fiber itself is not part of the physical spacetime but serves as a *tracking device* that accounts for the variation of the axion-dilaton τ. As seen from the solution (1.61), at the location of 7-branes the axion-dilaton field diverges. If the complex structure of an elliptic curve diverges, this indicates that a one-cycle of the torus is pinched and consequently the elliptic curve is degenerate. Thus, 7-branes appear at points in the base B_3 at which the fibration becomes singular, corresponding to 4-cycles S wrapped by the 7-brane.

It is well known from constructions with intersecting D-branes that gauge symmetries emerge when more than one D-branes coincide. While a single D-brane is associated to a $U(1)$ symmetry, when we consider the possibility of having N D-branes of the same kind on top of each other (a stack of branes), then this gauge symmetry will be $U(N)$. In a similar logic, in F-theory when 7 branes coincide at a certain point, there is a gauge symmetry associated to these branes. Since at this point there is a singularity of the elliptic fibration, we expect that there is a connection between elliptic singularities and gauge symmetries. Indeed, a systematic analysis of these singularities has started long time ago with the work of Kodaira [133].

1.5.2 Tate's Algorithm and Gauge Symmetries

According to the discussion above, in F-theory the gauge symmetry is connected with the singularities of the internal compact manifold. Thanks to Kodaira we have a systematic classification of these singularities in ADE type groups. The Kodaira classification depends on the vanishing order of the discriminant Δ and the polynomials f, g of the Weirstraß equation given in (1.58). The results can be found in many recent works [134], [135], [136],[137]. Here are summarized in Table 1.5 and as we can see the classification contains also the exceptional groups E_6, E_7 and E_8.

In the present thesis we will focus mostly in local F-theory constructions. A useful description which emphasizes the local properties of the singularities under discussion is given in terms of *Tate's algorithm* [138]. Tate's procedure is based in a local coordinate redefinition that brings the Weierstraß equation in to the following form

$$y^2 + a_1 x\, y + a_3 y = x^3 + a_2\, x^2 + a_4 x + a_6. \tag{1.62}$$

This is known as the inhomogeneous *Tate form*. The a_i's are functions of the complex coordinate z of the base B_3 and as we expected are related with the f and g polynomials of the initial Weirstrass equation. In particular, the polynomials f, g and consequently the discriminant Δ, can be expressed as functions of the a_i's. In order to see this we have to convert the Tate's equation (1.62) in to the Weirstraß form (1.58). This can be achieved by complete the square on the left hand side and the cube on the right hand side of equation (1.62) and then comparing with the Weirstraß equation. That way we find that:

ord(f)	ord(g)	ord(Δ)	fiber type	Singularity
0	0	n	I_n	A_{n-1}
≥ 1	1	2	II	none
1	≥ 2	3	III	A_1
≥ 2	2	4	IV	A_2
2	≥ 3	$n+6$	I_n^*	D_{n+4}
≥ 2	3	$n+6$	I_n^*	D_{n+4}
≥ 3	4	8	IV^*	E_6
3	≥ 5	9	III^*	E_7
≥ 4	5	10	II^*	E_8

Table 1.5: Kodaira's classification of elliptic singularities [133].

$$f = -\frac{1}{48}\left(\beta_2^2 - 24\beta_4\right) , \tag{1.63}$$

$$g = -\frac{1}{864}\left(-\beta_2^3 + 36\beta_2\beta_4 - 216\beta_6\right) , \tag{1.64}$$

and replacing f, g in (1.59), the discriminant takes the form

$$\Delta = \frac{1}{8}\left(\beta_8\beta_2^2 - 9\beta_2\beta_4\beta_6 + 8\beta_4^3 + 27\beta_6^2\right) \tag{1.65}$$

where for shorthand we made the redefinitions

$$\beta_2 = a_1^2 + 4a_2 \, , \tag{1.66}$$

$$\beta_4 = a_1 a_3 + 2a_4 \, , \tag{1.67}$$

$$\beta_6 = a_3^2 + 4a_6 \, , \tag{1.68}$$

$$\beta_8 = \frac{1}{4}(\beta_2\beta_6 - \beta_4^2) \, . \tag{1.69}$$

Now all the symmetry properties of the singularities on the elliptic fibration are encoded on the vanishing degree of the polynomials $a_i \sim b_i z^n$ and the discriminant Δ. The discriminant will factorize with each factor describing the location of a 7-brane on a divisor S in B_3. The results are presented in Table 1.6 and the various cases have been analysed in detail in [134]. Here we are interested in some specific cases, like the popular GUT groups $SU(5)$, $SO(10)$ and E_6. Since most of the work presented in this thesis deals with $SU(5)$ GUT constructions, lets discuss this case in more detail.

Let's assume that a_i receives the following forms

$$a_1 = -b_5, \, a_2 = b_4 z, \, a_3 = -b_3 z^2, \, a_4 = b_2 z^3, \, a_6 = z^5 b_0 \tag{1.70}$$

where b_k's are independent of z. This choice returns the following Tate equation

$$y^2 = x^3 + b_0 z^5 + b_2 x z^3 + b_3 y z^2 + b_4 x^2 z + b_5 x y \tag{1.71}$$

which as can be seen from Table 1.6 (9^{th} row on the Table) implies an $SU(5)$ singularity. The coefficients b_k are in general non-vanishing and can be seen as sections of line-bundles on S. Their homology classes are given by

$$[b_k] = \eta - k\, c_1 \tag{1.72}$$

where $\eta = 6c_1 - t$ with c_1 the 1^{st} Chern class of the tangent bundle to S and -t the 1^{st} Chern class of the normal bundle to S.

Substituting the relations (1.70) in to the β_k's defined in (1.66)-(1.69) , we find

$$\beta_2 = b_5^2 + 4b_4 z\,, \tag{1.73}$$
$$\beta_4 = b_3 b_5 z^2 + 2b_2 z^3\,, \tag{1.74}$$
$$\beta_6 = b_3^2 z^4 + 4b_0 z^5\,, \tag{1.75}$$
$$\beta_8 = z^5(\mathcal{R} + z(4b_0 b_4 - b_2^2)) \tag{1.76}$$

where

$$\mathcal{R} = b_3^2 b_4 - b_2 b_3 b_5 + b_0 b_5^2 \tag{1.77}$$

Further substitution of the above relations in the discriminant (1.65), returns that $\Delta \sim \frac{1}{8} z^5$ as required for an $SU(5)$ singularity described in Table 1.6.

The matter representations of the effective theory model, reside at the intersections of the 7 branes wrapping the $SU(5)$ divisor S, with other 7 branes spanning different dimensions of the internal space. In the language of F-theory these intersections are called *matter curves*, but in fact are Riemann surfaces along which symmetry is further enhanced.

We can check how the symmetry is enhanced for certain choices. For example, choosing $b_5 = 0$ we see that the discriminant becomes $\Delta \propto z^7$. Comparing with Tate's results in Table 1.6, we see that this corresponds to an $SO(10)$ singularity. Thus, a matter curve is defined along the intersection with another brane where we expect to find the **10** of $SU(5)$ in the adjoint decomposition of $SO(10)$, therefore we write

$$\Sigma_{10} = \{b_5 = 0\}\,. \tag{1.78}$$

Similar by putting $\mathcal{R} = 0$, we see that $\Delta \sim z^6$ and this translates in to an $SU(6)$ singularity. The $SU(6)$ adjoint induces the **5** of $SU(5)$, therefore we define the matter curve for the fiveplet as

$$\Sigma_5 = \{\mathcal{R} = b_3^2 b_4 - b_2 b_3 b_5 + b_0 b_5^2 = 0\}\,. \tag{1.79}$$

Further enhancements are obtained setting additional coefficients equal to zero. This time we receive triple intersections of branes which define points in the internal space where the Yukawa couplings are formed. Choosing $b_4 = b_5 = 0$, we see that $\Delta \sim z^8$ which corresponds to an E_6 symmetry enhancement. This implies the existence of the top Yukawa coupling. Similarly, the choice $b_3 = b_5 = 0$ implies an $SO(12)$ point of enhancement which is the origin of the bottom/tau Yukawa coupling. Collectively we have:

$$Y_t \to \{b_5 = b_4 = 0\},\ Y_b \to \{b_5 = b_3 = 0\}\,.$$

Type	**Group**	a_1	a_2	a_3	a_4	a_6	Δ
I_0	0	0	0	0	0	0	0
I_1	–	0	0	1	1	1	1
I_2	$SU(2)$	0	0	1	1	2	2
I_3^{ns}	–	0	0	2	2	3	3
I_3^{s}	–	0	1	1	2	3	3
I_{2n}^{ns}	$Sp(n)$	0	0	n	n	$2n$	$2n$
I_{2n}^{s}	$SU(2n)$	0	1	n	n	$2n$	$2n$
I_{2n+1}^{ns}	–	0	0	$n+1$	$n+1$	$2n+1$	$2n+1$
I_{2n+1}^{s}	$\mathbf{SU(2n+1)}$	0	1	n	$n+1$	$2n+1$	$2n+1$
II	–	1	1	1	1	1	2
III	$SU(2)$	1	1	1	1	2	3
IV^{ns}	–	1	1	1	2	2	4
IV^{s}	$SU(3)$	1	1	1	2	3	4
I_0^{*ns}	G_2	1	1	2	2	3	6
I_0^{*ss}	$SO(7)$	1	1	2	2	4	6
I_0^{*s}	$SO(8)$	1	1	2	2	4	6
I_1^{*ns}	$SO(9)$	1	1	2	3	4	7
I_1^{*s}	$SO(10)$	1	1	2	3	5	7
I_2^{*ns}	$SO(11)$	1	1	3	3	5	8
I_2^{*s}	$SO(12)$	1	1	3	3	5	8
I_{2n-3}^{*ns}	$SO(4n+1)$	1	1	n	$n+1$	$2n$	$2n+3$
I_{2n-3}^{*s}	$SO(4n+2)$	1	1	n	$n+1$	$2n+1$	$2n+3$
I_{2n-2}^{*ns}	$SO(4n+3)$	1	1	$n+1$	$n+1$	$2n+1$	$2n+4$
I_{2n-2}^{*s}	$SO(4n+4)$	1	1	$n+1$	$n+1$	$2n+1$	$2n+4$
IV^{*ns}	F_4	1	2	2	3	4	8
IV^{*s}	E_6	1	2	2	3	5	8
III^{*}	E_7	1	2	3	3	5	9
II^{*}	E_8	1	2	3	4	5	10

Table 1.6: Results from Tate's algorithm. (For a detailed description see [134, 138].) The order of vanishing of the coefficients $a_i \sim z^{n_j}$, the discriminant Δ and the corresponding gauge group. The highest singularity allowed in the elliptic fibration is the exceptional group E_8.

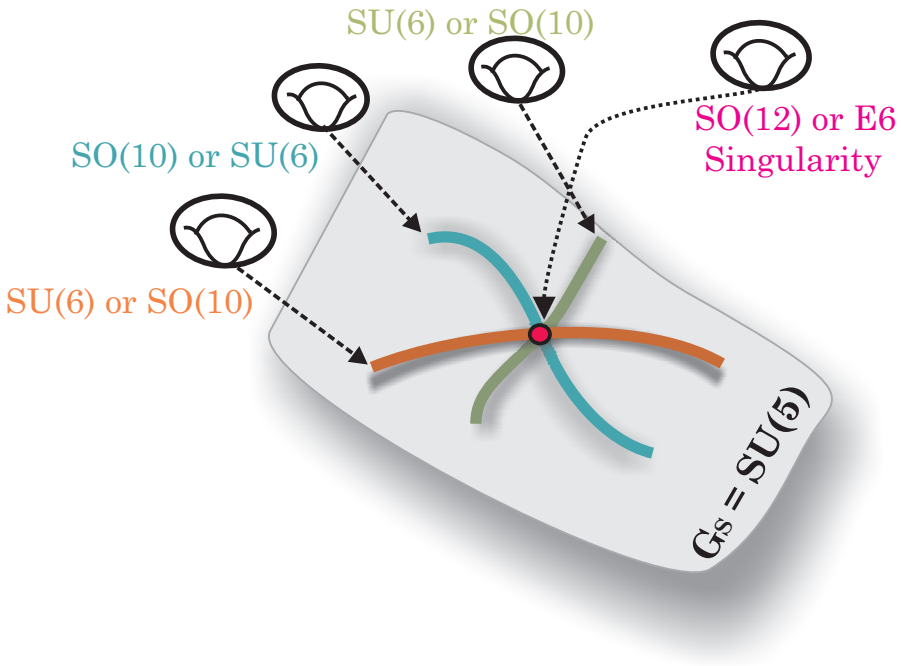

Figure 1.8: Graphic illustration of matter curves and Yukawa points in F-theory $SU(5)$ GUT. The grey region represents the $SU(5)$ GUT surface of the internal space wrapped by 7-branes. Matter curves (colored lines) are defined at the intersection with other 7-branes. A Yukawa coupling is defined at the point where three matter curves intersect. Since the singularity is further enhanced at these points we can find that the bottom/tau coupling is defined at an $SO(12)$ point while the top coupling corresponds to an E_6 symmetry enhancement.

The concepts of matter curves and Yukawa points described above graphically presented in Figure 1.8.

In the vincinity of the Yukawa points, F-theory allows for the computation of the Yukawa couplings something that have been studied extensively in the literature [139]-[154]. We will return on this interesting topic on Chapter 4 where we use known techniques in order to compute the strength of trilinear RPV couplings.

1.5.3 Semi-local approach and the Spectral cover

In the so called *semi-local* approach in F-theory we assume that a parent E_8 symmetry (which is the maximum singularity allowed in the elliptic fibration) is broken by a position dependent VEV for an adjoint Higgs field [121]. In this picture we concentrate in the vicinity of the chosen surface S associated to the GUT group G_S, while its neighborhood is described by a *spectral cover* surface which is associated to the commutant group of G_S with respect to E_8.

Of particular interest are the cases where G_S is one of the well known GUT groups E_6, $SO(10)$ or $SU(5)$. We recall that these gauge groups are embedded in E_8:

$$E_8 \supset G_S \times SU(N)_\perp \tag{1.80}$$

with $G_S = E_6, SO(10), SU(5)$ for $N = 3, 4, 5$ respectively. From these specific cases we see that

the commutant group is the $SU(N)_\perp$ factor where the subscript "$\perp$" is used here mostly to discriminate the case with $G_S = SU(5)$ from its commutant group. However sometimes we will refer to the commutant group also as the *perpendicular* group.

We focus again in the case with $G_S = SU(5)$. Matter resides in the adjoint representation of E_8 which in this case decomposes as

$$248 \to (24,1) + (1,24) + (5,10) + (\bar{5},\overline{10}) + (10,\bar{5}) + (\overline{10},5)\,. \tag{1.81}$$

The decomposition appears under $SU(5)_{GUT} \times SU(5)_\perp$ where the $SU(5)_\perp$ is the group describing the bundle in the vicinity.

The corresponding spectral cover equation is obtained by defining the homogeneous coordinates

$$z \to U,\ x \to V^2,\ y \to V^3$$

so that the $SU(5)$ singularity of the Tate equation (1.71) becomes

$$0 = b_0U^5 + b_2V^2U^3 + b_3V^3U^2 + b_4V^4U + b_5V^5$$

Then we can bring this equation to the form of a fifth degree polynomial by introduce the affine parameter $s = U/V$:

$$C_5 = \sum_{k=0}^{5} b_k s^{5-k} \ = \ b_5 + b_4 s + b_3 s^2 + b_2 s^3 + b_1 s^4 + b_0 s^5\,. \tag{1.82}$$

This is the spectral cover equation (or spectral cover polynomial) in the case of $SU(5)$. Furthermore, the roots of the spectral cover equation are identified [155] as the weights of the $SU(5)_\perp$ group. Lets denote this weights as t_i with $i = 1,2,3,4,5$, then we write

$$0 = b_5 + b_4 s + b_3 s^2 + b_2 s^3 + b_0 s^5 \propto \prod_{i=1}^{5}(s + t_i) \tag{1.83}$$

Using the above relation then it is a trivial task to express the b_k's as functions of the roots t_i. Then one can see that the coefficient b_1 is taken to be zero since it corresponds to the sum of the roots which for $SU(N)$ groups is always zero, $\sum t_i = 0$. Furthermore, it can be seen that the $s = 0$ part of the spectral cover polynomial is equal to the product of the roots: $b_5 = t_1t_2t_3t_4t_5$. We recall now from (1.78) that b_5 define the Σ_{10} matter curves where the corresponding matter multiplets are localised. Then, in the spectral cover description the tenplets of the $SU(5)$ correspond to the five zeros:

$$\mathbf{\Sigma_{10_i}}: \quad \mathcal{P}_{10} = b_5 = \prod_{i=1}^{5} t_i = 0 \to t_i = 0, \quad i = 1,2,3,4,5\,. \tag{1.84}$$

Similar, since the fiveplets of $SU(5)$ are defined by the equation (1.77) we can use the functions $b_k(t_i)$ with respect to (1.83) and translate (1.77) in terms of t_i's. Then we derive that:

$$\mathbf{\Sigma_{\bar{5}_{ij}}}: \quad \mathcal{P}_5 = \mathcal{R} = b_3^2b_4 - b_2b_3b_5 + b_0b_5^2 \propto \prod_{t_i \neq t_j} (t_i + t_j) = 0 \tag{1.85}$$

which implies that we have ten fiveplets. This can be read also from the decomposition of the E_8 adjoint as displayed in (1.81). There the 10 matter of $SU(5)_{GUT}$ is paired with the $\bar{5}_\perp$ of $SU(5)_\perp$ while the $\bar{5}$ GUT matter is paired with $10_\perp$. Furthermore, we see that the GUT singlets are paired with adjoint of $SU(5)_\perp$. Thus, in general there are 24 singlet curves $\Sigma_{1_{ij}}$ defined as:

$$\mathbf{\Sigma_{\bar{1}_{ij}}}: \quad \mathcal{P}_0 = \prod(\pm(t_i - t_j)) = 0 \tag{1.86}$$

which is actually the discriminant of the spectral polynomial.

In general, the model effectively appears with a symmetry $SU(5)_{GUT} \times U(1)^4$. Then, any possible Yukawa term should be invariant under this symmetry. Thus, writing the coupling involving the up quark masses

$$\mathcal{W} \supset 10_{t_i}\, 10_{t_j}\, 5_{-t_i-t_j}$$

would appear to involve two different generations. On the other hand, phenomenological reasons requires a rank-1 mass matrix at tree-level to account for the heavy top quark mass. A similar conclusion holds for the bottom mass term. More generally, the known hierarchical fermion mass spectrum and the heaviness of the third generation in particular, is compatible with rank-1 mass matrices at tree-level. This requires a solution where at least two of the curves are identified through some (discrete) symmetry acting on the weights t_i.

The above idea of matter curves identification is supported also by the following fact. In the spectral cover approach, the properties of the internal compact space are encoded into the coefficients b_k. Matter curves on the other hand are associated to the roots t_i which are polynomial solutions with factors combinations of b_k's, thus

$$b_k = b_k(t_i)$$

However, the inversion of these equations is not an easy task and usually lead to branchcuts. The solutions $t_j = t_j(b_i)$ are then subject to *monodromy* actions between the t_i roots.

To get a feeling of described above we present a simple example (given in [156]). Consider the simplest case of the Z_2 monodromy and suppose that two of the roots in (1.83) do not factorize. This implies that the second degree polynomial

$$a_1 + a_2 s + a_3 s^2 = 0$$

cannot be expressed in simple polynomials of the base coordinates. The roots can be written

$$s_1 = \frac{-a_2 + \sqrt{w}}{2a_3},\ s_2 = \frac{-a_2 - \sqrt{w}}{2a_3}$$

with $w = a_2^2 - 4a_1a_3$. These exhibit branchcuts and since

$$\sqrt{w} = e^{i\theta/2}\sqrt{|w|}$$

under a 2π rotation around the brane configuration $\theta \to \theta + 2\pi$ we get $\sqrt{w} \to -\sqrt{w}$ and

$$s_1 \leftrightarrow s_2$$

This means that the two branes interchange locations $s = s_1$ and $s = s_2$. This is equivalent of taking the quotient of the parent theory with a Z_2 symmetry. If this is among $t_1 \leftrightarrow t_2$ the coupling now reads

$$\mathcal{W} \supset 10_{t_1}\, 10_{t_2}\, 5_{-t_1-t_2} \to 10_{t_1}\, 10_{t_1}\, 5_{-2t_1}$$

providing a diagonal mass term since the two curves are identified.

Since the $SU(5)$ spectral cover is described by the 5-degree polynomial C_5, the various monodromy actions on the roots will be associated to the possible ways of splitting the polynomial. All the possible factorisations of the C_5 polynomial are listed bellow:

$$\begin{aligned}
C_2 \times C_1 \times C_1 \times C_1 &: (a_1 + a_2 s + a_3 s^2)(a_4 + a_5 s)(a_6 + a_7 s)(a_8 + a_9 s)\ , \\
C_2 \times C_2 \times C_1 &: (a_1 + a_2 s + a_3 s^2)(a_4 + a_5 s + a_6 s^2)(a_7 + a_8 s)\ , \\
C_3 \times C_1 \times C_1 &: (a_1 + a_2 s + a_3 s^2 + a_4 s^3)(a_5 + a_6 s)(a_7 + a_8 s)\ , \\
C_3 \times C_2 &: (a_1 + a_2 s + a_3 s^2 + a_4 s^3)(a_5 + a_6 s + a_7 s^2)\ , \\
C_4 \times C_1 &: (a_1 + a_2 s + a_3 s^2 + a_4 s^3 + a_5 s^4)(a_6 + a_7 s)\ .
\end{aligned}$$

In the simplest case the roots of C_2, C_3 and C_4 polynomials can be related with Z_n discrete monodromies. For the SU(5) case at hand, under specific circumstances (related mainly to the properties of the internal manifold and flux data) the monodromies can be described by any possible subgroup of the Weyl group S_5 of $SU(5)_\perp$. In the following Chapter we discuss some interesting cases of non-trivial monodromies.

Chapter 2

F-theory $SU(5)$ GUT with Klein monodromy action

2.1 Introduction

Over the last decades string theory GUTs have aroused considerable interest. Recent progress has been focused in F-theory effective models [157]-[177] which incorporate several constraints attributed to the topological properties of the compactified space. Indeed, in this context the gauge symmetries are associated to the singularities of the elliptically fibred compactification manifold. As such, GUT symmetries are obtained as a subgroup of E_8 and the matter content emerges from the decomposition of the E_8-adjoint representation.

In the present Chapter we will revisit a class of $SU(5)$ SUSY GUT models which arise in the semi-local approach of the spectral cover surface. The reason is that the recent developments in F-theory provide now a clearer insight and a better perspective of these constructions. For example, developments on computations of the Yukawa couplings[139]-[148] have shown that a reasonable mass hierarchy and mixing may arise even if more than one of the fermion families reside on the same matter curve. This implies that effective models left over with only a few matter curves after certain monodromy identifications could be viable and it would be worth reconsidering them. More specifically, among the many possible monodromy groups here we will study the case of the Klein Group monodromy $V_4 = Z_2 \times Z_2$ [156, 157, 158, 159, 162]. Interestingly, with this particular spectral cover, there are two main ways to implement its monodromy action, depending on whether V_4 is a *transitive* or *non-transitive* subgroup of S_4. A significant part of the present analysis will be devoted to the viability of the corresponding two kinds of effective models. Another ingredient related to the predictability of the model, is the implementation of R-parity conservation, or equivalently a Z_2 Matter Parity, which can be realised with the introduction of new geometric symmetries [143] respected from the spectral cover.

The Chapter is organised as follows. In section 2.2 we describe the action of monodromies and their importance in F-theory model building. We focus on the Klein Group monodromy and the corresponding spectral cover factorisations which is the main topic of the present chapter.

In section 2.3 we review a few well known Galois theory results and theorems which will be used in model building of the subsequent sections. In section 2.4 we discuss effective field theory models with Klein Group monodromy and implement the idea of matter parity of geometric origin. Section 2.5 deals with the particle content, the Yukawa sector and other properties and predictions of the effective model obtained from the above analysis. Finally a discussion for possible further applications of the results is given in section 2.6.

2.2 The Importance of Monodromy

In the case of F-theory $SU(5)_{GUT}$ model we study here, we have seen that any possible remnant symmetries (embedable in the E_8 singularity) must be contained in $SU(5)_\perp$ of the spectral cover. We have already explained that in the spectral cover approach we quotient the theory by the action of a finite group [156] which is expected to descend from a geometrical symmetry of the compactification. Starting from an C_5 spectral cover, the local field theory is determined by the $SU(5)$ GUT group and the Cartan subalgebra of $SU(5)_\perp$ modulo the Weyl group $W(SU(5)_\perp)$. This is the group S_5, the permutation symmetry of five elements which in the present case correspond to the Cartan weights $t_{1,\dots 5}$.

Depending on the geometry of the manifold, C_5 may split to several factors

$$C_5 = \prod_j C_j$$

In the present chapter, we will focus in two cases where the compactification geometry implies the splitting of the spectral cover to:

$$C_5 \to C_4 \times C_1 \quad \text{or} \quad C_5 \to C_2 \times C_2' \times C_1.$$

Assuming the first splitting, $C_5 \to C_4 \times C_1$, the permutation takes place between the four roots, say $t_{1,2,3,4}$ of the C_4 polynomial and the corresponding Weyl group is S_4. Notwithstanding, under specific conditions to be discussed in what follows, the monodromy action may be described by the Klein group $V_4 \in S_4$, which might be either transitive or non transitive. As we will show, the second case implies the spectral cover factorisation $C_4 \to C_2 \times C_2'$. As a result, there are two non-trivial identifications acting on the pairs (t_1, t_2) and (t_3, t_4) respectively while both are described by the Weyl group $W(SU(2)_\perp) \sim S_2$. Since $S_2 \sim Z_2$, we conclude that in the second case of spectral cover factorisation ($C_2 \times C_2' \times C_1$.) the monodromy action is the non-transitive Klein group $Z_2 \times Z_2$. Next section describes the basic features of these two spectral cover factorisations.

2.2.1 S_4 Subgroups and Monodromy Actions

The group of all permutations of four elements, S_4, has a total of $4! = 24$ elements. These include 2,3,4 and 2+2-cycles, all of which are presented in Table 2.1. These cycles form a *web* of 30 subgroups of S_4, graphically presented in Figure 2.1. These subgroups can be classified

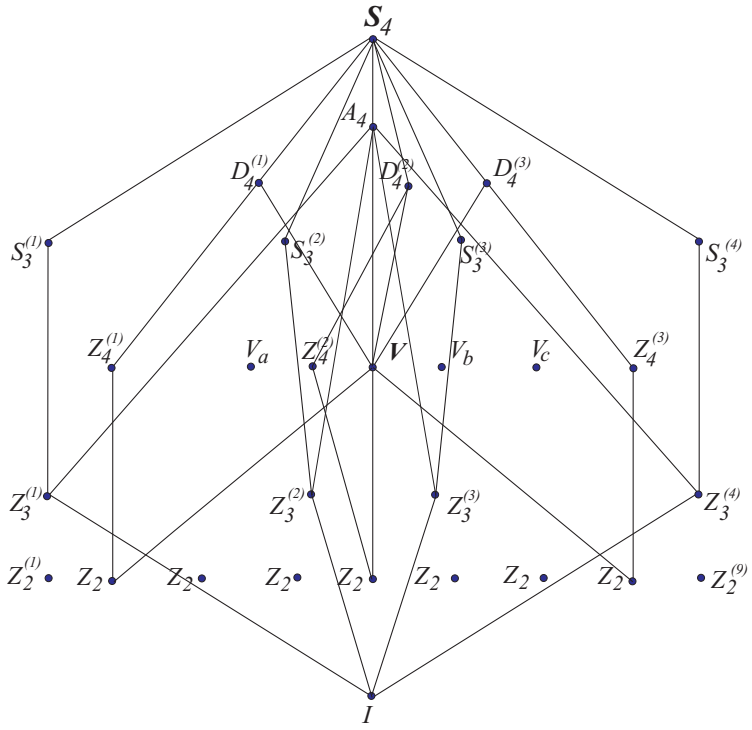

Figure 2.1: Pictorial summary of the subgroups of S_4, the group of all permutations of four elements.

	S_4 cycles	Transitive A_4	Transitive V_4
4-cycles	(1234), (1243), (1324), (1342), (1423), (1432)	No	No
3-cycles	(123), (124), (132), (134), (142), (143), (234), (243)	Yes	No
2+2-cycles	(12)(34), (13)(24), (14)(23)	Yes	Yes
2-cycles	(12), (13), (14), (23), (24), (34)	No	No
1-cycles	e	Yes	Yes

Table 2.1: A summary of the permutation cycles of S_4, categorised by cycle size and whether or not those cycles are contained within the transitive subgroups A_4 and V_4. This also shows that V_4 is necessarily a transitive subgroup of A_4, since it contains all the $2+2$-cycles of A_4 and the identity only.

in two main categories, transitive and non-transitive subgroups of S_4. For example the whole group, A_4, D_4, Z_4 and the Klein group V_4 are transitive subgroups.

In this Chapter we focus only in compactification geometries consistent with the Klein group monodromy $V_4 = Z_2 \times Z_2$. From Table 2.1 we observe that there are three non-transitive V_4 subgroups within S_4 and only one (non-trivial) transitive subgroup. This transitive Klein group is the subgroup of the A_4 subgroup of S_4. Considering Table 2.1, one can see that A_4 is the group of all even permutations of four elements and the transitive V_4 is that group excluding 3-cycles. The significance of this is that in the case of Galois theory, to be discussed in Section 2.4, the transitive subgroups A_4 and V_4 are necessarily connected with irreducible quartic polynomials, while the non-transitive V_4 subgroups of S_4 should be the Galois group of a reducible quartic polynomial.

In terms of group elements, the Klein group that is transitive in S_4 has the elements:

$$\{(1), (12)(34), (13)(24), (14)(23)\} \tag{2.1}$$

which are the 2+2-cycles shown in Table 2.1 along with the identity. On the other hand, the non-transitive Klein groups within S_4 are isomorphic to the subgroup containing the elements:

$$V_4 = \{(1), (12), (34), (12)(34)\}. \tag{2.2}$$

The distinction here is clear. In the first case (2.1) the group elements are all 2-2 cycles while in the second case (2.2) the group elements are not all within one cycle, since we have two types of cycles in the non-transitive case (2-cycles and one 2+2-cycle). These types of subgroup must lead to a factorisation of the quartic polynomial, as we shall discuss in Section 2.4. Regarding the Figure 2.1, the non-transitive Klein groups are those disconnected from the web, while the central V_4 is the transitive group.

2.2.2 Spectral cover factorisation

In this section we will discuss the two possible factorisations of the spectral surface compatible with a Klein Group monodromy, in accordance with the previous analysis. In particular, we shall be examining the implications of a monodromy action that is a subgroup of S_4 - the most general monodromy action relating four weights. In particular we shall be interested in the chain of subgroups $S_4 \to A_4 \to V_4$, which we shall treat as a problem in Galois theory.

The $C_4 \times C_1$ spectral cover

This set of monodromy actions implies that the spectral cover polynomial of Equation (1.83) should be factorise in the following way:

$$\begin{aligned} &\mathcal{C}_5 \to \mathcal{C}_4 \times C_1 : \\ &\quad (a_5 s^4 + a_4 s^3 + a_3 s^2 + a_2 s + a_1)(a_6 + a_7 s) \end{aligned} \tag{2.3}$$

which implies the 'breaking' of the $SU(5)_\perp$ to the monodromy group S_4, or one of its subgroups such as V_4, associated with the fourth degree polynomial,

$$\mathcal{C}_4 : \qquad \sum_{k=1}^{5} a_k s^{k-1} = 0 \tag{2.4}$$

along with a perpendicular $U(1)$ connected with the linear part $\mathcal{C}_1$. New and old polynomial coefficients satisfy trivial relations of the form, $b_k = b_k(a_j)$, which can be easily extracted comparing same powers of (1.82) and Equation (2.3) with respect to the parameter s. Then we have the following relations between the coefficients of the unfactorised spectral cover and the a_j coefficients:

$$\begin{aligned} b_0 &= a_5 a_7 \\ b_1 &= a_5 a_6 + a_4 a_7 \\ b_2 &= a_4 a_6 + a_3 a_7 \\ b_3 &= a_3 a_6 + a_2 a_7 \\ b_4 &= a_2 a_6 + a_1 a_7 \\ b_5 &= a_1 a_6 . \end{aligned} \tag{2.5}$$

Since the homologies of the b-coefficients are known (see 1.72) we can easily derive the homologies of the a-coefficients using the relations (2.5). These homologies are:

$$\begin{aligned} [a_j] &= \eta + (j-6)c_1 - \chi \, , \\ [a_6] &= \chi \, , \\ [a_7] &= c_1 + \chi \end{aligned} \tag{2.6}$$

with $j = 1, 2, 3, 4, 5$. Because there are more a-coefficients than the number of relations in (2.5) (the system is over-defined) the homology class $[a_6] = \chi$ stands as an unspecified parameter of the model. In addition, we have to take into account the $SU(5)$ tracelessness condition, $b_1 = 0$. In terms of a's the condition reads

$$a_5 a_6 + a_4 a_7 = 0 \tag{2.7}$$

and can be solved by the following *ansatz*:

$$\begin{aligned} a_4 &= \pm a_0 a_6 \, , \\ a_5 &= \mp a_0 a_7 \end{aligned} \tag{2.8}$$

where we have introduced a new unspecified holomorphic section a_0. The homology class of the new section can be computed from the above ansatz by using the relations (2.6), as follows:

$$[a_0] = [a_4] - [a_6] = \eta - 2(c_1 + \chi).$$

In a last step, the relations (2.5) has to be enforced with the above ansatz solution and further substitution of them into the defining equations for the tenplets (1.84) and fiveplets (1.85) gives:

$$\mathcal{P}_{10} \, := a_1 \times a_6 \, , \tag{2.9}$$

$$\mathcal{P}_5 \, := (a_2^2 a_7 + a_2 a_3 a_6 \mp a_0 a_1 a_6^2) \times (a_3 a_6^2 + (a_2 a_6 + a_1 a_7) a_7) \tag{2.10}$$

which is the most general, pertaining to an S_4 monodromy action on the roots. Hence, this spectral cover factorisation defines two matter curves for the tenplets and two matter curves for the fiveplets.

The $C_2 \times C_2' \times C_1$ case

If the V_4 actions are not derived as transitive subgroups of S_4, then the Klein group is isomorphic to:

$$A_4 \not\supset V_4 : \ \{(1), (12), (12)(34), (34)\}. \tag{2.11}$$

This is not contained in A_4, but is admissible from the spectral cover in the form of a monodromy $C_5 \to C_2 \times C_2' \times C_1$.

In this case the spectral cover polynomial (1.82) splits into three factors as follows:

$$\begin{aligned} &\mathcal{C}_5 \to \mathcal{C}_2 \times C_2' \times C_1 : \\ &\quad (a_1 + a_2 s + a_3 s^2)(a_4 + a_5 s + a_6 s^2)(a_7 + a_8 s). \end{aligned} \tag{2.12}$$

We may now match the coefficients of this polynomial in each order in s to the ones of the spectral cover with the b_k coefficients. This trivial task returns the following relations:

$$\begin{aligned} b_0 &= a_{368} \\ b_1 &= a_{367} + a_{358} + a_{268} \\ b_2 &= a_{357} + a_{267} + a_{348} + a_{258} + a_{168} \\ b_3 &= a_{347} + a_{257} + a_{167} + a_{248} + a_{158} \\ b_4 &= a_{247} + a_{157} + a_{148} \\ b_5 &= a_{147} \end{aligned} \tag{2.13}$$

where for simplicity we follow the notation $a_{ijk} = a_i a_j a_k$ in [157].

We turn now to the computation of the homology classes of the a_i coefficients. Comparing to the homologies of the unsplit spectral cover, a solution for the $[a_i]$ can be found by using the relations (2.13). Notice, though, that we have 8 a_i-coefficients and only 6 relations with well defined homology classes for b_j, therefore the homologies of a_i are defined up to two homology classes:

$$\begin{aligned} [a_{n=1,2,3}] &= \chi_1 + (n-3)c_1, \\ [a_{n=4,5,6}] &= \chi_2 + (n-6)c_1, \\ [a_{n=7,8}] &= \eta + (n-8)c_1 - \chi_1 - \chi_2. \end{aligned} \tag{2.14}$$

We have also to enforce the $SU(5)$ tracelessness condition, $b_1 = 0$. An *ansatz* for the solution was put forward in [157],

$$\begin{aligned} a_2 &= -c(a_6 a_7 + a_5 a_8) \\ a_3 &= c a_6 a_8 \end{aligned} \tag{2.15}$$

which again introduces a new section, c. The homology class of this new secton is completely defined by

$$[c] = -\eta + 2\chi_1 \, . \tag{2.16}$$

Using (2.13) along with the ansatz (2.15) we derive the defining equations of the tenplets and fiveplets in terms of the a-coefficients and the new section c. In particular, for the tenplets we receive that

$$\mathcal{P}_{10} = a_1 a_4 a_7 \tag{2.17}$$

while the P_5 splits into five factors as follows:

$$\begin{aligned}\mathcal{P}_5 =& a_5(a_6 a_7 + a_5 a_8)(a_6 a_7^2 + a_8(a_5 a_7 + a_4 a_8))(a_1 - a_5 a_7 c) \\ & (a_1^2 - a_1(a_5 a_7 + 2a_4 a_8)c + a_4(a_6 a_7^2 + a_8(a_5 a_7 + a_4 a_8))c^2).\end{aligned} \tag{2.18}$$

So this specific factorization predicts more matter curves in comparison with the previous case. In particular, we receive three tenplets and five fiveplets. A more detailed analysis of this interesting case will be presented in the subsequent sections.

2.3 A little bit of Galois theory

So far, we have discussed the basic properties of the most general spectral cover with a monodromy action acting on four of the roots of the $SU(5)_\perp$ group. This monodromy action is the Weyl group S_4, however a subgroup is equally admissible as the action. Transitive subgroups are subject to the theorems of Galois theory, which will allow us to determine what properties the a_i coefficients of the quartic factor of Equation (2.3) must have in order to have roots with a particular symmetry [171]-[1]. In the present Chapter emphasis is given on the case of the Klein group, $V_4 \cong Z_2 \times Z_2$. As already mentioned, the transitive V_4 subgroup of S_4 is contained within the A_4 subgroup of S_4, and so shall share some of the same requirements on the coefficients.

Galois theory is a field of Mathematics with an extensive literature. A brief introduction into the subject is given in Appendix A. Here we need only reference a handful of key theorems. Proofs for these theorems will be omitted as they are readily available in the literature and are not relevant for the purpose at hand.

Theorem 1. *Let K be a field with characteristic different than 2, and let $f(X)$ be a separable, polynomial in $K(X)$ of degree n.*

- *If $f(X)$ is irreducible in $K(X)$ then its Galois group over K has order divisible by n.*
- *The polynomial $f(X)$ is* irreducible *in $K(X)$* if and only if *its Galois group over K is a transitive subgroup of S_n.*

This first theorem offers the key point that any polynomial of degree n, that has non-degenerate roots, but cannot be factorised into polynomials of lower order with coefficients remaining in the same field must necessarily have a Galois group relating the roots that is S_n or a transitive subgroup thereof.

Theorem 2. *Let K be a field with characteristic different than 2, and let $f(X)$ be a separable, polynomial in $K(X)$ of degree n. Then the Galois group of $f(X)$ over K is a subgroup of A_n* if and only if *the discriminant of f is a square in K.*

As already stated, we are interested specifically in transitive V_4 subgroups. Theorem 2 gives us the requirement for a Galois group that is A_4 or its transitive subgroup V_4 - both of which are transitive in S_4. Note that no condition imposed on the coefficients of the spectral cover should split the polynomial ($C_4 \to C_2 \times C_2$), due to Theorem 1. We also know by Theorem 2 that both V_4 and A_4 occur when the discriminant of the polynomial is a square, so we necessarily require another constraint in order to distinguish the two.

2.3.1 The Cubic Resolvent polynomial

In Galois theory, the so-called *Cubic Resolvent*, is an auxiliary polynomial defined in terms of the roots of the original quartic polynomial we are attempting to classify. The roots of the cubic resolvent are defined as symmetric functions of the t_i roots of the initial quartic polynomial, as follows

$$x_1 = (t_1t_2 + t_3t_4),\ x_2 = (t_1t_3 + t_2t_4),\ x_3 = (t_1t_4 + t_2t_3) \tag{2.19}$$

and one can easily check that the initial quartic and the cubic resolvent polynomial share the same discriminant. Furthermore, under any permutation of the S_4 group, the x_i-roots transform between one another. However, this is not always true when the Galois group relation is a subgroup of S_4. The cubic resolvent itself is defined trivially as:

$$(x - (t_1t_2 + t_3t_4))(x - (t_1t_3 + t_1t_4))(x - (t_1t_4 + t_3t_2)) = g_3x^3 + g_2x^2 + g_1x + g_0 \tag{2.20}$$

The coefficients g_i of the above equation can be determined by relating them to the original $\mathcal{C}_4$ coefficients through the the t_i roots. The procedure returns the following expression:

$$g(x) \approx a_5^3x^3 - a_3a_5^2x^2 + (a_2a_4 - 4a_1a_5)\,a_5x - a_2^2a_5 + 4a_1a_3a_5 - a_1a_4^2 \tag{2.21}$$

and can be further simplified by making the replacement $y = a_5x$. In this case we receive the simplest form:

$$g(y) = y^3 - a_3y^2 + (a_2a_4 - 4a_1a_5)\,y - a_2^2a_5 + 4a_1a_3a_5 - a_1a_4^2 \tag{2.22}$$

If the cubic resolvent is factorisable in the field K, then the Galois group does not contain any three cycles. For example, if the Galois group is V_4, then the roots will transform only under the 2+2-cycles:

$$V_4 \subset A_4 = \{(1), (12)(34), (13)(24), (14)(23)\}\,. \tag{2.23}$$

Each of these actions leaves the first of the roots in Equation (2.19) invariant, thus implying that the cubic resolvent is reducible in this case. If the Galois group were A_4, the 3-cycles present in the group would interchange all three roots, so the cubic resolvent is necessarily irreducible. This leads us to a third theorem, which classifies all the Galois groups of an irreducible quartic polynomial (see also Table 2.2).

Theorem 3. *The Galois group of a quartic polynomial $f(x) \in K$, can be described in terms of whether or not the discriminant of f is a square in K and whether or not the cubic resolvent of f is reducible in K.*

Group	Discriminant Δ	Cubic Resolvent
S_4	$\Delta \neq \delta^2$	Irreducible
A_4	$\Delta = \delta^2$	Irreducible
D_4 or Z_4	$\Delta \neq \delta^2$	Reducible
V_4	$\Delta = \delta^2$	Reducible

Table 2.2: A summary of the conditions on the partially symmetric polynomials of the roots and their corresponding Galois group.

2.3.2 The Discriminant

According to the previous analysis, classification of the Galois groups of a quartic polynomial depends also on the properties of the discriminant. From the effective model point of view, all the useful information is encoded in the properties of the polynomial coefficients a_k and if we wish to distinguish the various cases further assumptions for the latter coefficients have to be made.

We focus now on the cases where the symmetry acting on roots is the subgroup A_4 or the transitive V_4, then the coefficients a_k must respect certain conditions in order to distinguish the various cases. Such constraints emerge from the study of partially symmetric functions of roots. In the present case in particular, we recall that the A_4 discrete symmetry is associated only to even permutations of the four roots t_i. Further, we note now that the partially symmetic function

$$\delta = (t_1 - t_2)(t_1 - t_3)(t_1 - t_4)(t_2 - t_3)(t_2 - t_4)(t_3 - t_4)$$

is invariant only under the even permutations of roots. The quantity δ is the square root of the discriminant,

$$\Delta = \delta^2 \tag{2.24}$$

and as such δ should be written as a function of the polynomial coefficients a_k. The discriminant is computed easily by applying standard formulas and is turn out to be

$$\begin{aligned}\Delta(a_k) = {} & 256a_1^3a_5^3 - \left(27a_2^4 - 144a_1a_3a_2^2 + 192a_1^2a_4a_2 + 128a_1^2a_3^2\right)a_5^2 \\ & - 2\left(2\left(a_2^2 - 4a_1a_3\right)a_3^3 - \left(9a_2^2 - 40a_1a_3\right)a_2a_4a_3 + 3\left(a_2^2 - 24a_1a_3\right)a_1a_4^2\right)a_5 \\ & - a_4^2\left(4a_4a_2^3 + a_3^2a_2^2 - 18a_1a_3a_4a_2 + \left(4a_3^3 + 27a_1a_4^2\right)a_1\right).\end{aligned} \tag{2.25}$$

In order to examine the implications of (2.24) we write the discriminant as a polynomial of the coefficient a_3 [172]

$$\Delta \equiv f(a_3) = \sum_{n=0}^{4} c_n a_3^n \tag{2.26}$$

where the c_n are functions of the remaining coefficients a_k, $k \neq 3$ and can be easily computed by comparison with (2.25). We may equivalently demand that $f(a_3)$ is a square of a second degree polynomial

$$f(a_3) = (\kappa a_3^2 + \lambda a_3 + \mu)^2.$$

A necessary condition that the polynomial $f(a_3)$ is a square, is its own discriminant Δ_f to be zero. By computing the discriminant of $f(a_3)$ we find that has the following form

$$\Delta_g \propto D_1^2 D_2^3$$

where

$$\begin{aligned} D_1 &= a_2^2 a_5 - a_1 a_4^2 \\ D_2 &= \left(27 a_1^2 a_4 - a_2^3\right) a_4^3 - 6 a_1 a_2^2 a_5 a_4^2 + 3 a_2 \left(9 a_2^3 - 256 a_1^2 a_4\right) a_5^2 + 4096 a_1^3 a_5^3 \end{aligned} \tag{2.27}$$

Consequently there are two ways to eliminate the discriminant of the polynomial, either putting $D_1 = 0$ or by demanding $D_2 = 0$ [172].

In the first case, we can achieve $\Delta = \delta^2$ if we solve the constraint $D_1 = 0$ as follows

$$\begin{aligned} a_2^2 &= 2 a_1 a_3 \\ a_4^2 &= 2 a_3 a_5. \end{aligned} \tag{2.28}$$

Substituting the solutions (2.28) in the discriminant one finds

$$\Delta \;=\; \delta^2 \;=\; \left[a_2 a_4 \left(a_3^2 - 2\, a_2 a_4\right) \left(a_3^2 - a_2 a_4\right) / a_3^3\right]^2 . \tag{2.29}$$

The above constitute the necessary conditions to obtain the reduction of the symmetry [172] down to the Klein group V_4. Indeed, as we can see the conditions (2.28) elliminates the constant term of the cubic resolvent and made it reducible.

On the other hand, the second condition $D_2 = 0$, implies a non-trivial relation among the coefficients

$$(a_2^2 a_5 - a_4^2 a_1)^2 \;=\; \left(\frac{a_2 a_4 - 16 a_1 a_5}{3}\right)^3 \tag{2.30}$$

If we further apply the $b_1 = 0$ solution, the constraint (2.65) receives the form

$$(a_2^2 a_7 + a_0 a_1 a_6^2)^2 \;=\; a_0 \left(\frac{a_2 a_6 + 16 a_1 a_7}{3}\right)^3 \tag{2.31}$$

which is just the condition on the polynomial coefficients to obtain the transition $S_4 \to A_4$.

2.4 Klein monodromy and the origin of matter parity

In this section we will analyse a class of four-dimensional effective models obtained under the assumption that the compactification geometry induces a $Z_2 \times Z_2$ monodromy. As we have seen in the previous section, there are two distinct ways to realise this scenario, which depends on whether the corresponding Klein group is transitive or non-transitive.

There are significant differences in the phenomenological implications of these models since in a factorised spectral surface matter and Higgs are associated with different irreducible components [1].

[1] Further phenomenological issues concerning proton decay and unbroken $U(1)$ factors beyond a local spectral cover can be found in [159, 160]

In the present work we will choose to explore the rather promising case where the monodromy Klein group is non-transitive. In other words, this essentially means that the spectral cover admits a $C_2 \times C_2' \times C_1$ factorisation. As was shown above by analyzing the properties of the discriminant, the case of a transitive Klein group is more involved due to the non-trivial relations among the coefficients (Eq: 2.28), hence it is not an easy task to obtain a viable effective model. This requires further investigation.

Hence, turning our attention to the non-transitive case, the basic structure of the model obtained in this case corresponds to one of those initially presented in [156] and subsequently elaborated by other authors [157]-[162]. This model possesses several phenomenologically interesting features and we consider it is worth elaborating it further.

2.4.1 Analysis of the $Z_2 \times Z_2$ model

To set the stage, we first present a short review of the basic characteristics of the model following mainly the notation of [157]. The $Z_2 \times Z_2$ monodromy case implies a $2+2+1$ splitting of the spectral cover equation which has already been given in (2.12). Under the action (2.11), for each element, either x_2 and x_3 roots defined in (2.19) are exchanged or the roots are unchanged.

As was analyzed explicitly, the model will be characterized by three distinct 10 matter curves, while we have two more matter curves for the fiveplets. The defining equations along with their t_i charges and the corresponding homologies of the matter curves are presented in Table 2.3.

Curve	$U(1)$ Charge	Defining Equation	Homology Class
10_1	t_1	a_1	$-2c_1 + \chi_1$
10_3	t_3	a_4	$-2c_1 + \chi_2$
10_5	t_5	a_7	$\eta - c_1 - \chi_1 - \chi_2$
5_1	$-2t_1$	$a_6 a_7 + a_5 a_8$	$\eta - c_1 - \chi_1$
5_{13}	$-t_1 - t_3$	$a_1^2 - a_1(a_5 a_7 + 2a_4 a_8)c + a_4(a_6 a_7^2 + a_8(a_5 a_7 + a_4 a_8))c^2$	$-4c_1 + 2\chi_1$
5_{15}	$-t_1 - t_5$	$a_1 - a_5 a_7 c$	$-2c_1 + \chi_1$
5_{35}	$-t_3 - t_5$	$a_6 a_7^2 + a_8(a_5 a_7 + a_4 a_8)$	$2\eta - 2c_1 - 2\chi_1 - \chi_2$
5_3	$-2t_3$	a_5	$-c_1 + \chi_2$

Table 2.3: Matter curves along with their *perpendicular* charges, the defining equations and the corresponding homology classes

Now we turn our attention to the symmetry breaking procedure. Knowing the homology classes associated with each matter curve allows us to determine the spectrum of the theory through the units of abelian fluxes that pierce the matter curves [120], [119]. Indeed, one of the advantages of F-theory model building toolbox, is the fact that the properties of its internal space allows the implementation of alternative symmetry breaking mechanisms. Namely, by turning on a magnetic flux in the $U(1)_X$ directions, we can endow our spectrum with chirality and break the perpendicular group. In order to retain an anomaly free spectrum we need to

allow for [157], [161]

$$\sum M_5 + \sum M_{10} = 0, \tag{2.32}$$

where M_5 (M_{10}) denote $U(1)_X$ flux units piercing a certain 5 (10) matter curve.

A non-trivial flux can also be turned on along the direction of the Hypercharge generator. This will allow us to split the SM states into the GUT representations providing that way an elegant solution for the doublet-triplet splitting problem. In order for the Hypercharge to remain ubroken, the flux configuration should not allow for a heavy Green-Schwarz mass. This problem can be avoided if the following conditions hold [120]

$$F_Y \cdot c_1 = 0, \;\; F_Y \cdot \eta = 0. \tag{2.33}$$

For the new, unspecified, homology classes, χ_1 and χ_2 we let the flux units piercing them to be

$$F_Y \cdot \chi_1 = N_1, \;\; F_Y \cdot \chi_2 = N_2, \tag{2.34}$$

where N_1 and N_2 are flux integer units, and are treated as free parameters of the model.

For a fiveplet 5 one can use the above construction as

$$\begin{aligned} n(3,1)_{-1/3} - n(\overline{3},1)_{1/3} &= M_5, \\ n(1,2)_{1/2} - n(1,2)_{-1/2} &= M_5 + N, \end{aligned} \tag{2.35}$$

where for $N \neq 0$ the doublet-triplet splitting problem is easily evaded. Similar, for a 10 of $SU(5)$ we have

$$\begin{aligned} n(3,2)_{1/6} - n(\overline{3},2)_{-1/6} &= M_{10}, \\ n(\overline{3},1)_{-2/3} - n(3,1)_{2/3} &= M_{10} - N, \\ n(1,1)_{1} - n(1,1)_{-1} &= M_{10} + N. \end{aligned} \tag{2.36}$$

In the end, by choosing appropriate values for the flux parameters (M_5, M_{10}, N_1, N_2) the spectrum of the theory is fully defined as can be seen in Table 2.4. Note also that well known problems with unappropriate fermion mass relations at the GUT scale, may can be easily avoided here since the fluxes piercing matter generations in to different matter curves.

2.4.2 Matter Parity from geometry

In the first Chapter we saw that a crucial problem of SUSY GUTs is the presence of dangerous terms leading to fast proton decay and other unwanted processes at unacceptable rates. These issues can be evaded by introducing the concept of R-parity/Matter parity. In early F-theory model building[157, 173], such matter parity symmetries where introduced by hand. Here, in the present approach, the conjecture is that as in the case of the GUT symmetries which are associated with the manifold singularities, R-parity can also be connected to the geometric properties of the manifold[2].

[2] Another way to deal with the annihilation of unwanted Yukawa terms is to introduce new symmetries emerging from specific elliptic fibrations with rational sections. Indeed, these imply the existence of new $U(1)$ symmetries of Mordell-Weil type [178, 168]. These type of symmetries may prevent unwanted couplings.

Curve	Weight	Homology	N_Y	N_X	Spectrum
10_1	t_1	$-2c_1+\chi_1$	N_1	M_{10_1}	$M_{10_1}Q+(M_{10_1}-N_1)u^c+(M_{10_1}+N_1)e^c$
10_3	t_3	$-2c_1+\chi_2$	N_2	M_{10_3}	$M_{10_3}Q+(M_{10_3}-N_2)u^c+(M_{10_3}+N_2)e^c$
10_5	t_5	$\eta-c_1-\chi_1-\chi_2$	$-N_1-N_2$	M_{10_5}	$M_{10_5}Q+(M_{10_5}+N)u^c+(M_{10_5}-N)e^c$
5_1	$-2t_1$	$\eta-c_1-\chi_1$	$-N_1$	M_{5_1}	$M_{5_1}\overline{d^c}+(M_{5_1}-N_1)\overline{L}$
5_{13}	$-t_1-t_3$	$-4c_1+2\chi_1$	$2N_1$	$M_{5_{13}}$	$M_{5_{13}}\overline{d^c}+(M_{5_{13}}+2N_1)\overline{L}$
5_{15}	$-t_1-t_5$	$-2c_1+\chi_1$	N_1	$M_{5_{15}}$	$M_{5_{15}}\overline{d^c}+(M_{5_{15}}+N_1)\overline{L}$
5_{35}	$-t_3-t_5$	$2\eta-2c_1-2\chi_1-\chi_2$	$-2N_1-N_2$	$M_{5_{35}}$	$M_{5_{35}}\overline{d^c}+(M_{5_{35}}-2N_1-N_2)\overline{L}$
5_3	$-2t_3$	$-c_1+\chi_2$	N_2	M_{5_3}	$M_{5_3}\overline{d^c}+(M_{5_3}+N_2)\overline{L}$

Table 2.4: Matter curve spectrum parametrized by the integer flux parameters M_i and $N_{1,2}$. Note that $N=N_1+N_2$ has been used as short hand.

Given the fact that the GUT symmetries in F-theory are linked to geometric singularities of the internal space, it is also worth exploring the possibility whether matter parity can be of a similar nature.

It was first proposed before [143], in local F-Theory constructions there are geometric discrete symmetries of the spectral cover that manifest on the final field theory. To understand this, note that the spectral cover equation is invariant, up to a phase, under the phase transformation $\sigma : s \mapsto \sigma s$ of the fibration coordinates

$$s(\sigma(p)) = s(p)\, e^{i\phi}, \;\; b_k(\sigma(p)) \;=\; b_k(p)\, e^{i(\chi-(6-k)\phi)}.$$

Under this action, each term in the spectral cover polynomial transforms the same way

$$b_k s^{5-k} \to e^{i(\chi-\phi)} b_k s^{5-k}$$

It can be readily observed that a non-trivial solution accommodates a Z_N symmetry for $\phi=\frac{2\pi}{N}$. Thus, for $N=2$, we have $\phi=\pi$ and the transformation reduces to

$$s \to -s, \; b_k \to (-1)^k e^{i\chi}\, b_k \tag{2.37}$$

We may now assume that this symmetry is communicated from the $\mathcal{C}_5$ theory to the split spectral cover geometry. Further, for curves accommodating MSSM matter fields we will assume that matter parity is defined by the corresponding 'parity' of its defining equation, which is fixed through its relation with the b_i coefficients of the initial $\mathcal{C}_5$ spectral equation.

For the specific models presented here, we can use [162] the equations relating

$$b_k \propto a_l a_m a_n, \; with \;\; k+l+m+n=17 \tag{2.38}$$

to find the transformation rules of the a_k such that the spectral cover equation respects the symmetry of Equation (2.38). Consistency with Equation (2.38) implies that the coefficients a_n should transform as

$$a_n \to e^{i\psi_n} e^{i(11/3-n)\phi} a_n. \tag{2.39}$$

We now note that the above transformations can be achieved by a Z_N symmetry if $\phi = 3\frac{2\pi}{N}$. In that case one can find, by looking at the equations (2.13) for $b_k \propto a_l a_m a_n$ that we have

$$\psi_1 = \psi_2 = \psi_3 \tag{2.40}$$

$$\psi_4 = \psi_5 = \psi_6 \tag{2.41}$$

$$\psi_7 = \psi_8 \tag{2.42}$$

meaning that there are three distinct cycles, and

$$\chi = \psi_1 + \psi_4 + \psi_7. \tag{2.43}$$

Furthermore, the section c introduced to solve the tracelness condition (2.15) has to transform as

$$c \to e^{i\phi_c} c, \tag{2.44}$$

with

$$\phi_c = \psi_3 - \psi_6 - \psi_7 + \left(-\frac{11}{3} + 11\right)\phi \quad , \quad \phi_c = \psi_2 - \psi_5 - \psi_8 + \left(-\frac{11}{3} + 11\right)\phi. \tag{2.45}$$

We can now deduce what would be the matter parity assignments for Z_2 with $\phi = 3(2\pi/2)$. Let $p(x)$ be the parity of a section (or products of sections), x. We notice that there are relations between the parities of different coefficients, for example one can easily find

$$\frac{p(a_1)}{p(a_2)} = -1 \tag{2.46}$$

amongst others, which allow us to find that all parity assignments depend only on three independent parities

$$p(a_1) = -p(a_2) = p(a_3) = i \tag{2.47}$$

$$p(a_4) = -p(a_5) = p(a_6) = j \tag{2.48}$$

$$p(a_7) = -p(a_8) = k, \tag{2.49}$$

where we note that $p(c) = ijk$ and the trivial condition $i^2 = j^2 = k^2 = +$. With the analysis above in hand we are ready to write down all the parities for each matter curve as a function of i, j, k. This, along with all the possible parity assignments, are presented in the table 2.5.

As such, F-theory $SU(5)$ models with a $Z_2 \times Z_2$ monodromy are completely specified by the information present in table 2.6.

2.4.3 The Singlets

In the context of F-theory GUTs, the local geometry cannot tell us everything about the singlets of the theory. A definite and reliable consideration of this issue would require an analysis of the model in terms of global geometry but this goes beyond the scope of the present work. Bearing in mind the limitations of the spectral cover approach, we will take a conservative point of view

Curve	Charge	Parity	All possible assignments							
10_1	t_1	i	+	−	+	−	+	−	+	−
10_3	t_3	j	+	+	−	−	+	+	−	−
10_5	t_5	k	+	+	+	+	−	−	−	−
5_1	$-2t_1$	jk	+	+	−	−	−	−	+	+
5_{13}	$-t_1-t_3$	+	+	+	+	+	+	+	+	+
5_{15}	$-t_1-t_5$	i	+	−	+	−	+	−	+	−
5_{35}	$-t_3-t_5$	j	+	+	−	−	+	+	−	−
5_3	$-2t_3$	$-j$	−	−	+	+	−	−	+	+

Table 2.5: All the possible matter parity assignments for the matter curves of the model under consideration.

Curve	Charge	Matter Parity	Spectrum
10_1	t_1	i	$M_{10_1}Q+(M_{10_1}-N_1)u^c+(M_{10_1}+N_1)e^c$
10_3	t_3	j	$M_{10_3}Q+(M_{10_3}-N_2)u^c+(M_{10_3}+N_2)e^c$
10_5	t_5	k	$M_{10_5}Q+(M_{10_5}+N_1+N_2)u^c+(M_{10_5}-N_1-N_2)e^c$
5_1	$-2t_1$	jk	$M_{5_1}\overline{d^c}+(M_{5_1}-N_1)\overline{L}$
5_{13}	$-t_1-t_3$	+	$M_{5_{13}}\overline{d^c}+(M_{5_{13}}+2N_1)\overline{L}$
5_{15}	$-t_1-t_5$	i	$M_{5_{15}}\overline{d^c}+(M_{5_{15}}+N_1)\overline{L}$
5_{35}	$-t_3-t_5$	j	$M_{5_{35}}\overline{d^c}+(M_{5_{35}}-2N_1-N_2)\overline{L}$
5_3	$-2t_3$	$-j$	$M_{5_3}\overline{d^c}+(M_{5_3}+N_2)\overline{L}$

Table 2.6: All the relevant information for model building with $Z_2\times Z_2$ monodromy in F-theory $SU(5)$ semi-local constructions. The exact spectrum of the model is specified by the flux parameters M_i and N_j.

and present a discussion of these fields focusing only on a less general case where the spectral cover analysis is reliable.

For the singlets on the GUT surface we start by looking at the splitting equation for singlet states, P_0. For $SU(5)$ case we study here, these are found to be

$$\begin{aligned}P_0 = {} & 3125b_5^4b_0^4+256b_4^5b_0^3-3750b_2b_3b_5^3b_0^3+2000b_2b_4^2b_5^2b_0^3+2250b_3^2b_4b_5^2b_0^3\\ & -1600b_3b_4^3b_5b_0^3-128b_2^2b_4^4b_0^2+144b_2b_3^2b_4^3b_0^2-27b_3^4b_4^2b_0^2+825b_2^2b_3^2b_5^2b_0^2\\ & -900b_2^3b_4b_5^2b_0^2+108b_3^5b_5b_0^2+560b_2^2b_3b_4^2b_5b_0^2-630b_2b_3^3b_4b_5b_0^2+16b_2^4b_4^3b_0\\ & -4b_2^3b_3^2b_4^2b_0+108b_2^5b_5^2b_0+16b_2^3b_3^3b_5b_0-72b_2^4b_3b_4b_5b_0\ .\end{aligned} \tag{2.50}$$

Applying the solution for the $Z_2\times Z_2$ monodromy from Eq.(2.13,2.15) we end up with 13 factors

$$P_0 = a_6^2 a_8^2 c \left(a_5^2 - 4a_4 a_6\right) \left(a_8(a_4 a_8 - a_5 a_7) + a_6 a_7^2\right)^2 \left(c(a_5 a_8 + a_6 a_7)^2 - 4a_1 a_6 a_8\right) \left(a_1 a_8 + a_7 c(a_5 a_8 + 2a_6 a_7)\right)^2 \left(a_1^2 a_6 + a_1 c\left(-2a_4 a_6 a_8 + 2a_5^2 a_8 + a_5 a_6 a_7\right) + a_4 c^2 \left(a_6 a_8(a_4 a_8 + 3a_5 a_7) + 2a_5^2 a_8^2 + a_6^2 a_7^2\right)\right)^2 . \tag{2.51}$$

Their homologies and geometric parities can be founded by applying the techniques from the previous section for the fiveplets and tenplets. The results are presented in Table 2.7. Note that not all the factors of Equation (2.51) appear to be singlets incident at points on the GUT surface. In particular, the fields associated to the factors c, $a_5^2 - \ldots$ and $c(a_5 a_8 + \ldots$ are uncharged under the perpendicular group weights. As such these cannot be incident upon the GUT surface and we shall not include them to participate in any coupling for the rest of the analysis.

Name	Equation	Power	Charge	Homology Class	Matter Parity
θ_1	a_6	2	$\pm(t_1 - t_3)$	χ_2	j
θ_2	a_8	2	$\pm(t_1 - t_5)$	$\eta - \chi_1 - \chi_2$	$-k$
θ_3	$a_8(a_4 a_8 - \ldots$	2	$\pm(t_3 - t_5)$	$2\eta - 2c_1 - 2\chi_1 - \chi_2$	j
θ_4	$(a_1 a_8 + \ldots$	2	$\pm(t_1 - t_5)$	$\eta - 2c_1 - \chi_2$	$-ik$
θ_5	$(a_1^2 a_6 + \ldots$	2	$\pm(t_1 - t_3)$	$-4c_1 + 2\chi_1 + \chi_2$	j

Table 2.7: Defining equations, multiplicity, perpendicular $(t_i - t_j)$-charges, homology classes and matter parity of the singlet spectrum. Note that the properties of the singlet fields described by the factors c, $a_5^2 - \ldots$ and $c(a_5 a_8 + \ldots$ cannot be deduced in this approach (see text) and as a result have not included here.

Finally, in the construction of a realistic model we have also to take into account the geometric parity signs of these singlet states. All possible geometric parities of the singlets can be seen in Table 2.8, where the charge conjugated partner is included in the same row - i.e. θ_i has the same parity as $\overline{\theta}_i$.

2.5 Deriving the MSSM with two right-handed neutrinos

The number of possible models that can be constructed is very large as we can see from the analysis so far. Because of the plethora of reasonable combinations of fluxes, multiplicities and choices of geometric parities we need some model building guiding principles. There are a number of ways to narrow the parameter space of any search, for example requiring that there be no exotics present in the spectrum, or contriving there to be only one tree-level Yukawa coupling to enable a heavy top quark. Furthermore, the observed large hierarchy of the up-quark mass

Name	Charge	All possible assignments							
θ_1	$\pm(t_1 - t_3)$	+	+	−	−	+	+	−	−
θ_2	$\pm(t_1 - t_5)$	−	−	−	−	+	+	+	+
θ_3	$\pm(t_3 - t_5)$	+	+	−	−	+	+	−	−
θ_4	$\pm(t_1 - t_5)$	−	+	−	+	+	−	+	−
θ_5	$\pm(t_1 - t_3)$	+	+	−	−	+	+	−	−

Table 2.8: All the possible geometric parities of the singlets participating to the model.

spectrum emerges naturally from a rank one mass matrix and this means that the associated gauge invariant term $10_{t_i}10_{t_j}5_{-t_i-t_j}$ can account for it only under a monodromy action such that two matter curves are identified $t_i = t_j$.

We note however that in general monodromies allow more than one tree-level coupling in the superpotential and therefore it is necessary to implement some form of R-parity or matter parity in F-theory GUT models.

Using the Mathematica package presented in [179], it is easy to produce the spectrum of operators up to an arbitrary mass dimension for various choices of the parameters involved in to the analysis. In most of the models with a tree level top quark operator, there is a conflict between dangerous bilinear R-parity violation terms and the mass of exotics. So, in order to proceed we relax the requirement for a tree level top quark term and we search for models with conventional MSSM matter parity and no exotics.

That way we make a choice for the flux parameters and phases that enables the implementation of a standard matter parity:

$$\begin{aligned}
&\{N_1 = 1, N_2 = 0\},\\
&\{M_{10_1} = -M_{5_{13}} = 2,\\
&M_{10_5} = -M_{5_3} = 1,\\
&M_{10_3} = M_{5_1} = M_{5_{15}} = M_{5_{35}} = 0\},\\
&\{i = -j = k = -\}.
\end{aligned} \tag{2.52}$$

The matter spectrum of this model is summarised in Table 2.9. With this choice, Table 2.8 will select the column with only the singlets θ_4 and $\overline{\theta}_4$ having a negative matter parity. Provided this singlet does not acquire a vacuum expectation it will then be impossible for Bilinear R-parity violating terms due to the nature of the parity assignments. This will also conveniently give us candidates for right-handed neutrinos, θ_4 and $\overline{\theta}_4$.

2.5.1 Quarks and Charged Leptons Yukawas

Having written down a spectrum that has the phenomenologically preferred R-parity, we must now examine the allowed couplings of the model. The model only allows Yukawa couplings to arise at non-renormalisable levels, however the resulting couplings give rise to rank three mass

Curve	Charge	Matter Parity	Spectrum
10_1	t_1	$-$	$Q_3 + Q_2 + u_3^c + 3e^c$
10_3	t_3	$+$	$-$
10_5	t_5	$-$	$Q_1 + u_2^c + u_1^c$
5_1	$-2t_1$	$-$	$-\overline{L}_1$
5_{13}	$-t_1 - t_3$	$+$	$2H_u$
5_{15}	$-t_1 - t_5$	$-$	$-\overline{d}_2^c - \overline{d}_1^c - \overline{L}_2$
5_{35}	$-t_3 - t_5$	$+$	$-2\overline{H}_d$
5_3	$-2t_3$	$-$	$-\overline{d}_3^c - \overline{L}_3$
$1_{15} = \theta_4$	$t_1 - t_5$	$-$	N_R^a
$1_{51} = \overline{\theta}_4$	$t_5 - t_1$	$-$	N_R^b

Table 2.9: Matter content for a model with the standard matter parity arising from a geometric parity assignment .

matrices. This is because the perpendicular group charges must be canceled out in any Yukawa couplings. For example, the Yukawa arising from $10_1 \cdot 10_1 \cdot 5_{13}$ has a charge $t_1 - t_3$, which may be canceled by the $\theta_{1/5}$ singlets. Consider the Yukawas of the Top sector,

$$\begin{aligned} 10_1 \cdot 10_1 \cdot 5_{13} \cdot (\overline{\theta}_1 + \overline{\theta}_5) &\longrightarrow (Q_3 + Q_2) u_3 H_u (\overline{\theta}_1 + \overline{\theta}_5) \\ 10_1 \cdot 10_5 \cdot 5_{13} \cdot \theta_3 &\longrightarrow ((Q_3 + Q_2)(u_1 + u_2) + Q_1 u_3) H_u \theta_3 \\ 10_5 \cdot 10_5 \cdot 5_{13} \cdot \theta_2 \cdot \theta_3 &\longrightarrow Q_1 (u_1 + u_2) H_u \theta_2 \theta_3 \end{aligned} \tag{2.53}$$

where the numbers indicate generations (1, 2 and 3). The resulting mass matrix should be rank three, however the terms will not all be created equally and the rank theorem [141] should lead to suppression of operators arising from the same matter curve combination:

$$M_{u,c,t} \sim v_u \begin{pmatrix} \epsilon\theta_2\theta_3 & \theta_2\theta_3 & \theta_3 \\ \epsilon^2\theta_3 & \epsilon\theta_3 & \epsilon(\overline{\theta}_1 + \overline{\theta}_5) \\ \epsilon\theta_3 & \theta_3 & \overline{\theta}_1 + \overline{\theta}_5 \end{pmatrix} \tag{2.54}$$

where each element of the matrix has some arbitrary coupling constant. We use here ϵ to denote suppression due to the effects of the computation of Yukawa couplings [141] for Yukawas arising from the same GUT operators. The lightest generation will have the lightest mass due to an extra GUT scale suppression arising from the second singlet involved in the Yukawa term. There are a large number of corrections at higher orders from singlet VEVs, which we have not included here for brevity. These corrections will also be less significant compared to the lowest order contributions.

In a similar way, the Down-type Yukawa couplings arise as non-renormalisable operators, coming from four different combinations. The operators for this sector often exploit the tracelessness of $SU(5)$, so that the sum of the GUT charges must vanish. The leading order Yukawa

operators are,

$$\begin{aligned} 10_1 \cdot \overline{5}_3 \cdot \overline{5}_{35} \cdot (\theta_1 + \theta_5) &\longrightarrow (Q_3 + Q_2) d_3 H_d (\theta_1 + \theta_5) \\ 10_1 \cdot \overline{5}_{15} \cdot \overline{5}_{35} \cdot \theta_3 &\longrightarrow (Q_3 + Q_2)(d_1 + d_2) H_d \theta_3 \\ 10_5 \cdot \overline{5}_3 \cdot \overline{5}_{35} \cdot (\theta_1 + \theta_5)\theta_2 &\longrightarrow Q_1 d_3 H_u (\theta_1 + \theta_5)\theta_2 \\ 10_5 \cdot \overline{5}_{15} \cdot \overline{5}_{35} \cdot \theta_2 \cdot \theta_5 &\longrightarrow Q_1 (d_1 + d_2) H_u \theta_2 \theta_5 \end{aligned} \tag{2.55}$$

and like in the case of the Top sector, the above terms return a rank three mass matrix which has the following form:

$$M_{d,s,b} \sim v_d \begin{pmatrix} \epsilon\theta_2\theta_3 & \theta_2\theta_3 & (\theta_1 + \theta_5)\theta_2 \\ \epsilon^2\theta_3 & \epsilon\theta_3 & \epsilon(\theta_1 + \theta_5) \\ \epsilon\theta_3 & \theta_3 & \theta_1 + \theta_5 \end{pmatrix}. \tag{2.56}$$

The structure of the Top and Bottom sectors appears to be quite similar in this model, which should provide a suitable hierarchy to both sectors.

Usually the Charged Lepton and the the Bottom sector shares a similar structure, but this is not the case in the present model, due primarily to the fact the e_i^c matter is localised on one GUT tenplet. The Lepton doublets however all reside on different $\overline{5}$ representations, which will fill out the matrix in a non-trivial way, with the operators:

$$\begin{aligned} 10_1 \cdot \overline{5}_3 \cdot \overline{5}_{35} \cdot (\overline{\theta}_1 + \overline{\theta}_5) &\longrightarrow L_3 (e_1^c + e_2^c + e_3^c) H_d (\overline{\theta}_1 + \overline{\theta}_5) \\ 10_1 \cdot \overline{5}_{15} \cdot \overline{5}_{35} \cdot \theta_3 &\longrightarrow L_2 (e_1^c + e_2^c + e_3^c) H_d \theta_3 \\ 10_1 \cdot \overline{5}_1 \cdot \overline{5}_{35} \cdot (\theta_1 + \theta_5) &\longrightarrow L_1 (e_1^c + e_2^c + e_3^c) H_d (\theta_1 + \theta_5) \end{aligned} \tag{2.57}$$

The mass matrix for the Charged Lepton sector will be subject to suppressions arising due to the effects discussed above. Next we discuss the Neutrino sector of the model.

2.5.2 Neutrino Masses

The spectrum contains two singlets that do not have VEV's, which protects the model from certain classes of unwanted terms. These singlets, $\theta_4/\overline{\theta}_4$, also serve as candidates for RH-neutrinos. Let us make the assignment $\theta_4 = N_R^a$ and $\overline{\theta}_4 = N_R^b$. This gives Dirac masses from two sources, the first of which involve all lepton doublets and N_R^a:

$$\begin{aligned} \overline{5}_3 \cdot 5_{13} \cdot \theta_4 \cdot \overline{\theta}_3 &\longrightarrow L_3 N_R^a H_u \overline{\theta}_3 \\ \overline{5}_{15} \cdot 5_{13} \cdot \theta_4 \cdot (\overline{\theta}_1 + \overline{\theta}_5) &\longrightarrow L_2 N_R^a H_u (\overline{\theta}_1 + \overline{\theta}_5) \\ \overline{5}_1 \cdot 5_{13} \cdot \theta_4 \cdot (\overline{\theta}_1 + \overline{\theta}_5) \cdot \theta_2 &\longrightarrow L_1 N_R^a H_u (\overline{\theta}_1 + \overline{\theta}_5)\theta_2. \end{aligned} \tag{2.58}$$

This generates a hierarchy for neutrinos, however the effect will be mitigated by the operators arising from the N_R^b singlet:

$$\begin{aligned} \overline{5}_3 \cdot 5_{13} \cdot \overline{\theta}_4 \cdot (\overline{\theta}_1 + \overline{\theta}_5) \cdot \theta_2 &\longrightarrow L_3 N_R^b H_u (\overline{\theta}_1 + \overline{\theta}_5)\theta_2 \\ \overline{5}_{15} \cdot 5_{13} \cdot \overline{\theta}_4 \cdot \theta_2 \cdot \theta_3 &\longrightarrow L_2 N_R^b H_u \theta_2 \theta_3 \\ \overline{5}_1 \cdot 5_{13} \cdot \overline{\theta}_4 \cdot \theta_3 &\longrightarrow L_1 N_R^b H_u \theta_3. \end{aligned} \tag{2.59}$$

If all these Dirac mass operators are present in the low energy spectrum, then the neutrino sector should have masses that mix greatly. This is compatible with our understanding of neutrinos from experiments, which requires large mixing angles compared to the quark sector.

A light mass scale for the neutrinos can be generated using the standard seesaw mechanism, which requires large right-handed Majorana masses to generate light physical left-handed Majorana neutrino mass at low scales. The singlets involved in this scenario has perpendicular charges that must be canceled out, similar to the quark and charged lepton operators of the model. Fortunately, this can be achieved, in part due to the presence of $\theta_2/\overline{\theta}_2$, which have the same charge combinations as $N_R^{a,b}$. The leading contribution to the mass term will come from the off diagonal $\theta_4\overline{\theta}_4$ term, however there are diagonal contributions:

$$\frac{\langle\theta_2\rangle^2}{\Lambda}\overline{\theta}_4^2 \;+\; \frac{\langle\overline{\theta}_2\rangle^2}{\Lambda}\theta_4^2 \;+\; M\theta_4\overline{\theta}_4. \tag{2.60}$$

Two RH neutrinos are capable to generate the observed physical light neutrinos masses as suggested by the experiments [180, 181].

2.5.3 Other Features

μ-term(s)

The model is free from heavy exotic colour triplets, however an extra pair of Higgs doublets fields appear in the spectrum. Because of the flux choices and the requirement for a realistic doublet-triplet splitting mechanism, it is necessary to have two copies of the up and down-type Higgs supermultiplets. This insures that the model is free of exotic colour triplets, D_u/D_d and at the same time allowing for a positive parity assignment to matter curves accommodating the Higgs doublets. As a result, the μ-term for the Higgs mass would seem to give four Higgs operators of the same mass: $M_{ij}H_u^iH_d^j$, with $i,j=1,2$. However, since for both the up and down-types there are two copies on the same matter curve, we can call upon the rank theorem [141]. Consider the operator for the μ-term:

$$5_{13}\cdot\overline{5}_{35}\cdot\theta_2 \to M_{ij}H_u^iH_d^j \to M\begin{pmatrix}\epsilon_h^2 & \epsilon_h\\ \epsilon_h & 1\end{pmatrix}\begin{pmatrix}H_u^1\\ H_u^2\end{pmatrix}\begin{pmatrix}H_d^1 & H_d^2\end{pmatrix}. \tag{2.61}$$

This operator will give a mass that is naturally large for one generation of the Higgs, while the second mass should be suppressed due to non-perturbative effects. This is parameterised by ϵ_h, which represents here the effects of local F-theory effects and is required to be sufficiently small in order to allow for a Higgs to be present at low energy scales, while the leading order Higgs must be heavy enough to remain at a reasonably high scale and not create conflict with unification of gauge couplings. Thus we should have a light Higgs boson as well as a heavier copy which is undetected from the present days experiments.

Proton decay

The spectrum is free of the Higgs colour triplets D_u/D_d, however we must still consider operators of the types $QQQL$ and $d^cu^cu^ce^c$, since the colour triplets may appear in the spectrum at the

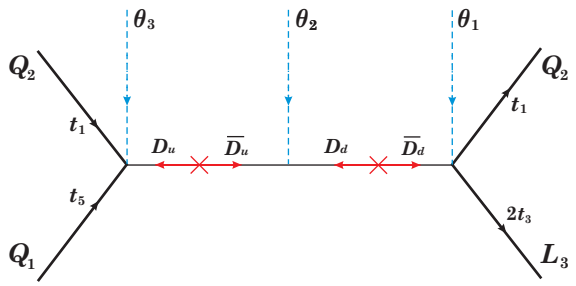

Figure 2.2: Proton decay effects due to extra color triplets.

string scale. Of these types of operator, most are forbidden at leading order thanks to the t_i-charges of the perpendicular group. However, one operator is allowed and we must consider this process:

$$10_1 10_1 10_5 \bar{5}_3 \to (Q_3 + Q_2)(Q_3 + Q_2)Q_1 L_3 + (u_2^c + u_1^c)u_3^c d_3^c (e_1^c + e_2^c + e_3^c). \tag{2.62}$$

None of the operators arising are solely first generation matter, however due to mixing they may contribute to any proton decay rate. The model in question only has one of each type of Higgs matter curve, which means any colour triplet partners must respect the perpendicular charges of those curves. The result of this requirement is that the vertex between the initial quarks and the D_u colour triplet must also include a singlet to balance the t_i charges, with the same requirement for the final vertex. The resulting operator should be suppressed by some high scale where the colour triplets are appearing in the spectrum - Λ_s. The most dangerous contribution of this operator can be assume to be the $Q_2 Q_1 Q_2 L_3$ component, which will mix most strongly with the lightest generation. It can be estimated that, given the quark mixing and the mixing structure of the charged Leptons in particular, the suppression scale should be in the region $\sim 10^{4-6}\Lambda_s$. This estimate seems to place the suppression of proton decay at too small a value, though not wildly inconsistent.

However, by considering Figure 2.2, one can see that while the sum of the t_i-charges of the external legs is zero, the inner vertices require singlet contributions. For example, the first vertex is $Q_2 Q_1 D_u$ and returns a non-zero perpendicular charge equals to $(t_3 - t_5)$ which is canceled by the θ_3 singlet. That way we have the nonrenormalisable operator $Q_2 Q_1 D_u \theta_3$ contribute to the process and we cannot write down a series of renormalisable operators to mediate this effective operator. This is because the combination of perpendicular group and GUT charges constrain heavily the operators we can write down, which means proton decay can be seen to be suppressed here by the dynamics as well as the symmetries required by the F-theory formalism. The full determination of the coupling strengths of any process of this type in F-theory should be found through computing the overlap integral of the wavefunctions involved [148].

2.6 Discussions and outlook

Before closing this chapter, we briefly comment on some alternatives spectral cover constructions where the techniques that have been presented in this chapter can also be applied.

First, we mention that a cubic polynomial is also subject to Galois theory, which means that Galois knowledge is also applicable in cases where the spectral cover splitting contains a cubic factor. In the case of $SU(5)$ GUT with a spectral cover description, there are two such possible cases:

$$(i). \quad \mathcal{C}_3 \times \mathcal{C}_2 \quad and \quad (ii). \quad \mathcal{C}_3 \times \mathcal{C}_1 \times \mathcal{C}'_1$$

.

Just for illustrating reasons we focus on the first case where we assume that the spectral cover polynomial factors into a cubic and a quadratic term:

$$\mathcal{C}_5 = \sum_k b_k s^{5-k} = P_a P_b = (a_0 + a_1 s + a_2 s^2 + a_3 s^3)\,(a_4 + a_5 s + a_6 s^2). \tag{2.63}$$

The equations connecting b_k's with a_i's are of the form $b_k \sim \sum_n a_n a_{9-n-k}$, the sum referring to appropriate values of n which can be read off from (2.63). We recall that the b_k coefficients are characterised by homologies $[b_k] = \eta - k\,c_1$. Using this fact as well as the corresponding equations $b_k(a_i)$, we can determine the corresponding homologies of the a_i's in terms of only one arbitrary parameter which we may take to be the homology $[a_6] = \chi$. Furthermore the constraint $b_1 = a_2 a_6 + a_3 a_5 = 0$ is solved by introducing a suitable section λ such that $a_3 = -\lambda\, a_6$ and $a_2 = \lambda\, a_5$.

The Galois group of a cubic polynomial is completely determined by its discriminant. The permutation action of the Galois group of a cubic polynomial on its roots turns the Galois group into a transitive subgroup of S_3. The only transitive subgroups of S_3 are A_3 and S_3, and we can decide when the Galois group is in A_3 or not using the discriminant. More precisely, if the discriminant of the cubic polynomial is a square in the field of the coefficients of the polynomial then the Galois group of the polynomial is A_3. In a different case (the discriminant it's not a square) the Galois group is S_3.

Returning in to our case, apart from the constraint $b_1 = 0$, there are no other restrictions on the coefficients a_i in the case of the S_3 symmetry. If, however, we wish to reduce the S_3 symmetry to A_3 (which from the point of view of low energy phenomenology is essentially Z_3), additional conditions should be imposed. As in the case of A_4 discussed previously, in order to derive the constraints on a_k's for the symmetry reduction $S_3 \to Z_3$ we compute the discriminant which turns out to be

$$\begin{aligned} \Delta &= -4a_3 a_1^3 + a_2^2 a_1^2 + 18 a_0 a_2 a_3 a_1 - 4 a_0 a_2^3 - 27 a_0^2 a_3^2 \\ &= \left(a_1^2 - 4 a_0 a_2\right) a_2^2 - 27 a_0^2 a_3^2 + 2 a_1 \left(9 a_0 a_2 - 2 a_1^2\right) a_3 \end{aligned} \tag{2.64}$$

and demand $\Delta = \delta^2$. In analogy with the method followed in the case of the quartic polynomial we re-organise the terms in powers of the ficticious variable $x \equiv a_1$

$$\Delta \to f(x) = -4a_3 x^3 + a_2^2 x^2 + 18 a_0 a_2 a_3 x - a_0 \left(4 a_2^3 + 27 a_0 a_3^2\right) \tag{2.65}$$

First, we observe that in order to write the above expression as a square, the product $a_1 a_3$ must be positive definite $\text{sign}(a_1 a_3) = -$. Provided this condition is fulfilled, then we require the vanishing of the discriminant Δ_f of the cubic polynomial $f(x)$, namely:

$$\Delta_f = -64 a_0 a_3 \left(27 a_0 a_3^2 - a_2^3\right)^3 = 0$$

This can occur if the non-trivial relation $a_2^3 = 27 a_0 a_3^2$ holds. Substituting back to (2.64) we find that the condition is fulfilled for $a_2^2 \propto a_1 a_3$. The two constraints can be combined to give the simpler ones

$$a_0 a_3 + a_1 a_2 = 0, \quad a_2^2 + 27 a_1 a_3 = 0.$$

The details concerning the spectrum, homologies and flux restrictions of this model can be found in [157, 162]. Identifying $t_{1,2,3} = t_a$ and $t_{4,5} = t_b$ (due to monodromies) we distribute the matter and Higgs fields over the curves as follows

$$10_M \equiv 10_{t_b},\ \bar{5}_{h_d} \equiv \bar{5}_{t_a + t_b},\ 5_{h_u} \equiv 5_{-2t_b},\ \bar{5}_{2t_a} = \bar{5}_M,$$

and the allowed tree-level couplings with non-trivial $SU(5)$ representations are

$$\mathcal{W} = y_u\, 10_M\, 10_M\, 5_{h_u} + y_d\, 10_M\, \bar{5}_M\, \bar{5}_{h_d} \tag{2.66}$$

where the second term survives due to the $SU(5)$ traceless condition, $\sum t_i = 3t_a + 2t_b = 0$. Due to the limited number of matter curves, this specific example of spectral cover factorisation does not lead to a suitable effective model. From the point of view of model building and phenomenology, novel interesting features are found in $\mathcal{C}_3 \times \mathcal{C}_1 \times \mathcal{C}'_1$ splitting which an S_3 variant of the model have been analysed in our previous work [1].

Another interesting scenario is the case of F-theory $SO(10)$ models. In this case our effective theory has a GUT group $G_S = SO(10)$, then the spectral cover group corresponds to its commutant with respect to E_8 under the decomposition:

$$E_8 \to SO(10) \times SU(4)_\perp. \tag{2.67}$$

Similar to the $SU(5)$ case, important properties of the local model are also *encoded* in the spectral cover equation which for the $SU(4)_\perp$ is described by the quartic polynomial

$$\mathcal{C}_4 = \sum_{k=1}^{4} b_k s^{4-k} = b_0 s^4 + b_1 s^3 + b_2 s^2 + b_1 s + b_0 \tag{2.68}$$

with roots $t_{i=1,2,3,4}$ the weights of the $SU(4)$ which implies that $b_1 = \sum t_i = 0$. A realistic low energy model implies the existence of monodromies along the t_i's and the most interesting cases correspond to the following spectral cover factorizations[3]:

$$\mathcal{C}_2 \times \mathcal{C}_1 \times \mathcal{C}'_1, \quad \mathcal{C}_2 \times \mathcal{C}'_2, \quad \mathcal{C}_3 \times \mathcal{C}_1.$$

[3] A study of the various F-theory $SO(10)$ models is given in [162].

The first case implies the existence of a Z_2 monodromy while for the other two cases we expect that they are subject to the analysis presented in this chapter so far. Most precisely, without further investigation, we can conclude that the $\mathcal{C}_2 \times \mathcal{C}_2'$ spectral factorisation corresponds to the Klein group $Z_2 \times Z_2$ which is transitive subgroup of S_4. Similar the case with a $\mathcal{C}_3 \times \mathcal{C}_1$ spectral cover split will be subject to the Galois theory of a cubic polynomial described previously. In this specific scenario, a study of a S_3 variant of the model presented in [162] will be interesting for further investigation. Indeed, explanation of results of the neutrino oscillations experiments strongly suggests the existence of a discrete family symmetry.

In [1], the emergence of discrete symmetries in semi-local F-theory models have been discussed and realistic models based on the cases of A_4 and S_3 combined with $SU(5)$ GUT have been analysed. Notice that from the possible discrete monodromies listed in Table 2.2 we didn't consider so far the case of the dihedral group D_4 in the spectral cover equation. This is the subject of the next chapter where we threat the discrete monodromy as a discrete symmetry of the effective theory and we present a model with some interesting phenomenological consequences.

Chapter 3

D_4 discrete symmetry from F-theory $SU(5)$

3.1 Introduction

This Chapter focus on non-Abelian discrete symmetries emerging in the context of the spectral cover equation, accompanied by continuous Abelian symmetry. It is well known that the discrete symmetries play an important role in model building, since they lead to suppression of undesired nucleon decay effects and generate a hierarchical fermion mass spectrum [1]. Furthermore, non-Abelian discrete groups were introduced to interpret the observed mixing properties of the neutrino sector. Indeed the results of the neutrino oscillation experiments are in agreement with an almost maximal atmospheric mixing angle θ_{23}, a large solar mixing θ_{12}, and a non-vanishing reactor angle θ_{13}, all of which could be explained by an underlying non-Abelian discrete family symmetry [194, 195, 196, 197].

Here, we continue our analysis of the previous chapter to investigate further the grid of discrete symmetries emerging as subgroups of the $SU(5)_\perp$ spectral cover group. Motivated by the successful implementation of a class of such symmetries to the neutrino sector, we focus on the subgroups of S_4 and especially on the dihedral group D_4. Again, we show how a geometric discrete Z_2 symmetry can additionally emerge, leading to matter parity which can protect the effective models from dangerous proton decay terms. However, due to the geometric origin and the flux mechanism, this time matter parity does not completely coincide with the well known matter parity of the MSSM. In the particular example we develop, based on $D_4 \times U(1)$ family symmetry, with an $SU(5)$ GUT group, broken by fluxes, the geometric Z_2 matter parity, while suppressing proton decay, allows neutron-antineutron oscillations, providing a distinctive signature of the model. To be precise, while QLd^c is forbidden, the baryon violating operator $u^c d^c d^c$ is present leading to neutron-antineutron oscillations at a calculable rate.

The Chapter is organised as follows. In section 3.2 we study the conditions on the coefficients of the spectral cover polynomial for the implementation of a D_4 symmetry in F-theory $SU(5)$

[1] For discussions in a wider framework of discrete symmetries in String Theory see references [182]-[193].

semi-local approach. We further introduce the basic ingredients of the set-up by defining its matter curves the corresponding homologies and geometric parity assignments. In section 3.3 a specific model is analysed. We compute the quark and lepton mass matrices of the effective model while special attention is given on the neutrino sector where the neutrino observables can be explained through the implementation of the see-saw mechanism. Finally, in section 3.4 we discuss baryon violation effects, like neutron-antineutron oscillations that appear in our model due to the presence of the geometric parity.

3.2 D_4 symmetry from the spectral cover

The techniques and approaches presented in the subsequent sections will rely mainly on the analysis of the previous Chapter and the work of ref [156] as well as in [171] and especially [172] where non-Abelian fluxes are conjectured to give rise to non-Abelian discrete family symmetries in the low energy effective theory. The origin of such a symmetry is the non-Abelian $SU(5)_\perp$ which paired up with the $SU(5)_{GUT}$ at the E_8 point of enhancement. The existence of such a non-Abelian symmetry in the low energy theory will strongly depend on the geometry of the internal compact space and the fluxes present. The usual assumption is that the $SU(5)_\perp$ is first broken to a product of $U(1)_\perp$ groups which are then further broken by the action of discrete symmetries associated with the monodromy action group. Instead here we are following the conjecture in [172] that *non-Abelian fluxes* can break $SU(5)_\perp$ first to a non-Abelian discrete group S_4 then to a smaller group such as D_4 which acts as a family symmetry group in the low energy effective theory. It is emphasised that this is a conjecture since there is no proof that non-Abelian fluxes can do this. In the aforementioned works, discrete symmetries were used to deal with fundamental problems of the effective model, such as the fermion mixing and especially the neutrino sector, the μ term etc.

In the context of F-theory in particular, the D_4 symmetry was suggested in [156] for a successful implementation of a consistent effective model. This was considered in the context of a model where all Yukawa hierarchies emerge from a single E_8 enhancement point. It was further shown that the D_4 symmetry is one of the few possible monodromy groups accommodating just only the minimal matter, and at the same time being compatible with viable right-handed neutrino scenarios. In the present Chapter, we will try to exploit the non-abelian nature of this discrete group in order to construct realistic fermion mass textures which interpret the neutrino data and make possible predictions for other interesting processes of our effective model.

Since we are interested in D_4 symmetry we can approach the above picture using the spectral cover description and in particular the $\mathcal{C}_4 \times \mathcal{C}_1$ case. The basic properties (number of matter curves, t_i charges and homology classes) of the $\mathcal{C}_4 \times \mathcal{C}_1$ spectal cover split have been analysed in Section 2.3.

In the context of F-theory with an $SU(5)$ GUT group, if the remaining discrete group is D_4, then the four of the roots of the original $SU(5)_\perp$ group are permuted in accordance to the

specific D_4 rules and the overall symmetry structure is:

$$\begin{aligned} E_8 \rightarrow & SU(5)_{\text{GUT}} \times SU(5)_{\perp} \\ \rightarrow & SU(5)_{\text{GUT}} \times D_4 \times U(1)_{\perp} . \end{aligned}$$

In order to have a D_4 symmetry relating the four roots $t_{1=1,2,3,4}$ of the C_4 spectral factor, rather the general S_4 case, we must appeal again to Galois theory. From Table 2.2, we can see that this means the discriminant of the quartic part of the spectral cover split must not be a square, while the cubic resolvent of the $\mathcal{C}_4$ polynomial must be reducible.

If we assume the roots $t_{i=1,2,3,4}$, then the C_4 part of the spectral equation has a cubic resolvent of the form given in (2.21) where the roots x_i are the symmetric polynomials of the weights t_i given in (2.19).

It can be shown that the discriminant (Δ_f) of Equation (**??**) is:

$$27\Delta_f = 4\left(a_3^2 - 3a_2a_4 + 12a_1a_5\right)^3 - \left(2a_3^3 - 9\left(a_2a_4 + 8a_1a_5\right)a_3 + 27\left(a_5a_2^2 + a_1a_4^2\right)\right)^2 \tag{3.1}$$

which is also equal to the discriminant of the quartic polynomial relating the four roots given by Equation 2.25 - this is a standard property of all cubic resolvents[2].

The simplest way to make this polynomial reducible, is to demand the zero order term to vanish, $g(0) = 0$. By setting $g(0) = 0$ and using the $SU(5)$ tracelessness constraint ($b_1 = 0$[3]) we take the following known condition [172] between the a_i's :

$$a_2^2a_7 = a_1(a_0a_6^2 + 4a_3a_7)\,, \tag{3.2}$$

Further substitution of this into the equation for the fiveplets of the GUT group, (2.10), returns back an equation factorised into 3 parts,

$$P_5 = a_3(a_2a_6 + 4a_1a_7)(a_3a_6^2 + a_7(a_2a_6 + a_1a_7))\,, \tag{3.3}$$

which show us that we have at least 3 distinct matter curves by the usual interpretation. Thus, it seems that in this simple approach the D_4 conditions introduce extra matter curves.
The so obtained splitings of the non-trivial $SU(5)$ representations are collected in Table 3.1. The first column indicates the $SU(5)$ representation, while the defining equation of each corresponding matter curve is shown in the second column. In the third column we designate the associated homologies given by Equation (2.6).

3.2.1 Irreducible Representations

Thus far we have largely ignored how the group theory must be applied to matter curves in this construction. We shall now examine this side of the problem, with a particular view being taken to find the irreducible representations where possible. Given the earlier conjecture that

[2] An alternative definition for the roots of the cubic resolvent is presented in Appendix A.
[3] Note that $b_1 = a_5a_6 + a_4a_7 = 0$ is solved as shown in Equation (2.8)

$SU(5)$ Rep.	Equation	Homology
10_a	a_1	$\eta - 5c_1 - \chi$
10_b	a_6	χ
5_a	a_3	$\eta - 3c_1 - \chi$
5_b	$a_2a_6 + 4a_1a_7$	$\eta - 4c_1$
5_c	$a_3a_6^2 + a_7(a_2a_6 + a_1a_7)$	$\eta - 3c_1 + \chi$

Table 3.1: Summary of the default matter curve splitting from spectral cover equation in the event of a D_4 monodromy accompanying an $SU(5)$ GUT group. Note that the D_4 Galois theory constraint introduces an extra fiveplet in comparison with the unconstraint spectarl cover split $C_4 \times C_1$.

non-Abelian fluxes can break $SU(5)_\perp$ to $D_4 \times U(1)_\perp$, which acts as a family symmetry group in the low energy effective theory, it then follows that the low energy states must transform according to irreducible representations of D_4. In Appendix B we show how reducible 4 and 6 dimensional representations of D_4 decompose into irreducible representations. The argument in Appendix B is summarised as follows.

Knowing that we have four weights $t_{i=1,2,3,4}$, that have a relation under a D_4 symmetry, we might exploit the nature of D_4. Specifically, since D_4 can be physically interpreted as the symmetries of a square, we might label the corner of such a square with our four weights $(t_{1,2,3,4})$ and see how they must transform based on this. Similar to the symmetries of a square, it is clear that there should be two generators: a rotation about the centre by $\frac{\pi}{2}$ and a reflection along one of the lines of symmetry, which we will call a and b respectively. Then these generators are obey the following relations :

$$a^4 = e, \;\; b^2 = e, \;\; bab = a^{-1}\,, \tag{3.4}$$

where e is the identity.

It can be shown that this quadruplet of weights can be rotated into a basis with irreducible representations of D_4 - see Appendix B - by use of appropriate unitary transformations. It transpires that the irreducible basis includes a trivial singlet, a non-trivial singlet and a doublet, as summarised in Table 3.2. Note that we also have an extra singlet that is charged under the fifth weight (10_δ), which must logically be a trivial singlet since it is uncharged under the D_4 symmetry.

The fiveplets of the GUT group have a maximum of 10 weights before the reduction of the $SU(5)$ down to D_4 symmetry. These have weights related to the 10's of the GUT group: $\pm(t_i + t_j)$. By consistency these must transform in the same manner as the weights of the 10s, allowing us to unambiguously write down the generators a and b.

Following the same procedure as previously, we may decompose this tenplet under D_4 into

Curve	D_4rep.	t_5
10_α	1_{++}	0
10_β	1_{+-}	0
10_γ	2	0
10_δ	1_{++}	1

Table 3.2: Summary of the representations of the tenplets of $SU(5)_{\rm GUT}$ along with their representations under D_4 and the corresponding perpendicular charges t_i.

Curve	D_4 rep.	t_5 charge	weight relation
$\bar{5}_\alpha$	1_{++}	1	$\sum_{i=1}^4 t_i$
$\bar{5}_\beta$	1_{+-}	1	$(t_1+t_3)-(t_2+t_4)$
$\bar{5}_\gamma$	2	1	$\begin{pmatrix} t_1-t_3 \\ t_2-t_4 \end{pmatrix}$
$\bar{5}_\delta$	1_{++}	0	$\sum_{i=1}^4 t_i$
$\bar{5}_\epsilon$	1_{++}	0	$\sum_{i=1}^4 t_i$
$\bar{5}_\zeta$	1_{++}	0	$\sum_{i=1}^4 t_i$
$\bar{5}_\eta$	1_{+-}	0	$(t_1+t_3)-(t_2+t_4)$
$\bar{5}_\theta$	2	0	$\begin{pmatrix} t_1-t_3 \\ t_2-t_4 \end{pmatrix}$

Table 3.3: Summary of the of the $SU(5)_{\rm GUT}$ fiveplets, their represantation under D_4 and the corresponding perpendicular t_i-charges.

irreducible representations of the group. Referring to the Appendix once again, we may obtain a total of eight representations, as shown in Table 3.3. However, we note that three of the representations[4] are entirely indistinguishable as they are trivial singlets with only charges under $t_{i=1,2,3,4}$.

A full decomposition of the $SU(5)_{GUT}$ representations in terms of D_4 is included in the Appendix, including the decomposition of the GUT singlets, which will be important for model building in what follows.

3.2.2 Reconciling Interpretations

It is clear at this point that there is some tension between the two angles of attack for this problem. Obviously we must be able to describe both the non-abelian discrete group representations of the matter curves, while also being able to obtain them in some manner from the spectral cover approach. In order to achieve this, we shall attempt some form of multifurcation of the spectral cover by definition of new sections in a consistent manner.

[4] $\bar{5}_\delta$, $\bar{5}_\epsilon$, and $\bar{5}_\zeta$

Constraints	P_a	P_b	P_{10}
$a_1 = \kappa a_2$ $a_3 = \lambda a_7$ $a_6 = \mu a_2$	$a_2^2\left(a_7 + \lambda\mu a_7 - \alpha_0\kappa\mu^2 a_2\right)$	$a_2 a_7\left(\kappa a_7 + (\lambda\mu + 1)\mu a_2\right)$	$\kappa\mu a_2^2$

Table 3.4: A promising splitting option of the matter curves, respecting the Galois theory constraint $\Delta \neq \delta^2$ as required for a D_4 symmetry action among the roots of the spectral cover polynomial.

We begin by defining two new sections κ and λ such that

$$a_2 \to \lambda\, a_6, \quad a_3 \to \kappa\, a_7\,. \tag{3.5}$$

It is clear that this approach has some similarity with the $b_1 = 0$ tracelessness ansatz solution usually employed. Furthermore, these definitions do not generate new unwanted sections. For example, the b_k's

$$b_0 = -a_0 a_7^2, b_1 = 0, b_2 = a_7^2\kappa + a_0 a_6^2, b_3 = (\kappa + \lambda)a_6 a_7, b_4 = \lambda a_6^2 + a_1 a_7, b_5 = a_1 a_6\,, \tag{3.6}$$

do not acquire an overall common factor, while the discriminant

$$\Delta = 108 a_0\left(\lambda a_6^2 + 4a_1 a_7\right)\left(\kappa^2 a_7^2 + a_0\left(\lambda a_6^2 + 4a_1 a_7\right)\right)^2 \neq \delta^2 \tag{3.7}$$

is not a square - as required for the case of a D_4 monodromy group. On the contrary, substitution to equation for the fiveplets returns

$$P_a = a_6^2\left((\kappa + \lambda)\lambda a_7 - a_0 a_1\right) \tag{3.8}$$

and

$$P_b = a_7\left((\kappa + \lambda)a_6^2 + a_1 a_7\right)\,. \tag{3.9}$$

This appears to generate extra matter curves by increasing the number of factors available, with the added advantage that we can easily find the homologies of our matter curves and consequently the flux restraints for each. We can interpret these results as a multifurcation to irreducible representations of the D_4 group.

If we further assume $a_1 \to \mu a_6$, then

$$P_b = a_6 a_7\left(a_6(\kappa + \lambda) + \mu a_7\right)\,, \tag{3.10}$$

and the tens of the GUT group now become:

$$P_{10} \to b_5 = \mu\, a_6 a_6\,. \tag{3.11}$$

So we add extra curves here as well.

This is not a unique choice of splitting, and in fact we have a number of possible options that would be compatible with the requirement to prevent unwanted overall factors. A second option is the splitting:

$$a_1 \to \lambda a_2, \quad a_3 \to \kappa a_7\,. \tag{3.12}$$

With this choice, the fiveplets are now

$$P_a = a_2 \left(a_7 \left(a_6 \kappa + a_2 \right) - a_0 a_6^2 \lambda \right) \tag{3.13}$$

and

$$P_b = a_7 \left(a_6^2 \kappa + a_2 \left(a_7 \lambda + a_6 \right) \right) . \tag{3.14}$$

The tens now reads $P_{10} = a_1 a_6 \to \lambda a_2 a_6$.

In the same way we can find a number of available combinations that leads in suitable splits. In Table 3.4 we show the most interesting case

$$a_1 \to \kappa a_2, \quad a_3 \to \lambda a_7, \quad \text{and} \quad a_6 \to \mu a_2. \tag{3.15}$$

As we can see (3.15) leads in a maximal factorisation for the fiveplets (six factors) and the tenplets (four factors). The discriminant is computed to be

$$\Delta = -a_0^2 a_2^2 (a_6 + 4 a_7 \kappa)^2 (4 a_0 a_2 a_6 - 16 a_0 a_2 a_7 \kappa - a_7^2 \lambda^2) \tag{3.16}$$

and as we can see it is not a square, while at the same time the b_k's do not asquire a common factor. Very important for model building reasons are the homologies of the matter curves. Thus we need to compute the homologies of the new coefficients κ, λ and μ. These can be computed easily from (3.15), since we already know the homologies of a_i's coefficients. We find that:

$$[\kappa] = -c_1, \quad [\mu] = -[\lambda] = 4c_1 + 2\chi - \eta. \tag{3.17}$$

Using the above, we can calculate the homologies of the all new factors of the tenplets and fiveplets. Notice that the distribution of the the tenplets and fiveplets on the various matter curves has be done in an almost arbitrary way. This case is of particular interest because we have seen that we have four tenplets of the GUT group, while we will also have six of the fiveplets provided we interpret the trivial singlets as one representation. This last assumption seems reasonable given that they are otherwise indistinguishable.

Flux Restrictions

In order to finally marry the two understandings present so far, we must appeal to flux restrictions. We summarise the homologies of the various matter curves in Table 3.5 and Table 3.6 with this in mind. Let us assume the usual flux restriction rules. We denote with $\mathcal{F}_Y$ the $U(1)_Y$ flux which breaks $SU(5)$ to the SM and at the same time generates chirality to the fermions. In order to avoid a Green-Schwarz mass for the corresponding gauge boson we must require $\mathcal{F}_Y \cdot \eta = \mathcal{F}_Y \cdot c_1 = 0$. For the unspecified homology χ we parametrise the corresponding flux restriction with an arbitrary integer $N = \mathcal{F}_Y \cdot \chi$, hence we have the constraints:

$$\mathcal{F}_Y \cdot \chi = N, \ \mathcal{F}_Y \cdot c_1 = \mathcal{F}_Y \cdot \eta = 0 \, . \tag{3.18}$$

$P_{10} = \kappa\mu a_2^2$		
Curve	factor	Homology
10_1	κ	$-c_1$
10_2	a_2	$\eta - 4c_1 - \chi$
10_3	a_2	$\eta - 4c_1 - \chi$
10_4	μ	$-\eta + 4c_1 + 2\chi$

Table 3.5: Distribution of the tenplets of the model along with the corresponding homologies according to the new factorisation, $P_{10} = \kappa\mu a_2^2$.

$P_b = a_2 a_7 \left(\kappa a_7 + (\lambda\mu + 1)\mu a_2\right)$			
Curve	t_5 charge	factor	Homology
$\bar{5}_a$	1	a_2	$\eta - 4c_1 - \chi$
$\bar{5}_b$	1	a_7	$c_1 + \chi$
$\bar{5}_c$	1	$\kappa a_7 + (\lambda\mu + 1)\mu a_2$	χ
$P_a = a_2^2 \left(a_7 + \lambda\mu a_7 - \alpha_0 \kappa \mu^2 a_2\right)$			
Curve	t_5 charge	factor	Homology
$\bar{5}_d$	0	a_2	$\eta - 4c_1 - \chi$
$\bar{5}_e$	0	a_2	$\eta - 4c_1 - \chi$
$\bar{5}_f$	0	$a_7 + \lambda\mu a_7 - \alpha_0 \kappa \mu^2 a_2$	$c_1 + \chi$

Table 3.6: Distribution of the fiveplets into P_a and P_b along with their perpendicular charges, defining factors and the corresponding homology classes. As we can see P_b is related with the t_5 charge.

We shall also assume the doublet-triplet splitting mechanism to be powered by this flux. Indeed, assuming N units of hyperflux piercing a given matter curve, the $5/\bar{5}$ split according to:

$$\begin{aligned} n(3,1)_{-1/3} - n(\bar{3},1)_{+1/3} &= M_5 \,, \\ n(1,2)_{+1/2} - n(1,2)_{-1/2} &= M_5 + N \,. \end{aligned} \tag{3.19}$$

Thus, as long as $N \neq 0$, for the fives residing on a given matter curved the number of doublets differs from the number of triplets in the effective theory. Choosing $M_5 = 0$ for a Higgs matter curve the coloured triplet-antitriplet fields appear only in pairs which under certain conditions [118, 155] form heavy massive states. On the other hand, the difference of the doublet-antidoublet fields is non-zero and is determined solely from the hyperflux integer parameter N. Similarly, on a matter curve accommodating fermion generations, Equation (3.19) implies different numbers of lepton doublets and down quarks on this particular matter curve. As a consequence, the corresponding mass matrices are expected to differ, avoided that way unwanted mass relations at the GUT scale.

Similarly, the 10s decompose under the influence of N hyperflux units to the following SM-

GUT rep	Def. Eqn.	Parity:	Matter content
10_1	κ	$-$	$M_1 Q_L + u_L^c M_1 + e_L^c M_1$
10_2	a_2	a	$M_2 Q_L + u_L^c (M_2 + N) + e_L^c (M_2 - N)$
10_3	a_2	a	$M_3 Q_L + u_L^c (M_3 + N) + e_L^c (M_3 - N)$
10_4	μ	$\frac{parity(a_6)}{a}$	$M_4 Q_L + u_L^c (M_4 - 2N) + e_L^c (M_4 + 2N)$
5_a	a_2	a	$M_a \bar{d}_L^c + (M_a - N)\bar{L}$
5_b	a_7	b	$M_d D_u + (M_d + N) H_u$
5_c	κa_7	$-b$	$M_c \bar{d}_L^c + (M_c + N)\bar{L}$
5_d	a_2	a	$M_b \bar{D}_d + (M_b - N)\bar{H}_d$
5_e	a_2	a	$M_e \bar{d}_L^c + (M_e - N)\bar{L}$
5_f	a_7	b	$M_f \bar{d}_L^c + (M_f + N)\bar{L}$

Table 3.7: The generalized matter spectrum of the model. The table shows the GUT matter curves along with their defining spectral cover equations, the geometric parity assignments and the flux data. Here $a = parity(a_2)$ and $b = parity(a_7)$, by convention.

representations:

$$\begin{aligned} n(3,2)_{+1/6} - n(\bar{3},2)_{-1/6} &= M_{10}\,, \\ n(\bar{3},1)_{-2/3} - n(3,1)_{+2/3} &= M_{10} - N\,, \\ n(1,1)_{+1} - n(1,1)_{-1} &= M_{10} + N\,. \end{aligned} \tag{3.20}$$

Hence, similar to the fivplets above, the flux effects have analogous implications on the tenplets. The first line in (3.20) in particular, generates the required up-quark chirality since for $M_{10} \neq 0$ the number of $Q = (3,2)_{1/6}$ differs from $\bar{Q} = (\bar{3},2)_{-1/6}$ representations. Moreover, from the second line it is to be observed that $N \neq 0$ leads to further splitting between the $Q = (3,2)_{1/6}$ and $u^c = (\bar{3},1)_{-2/3}$ multiplicities. This fact as we will see provides interesting non-trivial quark mass matrix textures.

3.3 Constructing An $N = 1$ Model

Referring to the aforementioned geometric symmetry discussed at length in previous Chapter (see also the Appendix B for the implementation of a geometric parity on the $C_4 \times C_1$ case discussed here), we may start out by assigning a Z_2 symmetry to our matter curves, Table 3.8. We shall demand some doublet-triplet splitting in our model, so we take the liberty of setting $N = 1$, motivated by a desire to produce a spectrum free of Higgs colour triplets.

The Z_2 parity has arbitrary phases connecting the coefficients in two cycles: $a_{1,\ldots,5}$ and $a_{6,7}$, which we must choose so that we can best fit the standard matter parity of the MSSM. The generalised parities of the matter curves are presented in Table 3.7. If we start with a handful of basic requirements it becomes quickly apparent how to do this and guides our assignments of the D_4 irreducible representations.

GUT rep	Def. Eqn.	Parity:	$(-,-)$	$(+,-)$	$(-,+)$	$(+,+)$	$N=1$ Matter spectrum
10_1	κ	$-$	$-$	$-$	$-$	$-$	$M_1 Q_L + u_L^c M_1 + e_L^c M_1$
10_2	a_2	a	$-$	$+$	$-$	$+$	$M_2 Q_L + u_L^c (M_2+1) + e_L^c (M_2-1)$
10_3	a_2	a	$-$	$+$	$-$	$+$	$M_3 Q_L + u_L^c (M_3+1) + e_L^c (M_3-1)$
10_4	μ	$\frac{parity(a_6)}{a}$	$-$	$+$	$+$	$-$	$M_4 Q_L + u_L^c (M_4-2) + e_L^c (M_4+2)$
5_a	a_2	a	$-$	$+$	$-$	$+$	$M_a \bar{d}_L^c + (M_a-1)\bar{L}$
5_b	a_7	b	$-$	$-$	$+$	$+$	$M_d D_u + (M_d+1) H_u$
5_c	κa_7	$-b$	$+$	$+$	$-$	$-$	$M_c \bar{d}_L^c + (M_c+1)\bar{L}$
5_d	a_2	a	$-$	$+$	$-$	$+$	$M_b \bar{D}_d + (M_b-1)\bar{H}_d$
5_e	a_2	a	$-$	$+$	$-$	$+$	$M_e \bar{d}_L^c + (M_e-1)\bar{L}$
5_f	a_7	b	$-$	$-$	$+$	$+$	$M_f \bar{d}_L^c + (M_f+1)\bar{L}$

Table 3.8: General properties of a model with flux parameter $N=1$. All the possible parity options are parametrized in two cycles ($a=\pm, b=\pm$). Any matter curve that has a D_4-doublet must produce doublets - i.e. split twice as fast.

- We must ensure the existence of a tree-level top Yukawa coupling.
- We wish to forbid all the dangerous dimension 4 proton decay terms- which may be achieved if our Higgs have $+$ parity and our matter $-$ parity similar to the conventional R-parity of the MSSM.
- We want a spectrum that resembles the MSSM.

If we examine Table 3.8, we can see that in order to be free from $D_{u,d}$ matter, we should choose the parity option $a=b=+$. The subtlety here is that the H_u and H_d must be on matter curves that have different homologies so that if we set the multiplicity for those curves to zero (preventing the $D_{u,d}$ matter), the flux naturally pushes the H_u to be on a 5 of the GUT group, while it pushes the H_d to be a $\bar{5}$.

We now select our multiplicities M_i as follows:

$$\begin{aligned} M_2 =& M_3 = M_b = M_d = 0, \\ M_1 =& M_a = M_e = -M_f = 1, \\ M_4 =& 2, \\ M_c =& -4. \end{aligned}$$

This returns a spectrum that has only a tree-level top Yukawa coupling, the desired number of matter generations, and only $u^c d^c d^c$ dimension 4 parity violating operators, which should shield us from the most dangerous proton decay effects. The spectrum is summarized in Table 3.9.

GUT rep	Def. Eqn.	Parity	Matter content	D_4 rep.	t_5 charge
10_1	κ	$-$	$Q_L + u_L^c + e_L^c$	1_{+-}	0
10_2	a_2	$+$	$u_L^c - e_L^c$	1_{++}	0
10_3	a_2	$+$	$u_L^c - e_L^c$	1_{++}	1
10_4	μ	$-$	$2Q_L + 4e_L^c$	2	0
5_a	a_2	$+$	$2\bar{d}_L^c$	2	0
5_b	a_7	$+$	H_u	1_{++}	0
5_c	κa_7	$-$	$-4\bar{d}_L^c - 3\bar{L}$	1_{+-}	0
5_d	a_2	$+$	$-\bar{H}_d$	1_{++}	-1
5_e	a_2	$+$	$\bar{d}_L^c$	1_{+-}	-1
5_f	a_7	$+$	$-2\bar{d}_L^c$	2	-1

Table 3.9: Full spectrum for an $SU(5) \times D_4 \times U(1)_{t_5}$ model from an F-theory background. Note that the $-t_5$ charge corresponds to the 5, while any representations that are a $\bar{5}$ will instead have t_5.

Singlet	Parity	D_4 rep.	t_5 charge	Vacuum Expectation
θ_α	$+$	1_{++}	-1	$\langle\theta_\alpha\rangle = \alpha$
θ_β	$-$	1_{+-}	-1	$\langle\theta_\beta\rangle = \beta$
θ_γ	$+$	2	-1	$\langle\theta_\gamma\rangle = (\gamma_1, \gamma_2)$
θ_a	$+$	2	0	$\langle\theta_a\rangle = (a_1, a_2)$
ν_r	$-$	1_{+-}	0	$-$
ν_R	$-$	2	0	$-$

Table 3.10: Spectrum and general properties of the require singlets to construct full Yukawa matrices with the model outlined in Table 3.9.

3.3.1 Fermion Textures

Models of the form presented here allow for a large number of GUT operators, however we must ensure that all symmetries are respected. This being the case, we find that the tree-level operators found in Table 3.12, and constructed from the low energy spectrum summarised in Table 3.11, form the basis for our model, assuming the D_4 algebra rules:

$$\begin{aligned} 2{\times}2 &= 1_{++} + 1_{+-} + 1_{-+} + 1_{--}\,, \\ 1_{a,b}{\times}1_{c,d} &= 1_{ac,bd}\,, \\ \text{with: } & a, b, c, d = \pm \end{aligned}$$

As well as the expected Yukawas for the quarks and charged leptons, there are also a number of parity violating operators that could lead to dangerous and unacceptable rates of proton decay. However, provided the singlet spectrum is aligned correctly it is possible to avoid unacceptable proton decay rates via dimension 4 operators. It will not be possible to remove all parity violating operators from the spectrum though, and we will be left with $u^c d^c d^c$ operators that may facilitate neutron-antineutron oscillations. It is also possible to remove vectorlike pairs

Low Energy Spectrum	D_4 rep	$U(1)_{t_5}$	Z_2
Q_3, u_3^c, e_3^c	1_{+-}	0	$-$
u_2^c	1_{++}	1	$+$
u_1^c	1_{++}	0	$+$
$Q_{1,2}, e_{1,2}^c$	2	0	$-$
L_i, d_i^c	1_{+-}	0	$-$
ν_3^c	1_{+-}	0	$-$
$\nu_{1,2}^c$	2	0	$-$
H_u	1_{++}	0	$+$
H_d	1_{++}	-1	$+$

Table 3.11: A summary of the low energy spectrum of the model considered. The charges include the Standard Model matter content, the D_4 family symmetry, the remaining $U(1)_{t_5}$ from the commutant $SU(5)$ descending from E_8 orthogonally to the GUT group, and finally the geometric Z_2 symmetry assignments.

Operator$\rightarrow$ type	D_4 irrep.	t_5 charge	Z_2 parity
$10_1 10_1 5_b \rightarrow QUH$	1_{++}	0	$+$
$10_1 10_2 5_b \rightarrow QUH$	1_{+-}	0	$-$
$10_1 10_3 5_b \rightarrow QUH$	1_{+-}	1	$-$
$10_4 10_1 5_b \rightarrow QUH$	2	0	$+$
$10_4 10_2 5_b \rightarrow QUH$	2	0	$-$
$10_4 10_3 5_b \rightarrow QUH$	2	1	$-$
$10_1 \bar{5}_c \bar{5}_d \rightarrow QDH$	1_{++}	1	$+$
$10_4 \bar{5}_c \bar{5}_d \rightarrow QDH$	2	1	$+$
$10_1 \bar{5}_c \bar{5}_d \rightarrow LEH$	1_{++}	1	$+$
$10_4 \bar{5}_c \bar{5}_d \rightarrow LEH$	2	1	$+$
$10_1 \bar{5}_c \bar{5}_c \rightarrow UDD$	1_{+-}	0	$-$
$10_2 \bar{5}_c \bar{5}_c \rightarrow UDD$	1_{++}	0	$+$
$10_3 \bar{5}_c \bar{5}_c \rightarrow UDD$	1_{++}	1	$+$
$10_1 \bar{5}_c \bar{5}_c \rightarrow QLD$	1_{+-}	0	$-$
$10_4 \bar{5}_c \bar{5}_c \rightarrow QLD$	2	0	$-$
$10_1 \bar{5}_c \bar{5}_c \rightarrow ELL$	1_{+-}	0	$-$
$10_4 \bar{5}_c \bar{5}_c \rightarrow ELL$	2	0	$-$

Table 3.12: List of all the possible trilinear couplings available in the SU(5) $\times D_4 \times U(1)$ model presented. At tree-level, these operators are not all immediately allowed, since the combined $D_4 \times U(1)$ family symmetry along with the geometric Z_2 parity must be respected.

from the spectrum to insure a low energy matter content similar to the MSSM.

Quark sector

The up-type quark sector have four operators which contribute to the corresponding Yukawa matrix. Firstly, we have a tree level top quark coming from the operator $10_1 10_1 5_b$, which is the only tree level Yukawa operator found in the quark and charged Lepton sectors. The remaining three terms are non-renormalisable operators subject to suppression. We shall assume that the up-type Higgs gets a vacuum expectation value, $\langle H_u \rangle = v_u$. The singlets involved must have VEVs as summarised in Table 3.10. The following mass terms are generated

$$\begin{aligned} 10_1 10_1 5_b &\to y_1 v_u Q_3 u_3^c \\ 10_4 10_1 5_b \theta_a &\to y_2 v_u (Q_2 a_2 + Q_1 a_1) u_3^c \\ 10_4 10_3 5_b \theta_a \theta_\beta &\to y_3 v_u \beta (Q_2 a_2 + Q_1 a_1) u_2^c \\ 10_1 10_3 5_b \theta_\beta &\to y_4 v_u \beta Q_3 u_2^c \end{aligned}$$

giving rise to the following texture for the up-quark mass matrix

$$M_{u,c,t} = v_u \begin{pmatrix} 0 & y_3 a_1 \beta & y_2 a_1 \\ 0 & y_3 a_2 \beta & y_2 a_2 \\ 0 & y_4 \beta & y_1 \end{pmatrix}.$$

The lightest generation does not get an explicit mass from this mechanism, but we can expect a small correction to come from non-commutative fluxes or instanton effects [141, 147, 152], thus generating a small mass for the first generation.

The down-type quarks contribute a further two operators to the model. These will be symmetric across the right-handed d^c since all three generations are found on the 5_c matter curve. We once again assume the down type Higgs to receive a VEV, $\langle H_d \rangle = v_d$. Similar to the up-sector, we also give the singlets a vacuum expectation value: $\langle \theta_\alpha \rangle = \alpha$ and $\langle \theta_\gamma \rangle = (\gamma_1, \gamma_2)^T$. As a result, we get the following Yukawa contributions

$$\begin{aligned} 10_1 \bar{5}_c \bar{5}_d \theta_\alpha &\to y_{4,i} v_d Q_3 d_i^c \alpha \\ 10_4 \bar{5}_c \bar{5}_d \theta_\gamma &\to y_{5,i} v_d (Q_2 \gamma_2 + Q_1 \gamma_1) d_i^c \end{aligned}$$

and consequently, the down quark mass matrix form

$$M_{d,s,b} = v_d \begin{pmatrix} y_{5,1}\gamma_1 & y_{5,2}\gamma_1 & y_{5,3}\gamma_1 \\ y_{5,1}\gamma_2 & y_{5,2}\gamma_2 & y_{5,3}\gamma_2 \\ y_{4,1}\alpha & y_{4,2}\alpha & y_{4,3}\alpha \end{pmatrix}.$$

However, this mass matrix will be subject to the rank theorem, requiring that there be some suppression factor between the copies of the operator, which we indicate by the second index, $y_{i,j}$.

Charged Leptons

The Charged Lepton Yukawas are determined by the same operators as the Down-type quarks, subject to a transpose. As such their mass matrix is as follows:

$$10_1\bar{5}_c\bar{5}_d\theta_\alpha \to y_{6,i}v_d L_i e_3^c\alpha$$
$$10_4\bar{5}_c\bar{5}_d\theta_\gamma \to y_{7,i}v_d L_i(e_2^c\gamma_2 + e_1^c\gamma_1)$$
$$M_{e,\mu,\tau} = v_d \begin{pmatrix} y_{7,1}\gamma_1 & y_{7,1}\gamma_2 & y_{6,1}\alpha \\ y_{7,2}\gamma_1 & y_{7,2}\gamma_2 & y_{6,2}\alpha \\ y_{7,3}\gamma_1 & y_{7,3}\gamma_2 & y_{6,3}\alpha \end{pmatrix}.$$

The mass relations between charged leptons and down-type quarks will not be constrained to be exact as the operators can be assumed to be localized to different parts of the GUT surface. Once again this is subject to the rank theorem, but will be able to produce a light first generation through other mechanisms.

Neutrino sector

Various ideas and mechanisms have been proposed through the time for the description of light neutrino masses m_i and mixing angles θ_{ij}. As we have discussed in the first chapter, perhaps the most elegant choice is the classical see-saw mechanism, in which the observed smallness of neutrino masses is explained due to the existence of heavy right-handed Majorana neutrinos [32],

$$m^\nu = -m^D M_R^{-1}(m^D)^T,$$

where m^ν is the light effective Majorana neutrino mass matrix (i.e. the physical neutrino mass matrix), m^D is the Dirac mass matrix and M_R is the (heavy) Majorana mass matrix. In general, the see-saw mechanism predicts Majorana neutrinos, however has nothing to say about the neutrinos "mass hierarchy", nor does it yield any understanding of lepton mixing. In most of the cases, in order to overcome these difficulties, the see-saw mechanism must be supplemented by other ingredients (for reviews see e.g. [194, **?**, 196, 197]).

In F-theory, neutrinos may admit both Dirac and Majorana mass terms due to the existence of extra singlets states. As such, F-theory provides all the necessary ingredients to use the see-saw mechanism in order to achieve small neutrino masses via a GUT scale Majorana type mass. Any Dirac type mass comes from an operator of the form $m_D \sim \theta_\nu 5_b\bar{5}_c$, while the right-handed Majorana mass terms are of the form $M\theta_\nu\theta_\nu$.

For the model at hand, the singlet representations and parities, as detailed in the Appendix B, allow us up to nine singlets in the present model. Let us then match our right-handed neutrinos to the representations 1_{+-} and a doublet (under D_4), as allowed from our spectrum.

This will then give the following Dirac-type operators for the neutrino sector:

$$\begin{aligned}\theta_{\nu_r} 5_b \bar{5}_c &\to y_{8,i} v_u \nu_3^c L_i \ , \\ \theta_{\nu_R} 5_b \bar{5}_c \theta_a &\to y_{9,i} v_u (\nu_1^c a_1 + \nu_2^c a_2) L_i \ ,\end{aligned}$$

$$m_D = v_u \begin{pmatrix} y_{9,1}a_1 & y_{9,1}a_2 & y_{8,1} \\ y_{9,2}a_1 & y_{9,2}a_2 & y_{8,2} \\ y_{9,3}a_1 & y_{9,3}a_2 & y_{8,3} \end{pmatrix} .$$

It is trivial to check that the Dirac matrix above has zero determinant, which will cause one neutrino to be massless. While this is not explicitly ruled-out by the experimental observations, a small mass can be generated through some higher order operators from other singlets in the spectrum if required. For example, a singlet of the type 1_{--} with + parity. This will allow an explicit Dirac type mass, however similar analysis has been done in a previous work [1]), so we omit in depth discussion here.

The Majorana terms corresponding to this choice of neutrino spectrum are simply calculated, as one might expect:

$$\begin{aligned}\theta_{\nu_r}\theta_{\nu_r} &\to m\nu_3^c\nu_3^c \ , \\ \theta_{\nu_R}\theta_{\nu_R} &\to M\nu_1^c\nu_2^c \ , \\ \theta_{\nu_r}\theta_{\nu_R}\theta_a &\to y\nu_3^c\nu_2^c a_2 + y\nu_3^c\nu_1^c a_1 \ ,\end{aligned}$$

$$M_R = \begin{pmatrix} 0 & M & ya_1 \\ M & 0 & ya_2 \\ ya_1 & ya_2 & m \end{pmatrix} .$$

This may also be allowed corrections via extra singlets, though it will not be needed for the present study.

Having write down both Dirac and Majorana mass matrices, then the effective neutrino mass can be calculated from the see-saw mechanism via $m_\nu = -m_D M_R^{-1} m_D^T$. The resulting mass matrix appears complicated, with elements given in full as:

$$\begin{aligned} m_{11} &= M{y_{8,1}}^2 + 2a_1a_2y_{9,1}(my_{9,1} - 2y_{8,1}y) \ , \\ m_{12} = m_{21} &= My_{8,1}y_{8,2} - 2a_1a_2(y_{8,2}yy_{9,1} - my_{9,2}y_{9,1} + y_{8,1}yy_{9,2}) \ , \\ m_{13} = m_{31} &= My_{8,1}y_{8,3} - 2a_1a_2(y_{8,3}yy_{9,1} - my_{9,3}y_{9,1} + y_{8,1}yy_{9,3}) \ , \\ m_{22} &= M{y_{8,2}}^2 + 2a_1a_2y_{9,2}(my_{9,2} - 2y_{8,2}y) \ , \\ m_{23} = m_{32} &= My_{8,2}y_{8,3} - 2a_1a_2(y_{8,3}yy_{9,2} - my_{9,3}y_{9,2} + y_{8,2}yy_{9,3}) \ , \\ m_{33} &= M{y_{8,3}}^2 + 2a_1a_2y_{9,3}(my_{9,3} - 2y_{8,3}y) \ , \end{aligned}$$

with an overall scaling factor of $m_0 = v_u^2(Mm - 2a_1a_2y^2)^{-1}$.

In order to extract in an easiest way the mixing parameters and mass scales of the model, we redefine the parameters of the matrix elements in the following way:

$$X_i = \frac{y_{8,i}}{y_{8,1}}, \quad \frac{Z_i}{M} = \frac{y_{9,i}}{y_{8,1}}, \quad G = \frac{2a_1a_2}{M^2} \tag{3.21}$$

with $i = 1, 2, 3$. From the above definitions it is clear that $X_1 = 1$. Note that $X_{2,3}$ and Z_j, are not always required to be order one due to the new parametrization. In addition, the neutrino matrix is greatly simplified if we further assume that: $m \approx M$. With this reduction of parameters, the elements of the mass matrix are given by:

$$\begin{aligned}
m_{11} =& \tilde{m}_0[-1 + GZ_1(2y - Z_1)] \,, \\
m_{12} = m_{21} =& \tilde{m}_0[-X_2 + G(yX_2Z_1 + yZ_2 - Z_1Z_2)] \,, \\
m_{13} = m_{31} =& \tilde{m}_0[-X_3 + G(yX_3Z_1 + yZ_3 - Z_1Z_3)] \,, \\
m_{22} =& \tilde{m}_0[X_2^2 + G(2yX_2Z_2 - Z_2^2)] \,, \\
m_{23} = m_{32} =& \tilde{m}_0[-X_2X_3 + G(yX_3Z_2 + yX_2Z_3 - Z_2Z_3)] \,, \\
m_{33} =& \tilde{m}_0[-X_3^2 + G(2yX_3Z_3 - X_3^2)]
\end{aligned}$$

where now the overall scale factor is $\tilde{m}_0 = v_u^2 y_{8,1}^2 M^{-1}(Gy^2 - 1)^{-1}$. We this new matrix form in hand, we proceed with the study of the neutrino mixing parameters. Firstly, we fit the mass squared differences Δm_{ij}^2 in this model with the experimental constraints (see Table 1.2), allowing us to extract a reasonable mass scale for the neutrinos while at the same time fitting parameters to allow for acceptable mixing angles.

The results are shown in Figure 3.1. The plot on the left shows contours on the (X_2, X_3) plane, of the 3σ ranges of Δm_{31}^2 (red), Δm_{21}^2 (blue) and $R = \left|\frac{m_3^2 - m_2^2}{m_2^2 - m_1^2}\right|$ (black). Similar, the plot on the right deals with the neutrino mixing angles $\sin^2\theta_{12}$ (red), $\sin^2\theta_{23}$ (blue) and $\sin^2\theta_{13}$ (green). The plots show that there are overlap regions in the parameter space where the key variables describing the neutrino mixing, are allowed. For example, a typical set of input parameters is:

$$X_2 = 0.345,\ X_3 = 0.49,\ Z_1 = 1,\ Z_2 = 0.3,\ Z_3 = 0.204,\ G = 1.9,\ y = 0.7,\ y_{81} = 0.15$$

which returns the following values for the mass squared differences and the neutrino mixing angles

$$\begin{aligned}
&\Delta m_{21}^2 \simeq 7.41 \times 10^{-5} eV^2,\ \Delta m_{31}^2 \simeq 2.50 \times 10^{-3} eV^2,\ R = 33.78, \\
&\theta_{12} = 33.08,\ \theta_{13} = 8.63,\ \theta_{23} = 46.6.
\end{aligned} \tag{3.22}$$

This also allows us to extract the neutrino masses using the mass differences. Since the model predicts a rank-2 Dirac mass matrix, one neutrino will be massless. So then the remaining two masses are (within experimental errors) equal to the square root of the mass differences. For the input parameters given above we find :

$$m_1 = 0 \text{ meV} \,,\ m_2 \simeq 2.72 \text{ meV} \,,\ m_3 \simeq 50.8 \text{ meV} \,. \tag{3.23}$$

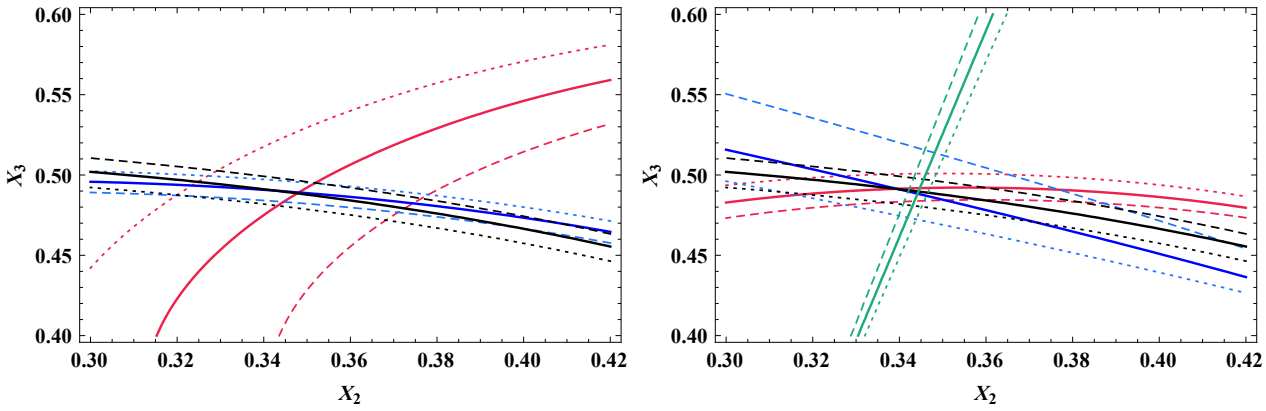

Figure 3.1: Plots of the neutrino mixing parameters of the model with respect to the experimental constraints presented in Table 1.2. The solid lines represent the best fit value (bfv) while the dashed/dotted lines display the lower/upper bounds of the 3σ range. Left: Plot of the mass square differences Δm^2_{31} (red), Δm^2_{21} (blue) and the ratio $R = |\Delta m^2_{31}|/|\Delta m^2_{21}|$ (black) for $R = 30$ (dashed), $R = 34$ (solid), $R = 38$ (dotted). Right: Plot of the neutrino mixing angles $\sin^2\theta_{12}$ (red), $\sin^2\theta_{23}$ (blue) and $\sin^2\theta_{13}$ (green). For comparison reasons with the plot on the left we have also include the ratio R (black lines). Both figures show solutions on (X_2, X_3) plane while the remaining parameters are set at values that yield consistent mixing parameters: $(Z_1 \approx 1, Z_2 \approx 0.3, Z_3 \approx 0.2, G \approx 1.9, y \approx 0.7, y_{81} \approx 0.15)$.

Of course, at this scale we are consistent with cosmological constraints for the sum of the neutrino masses (see Eq. (1.24)).

3.3.2 μ-Terms

In the model under consideration the standard Higgs sector μ-term requires coupling to a singlet in order to cancel the t_5-charges under the remaining $U(1)_\perp$ symmetry. The most suitable (trilinear) coupling allowed by the singlet sector is the following:

$$\lambda_1 \theta_\alpha H_u H_d \tag{3.24}$$

and consequently the μ-term is proportional to the VEV of the singlet θ_α:

$$\mu = \lambda_1 \langle \theta_\alpha \rangle \,. \tag{3.25}$$

Since this singlet is also participating to the charged lepton and the bottoms quark Yukawa matrices, the resulting VEV should allow a TeV scale μ-term while not affecting these Yukawas too strongly. Note that since the operators in the charged lepton and bottom quark sectors are non-renormalisable, the coupling should be suppressed by a large mass scale, making this possible. It is also shown in the D-flatness conditions (provided in the Appendix B) that we have a deal of freedom when choosing the VEV for θ_α.

A second non-renormalisable term of the type:

$$\lambda_2 \theta_a \theta_\gamma H_u H_d \tag{3.26}$$

will also contribute to the μ-term. This term should be suppressed by some large mass scale. Reffering to the flatness conditions and a cursory calculation of this coupling, we see that this

contributes proportionally to the product of the VEVs of the θ_a and θ_γ singlets. This again seems acceptable.

3.4 Baryon number violation effects

3.4.1 Proton decay

As was discussed in the first chapter, in the absence of particular types of symmetries such as R-parity, the MSSM as well as ordinary GUT symmetries are not adequate to ban rare processes leading to baryon and/or lepton number violation. Moreover, specific $SU(5)$ GUT representations include additional states leading to similar problems. Such states are the Higgs colour triplets being components of the very same fiveplets containing the up and down SM Higgs doublets. If both Higgs fields localise on the same matter curve they generate graphs contributing to proton decay from effective operators of the form $M_{GUT}^{-1}\,QQQL$. Since their Yukawa couplings are expected to be of order one, the suppression factor M_{GUT}^{-1} is not sufficient to reduce baryon number violating processes to acceptable rates.

In F-theory it is possible to turn on suitable fluxes so that the Higgs triplets are removed from the low energy spectrum. However even in this case their associated Kaluza-Klein modes generate the same type of non-renormalisable terms where now the suppression factor is replaced by the KK scale M_{KK}^{-1}. Since the M_{KK} mass scale is not expected to be substantially larger that the M_{GUT} scale, one would not expect a significant suppression of these operators. It is possible to achieve further suppression however, if the parts of the colour triplet-antitriplet pair emerge from different matter curves so that a direct tree-level mass term is not generated.

In practice, the realistic constructions are more complicated and the whole issue of baryon and lepton number violation is more involved. Firstly, as we have been analysed so far, the role of R-parity in this work is played by a Z_2 symmetry of geometric origin which does not necessarily coincide with the standard R-parity imposed in field theory supersymmetric models. Secondly, accompanying symmetries emerging from the $SU(5)_\perp$ breaking affix additional quantum numbers to the GUT representations and as such, they imply further restrictions on the superpotential of the effective theory.

We pursue our investigation, elaborating the above for the present model. Clearly, in order to establish the existence of a proton decay operator, we should pay heed to many more factors than in ordinary field theory GUTs, such as accompanying symmetries, geometric properties and flux effects. In the present model, there is a combination of constraints associated to the D_4 group, the Z_2 discrete symmetry of geometric origin as well as a $U(1)$ factor that should be respected. Although these symmetries eliminate a singificant number of unwanted operators, yet there remain trilinear terms which are potentially dangerous, which we now discuss. We start with the trilinear couplings, which take two forms,

$$10 \cdot \bar{5} \cdot \bar{5} \;\rightarrow\; Qd^cH_d + QD^cL + e^cLH_d + u^cd^cd^c \tag{3.27}$$

$$10 \cdot 10 \cdot 5 \;\rightarrow\; Qu^cH_u + u^ce^cD^c + QQD^c \tag{3.28}$$

which in principle, give rise to dimension 5 proton decay provided the following coupling exists for the Higgs colour triplet:

$$\Phi 5\bar{5} \to \langle\Phi\rangle D\, D^c \tag{3.29}$$

where Φ a suitable singlet field acquiring a non-zero vev. However, our flux choice eliminates the coloured triplets from Higgs fields (see Table 3.9) and as a result such terms do not exist.

In addition to the above type of operators, there are trilinear RPV terms that give rise to proton decay through similar graphs. Checking Table 3.12 one can see that there is a potentially dangerous baryon violating term, namely

$$10_2\bar{5}_c\bar{5}_c \tag{3.30}$$

giving rise to a $u^c d^c d^c$ operator (because of flux effects 10_2 does not contain Q, hence the operator Qd^cL does not exist). Thus, (3.30) contributes to proton decay only if analogous dimension-four operators from terms of the type $10_i 10_j 5_k$ are simultaneously present in the superpotential. In the present model such terms do not exist, hence proton stability is ensured. Nevertheless, there are other interesting implications of the above operator that could be the low energy imprint of the present model, which is discussed next.

3.4.2 Neutron-Antineutron oscillations

As mention in the previous section, the model presented is free from proton decay at the lowest orders. However, it is subject to operators which are classically considered to be parity violating. Since these operators are all of the type $u^c d^c d^c$, they will instead facilitate neutron-antineutron oscillations. While this is a seldom considered property of GUT models, work has been done to calculate transmission amplitudes of such processes by Mohapatra and Marshak [198] and later on by Goity and Sher [199] among others. The contributions to the process are generated from tree-level and box type graphs (see [199], the reviews [200, 74] and references therein), with typical cases shown in Figure 3.2.

In the paper of Goity and Sher, they argue that one can identify a competitive mechanism, with a fully calculable transition amplitude, which sets a bound on λ_{dbu}. This mechanism is based on the sequence of reactions $u_R d_R + d_L \to \tilde{b}_R^* + d_L \to (\tilde{b}_L^* + d_L \to \bar{d}_L + \tilde{b}_L) \to \bar{d}_L + \bar{u}_R \bar{d}_R$, where the intermediate transition in the parentheses, $\tilde{b}_L^* + d_L \to \bar{d}_L + \tilde{b}_L$, is due to a W boson and gaugino exchange box diagram . The choice of intermediate bottom squarks is the most favourable one in order to maximise factors such as m_b^2/m_W^2, which arise from the electroweak interactions of d-quarks in the box diagram (see 3.2).

Calculation of the diagram gives the following relation for the decay rate,

$$\Gamma = -\frac{3g^4\lambda_{dbu}^2 M_{\tilde{b}_{LR}}^2 m_{\tilde{w}}}{8\pi^2 M_{\tilde{b}_L}^4 M_{\tilde{b}_R}^4} |\psi(0)|^2 \sum_{j,j'}^{u,c,t} \xi_{jj'} J(M_{\tilde{w}}^2, M_W^2, M_{u_j}^2, M_{\tilde{u}_{j'}}^2) \tag{3.31}$$

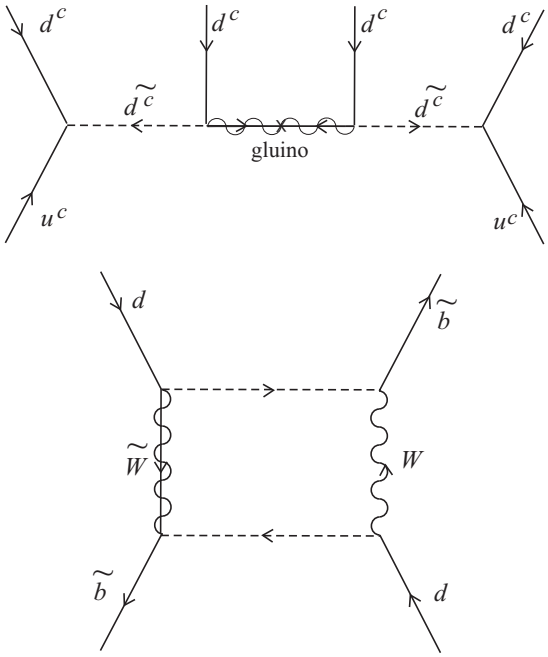

Figure 3.2: Feynman graphs for $n-\bar{n}$ oscillation processes. Top: oscillation via a gluino, Bottom: box-graph process.

where the mass term $M_{\tilde{b}_{LR}}$, which mixes $\tilde{b}_L$ and $\tilde{b}_R$, is given by $M_{\tilde{b}_{LR}} = Am_b$. Here A is the soft SUSY breaking parameter and in [199] was taken as $A = m_{\tilde{w}} = 200GeV$. Also $\xi_{jj'}$ is a combination of CKM matrix parameters,

$$\xi_{jj'} = V_{bu_j} V^{\dagger}_{u_j d} V_{bu_{j'}} V^{\dagger}_{u_{j'} d} \tag{3.32}$$

and the J functions are given by:

$$J(m_1, m_2, m_3, m_4) = \sum_{i=1}^{4} \frac{m_i^4 \ln(m_i^2)}{\prod_{k \neq i}(m_i^2 - m_k^2)} \,. \tag{3.33}$$

The n-$\bar{n}$ oscillation time is $\tau = 1/\Gamma$ and the current experimental limits gives, $\tau \gtrsim 10^8 sec.$ [200]. Finally $|\psi(0)|$ is the baryonic wave function matrix element for three quarks inside a nucleon. This parameter was calculated to be $|\psi(0)|^2 = 10^{-4}$ and $0.8 \times 10^{-4} GeV^{-6}$ in MIT Bag models[5].

Using the experimental limit on the neutron-antineutron oscillation time we can obtain bounds for the λ_{dbu} coupling. The results depend on CKM parameters and the squark masses. In Figure 3.3 we reproduce the results of Goity and Sher. As one can observe the upper bound on λ_{dbu} is between 0.005 and 0.1.

Next we use the equation (3.31) to recalculate the bounds on λ_{dbu} by consider the latest experimental results for the SUSY mass parameters. In Figure 3.4 the curves correspond to squark masses of 0.8, 1 and 1.2 TeV (solid, dashed and dotted curve accordingly). As we can

[5]Goity and Sher used a slightly more stringent bound, $\tau > 1.2 \times 10^8 sec.$ and for the matrix element they took $|\psi(0)|^2 = 3 \times 10^{-4} GeV^6$.

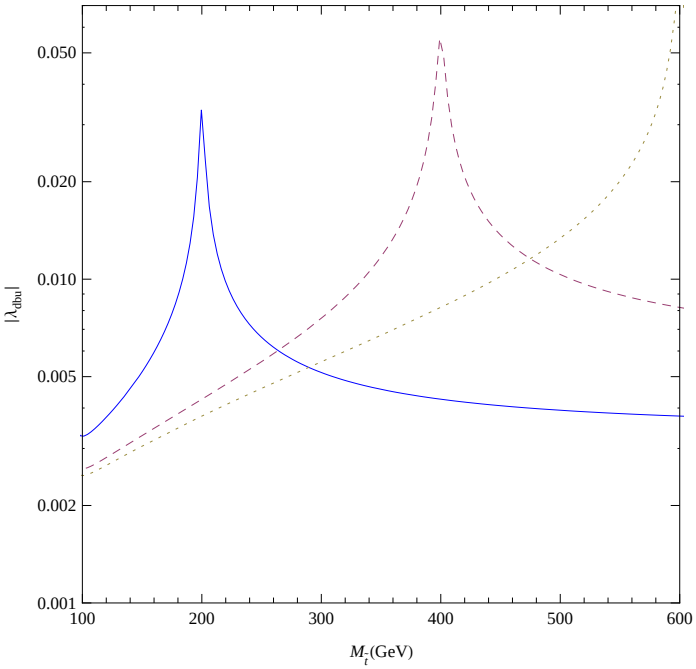

Figure 3.3: Goity and Sher bounds on the coupling λ_{dbu}. In their analysis they assumed that up and bottom squark masses are degenerate. Blue: $M_{\tilde{u}} = M_{\tilde{c}} = 200GeV$, Dashed: $M_{\tilde{u}} = M_{\tilde{c}} = 400GeV$, Dotted: $M_{\tilde{u}} = M_{\tilde{c}} = 600GeV$. Also we took $M_{\tilde{b}_L} = M_{\tilde{b}_R} = 350GeV$. The peaks corresponds to GIM cancellation mechanism effects.

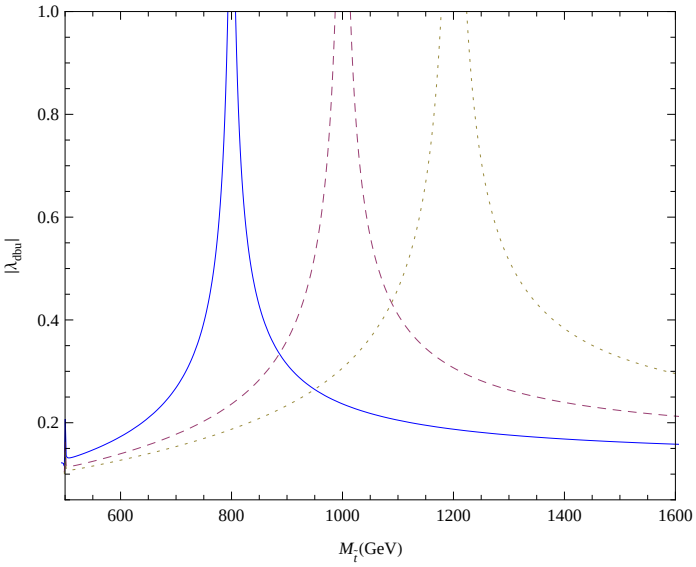

Figure 3.4: New bounds on λ_{dbu} using updated experimental limits for the SUSY parameters. Blue: $M_{\tilde{u}} = M_{\tilde{c}} = 0.8TeV$, Dashed: $M_{\tilde{u}} = M_{\tilde{c}} = 1TeV$, Dotted: $M_{\tilde{u}} = M_{\tilde{c}} = 1.2TeV$. For the other parameters participating in to the computation, the following values was used: $M_{\tilde{b}_L} = M_{\tilde{b}_R} = 0.5TeV$, $\tau = 10^8 sec.$ and $|\psi(0)| = 0.9 \times 10^{-4} GeV^{-6}$.

see the value of λ_{dbu} lies between 0.1 and ~ 0.5 for a stop mass in the range 0.5 and 1.6 TeV, neglecting the peaks coming from cancellation mechanism (GIM) effects.

In F-theory there is an associated wavefunction [139]-[150] to the state residing on each matter curve and it can be determined by solving the corresponding equations of motion [118]. The solutions show that each wavefunction is peaked along the corresponding matter curve. Yukawa couplings are formed at the point of intersection of three matter curves where the corresponding wavefunctions overlap. To estimate the corresponding Yukawa coupling we need to perform an integration over the three overlapping wavefunctions of the corresponding states participating in the trilinear coupling. Taking into account mixing effects this particular coupling is estimated to be of the order $\lambda_{dbu} \leq 10^{-1}$. From the figure it can be observed that recent $n-\bar{n}$ oscillation bounds on λ_{dbu} are compatible with such values.

On the next Chapter a more detailed analysis of RPV couplings in F-theory is presented.

Chapter 4

R-parity violation effects in F-theory

4.1 Introduction

In the previous Chapters we have analysed various phenomenological aspects of F-theory effective models using the spectral cover description. While in F-theory constructions, R-parity conservation (RPC) can emerge either as a remnant symmetry of extra $U(1)$ factors, or it can be imposed by appealing to some geometric property of the internal manifold and the flux [143], there is no compelling reason to assume this. Moreover, experimental bounds permit R-parity violating (RPV) interactions at small but non-negligible rates, providing a generic signature of F-theory models. In the field theory context, RPV proved to be the *Achilles heel* of many SUSY GUTs. The most dangerous such couplings induce the tree-level operators $QLd^c, d^cd^cu^c, e^cLL$ and in the absence of a suitable symmetry or some other kind of protecting mechanism, all of them appearing simultaneously can lead to Baryon and Lepton (B and L) violating processes at unacceptable rates [77]. On the other hand, in F-theory constructions, parts of GUT multiplets are typically projected out by fluxes, giving rise only to a part of the above operators. In other cases, due to symmetry arguments, the Yukawa couplings relevant to RPV operators are identically zero. As a result, several B/L violating processes, either are completely prevented or occur at lower rates in F-theory models, providing a controllable signal of RPV. This observation motivates a general study of RPV in F-theory, which is the subject of the present Chapter.

In the present Chapter, then, we study RPV in local F-theory constructions, trying to be as general as possible, with the goal of making a bridge connection between F-theory and experiment. An important goal of the chapter is to compute the strength of the RPV Yukawas couplings, which mainly depend on the topological properties of the internal space and are more or less independent of many details of a particular model, enabling us to work in a generic local F-theory set-up. We focus on F-theory SU(5) constructions, where a displacement mechanism, based on non-trivial fluxes, renders several GUT multiplets incomplete. This mechanism has already been suggested as a solution for the doublet-triplet splitting problem, so that dangerous dimension-5 proton decay operators are not present due to the elimination of the extra colour Higgs triplets. However, it turns out that, in several cases, not only the Higgs but also other matter multiplets are incomplete in a way that allows for trilinear RPV terms in the superpoten-

tial. In this context, it is quite common that not all of the RPV operators appear simultaneously, allowing observable RPV effects without catastrophic proton decay.

The goal here is twofold. Firstly, to present a detailed analysis of all possible combinations of RPV operators arising from a generic semi-local F-theory spectral cover framework, assuming an $SU(5)$ GUT. This includes a detailed analysis of the classification of all possible allowed combinations of RPV operators, originating from the $SU(5)$ term $10\cdot\bar{5}\cdot\bar{5}$, including the effect of $U(1)$ fluxes, with *global* restrictions, which are crucial in controlling the various possible multiplet splittings. Secondly, using F-theory techniques for the computation of Yukawa coefficients developed in the last few years, we perform explicit computations of the bottom/tau and RPV Yukawa couplings, assuming only *local* restrictions on fluxes, and comparing the results with the present experimental limits on the coupling for each specific RPV operator. The ingredients for this study have already appeared scattered through the literature, which we shall refer to as we go along.

The structure of the Chapter splits into two parts: in the first part, we consider semi-local F-theory constructions where global restrictions are imposed on the fluxes, which imply that they take integer values. In Section 4.2 we show that RPV is a generic expectation of semi-local F-theory constructions. In Section 4.2.1 we classify F-theory $SU(5)$ models in the spectral cover approach according to the type of monodromy which dictates the different curves on which the matter and Higgs fields can lie, with particular attention of the possibility for RPV operators in each case at the level of $10\cdot\bar{5}\cdot\bar{5}$ operators, involving complete $SU(5)$ multiplets, focussing on which multiplets contain the Higgs fields H_u and H_d. In Section 4.2.2 we introduce the notion of flux, quantised according to global restrictions, which, when switched on, leads to incomplete $SU(5)$ multiplets in the low energy (massless) spectrum, focussing on missing components of the multiplets projected out by the flux, and tabulating the type of physical process (RPV or proton decay) can result from particular operators involving different types of incomplete multiplets. Appendix C.1 details all possible sources of RPV couplings for all models classified with respect to the monodromies in semi-local F-theory constructions.

In the second part, we relax the global restrictions of the semi-local constructions, and allow the fluxes to take general values, subject only to local restrictions. In Section 4.3 we describe the calculation of a Yukawa coupling originating from an operator $10\cdot\bar{5}\cdot\bar{5}$ at an $SO(12)$ local point of enhancement in the presence of general local fluxes, with only local (not global) flux restrictions. In Section 4.4 we apply these methods to calculate the numerical values of Yukawa couplings for bottom, tau and RPV operators, exploring the parameter space of local fluxes. In Section 4.5 we finally consider RPV coupling regions and calculate ratios of Yukawa couplings from which the physical RPV couplings at the GUT scale can be determined and compared to limits on these couplings from experiment.

4.2 R-parity violation in F-theory semi-local approach

4.2.1 Multi-curve models in the spectral cover approach

In the present F-theory framework of $SU(5)$ GUT, third generation fermion masses are expected to arise from the tree-level superpotential terms $10_f \cdot \bar{5}_f \cdot \bar{5}_{\bar{H}}$, $10_f \cdot 10_f \cdot 5_H$ and $5_H \cdot \bar{5}_f \cdot 1_f$, where the index f stands for fermion, H for Higgs and we have introduced the notation

$$10_f = (Q, u^c, e^c),\ \bar{5}_f = (d^c, L),\ 1_f = \nu^c,\ 5_H = (D, H_u),\ \bar{5} = (\bar{D}, H_d) \tag{4.1}$$

The lighter generations receive masses from higher order terms, involving the same invariants, although suppressed by powers of $\langle\theta_i\rangle/M$, with θ_i representing available singlet fields with non-zero vacuum expectation values (vevs), while M is the GUT scale. The 4-d RPV couplings are obtained similarly with the replacements $\bar{5}_{\bar{H}} \to \bar{5}_f$ (provided that the symmetries of the theory permit the existence of such terms). At the level of the minimal supersymmetric standard model (MSSM) superpotential the RPV couplings read [74]:

$$W \supset 10_f \cdot \bar{5}_f \cdot \bar{5}_f \to \mu_i H_u L_i + \frac{1}{2}\lambda_{ijk} L_i L_j e^c_k + \lambda'_{ijk} L_i Q_j d^c_k + \frac{1}{2}\lambda''_{ijk} u^c_i d^c_j d^c_k \tag{4.2}$$

in the conventional notation for matter multiplets $Q_i, u^c_i, d^c_i, L_i, e^c_i$ where $i = 1, 2, 3$ is a flavour index. Notice that in the presence of vector-like pairs, $5_f + \bar{5}_f$, additional RPV couplings appear from the following decompositions

$$W \supset 10_f \cdot 10_f \cdot 5_f \to \kappa Q u^c \bar{L} + \kappa' u^c \bar{d}^c e^c + \frac{1}{2}\kappa'' Q Q \bar{d}^c \tag{4.3}$$

where we have introduced the notation $5_f = (\bar{d}^c, \bar{L})$ and dropped the flavour indices here for shorthand. However, as we will analyse in detail, Abelian fluxes and additional continuous or discrete symmetries which are always present in F-theory models, eliminate several of these terms. We will perform the analysis in the context of the spectral cover equation. Then, a crucial rôle on the RPV remaining terms in the effective superpotential is played by the specific assignment of fermion and Higgs fields on the various matter curves and the remaining $U(1)_\perp$'s after the monodromy action.

A classification of the set of models with simple Z-monodromies that retain some perpendicular $U(1)_\perp$ charges associated with the weights t_i has been put forward in [156, 171, 157]. In the following, we categorize these models in order to assess whether tree-level, renormalizable, perturbative RPV is generic if matter is allocated in different curves. More specifically, we present four classes, characterised by the factorisation of the spectral cover polynomial. These are:

- $2+1+1+1$-splitting, which retains three independent perpendicular $U(1)_\perp$. These models represent a Z_2 monodromy ($t_1 \leftrightarrow t_2$), and as expected we are left with seven **5** curves, and four **10** curves.

- $2+2+1$-splitting, which retains two independent perpendicular $U(1)_\perp$. These models represent a $Z_2 \times Z_2$ monodromy ($t_1 \leftrightarrow t_2$, $t_3 \leftrightarrow t_4$), and as expected we are left with five **5** curves, and three **10** curves.

- $3+1+1$-splitting, which retains two independent perpendicular $U(1)_\perp$. These models represent a Z_3 monodromy ($t_1 \leftrightarrow t_2 \leftrightarrow t_3$), and as expected we are left with five **5** curves, and three **10** curves.

- $3+2$-splitting, which retains a single perpendicular $U(1)_\perp$. These models represent a $Z_3 \times Z_2$ monodromy ($t_1 \leftrightarrow t_2 \leftrightarrow t_3$, $t_4 \leftrightarrow t_5$), and as expected we are left with three **5** curves, and two **10** curves.

In Appendix C.1 we develop the above classes of models, identifying which curve contains the Higgs fields and which contains the matter fields, in order to show that RPV is a generic phenomenon in semi-local F-theory constructions. Of course, if all the RPV operators are present, then proton decay will be a direct consequence. In the next subsection we show that this may be avoided in semi-local F-theory constructions when fluxes are switched on, which has the effect of removing some of the RPV operators, while at the same time leaving some observable RPV operators in the low energy spectrum.

4.2.2 Hypercharge flux with global restrictions and R-parity violating operators

In F-theory GUTs, the mechanism of flux breaking is introduced to reduce the GUT symmetry down to the SM gauge group. In the case of $SU(5)$ this can happen by turning on a non-trivial flux along the hypercharge generator in the internal directions. At the same time, the various components of the GUT multiplets living on matter curves, interact differently with the hypercharge flux. As a result, in addition to the $SU(5)$ symmetry breaking, on certain matter curves we expect the splitting of the 10 and $5, \bar{5}$ representations into different numbers of SM multiplets.

In a minimal scenario one might anticipate that the hyperflux is non-trivially restricted only on the Higgs matter curves in such a way that the zero modes of the colour triplet components are eliminated. This would be an alternative to the doublet-triplet scenario since only the two Higgs doublets remain in the light spectrum. The occurrence of this minimal scenario presupposes that all the other matter curves are left intact by the flux. However, in this section we show that this is usually not the case. Indeed, the common characteristic of a large class of models derived from the various factorisations of the spectral cover are that there are incomplete $SU(5)$ multiplets from different matter curves which comprise the three known generations and eventually possible extraneous fields. Interestingly, such scenarios leave open the possibility of effective models with only a fraction of RPV operators and the opportunity of studying exciting new physics implications leading to suppressed exotic decays which might be anticipated in the LHC experiments.

To analyse these cases, we assume that m_{10}, m_5 integers are units of $U(1)$ fluxes, with n_Y representing the corresponding hyperflux piercing the matter curves. The integer nature of these fluxes originates from the assumed *global* restrictions [156, 171, 157]. Then, the tenplets and

fiveplets split according to:

$$10_{t_i} = \begin{cases} \text{Representation} & \text{flux units} \\ n_{(3,2)_{1/6}} - n_{(\bar{3},2)_{-1/6}} & = m_{10} \\ n_{(\bar{3},1)_{-2/3}} - n_{(3,1)_{2/3}} & = m_{10} - n_Y \\ n_{(1,1)_{+1}} - n_{(1,1)_{-1}} & = m_{10} + n_Y \end{cases} \tag{4.4}$$

$$5_{t_i} = \begin{cases} \text{Representation} & \text{flux units} \\ n_{(3,1)_{-1/3}} - n_{(\bar{3},1)_{+1/3}} & = m_5 \\ n_{(1,2)_{+1/2}} - n_{(1,2)_{-1/2}} & = m_5 + n_Y \end{cases} \tag{4.5}$$

The integers $m_{10,5}, n_Y$ may take any positive or negative value, leading to different numbers of SM representations, however, for our purposes it is enough to assume the cases [1] $m, n_Y = \pm 1, 0$. Then, substituting these numbers in Eqs. (4.4,4.5) we obtain the cases of Table 4.1.

10	Flux units	10 content	$\bar{5}$	Flux units	$\bar{5}$ content
10_1	$m_{10} = 1, n_Y = 0$	$\{Q, u^c, e^c\}$	$\bar{5}_1$	$m_5 = 1, n_Y = 0$	$\{d^c, L\}$
10_2	$m_{10} = 1, n_Y = 1$	$\{Q, -, 2e^c\}$	$\bar{5}_2$	$m_5 = 1, n_Y = 1$	$\{d^c, 2L\}$
10_3	$m_{10} = 1, n_Y = -1$	$\{Q, 2u^c, -\}$	$\bar{5}_3$	$m_5 = 1, n_Y = -1$	$\{d^c, -\}$
10_4	$m_{10} = 0, n_Y = 1$	$\{-, \bar{u}^c, e^c\}$	$\bar{5}_4$	$m_5 = 0, n_Y = 1$	$\{-, L\}$
10_5	$m_{10} = 0, n_Y = -1$	$\{-, u^c, \bar{e}^c\}$	$\bar{5}_5$	$m_5 = 0, n_Y = -1$	$\{-, \bar{L}\}$

Table 4.1: Table of MSSM matter content originating from $10, \overline{10}, 5, \bar{5}$ of $SU(5)$ for various fluxes

Depending on the specific choice of m, n_Y integer parameters, we end up with incomplete $SU(5)$ representations. For convenience we collect all distinct cases of incomplete $SU(5)$ multiplets in Table 4.1.

We now examine all RPV operators formed by trilinear terms involving incomplete representations. Table 4.2 summarises the possible cases emerging form the various combinations $10_a \bar{5}_b \bar{5}_c$ of the incomplete representations shown in Table 4.1.

In the last column of Table 4.2 we also show the dominant RPV processes, which lead to baryon and/or lepton number violation. We notice however, that there exist other rare processes beyond those indicated in the tables which can be found in reviews (see for example [74].) We have already stressed, that in addition to the standard model particles, some vector-like pairs may appear too. For example, when fluxes are turned on, we have seen in several cases that the MSSM spectrum is accompanied in vector like states such as:

$$u^c + \bar{u}^c, L + \bar{L}, d + \overline{d}^c, Q + \overline{Q} \ldots$$

Of course they are expected to get a heavy mass but if some vector-like pairs remain in the light spectrum they may have significant implications in rare processes, such as contributions to diphoton events which are one of the primary searches in the ongoing LHC experiments [6].

[1] Of course there are several combinations of (m, n_Y) values which do not exceed the total number of three generations. Here, in order to illustrate the point, we consider only the cases with $m, n_Y = \pm 1, 0$.

$SU(5)$-invariant	matter content	operators	Dominant $\not{R}$-process
$10_1 \cdot \bar{5}_1 \cdot \bar{5}_1$	$(Q, u^c, e^c)(d^c, L)^2$	All	proton decay
$10_1 \cdot \bar{5}_2 \cdot \bar{5}_2$	$(Q, u^c, e^c)(d^c, 2L)^2$	All	proton decay
$10_1 \cdot \bar{5}_3 \cdot \bar{5}_3$	$(Q, u^c, e^c)(d^c, -)^2$	$u^c d^c d^c$	$n - \bar{n}$-osc.
$10_1 \cdot \bar{5}_4 \cdot \bar{5}_4$	$(Q, u^c, e^c)(-, L)^2$	LLe^c	$L_{e,\mu,\tau}$-violation
$10_1 \cdot \bar{5}_5 \cdot \bar{5}_5$	$(Q, u^c, e^c)(-, \bar{L})^2$	None	None
$10_2 \cdot \bar{5}_1 \cdot \bar{5}_1$	$(Q, -, e^c)(d^c, L)^2$	QLd^c, LLe^c	$L_{e,\mu,\tau}$-violation
$10_2 \cdot \bar{5}_2 \cdot \bar{5}_2$	$(Q, -, e^c)(d^c, 2L)^2$	QLd^c, LLe^c	$L_{e,\mu,\tau}$-violation
$10_2 \cdot \bar{5}_3 \cdot \bar{5}_3$	$(Q, -, e^c)(d^c, -)^2$	None	None
$10_2 \cdot \bar{5}_4 \cdot \bar{5}_4$	$(Q, -, e^c)(-, L)^2$	LLe^c	$L_{e,\mu,\tau}$-violation
$10_2 \cdot \bar{5}_5 \cdot \bar{5}_5$	$(Q, -, e^c)(-, \bar{L})^2$	None	None
$10_3 \cdot \bar{5}_1 \cdot \bar{5}_1$	$(Q, 2u^c, -)(d^c, L)^2$	$QLd^c, d^c d^c u^c$	proton decay
$10_3 \cdot \bar{5}_2 \cdot \bar{5}_2$	$(Q, 2u^c, -)(d^c, 2L)^2$	$QLd^c, d^c d^c u^c$	proton decay
$10_3 \cdot \bar{5}_3 \cdot \bar{5}_3$	$(Q, 2u^c, -)(d^c, -)^2$	$d^c d^c u^c$	$n - \bar{n}$-osc.
$10_3 \cdot \bar{5}_4 \cdot \bar{5}_4$	$(Q, 2u^c, -)(-, L)^2$	None	None
$10_3 \cdot \bar{5}_5 \cdot \bar{5}_5$	$(Q, 2u^c, -)(-, \bar{L})^2$	None	None

Table 4.2: Fluxes, incomplete representations and $\not{R}$-processes emerging from the trilinear coupling $10_a \bar{5}_b \bar{5}_c$ for all possible combinations of the incomplete multiplets given in Table 4.1

.

4.3 Yukawa couplings in local F-theory constructions: formalism

In what follows we relax the global constraints on fluxes, and consider the calculation of Yukawa couplings, imposing only local flux constraints. The motivation for doing this is to calculate the Yukawa couplings associated with the RPV operators in a rather model independent way, and then compare our results to experimental limits. Flavour hierarchies and Yukawa structures in F-theory have been studied in many works so far [139]-[154]. In this section we shall discuss Yukawa couplings in F-theory, following mainly the approach of [144, 147, 150].

In the previous section we saw how chirality is realised on different curves due to flux effects. These considerations take into account the global flux data and are therefore called semi-local models. The flux units considered in the examples above are integer valued as they follow from the Dirac flux quantisation contition

$$\frac{1}{2\pi}\int_{\Sigma \subset S} F = n \tag{4.6}$$

where n is an integer, Σ a matter curve (two-cycle in the GUT divisor S), and F the gauge field-strength tensor, i.e. the flux. In conjugation with the index theorems, the flux units piercing different matter curves Σ will tell us how many chiral states are globally present in a model.

While the semi-local approach defines the full spectrum of a model, the computation of localised quantities in a microscopic level, such as the Yukawa couplings, requires appropriate

description of the local geometry. A key quantity in this ultra local approach is the notion of *local* flux density, which is described below.

First we notice that the unification gauge coupling is related to the compactification scale through the volume of the compact space [119], [140]

$$\alpha_G^{-1} = m_*^4 \int_S 2\omega \wedge \omega = m_*^4 \int \mathrm{dVol}_S = \mathrm{Vol}(S) m_*^4 \tag{4.7}$$

where α_G is the unification gauge coupling, m_* is an F-Theory characteristic mass, S the GUT divisor with Kähler form

$$\omega = \frac{i}{2}(dz_1 \wedge d\bar{z}_1 + dz_2 \wedge d\bar{z}_2) \tag{4.8}$$

that defines the volume form

$$\mathrm{dVol}_S = 2\omega \wedge \omega = dz_1 \wedge dz_2 \wedge d\bar{z}_1 \wedge d\bar{z}_2. \tag{4.9}$$

As the volume of Σ is bounded by the volume of S, we assume that

$$\mathrm{Vol}(\Sigma) \simeq \sqrt{\mathrm{vol}(S)}, \tag{4.10}$$

and if we now consider that the background of F is constant, we can estimate the values that F takes in S by

$$F \simeq 2\pi\sqrt{\alpha_G} m_*^2 n. \tag{4.11}$$

This means that, in units of m_*, the background F is an $\mathcal{O}(1)$ real number. Since in the computation of Yukawa couplings it's the local values of F – and not the global quantisation constraints – that matter, we will from now on abuse terminology and refer to flux densities, F, as fluxes. Furthermore, as we will see later, the local values of F also define what chiral states are supported locally. This will be crucial for the study of the behaviour of the various RPV couplings in different parts of the flux parameter space.

Before dealing with the particular rare reaction, it is useful to recall a few basic facts about the Yukawa couplings in F-Theory.

4.3.1 The $SO(12)$ point of enhancement

In F-theory matter is localised along Riemann surfaces (matter curves), which are formed at the intersections of D7-branes with the GUT surface S. Yukawa couplings are then realised when three of these curves intersect at a single point on S. At the same time, due to the tripe intersection, the gauge symmetry is further enhanced at this point. The computation relies on the knowledge of the profile of the wavefunctions of the states participating in the intersection. When a specific geometry is chosen for the internal space (and in particular for the GUT surface) these profiles are found by solving the corresponding equations of motion [141]-[150]. Their values are obtained by computing the integral of the overlapping wavefunctions at the triple intersections.

In $SU(5)$ two basic Yukawa terms are relevant when computing the Yukawa matrices and interactions. These are $\mathbf{y_u 10 \cdot 10 \cdot 5}$ and $\mathbf{y_d 10 \cdot \bar{5} \cdot \bar{5}}$. The first one generates the top Yukawa

coupling while the symmetry at this intersection enhances to the exceptional group E_6. The relevant couplings that we are interested in, are related to the second coupling. This one is realised at a point where there is an $SO(12)$ gauge symmetry enhancement[2]. To make this clear, next we highlighted some of the basic analysis of [150].

The 4-dimensional theory can be obtained by integrating out the effective 8-dimensional one over the divisor S

$$W = m_*^4 \int_S \mathrm{Tr}(F \wedge \Phi) \tag{4.12}$$

where $F = dA - iA \wedge A$ is the field-strength of the gauge vector boson A and Φ is a $(2,0)$-form on S.

From the above superpotential, the F-term equations can be computed by varying A and Φ. In conjugation with the D-term

$$D = \int_S \omega \wedge F + \frac{1}{2}[\Phi, \bar{\Phi}], \tag{4.13}$$

where ω is the Kähler form of S, a 4-dimensional supersymmetric solution for the equations of motion of F and Φ can be computed.

Both A and Φ, locally are valued in the Lie algebra of the symmetry group at the Yukawa point. In the case in hand, the fibre develops an $SO(12)$ singularity at which point couplings of the form $\mathbf{10} \cdot \bar{\mathbf{5}} \cdot \bar{\mathbf{5}}$ arise. Away from the enhancement point, the background Φ breaks $SO(12)$ down to the GUT group $SU(5)$. The rôle of $\langle A \rangle$ is to provide a 4d chiral spectrum and to break further the GUT gauge group.

More systematically, the Lie-Algebra of $SO(12)$ is composed of its Cartan generators H_i with $i = 1, ..., 6$, and 60 step generators E_ρ. Together, they respect the Lie algebra

$$[H_i, E_\rho] = \rho_i E_\rho \tag{4.14}$$

where ρ_i is the i^{th} component of the root ρ. The E_ρ generators can be completely identified by their roots

$$(\underline{\pm 1, \pm 1, 0, 0, 0, 0, 0}) \tag{4.15}$$

where underline means all 60 permutations of the entries of the vector, including different sign combinations. To understand the meaning of this notation it is sufficient to consider a simpler example:

$$(0, \underline{1, 0, 0}, 0, 0, 0) \equiv \{(0,1,0,0,0,0), (0,0,1,0,0,0), (0,0,0,1,0,0)\} \tag{4.16}$$

The background of Φ will break $SO(12)$ away from the $SO(12)$ singular point. In order to see this consider it takes the form

$$\Phi = \Phi_{z_1 z_2} dz_1 \wedge dz_2 \tag{4.17}$$

where it's now explicit that it parametrises the transverse directions to S. The background we are considering is

$$\langle \Phi_{z_1 z_2} \rangle = m^2 \left(z_1 Q_{z_1} + z_2 Q_{z_2} \right) \tag{4.18}$$

[2]For a general E_8 point of enhancement that containing both type of couplings see [149, 152]. Similar, an E_7 analysis is given in [153].

where m is related to the slope of the intersection of 7-branes, and

$$Q_{z_1} = -H_1 \tag{4.19}$$

$$Q_{z_2} = \frac{1}{2}\sum_i H_i. \tag{4.20}$$

The unbroken symmetry group will be the commutant of $\langle \Phi_{z_1 z_2} \rangle$ in $SO(12)$. The commutator between the background and the rest of the generators is

$$[\langle \Phi_{z_1 z_2} \rangle, E_\rho] = m^2 q_\Phi(\rho) E_\rho \tag{4.21}$$

where $q_\Phi(\rho)$ are holomorphic functions of the complex coordinates z_1, z_2. The surviving symmetry group is composed of the generators that commute with $\langle \Phi \rangle$ on every point of S. With our choice of background, the surviving step generators are identified to be

$$E_\rho : (0, \underline{1, -1}, 0, 0, 0), \tag{4.22}$$

which, together with H_i, trivially commute with $\langle \Phi \rangle$, generating $SU(5) \times U(1) \times U(1)$.

When $q_\Phi(\rho) = 0$ in certain loci we have symmetry enhancement, which accounts for the presence of matter curves. This happens as at these loci, extra step generators survive and furnish a representation of $SU(5) \times U(1) \times U(1)$. For the case presented we identify three curves joining at the $SO(12)$ point, these are

$$\Sigma_a = \{z_1 = 0\} \tag{4.23}$$

$$\Sigma_b = \{z_2 = 0\} \tag{4.24}$$

$$\Sigma_c = \{z_1 = z_2\}, \tag{4.25}$$

and defining a charge under a certain generator as

$$[Q_i, E_\rho] = q_i(\rho) E_\rho \tag{4.26}$$

all the data describing these matter curves are presented in Table 4.3. Since the bottom and tau Yukawas come from such an $SO(12)$ point, in order to have such a coupling the point must have the a^+, b^+, and c^+.

In order to both induce chirality on the matter curves and break the two $U(1)$ factors, we have to turn on fluxes on S valued along the two Cartan generators that generate the extra factors.

We first consider the flux

$$\langle F_1 \rangle = i(M_{z_1} dz_1 \wedge d\bar{z_1} + M_{z_2} dz_2 \wedge d\bar{z_2}) Q_F, \tag{4.27}$$

with

$$Q_F = -Q_{z_1} - Q_{z_2} = \frac{1}{2}(H_1 - \sum_{j=2}^{6} H_j). \tag{4.28}$$

Curve	Roots	q_Φ	$SU(5)$ irrep	q_{z_1}	q_{z_2}
$\Sigma_{a^\pm}$	$(\pm 1, \underline{\mp 1, 0, 0, 0, 0})$	$\mp z_1$	$\bar{\mathbf{5}}/\mathbf{5}$	∓ 1	0
$\Sigma_{b^\pm}$	$(0, \underline{\pm 1, \pm 1, 0, 0, 0})$	$\mp z_2$	$\mathbf{10}/\bar{\mathbf{10}}$	0	± 1
$\Sigma_{c^\pm}$	$(\mp 1, \underline{\mp 1, 0, 0, 0, 0})$	$\pm(z_1 - z_2)$	$\bar{\mathbf{5}}/\mathbf{5}$	± 1	∓ 1

Table 4.3: Matter curves and respective data for an $SO(12)$ point of enhancement model with a background Higgs given by Equation 4.18. The underline represent all allowed permutations of the entries with the signs fixed

It's easy to see that the $SU(5)$ roots are neutral under Q_F, and therefore this flux does not break the GUT group. On the other hand, the roots on a, b sectors are not neutral. This implies that this flux will be able to differentiate $\bar{\mathbf{5}}$ from $\mathbf{5}$ and $\mathbf{10}$ from $\bar{\mathbf{10}}$

$$\int_{\Sigma_a,\ \Sigma_b} F_1 \neq 0 \Rightarrow \text{ Induced Chirality.} \tag{4.29}$$

This flux does not induce chirality in $c^\pm$ curves as $q_F = 0$ for all roots in $c^\pm$. To induce chirality in $c^\pm$ one needs another contribution to the flux

$$\langle F_2 \rangle = i(dz_1 \wedge d\bar{z_2} + dz_2 \wedge d\bar{z_1})(N_a Q_{z_1} + N_b Q_{z_2}) \tag{4.30}$$

that does not commute with the roots on the $c^\pm$ sectors for $N_a \neq N_b$.

Breaking the GUT down to the SM gauge group requires flux along the Hypercharge. Locally we may define it as

$$\langle F_Y \rangle = i[(dz_1 \wedge d\bar{z_2} + dz_2 \wedge d\bar{z_1})N_Y + (dz_2 \wedge d\bar{z_2} - dz_1 \wedge d\bar{z_1})\tilde{N}_Y]Q_Y \tag{4.31}$$

and the Hypercharge is embedded in our model through the linear combination

$$Q_Y = \frac{1}{3}(H_2 + H_3 + H_4) - \frac{1}{2}(H_5 + H_6). \tag{4.32}$$

Since this contribution to the flux does not commute with all elements of $SU(5)$, only with its SM subgroup, distinct SM states will feel this flux differently. As we have see many times so far, this known fact is used extensively in semi-local models as a mechanism to solve the doublet-triplet splitting problem. As we will see bellow, it can also be used to locally prevent the appearance of certain chiral states and therefore forbid some RPV in subregions of the parameter space.

The total flux will then be the sum of the three above contributions. It can be expressed as

$$\begin{aligned} \langle F \rangle =& i(dz_2 \wedge d\bar{z_2} - dz_1 \wedge d\bar{z_1})Q_P \\ &+ i(dz_1 \wedge d\bar{z_2} + dz_2 \wedge d\bar{z_1})Q_S \\ &+ i(dz_2 \wedge d\bar{z_2} + dz_1 \wedge d\bar{z_1})M_{z_1 z_2} Q_F \end{aligned} \tag{4.33}$$

Sector	Root	SM	q_F	q_{z_1}	q_{z_2}	q_S	q_P
a_1	$(1,\underline{-1,0,0},0,0,0)$	$(\bar{\mathbf{3}},\mathbf{1})_{-\frac{1}{3}}$	1	-1	0	$-N_a-\frac{1}{3}N_Y$	$M-\frac{1}{3}\tilde{N}_Y$
a_2	$(1,0,0,0,\underline{-1,0})$	$(\mathbf{1},\mathbf{2})_{\frac{1}{2}}$	1	-1	0	$-N_a+\frac{1}{2}N_Y$	$M+\frac{1}{2}\tilde{N}_Y$
b_1	$(0,\underline{1,1,0},0,0,0)$	$(\bar{\mathbf{3}},\mathbf{1})_{\frac{2}{3}}$	-1	0	1	$N_b+\frac{2}{3}N_Y$	$-M+\frac{2}{3}\tilde{N}_Y$
b_2	$(0,\underline{1,0,0},\underline{1,0})$	$(\mathbf{3},\mathbf{2})_{-\frac{1}{6}}$	-1	0	1	$N_b-\frac{1}{6}N_Y$	$-M-\frac{1}{6}\tilde{N}_Y$
b_3	$(0,0,0,0,1,1)$	$(\mathbf{1},\mathbf{1})_{-1}$	-1	0	1	N_b-N_Y	$-M-\tilde{N}_Y$
c_1	$(-1,\underline{-1,0,0},0,0,0)$	$(\bar{\mathbf{3}},\mathbf{1})_{-\frac{1}{3}}$	0	1	-1	$N_a-N_b-\frac{1}{3}N_Y$	$-\frac{1}{3}\tilde{N}_Y$
c_2	$(-1,0,0,0,\underline{-1,0})$	$(\mathbf{1},\mathbf{2})_{\frac{1}{2}}$	0	1	-1	$N_a-N_b+\frac{1}{2}N_Y$	$\frac{1}{2}\tilde{N}_Y$

Table 4.4: Complete data of sectors present in the three curves crossing in an $SO(12)$ enhancement point considering the effects of non-vanishing fluxes. The underline represent all allowed permutations of the entries with the signs fixed

with the definitions

$$Q_P = MQ_F + \tilde{N}_Y Q_Y \tag{4.34}$$

$$Q_S = N_a Q_{z_1} + N_b Q_{z_2} + N_Y Q_Y \tag{4.35}$$

and

$$M = \frac{1}{2}(M_{z_1} - M_{z_2}) \tag{4.36}$$

$$M_{z_1 z_2} = \frac{1}{2}(M_{z_2} + M_{z_1}). \tag{4.37}$$

As the Hypercharge flux will affect SM states differently, breaking the GUT group, we will be able to distinguish them inside each curve. The full split of the states present in the different sectors, and all relevant data, is presented in Table 4.4.

4.3.2 Wavefunctions and the Yukawa computation

In general, the Yukawa strength is obtained by computing the integral of the overlapping wavefunctions. More precisely, according to the discussion on the previous section one has to solve for the zero mode wavefunctions for the sectors a, b and c presented in Table (4.4). The physics of the D7-Branes wrapping on S can be described in terms of a twisted 8-dimensional $\mathcal{N}=1$ gauge theory on $R^{1,3}\times S$, where S is a Kähler submanifold of elliptically fibered Calabi-Yau 4-fold X. One starts with the action of the effective theory, which was given in [119]. The next step is to obtain the equations of motion for the 7-brane fermionic zero modes. This procedure has been performed in several of papers including [149, 147, 150] and will not repeat it here in detail. In order for this Chapter to be self-contained we highlight the basic computational steps.

The equations for a 4-dimensional massless fermionic field are of the Dirac form:

$$\mathcal{D}_A \Psi = 0 \tag{4.38}$$

where

$$\mathcal{D}_A = \begin{pmatrix} 0 & D_1 & D_2 & D_3 \\ -D_1 & 0 & -D_{\bar{3}} & D_{\bar{2}} \\ -D_2 & -D_{\bar{3}} & 0 & -D_{\bar{1}} \\ -D_3 & -D_{\bar{2}} & D_{\bar{1}} & 0 \end{pmatrix} \quad , \quad \Psi = \Psi E_\rho = \begin{pmatrix} -\sqrt{2}\eta \\ \psi_{\bar{1}} \\ \psi_{\bar{2}} \\ \chi_{12} \end{pmatrix} . \tag{4.39}$$

The indices here are a shorthand notation instead of the coordinates z_1, z_2, z_3. The components of Ψ are representing 7-brane degrees of freedom. Also the covariant derivatives are defined as $D_i = \partial_i - i[\langle A_i \rangle, \ldots]$ for $i = 1, 2, \bar{1}, \bar{2}$ and as $D_{\bar{3}} = -i[\langle \Phi_{12} \rangle, \ldots]$ for the transverse coordinate z_3. It is clear from equations (4.38,4.39) that we have to solve the equations for each sector. According to the detailed solutions in [150] the wavefunctions for each sector have the general form

$$\Psi \sim f(az_1 + bz_2) e^{M_{ij} z_i z_j} \tag{4.40}$$

where $f(az_1 + bz_2)$ is a holomorphic function and M_{ij} incorporates flux effects. In an appropriate basis this holomorphic function can be written as a power of its variables $f_i \sim (az_1 + bz_2)^{3-i}$ and in the case where the generations reside in the same matter curve, the index-i can play the rôle of a family index. Moreover the Yukawa couplings as a triple wavefunction integrals have to respect geometric $U(1)$ selection rules. The coupling must be invariant under geometric transformations of the form: $z_{1,2} \to e^{i\alpha} z_{1,2}$. In this case the only non-zero tree level coupling arises for $i = 3$ and by considering that, the index in the holomorphic function f_i indicates the fermion generation we obtain a non-zero top-Yukawa coupling. Hierarchical couplings for the other copies on the same matter curve can be generated in the presence of non commutative fluxes [141] or by incorporating non-perturbative effects [147]-[153].

The RPV couplings under consideration emerge from a tree level interaction. Hence, its strength is given by computing the integral where now the rôle of the Higgs $\bar{5}_H$ is replaced by $\bar{5}_M$. We consider here the scenario where the generations are accommodated in different matter curves. In this case the two couplings, the bottom/tau Yukawa and the tree level RPV, are localised at different $SO(12)$ points on $\mathcal{S}_{GUT}$, (see Figure 4.1). In this approach, at first approximation we can take the holomorphic functions f as constants absorbed in the normalization factors.

As a first approach, our goal is to calculate the bottom Yukawa coupling as well as the coupling without hypercharge flux and compare the two values. So, at this point we write down the wavefunctions and the relevant parameters in a more detailed form as given in [150] but without the holomorphic functions. The wavefunctions in the holomorphic gauge have the

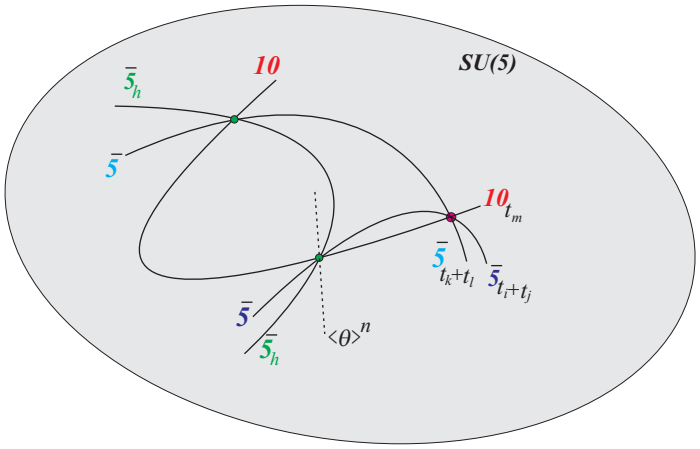

Figure 4.1: Intersecting matter curves, Yukawa couplings and the case of RPV in F-theory. The grey region represents the SU(5) GUT surface.

following form

$$\vec{\psi}^{(b)hol}_{10_M} = \vec{v}^{(b)}\chi^{(b)hol}_{10_M} = \vec{v}^{(b)}\kappa^{(b)}_{10_M} e^{\lambda_b z_2(\bar{z}_2-\zeta_b\bar{z}_1)} \tag{4.41}$$

$$\vec{\psi}^{(a)hol}_{5_M} = \vec{v}^{(a)}\chi^{(a)hol}_{5_M} = \vec{v}^{(a)}\kappa^{(a)}_{5_M} e^{\lambda_a z_1(\bar{z}_1-\zeta_a\bar{z}_2)} \tag{4.42}$$

$$\vec{\psi}^{(c)hol}_{5_H} = \vec{v}^{(c)}\chi^{(c)hol}_{5_H} = \vec{v}^{(c)}\kappa^{(c)}_{5_H} e^{(z_1-z_2)(\zeta_c\bar{z}_1-(\lambda_c-\zeta_c)\bar{z}_2)} \tag{4.43}$$

$$\vec{\psi}^{(c)hol}_{5_M} = \vec{v}^{(c)}\chi^{(c)hol}_{5_H} = \vec{v}^{(c)}\kappa^{(c)}_{5_M} e^{(z_1-z_2)(\zeta_c\bar{z}_1-(\lambda_c-\zeta_c)\bar{z}_2)}. \tag{4.44}$$

where

$$\zeta_a = -\frac{q_S(a)}{\lambda_a - q_P(a)} \tag{4.45}$$

$$\zeta_b = -\frac{q_S(b)}{\lambda_b + q_P(b)} \tag{4.46}$$

$$\zeta_c = \frac{\lambda_c(\lambda_c - q_P(c) - q_S(c)}{2(\lambda_c - q_S(c))} \tag{4.47}$$

and λ_ρ is the smallest eigenvalue of the matrix

$$m_\rho = \begin{pmatrix} -q_P & q_S & im^2 q_{z_1} \\ q_S & q_P & im^2 q_{z_2} \\ -im^2 q_{z_1} & -im^2 q_{z_2} & 0 \end{pmatrix}. \tag{4.48}$$

To compute the above quantities we make use of the values of q_i from Table 4.4. It is important to note that the values of the flux densities in this table depend on the $SO(12)$ enhancement point. This means that one can in principle have different numerical values for the strength of the interactions at different points.

The column vectors are given by

$$\vec{v}^{(b)} = \begin{pmatrix} -\frac{i\lambda_b}{m^2}\zeta_b \\ \frac{i\lambda_b}{m^2} \\ 1 \end{pmatrix}, \vec{v}^{(a)} = \begin{pmatrix} -\frac{i\lambda_a}{m^2} \\ \frac{i\lambda_a}{m^2}\zeta_a \\ 1 \end{pmatrix}, \vec{v}^{(c)} = \begin{pmatrix} -\frac{i\zeta_c}{m^2} \\ \frac{i(\zeta_c-\lambda_c)}{m^2} \\ 1 \end{pmatrix}. \tag{4.49}$$

Finally, the κ coefficients in equations (4.41-4.42) are normalization factors. These factors are fixed by imposing canonical kinetic terms for the matter fields. More precisely, for a canonically normalized field χ_i supported in a certain sector (e), the normalization condition for the wavefunctions in the real gauge is

$$1 = 2m_*^4||\vec{v}^{(e)}||^2 \int (\chi^{(e)real})_i^* \chi_i^{(e)real} \mathrm{dVol}_S \tag{4.50}$$

where $\chi_i^{(e)real}$ are now in the real gauge, and in our convention $\mathrm{Tr} E_\alpha^\dagger E_\beta = 2\delta_{\alpha\beta}$. The wavefunctions in real and holomorphic gauge are related by [144]

$$\psi^{real} = e^{i\Omega}\psi^{hol} \tag{4.51}$$

where

$$\Omega = \frac{i}{2}\left[\left(M_{z_1}|z_1|^2 + M_{z_2}|z_2|^2\right) Q_F - \tilde{N}_Y\left(|z_1|^2 - |z_2|^2\right) Q_Y + \left(z_1\bar{z}_2 + z_2\bar{z}_1\right) Q_S\right], \tag{4.52}$$

which only transforms the scalar coefficient of the wavefunctions, χ, leaving the $\vec{v}$ part invariant.

With the above considerations, one can find the normalization factors to be

$$|\kappa_{5_M}^{(a)}|^2 = -4\pi g_s\sigma^2 \cdot \frac{q_P(a)(2\lambda_a + q_P(a)(1+\zeta_a^2))}{\lambda_a(1+\zeta_a^2) + m^4}, \tag{4.53}$$

$$|\kappa_{10_M}^{(b)}|^2 = -4\pi g_s\sigma^2 \cdot \frac{q_P(b)(-2\lambda_b + q_P(b)(1+\zeta_b^2))}{\lambda_b(1+\zeta_b^2) + m^4}, \tag{4.54}$$

$$|\kappa_{5_H}^{(c)}|^2 = -4\pi g_s\sigma^2 \cdot \frac{2(q_P(c)+\zeta_c)(q_P(c)+2\zeta_c-2\lambda_c) + (q_S(c)+\lambda_c)^2}{\zeta_c^2 + (\lambda_c-\zeta_c)^2 + m^4}, \tag{4.55}$$

$$|\kappa_{5_M}^{(c)}|^2 = -4\pi g_s\sigma^2 \cdot \frac{2(q_P(c)+\zeta_c)(q_P(c)+2\zeta_c-2\lambda_c) + (q_S(c)+\lambda_c)^2}{\zeta_c^2 + (\lambda_c-\zeta_c)^2 + m^4}. \tag{4.56}$$

where we used the relation $\left(\frac{m}{m_*}\right)^2 = (2\pi)^{3/2} g_s^{1/2}\sigma$, making use of the dimensionless quantity $\sigma = (m/m_{st})^2$, where m_{st} the string scale. The expressions (4.53-4.56) above can be shown numerically to be always positive.

The superpotential trilinear couplings can be taken to be in the holomorphic gauge. For the bottom Yukawa, we consider that ψ_{10_M} and ψ_{5_M} contain the heaviest down-type quark generations. In this case the bottom and tau couplings can be computed:

$$\begin{aligned} y_{b,\tau} =& m_*^4\, t_{abc} \int_S \det(\vec{\psi}_{10_M}^{(b)hol}, \vec{\psi}_{5_M}^{(a)hol}, \vec{\psi}_{5_H}^{(c)hol}) \mathrm{dVol}_S \\ =& m_*^4\, t_{abc}\ \det(\vec{v}^{(b)}, \vec{v}^{(a)}, \vec{v}^{(c)}) \int_S \chi_{10_M}^{(b)hol} \chi_{5_M}^{(a)hol} \chi_{5_H}^{(c)hol} \mathrm{dVol}_S. \end{aligned} \tag{4.57}$$

The bottom and tau Yukawa couplings differ since they have different SM quantum numbers and arise from different sectors, leading to different q_S and q_P as shown in Table 4.4.
A similar formula can be written down for the RPV coupling

$$
\begin{aligned}
y_{RPV} =& m_*^4\ t_{abc} \int_S \det(\vec{\psi}^{(b)hol}_{10_M}, \vec{\psi}^{(a)hol}_{5_M}, \vec{\psi}^{(c)hol}_{5'_M}) \mathrm{dVol}_S \\
=& m_*^4\ t_{abc}\ \det(\vec{v}^{(b)}, \vec{v}^{(a)}, \vec{v}^{(c)}) \int_S \chi^{(b)hol}_{10_M} \chi^{(a)hol}_{5_M} \chi^{(c)hol}_{5_M} \mathrm{dVol}_S. \qquad (4.58)
\end{aligned}
$$

Here this RPV Yukawa coupling can in principle refer to any generations of squarks and sleptons, and may have arbitrary generation indices (suppressed here for simplicity).
The factor t_{abc} represents the structure constants of the $SO(12)$ group. The integral in the last term can be computed by applying standard Gaussian techniques. Computing the determinant and the integral, the combined result of the two is a flux independent factor and the final result reads:

$$
y_{b,\tau} = \pi^2 \left(\frac{m_*}{m}\right)^4 t_{abc} \kappa^{(b)}_{10_M} \kappa^{(a)}_{5_M} \kappa^{(c)}_{5_H}. \qquad (4.59)
$$

This is a standard result for the heaviest generations. As we observe the flux dependence is hidden on the normalization factors.

We turn now our attention in the case of a tree-level RPV coupling of the form $10_M \cdot \bar{5}_M \cdot \bar{5}_M$. This coupling can be computed in a different $SO(12)$ enhancement point p. As a first approach we consider that the hypercharge flux parameters are zero in the vicinity of p. From a different point of view, $\bar{5}_M$ replaces the Higgs matter curve in the previous computation. The new wavefunction ($\psi^{(c)}_{5_M}$) can be found by setting all the Hypercharge flux parameters on $\psi^{(c)}_{5_H}$, equal to zero. The RPV coupling will be given by an equation similar to that of the bottom coupling :

$$
y_{RPV} = \pi^2 \left(\frac{m_*}{m}\right)^4 t_{abc} \kappa^{(b)}_{10_M} \kappa^{(a)}_{5_M} \kappa^{(c)}_{5_M}. \qquad (4.60)
$$

and we notice that family indices are understood and this coupling is the same for every type of RPV interaction, depending on which SM states are being supported at the $SO(12)$ enhancement point. Notice that the κ's in equations (4.59, 4.60) are the modulus of the normalization factors defined in equations (4.53-4.56).

In the next section, using equations (4.59) and (4.60), we perform a numerical analysis for the couplings presented above with emphasis on the case of the RPV coupling. We notice that in our conventions for the normalization of the $SO(12)$ generators, the gauge invariant coupling supporting the above interactions has $t_{abc} = 2\cdot$.

4.4 Yukawa couplings in F-theory local approach: numerics

Using the mathematical machinery developed in the previous section, we can study the behaviour of $SO(12)$ points in F-theory - including both the bottom-tau point of enhancement and RPV operators. The former has been well studied in [150] for example. The coupling is primarily determined by five parameters - N_a, N_b, M, N_Y and $\tilde{N_Y}$. The parameters N_a and N_b give net chirality to the c-sector, while N_Y and $\tilde{N_Y}$ are components of hypercharge flux,

parameterising the doublet triplet splitting. M is related to the chirality of the a and b-sectors. There is also the $N_b = N_a - \frac{1}{3}N_Y$ constraint, which ensures the elimination of Higgs colour triplets at the Yukawa point. This can be seen by examining the text of the previous section, based on the work found in [150].

For a convenient and comprehensive presentation of the results we make the following redefinitions. In Eq. (4.59) and (4.60), one can factor out $4\pi g_s \sigma^2$ from inside Eq. (4.53),(4.54), and (4.55). In addition by noticing that $\left(\frac{m}{m_*}\right)^2 = (2\pi)^{3/2} g_s^{1/2} \sigma$, we obtain

$$y_{b,\tau} = 2g_s^{1/2}\sigma \; y'_{b,\tau} \tag{4.61}$$

$$y_{RPV} = 2g_s^{1/2}\sigma \; y'_{RPV} \tag{4.62}$$

where $y'_{b,\tau}$ and y'_{RPV} are functions of the flux parameters. Furthermore, we set the scale $m = 1$ and as such the remainder mass dimensions are given in units of m. The presented values for the strength of the couplings are then in units of $2g_s^{1/2}\sigma$.

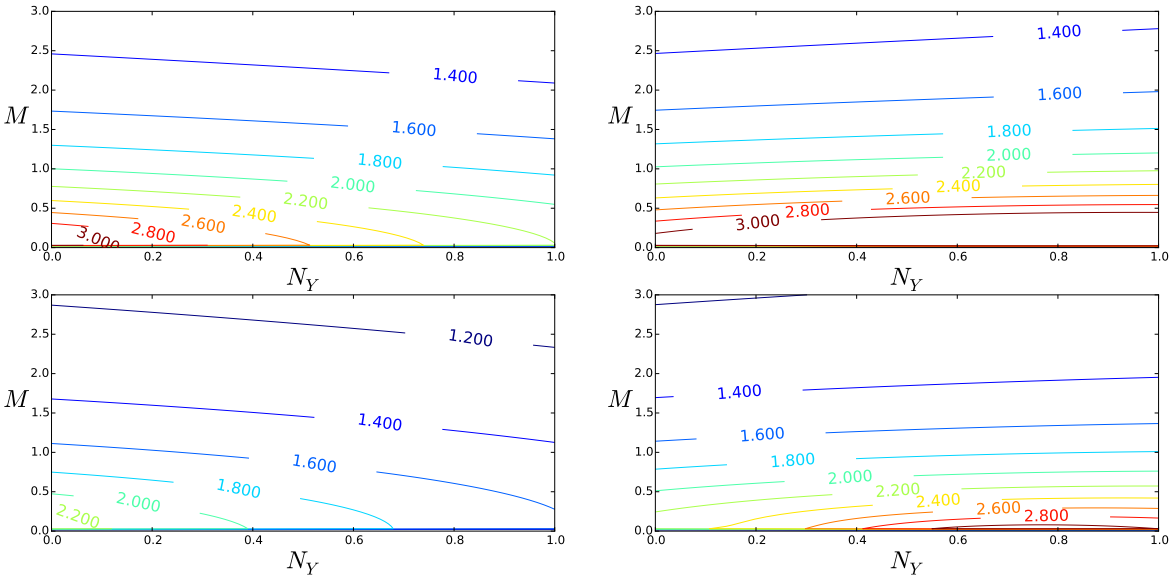

Figure 4.2: Ratio between bottom and tau Yukawa couplings, shown as contours in the plane (M, N_Y) of local fluxes. Plots on the left have $N_a = -1$, while those on the right $N_a = 1$. Also $\tilde{N}_Y = 1.8M$ (upper) and $\tilde{N}_Y = 1.3M$ (lower). The parameter N_b is fixed by the condition $N_b = N_a - \frac{1}{3}N_Y$.

Figure 4.2 shows the ratio of the bottom and tau Yukawa couplings at a point of $SO(12)$ in a region of the parameter space with reasonable values. These results are consistent with those in [150]. Note that the phenomenological desired ratio of the couplings at the GUT scale is $Y_\tau/Y_b = 1.37 \pm 0.1 \pm 0.2$ [201], which can be achieved within the parameter ranges shown in Figure 4.2. Having shown that this technique reproduces the known results for the bottom to tau ratio, we now go on to study the behaviour of an RPV coupling point in $SO(12)$ models.

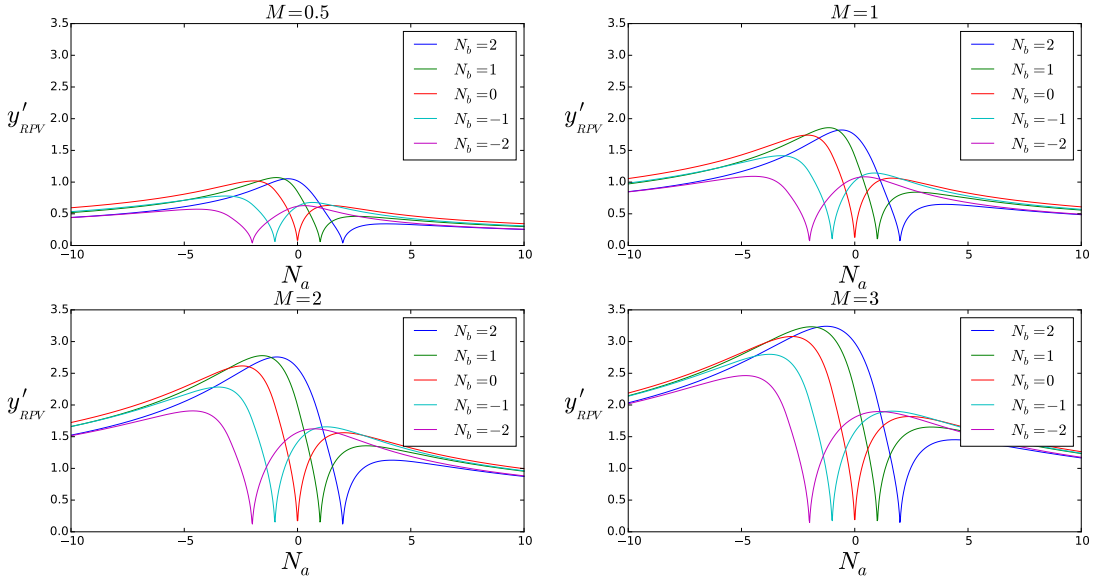

Figure 4.3: Dependency of the RPV coupling (in units of $2g_s^{1/2}\sigma$) on N_a in the absence of hypercharge fluxes, for different values of M and N_b.

4.4.1 Behaviour of $SO(12)$ points

The simplest scenario for an $SO(12)$ enhancement generating RPV couplings, would be the case where all three of the types of operator, QLD, UDD, and LLE arise with equal strengths, which would occur in a scenario with vanishing hypercharge flux, leading to an entirely "unsplit" scenario. This assumption sets N_Y and $\tilde{N_Y}$ to vanish, and we may also ignore the condition $N_b = N_a - \frac{1}{3}N_Y$. The remaining parameters determining are then N_a, N_b and M. Figure 4.3 shows the coupling strength in the N_a plane for differing N_b and M values. The general behaviour is that the coupling strength is directly related to M, while the coupling vanishes at the point where $N_a = N_b$. This latter point is due to the $N_Y = 0$ which for $N_a = N_b$ leads to $q_S = 0$ for the c-sector (see Table 4.4).

Figure 4.4 and Figure 4.5 also demonstrate this set of behaviours, but for contours of the coupling strength. Figure 4.4, showing all combinations of the three non-zero parameters, shows that in the $N_a - N_b$ plane there is a line of vanishing coupling strength about the $N_a = N_b$, chirality switch point for the c-sector. The figure also reinforces the idea that small values of M correspond to small values of the coupling strength, as close to the point of $M = 0$ the coupling again reduces to zero. Figure 4.5 again shows this behaviour, with the smallest values of M giving the smallest values of the coupling. From this we can infer that an RPV $SO(12)$ point is most likely to be compatible with experimental constraints if M takes a small value.

Figure 4.6(a) (and Figure 4.6(b)) shows the RPV coupling strength in the absence of flux for the N_a (N_b) plane, along with the "bottom" coupling strength for corresponding values. The key difference is that the Hypercharge flux is switched on at the bottom $SO(12)$ point, with values of $N_Y = 0.1$ and $\tilde{N_Y} = 3.6$. The figures show that for the bottom coupling, the fluxes always push the coupling higher, similarly to increasing the M values.

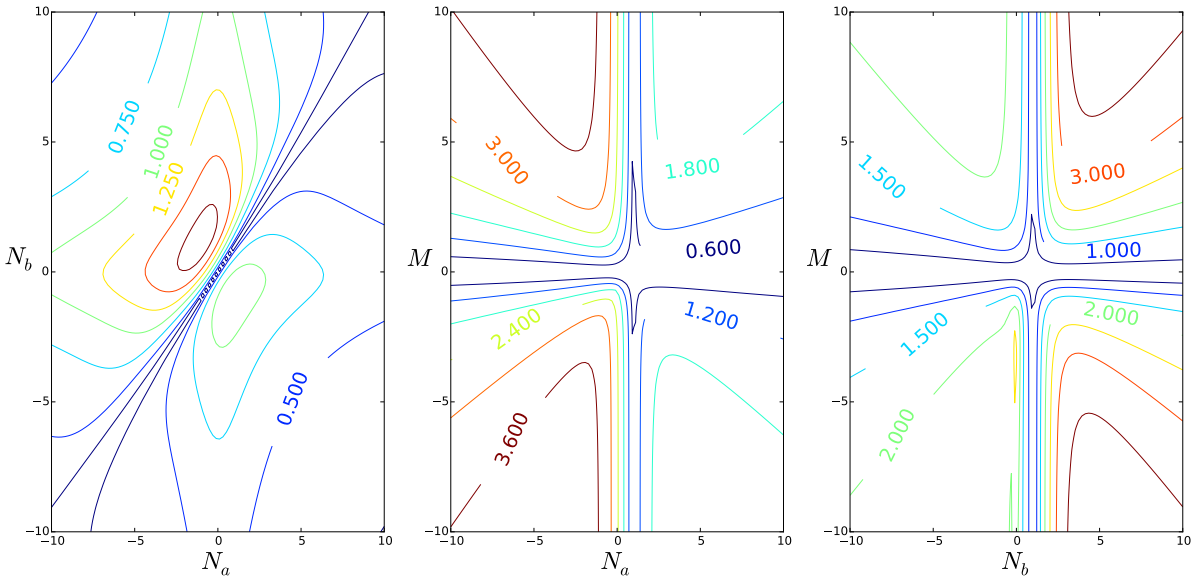

Figure 4.4: Dependency of the RPV coupling (in units of $2g_s^{1/2}\sigma$) on different flux parameters, in absence of Hypercharge fluxes. Any parameter whose dependency is not shown is set to zero.

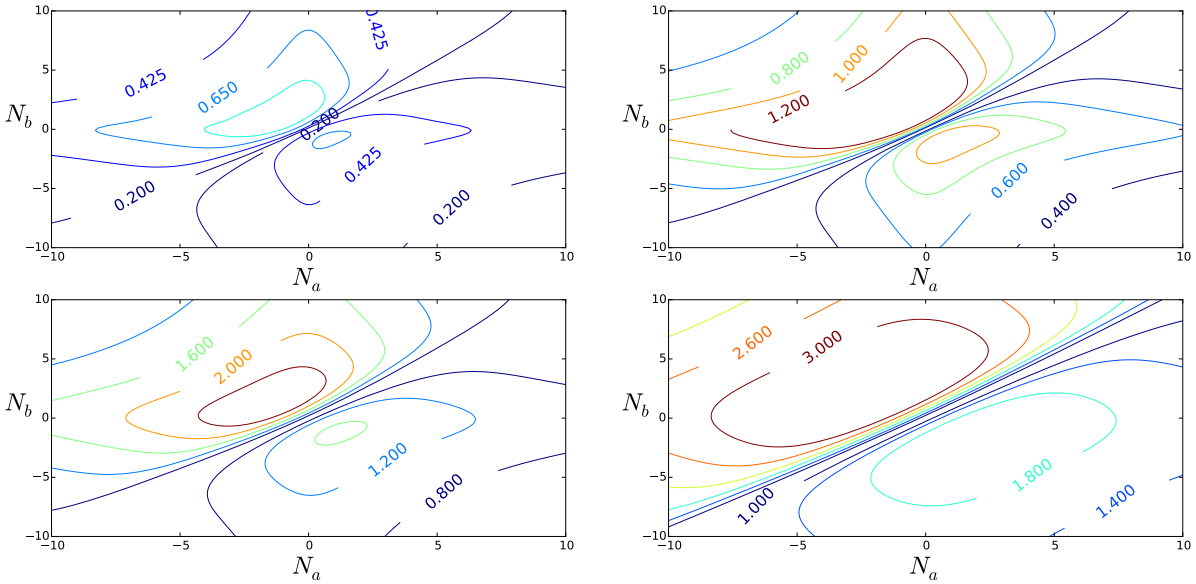

Figure 4.5: Dependency of the RPV coupling (in units of $2g_s^{1/2}\sigma$) on the (N_a, N_b)-plane, in absence of hypercharge fluxes and for different values of M. Top: left $M = 0.5$, right $M = 1.0$. Bottom: left $M = 2.0$, right $M = 3.0$.

Figure 4.6(c) plots out the two couplings in the M-plane, showing that the bottom Yukawa goes to zero for two values of M, while the RPV point has only one. Considering the form of Equation (4.59), we can see that the factors κ_{5_M} and κ_{10_M} are proportional to the parameter q_p. Referring to Table 4.4, one can see which values these take for each sector - namely, $q_p(a_1) = M - \frac{1}{3}\tilde{N_Y}$ and $q_p(b_2) = -M - \frac{1}{6}\tilde{N_Y}$. Solving these two equations shows trivially that zeros should occur when $M = \frac{1}{3}\tilde{N_Y}$ and $-\frac{1}{6}\tilde{N_Y}$, which is the exact behaviour exhibited in Figure

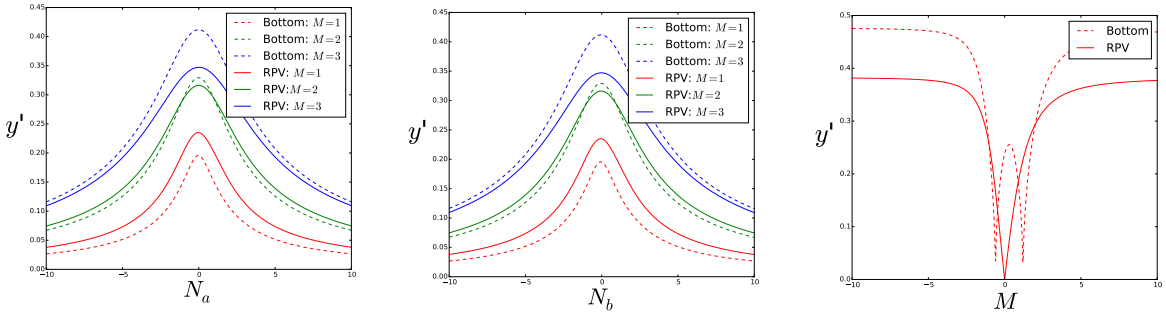

(a) Varying N_a with fixed M

(b) Varying N_b with fixed M

(c) Varying M with fixed N_a=1, $N_b = 29/30$, $N_Y = 0.1$, $\tilde{N}_Y = 3.6$

Figure 4.6: Dependency of the RPV and bottom Yukawa couplings (in units of $2g_s^{1/2}\sigma$) on different parameters at different regions of the flux parameter space

4.6(c).

4.5 RPV Yukawa couplings: allowed regions and comparison to data

In this section we focus on calculating the RPV Yukawa coupling constant at the GUT scale, which may be directly compared to the experimental limits, using the methods and results of the previous two sections. As a point of notation, we have denoted the RPV Yukawa coupling at the GUT scale to be generically y_{RPV}, independently of flavour or operator type indices. This coupling may be directly compared to the phenomenological RPV Yukawa couplings at the GUT scale λ_{ijk}, λ'_{ijk} and λ''_{ijk} as defined below.

Recall that, in the weak/flavour basis, the superpotential generically includes RPV couplings, in particular those from Eq. 4.2:

$$W \supset \frac{1}{2}\lambda_{ijk}L_iL_je^c_k + \lambda'_{ijk}L_iQ_jd^c_k + \frac{1}{2}\lambda''_{ijk}u^c_id^c_jd^c_k \tag{4.63}$$

In the local F-theory framework, each of the above Yukawa couplings (generically denoted as y_{RPV}) is computable through Eq. (4.60). What distinguishes different RPV couplings, say λ from λ', are the values of the flux densities, namely the hypercharge flux. This is because the normalization of matter curves depends on the hypercharge flux density. As such, different SM states will have different hypercharges and consequently different respective normalization coefficient.

Even though a given $SO(12)$ enhancement point can in principle support different types of trilinear RPV interactions, the actual effective interactions arising at such point depend on the local chiral spectrum present at each curve. For example, in order to have an LLe^c interaction, both Σ_a and Σ_c curves need to have chiral L states, and the Σ_b curve an e^c state at the enhancement point. In Figure 4.7 we show contours on the (N_a,N_b) plane for the different types of trilinear RPV couplings.

The local spectrum is assessed by local chiral index theorems [149]. In Appendix C.2 we outline the results for the constraints on flux densities such that different RPV points are allowed at a given $SO(12)$ enhancement point. These results are graphically presented in Figure 4.8 and may be compared to the operators presented in Table 4.2 in the semi-local approach. Thus, the green coloured region is associated with the $10_3\bar{5}_1\bar{5}_1$ operator of this Table, the blue colour with $10_1\bar{5}_3\bar{5}_3$, the pink with $10_2\bar{5}_4\bar{5}_4$ and so on. Thus different regions of the parameter space can support different types of RPV interactions at a given enhancement point. We can then infer that in F-theory the allowed RPV interactions can, in principle, be only a subset of all possible RPV interactions.

In the limiting cases where only one coupling is turned on, one can derive bounds on its magnitude at the GUT scale from low-energy processes [202]. In order to do so, one finds the bounds at the weak scale in the mass basis, performs a rotation to the weak basis and then evaluates the couplings at the GUT scale with the RGE. Since the effects of the rotation to the weak basis in the RPV couplings requires a full knowledge of the Yukawa matrices, we assume that the mixing only happens in the down-quark sector as we are not making any considerations regarding the up-quark sector in this work. Table 4.5 shows the upper bounds for the trilinear RPV couplings at the GUT scale.

The bounds presented in Table 4.5 have to be understood as being derived under certain assumptions on mixing and points of the parameter space [74, 203]. For example, the bound on λ_{12k} can be shown to have an explicit dependence on

$$\frac{\tilde{m}_{e_{k,R}}}{100\ \text{GeV}} \tag{4.64}$$

where $\tilde{m}_{e_{k,R}}$ refers to a 'right-handed' selectron soft-mass. The values presented in Table 4.5, as found in [202], were obtained by setting the soft-masses to 100 GeV, which are ruled out by more recent LHC results [204, 205, 206, 207, 208, 209] . By assuming heavier scalars, for example around 1 TeV, we would then get the bounds in Table 4.5 to be relaxed by one order of magnitude.

The results show that the λ type of coupling, corresponding to the LLe^c interactions, is bounded to be < 0.05 regardless of the indices taken. The red regions of Figures 4.11(a) and 4.9 show the magnitude of the coupling where it is allowed. A similar analysis can be carried out for the remaining couplings. The λ' coupling, which measures the strength of the LQd^c type of interactions, can be seen in the yellow regions of Figure 4.10. Finally, the derived values for λ'' coupling, related to the $u^c d^c d^c$ type of interactions, are shown in the blue regions of Figures 4.10 and 4.11(b). However these couplings shown are all expressed in units of $2g_s^{1/2}\sigma$, and so cannot yet be directly compared to the experimental limits.

In order to make contact with experiment we must eliminate the $2g_s^{1/2}\sigma$ coefficient. We do this by taking ratios of the couplings computed in this framework where the $2g_s^{1/2}\sigma$ coefficient cancels in the ratio. The ratio between any RPV coupling and the bottom Yukawa at the GUT scale is given by

$$r = \frac{y_{RPV}}{y_b} = \frac{y'_{RPV}}{y'_b}, \tag{4.65}$$

ijk	λ_{ijk}	λ'_{ijk}	λ''_{ijk}
111	-	1.5×10^{-4}	-
112	-	6.7×10^{-4}	4.1×10^{-10}
113	-	0.0059	1.1×10^{-8}
121	0.032	0.0015	4.1×10^{-10}
122	0.032	0.0015	-
123	0.032	0.012	1.3×10^{-7}
131	0.041	0.0027	1.1×10^{-8}
132	0.041	0.0027	1.3×10^{-7}
133	0.0039	4.4×10^{-4}	-
211	0.032	0.0015	-
212	0.032	0.0015	(1.23)
213	0.032	0.016	(1.23)
221	-	0.0015	(1.23)
222	-	0.0015	-
223	-	0.049	(1.23)
231	0.046	0.0027	(1.23)
232	0.046	0.0028	(1.23)
233	0.046	0.048	-
311	0.041	0.0015	-
312	0.041	0.0015	0.099
313	0.0039	0.0031	0.015
321	0.046	0.0015	0.099
322	0.046	0.0015	-
323	0.046	0.049	0.015
331	-	0.0027	0.015
332	-	0.0028	0.015
333	-	0.091	-

Table 4.5: Upper bounds of RPV couplings (ijk refer to flavour/weak basis) at the GUT scale under the assumptions: 1) Only mixing in the down-sector, none in the Leptons; 2) Scalar masses $\tilde{m} = 100$ GeV; 3) $\tan\beta(M_Z) = 5$; and 4) Values in parenthesis refer to non-perturbative bounds, when these are stronger than the perturbative ones. This Table is reproduced from [202].

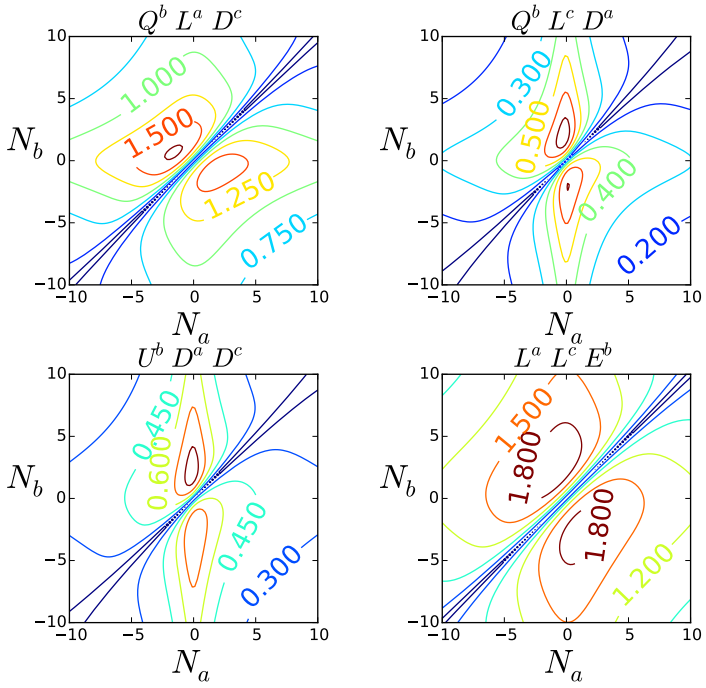

Figure 4.7: Strength of different RPV couplings (in units of $2g_s^{1/2}\sigma$) in the (N_a, N_b)-plane in the presence of Hypercharge fluxes $N_Y = 0.1$, $\tilde{N}_Y = 3.6$, and with $M = 1$. The scripts a, b, c refer to which sector each state lives.

as defined in Equation (4.61) and Equation (4.62). This ratio can be used to assess the absolute strength of the RPV at the GUT scale as follows.

First we assume that the RPV interaction is localised in an $SO(12)$ point far away from the bottom Yukawa point. This allows us to use different and independent flux densities at each point. We can then compute y_b' at a point in the parameter space where the ratio y_b/y_τ takes reasonable values, following [150]. Finally we take the ratio, r. In certain regions of the parameter space, r is naturally smaller than 1. This suppression of the RPV coupling in respect to the bottom Yukawa is shown in Figures 4.12(a), 4.12(b), 4.12(c), and 4.12(d), for different regions of the parameter space that allows for distinct types of RPV interactions.

Since r is the ratio of both primed and unprimed couplings, respectively unphysical and physical, at the GUT scale, we can extend the above analysis to find the values of the physical RPV couplings at the GUT scale. To do so, we use low-energy, experimental, data to set the value of the bottom Yukawa at the weak scale for a certain value of $\tan\beta$. Next, we follow the study in [201] to assess the value of the bottom Yukawa at the GUT scale through RGE runnings.

In order to make a connection with the bounds in Table 4.5, we pick $\tan\beta = 5$ and we find $y_b(M_{GUT}) \simeq 0.03$. The results for the value of the RPV couplings in different regions in the parameter space at the GUT scale are presented in Figures 4.13(a), 4.13(b), 4.13(c), and 4.13(d). These results show that, for any set of flavour indices, the strength of the coupling λ related to an LLe^c interaction is within the bounds. This means that this purely leptonic RPV operator, which violates lepton number but not baryon number, may be present with a

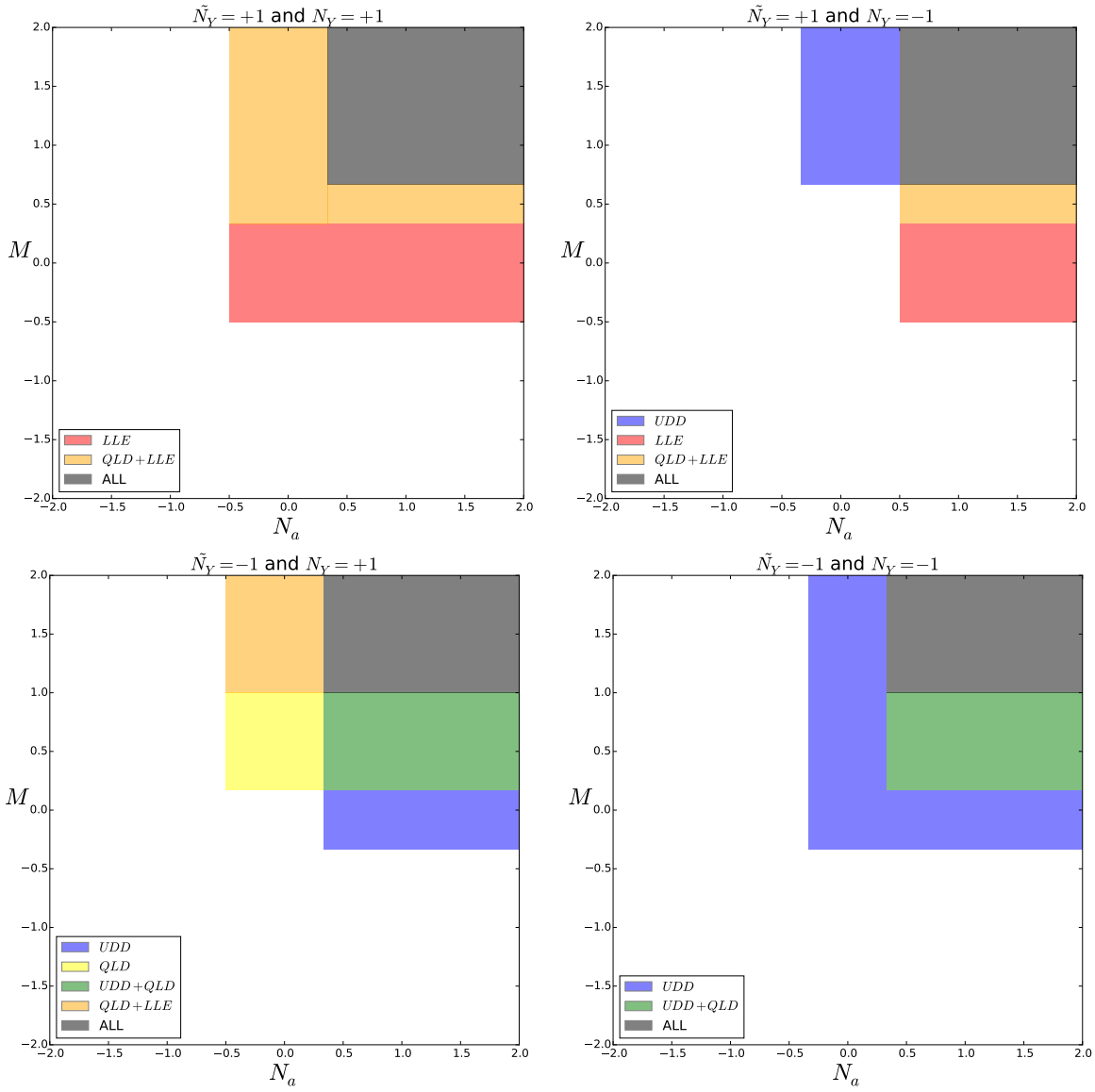

Figure 4.8: Allowed regions in the flux parameter space for the various RPV couplings. In all cases we have take for simplicity $N_b = 0$. Black and Green regions must be avoided since the combination of allowed RPV operators there can lead to proton decay effects. These figures should be seen in conjunction with the operators presented in Table 4.2.

sufficiently suppressed Yukawa coupling, according to our calculations. Therefore in the future lepton number violating processes could be observed.

By contrast, only for a subset of possible flavour index assignments for baryon number violating (but lepton number conserving) $u^c d^c d^c$ couplings are within the bounds in Table 4.5. The constraint on the first family up quark coupling λ''_{1jk} for the $u^c_1 d^c_j d^c_k$ interaction is so stringent, that this operator must only be permitted for the cases involving higher generation indices, like $u^c_2 d^c_j d^c_k$ and $u^c_3 d^c_j d^c_k$ (corresponding to the two heavy up-type quarks c^c, t^c), assuming no up-type quark mixing. However, if up-type quark mixing is allowed, then such operators could lead to an effective $u^c_1 d^c_j d^c_k$ operator suppressed by small mixing angles, in which case it could induce

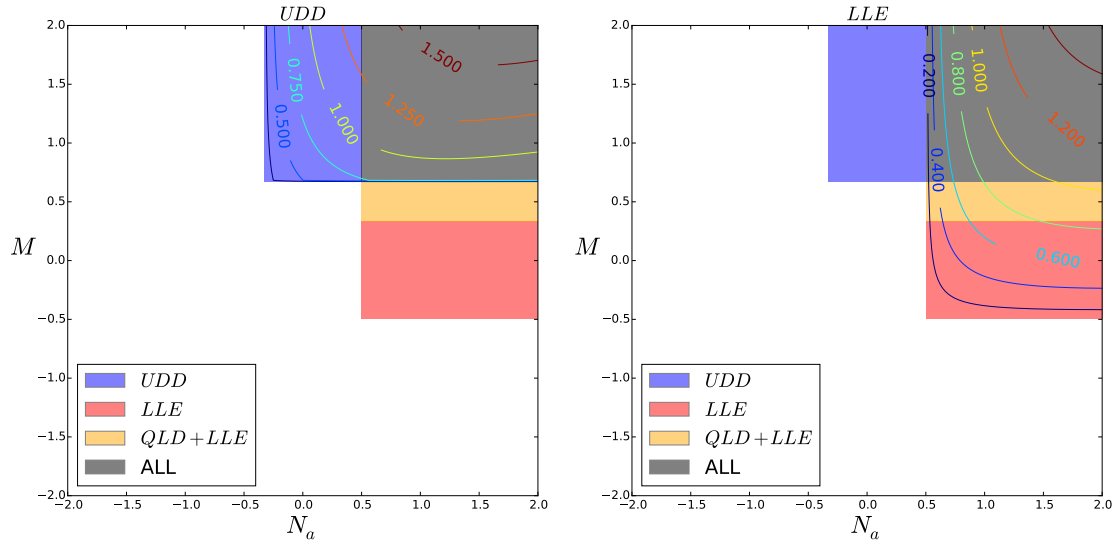

Figure 4.9: Allowed regions in the parameter space for different RPV couplings with $\tilde{N_Y} = -N_Y = 1$. We have also include the corresponding contours for the $u^c d^c d^c$ operator (left panel) and LLe^c (right panel). We see that the RPV couplings receive large values at this region of the parameter space so the Black corner must be avoided

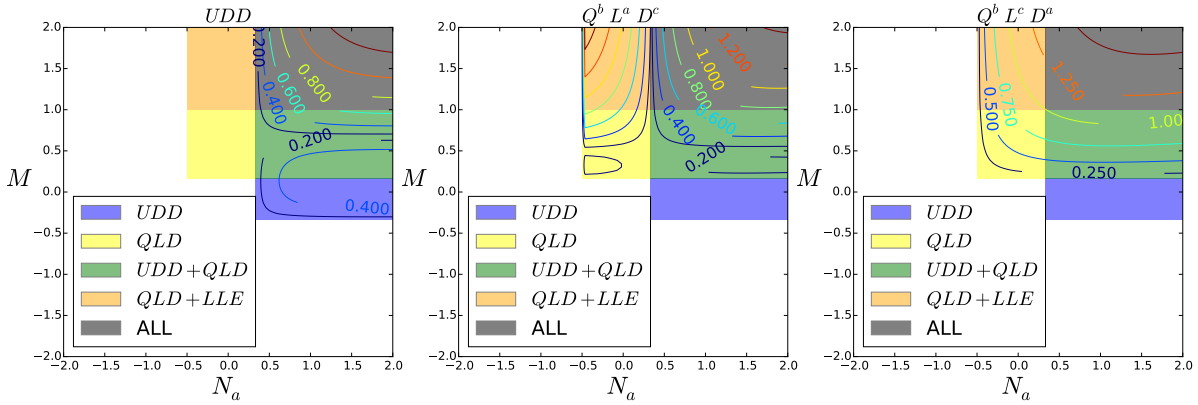

Figure 4.10: Allowed regions in the parameter space for different RPV couplings with $N_Y = -\tilde{N_Y} = 1$ and $N_b = 0$. We have also include the corresponding contours for the $u^c d^c d^c$ operator (left panel) and QLd^c (middle and right panel). The scripts a, b and c refer to which sector each state lives. Again, for this choice of parameters the Green and Black regions must be avoided since catastrophic proton decay can take place at there.

$n - \bar{n}$ oscillations.

Finally the QLd^c operator with Yukawa coupling λ' apparently must be avoided, since according to our calculations, there are regions with values of λ' that exceeds the experimental

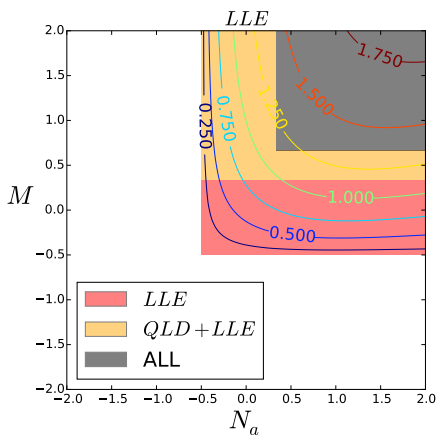

(a) LLe^c regions with $\tilde{N_Y} = N_Y = 1$

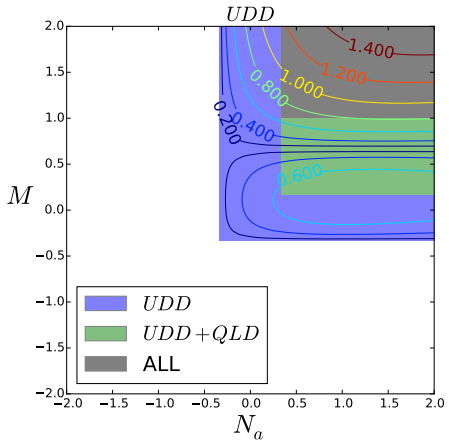

(b) $u^c d^c d^c$ regions with $\tilde{N_Y} = N_Y = -1$

Figure 4.11: Allowed regions in the parameter space for different RPV couplings.

limit, apart from λ'_{333} coupling corresponding to the $L_3 Q_3 d_3^c$ operator. This implies that we should probably eliminate such operators which violate both baryon number and lepton number, using the flux mechanism that we have described. However in some parts of parameter space, for certain flavour indices, such operators may be allowed leading to lepton number violating processes such as $K^+ \to \pi^- e^+ e^+$ and $D^+ \to K^- e^+ e^+$.

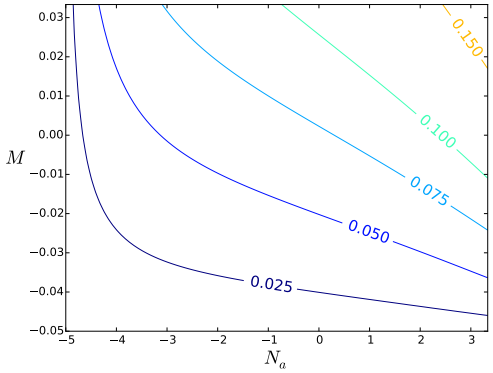

(a) LLe^c region with $N_Y = 10$, $\tilde{N}_Y = 0.1$

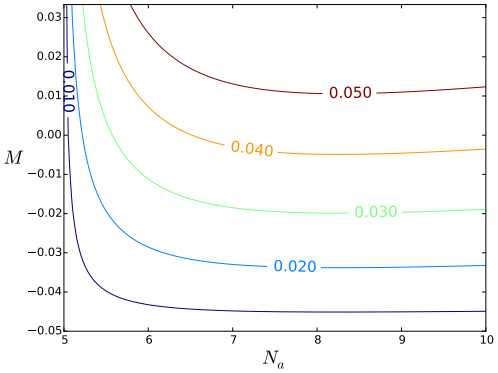

(b) LLe^c region with $N_Y = -10$, $\tilde{N}_Y = 0.1$

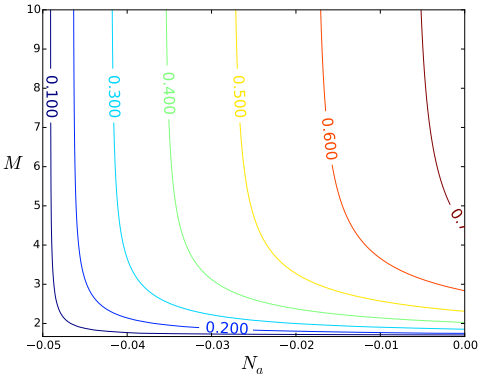

(c) QLd^c region with $N_Y = 0.1$, $\tilde{N}_Y = -10$

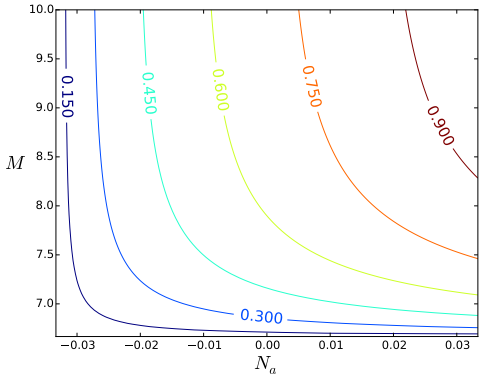

(d) $u^c d^c d^c$ region with $N_Y = -0.1$, $\tilde{N}_Y = -10$

Figure 4.12: y_{RPV}/y_b ratio. The bottom Yukawa was computed in a parameter space point that returns a reasonable y_b/y_τ ratio at the GUT scale [150]

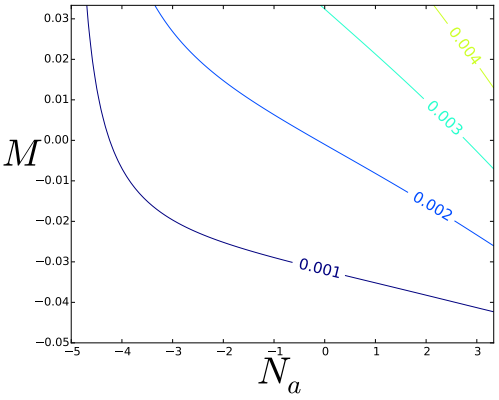

(a) λLLe^c region with $N_Y = 10$, $\tilde{N}_Y = 0.1$

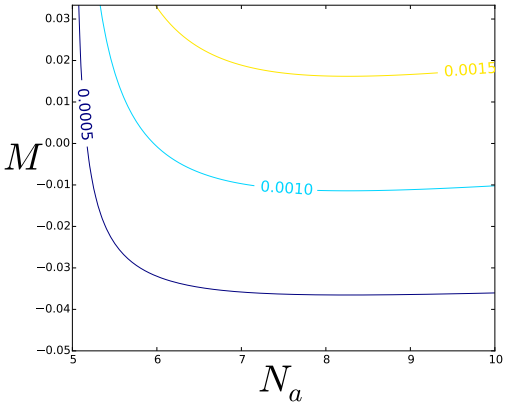

(b) λLLe^c region with $N_Y = -10$, $\tilde{N}_Y = 0.1$

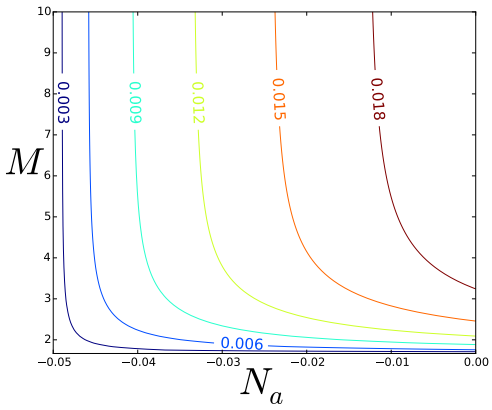

(c) $\lambda' QLd^c$ region with $N_Y = 0.1$, $\tilde{N}_Y = -10$

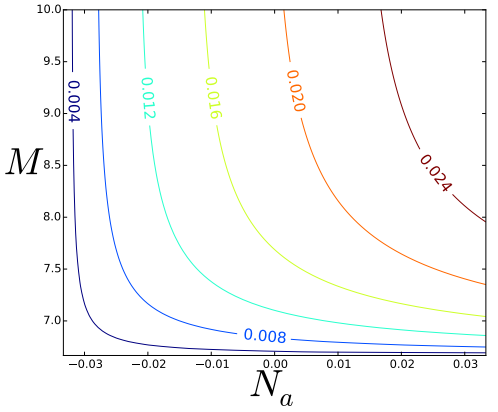

(d) $\lambda'' u^c d^c d^c$ region with $N_Y = -0.1$, $\tilde{N}_Y = -10$

Figure 4.13: y_{RPV} at GUT scale for $\tan\beta = 5$. All the plots have $N_b = 0$. The values here can be compared directly to the bounds presented in Table 4.5.

Chapter 5

Yukawa Unification in F-theory inspired E_6 models

5.1 Introduction

The existence of a neutral gauge boson Z' associated with a new $U(1)$ gauge symmetry spontaneously broken at a few TeV is an interesting possibility. It is well-motivated both experimentally as well as theoretically, and its implications have been extensively discussed in the literature [116, 210, 211]. The experimental bound on the mass of a Z' boson decaying only to ordinary quarks and leptons with couplings comparable to the SM Z boson, is about 3 TeV [212, 213, 214]. Theoretically, several extensions of the Standard Model and their supersymmetric versions, predict the existence of additional $U(1)$ symmetries. In the context of unified theories these are embedded in gauge groups larger than $SU(5)$ since the latter, which was the main GUT framework of the previous Chapters, contains only the SM gauge group.

One of the most interesting unified groups containing additional abelian factors of phenomenological interest is the exceptional group E_6 [106, 107, 108]. This has been extensively studied as a field theory unified model as well as in a string background. It emerges naturally in many string compactifications and, in particular, in an F-theory framework where several interesting features have been discussed [215, 216, 217, 218, 219, 220]. Under the breaking pattern $E_6 \supset SU(5)$, two abelian factors appear, usually dubbed $U(1)_\chi$ and $U(1)_\psi$. In general, after the spontaneous symmetry breaking of E_6, some linear combination of these $U(1)$'s may survive at low energies [113]. The corresponding neutral gauge boson receives mass at the TeV scale and may be found at LHC or its future upgrates.

In this Chapter we examine the implications of a TeV scale neutral gauge boson corresponding to various possible combinations of $U(1)_\psi$ and $U(1)_\chi$. In addition, motivated by string and in particular F-theory effective models, we consider the existence of additional vectorlike fields and neutral singlets at the TeV scale. We assume that the initial E_6 symmetry is broken by background fluxes which leave only one linear $U(1)$ combination unbroken, commutant with $SU(5)$. In the present Chapter the zero mode spectrum of the effective theory is derived from the decomposition of the 27 and $\overline{27}$ representations of E_6, and, we parametrise their multiplicities

in terms of a minimum number of (integer) flux parameters. In addition, since the flux-breaking mechanism splits the E_6 representations into incomplete multiplets [218, 216, 215, 219, 220], one may choose appropriately the flux parameters in order to retain only the desired components from the 27 and $\overline{27}$ representations.

We also perform a two-loop renormalisation group equations (RGE) analysis of the gauge and Yukawa couplings of the effective theory model for different choices of linear combinations of the $U(1)$ symmetries. Implementing the idea of incomplete E_6 representations motivated by F-theory considerations, we make use of zero mode spectra obtained from truncated E_6 representations. We use known mathematical packages [221], to derive and solve numerically the RGE's in the presence of additional matter such as vectorlike triplets, doublets and singlet fields with masses down to the TeV scale. Furthermore, we investigate possible gauge and Yukawa coupling unification by considering four different cases with respect to the unbroken $U(1)$ combination after breaking E_6 down to the SM. Finally, we perform an F-theory computation of the Yukawa couplings at the GUT scale and express them in terms of the various local flux parameters associated with the symmetry breaking.

5.2 E_6 GUT in an F-theory perspective

We start with a short description of the E_6 GUT breaking and the massless spectrum. The $U(1)$ symmetries we are interested in appear under the breaking pattern

$$E_6 \to SO(10) \times U(1)_\psi \to SU(5) \times U(1)_\psi \times U(1)_\chi. \tag{5.1}$$

In an effective E_6 model with an F-theory origin, matter fields, in general, arise from $27, \overline{27}$ and 78 representations. In the present work we restrict to the case where the three families, the Higgses and other possible matter fields emerge from the decomposition of the $27(\in E_6)$ under $SO(10) \times U(1)_\psi$,

$$27 \to 16_1 + 10_{-2} + 1_4. \tag{5.2}$$

The decompositions of the $SO(10)$ multiplets in (5.2) under the breaking of $SO(10)$ to $SU(5)$ are as follows

$$16_1 \to 10_{(1,-1)} + \bar{5}_{(1,3)} + 1_{(1,-5)},\ 10_{-2} \to 5_{(-2,2)} + \bar{5}_{(-2,-2)},\ 1_4 \to (1,1)_{(4,0)}, \tag{5.3}$$

where the two indices respectively refer to the charges under the two abelian factors $U(1)_\psi \times U(1)_\chi$.

The fermion families are accommodated in three 16-plets of $SO(10)$. The ordinary quark triplets, the right-handed electron and lepton doublets comprise the $10_{(1,-1)}$ and $\bar{5}_{(1,3)}$ of $SU(5)$, and in the standard description, the singlet $1_{(1,-5)}$ is identified with the right-handed neutrino. There are also vectorlike multiplets $5_{(-2,2)} + \bar{5}_{(-2,-2)}$ and $SO(10)$ singlets with charges $(4,0)$. The normalised charges $\tilde{Q}_a = N_a Q_a$ are defined so that $\mathrm{Tr}\, \tilde{Q}_a^2 = 3$, and therefore $N_\psi = \frac{1}{2\sqrt{6}}$ and $N_\chi = \frac{1}{2\sqrt{10}}$.

With the spontaneous breaking of $U(1)_\psi$ and $U(1)_\chi$, the corresponding neutral gauge bosons receive masses of the order of their breaking scale. Depending on the details of the particular

E_6	$SO(10)$	$SU(5)$	$\sqrt{24}Q_\psi$	$\sqrt{10}Q_N$	$\sqrt{15}Q_\eta$	SM
27	16	$\overline{5}_M$	1	1	$\frac{1}{2}$	d^c, L
27	16	10_M	1	$\frac{1}{2}$	-1	Q, u^c, e^c
27	16	1_ν	1	0	$-\frac{5}{2}$	ν^c
27	10	5_H	-2	-1	2	D, H_u
27	10	$\overline{5}_{\bar{H}}$	-2	$-\frac{3}{2}$	$\frac{1}{2}$	$\overline{D}, H_d$
27	1	1	4	$\frac{5}{2}$	$-\frac{5}{2}$	S

Table 5.1: 27 of E_6 and its $SO(10)$ and $SU(5)$ decompositions and $Q_{\psi,N,\eta}$ charges.

model, the breaking scale of these $U(1)$'s can be anywhere between M_{GUT} and a few TeV, with the latter determined by LHC. New Physics phenomena can be anticipated in the TeV range and possible deviations of the SM predictions are associated with the existence of a new neutral gauge boson in this range. In the present model, a Z' boson that may appear at low energies could be any linear combination of the form $Z' = Z_\chi \cos\phi + Z_\psi \sin\phi$. The corresponding $U(1)$ charge is defined by

$$Q = \tilde{Q}_\chi \cos\phi + \tilde{Q}_\psi \sin\phi. \tag{5.4}$$

Several values of the mixing angle ϕ lead to models consistent with the data. The following models are of our primary interest in the analysis presented in this Chapter.

• N-model [222, 223, 224]: We assign the right-handed neutrinos in $1_{(1,-5)}$, and require $Q_\nu = 0$. Then, from (5.4), we fix $\tan\phi = \sqrt{15}$ and as a result,

$$Q_N = \frac{1}{4}\sqrt{\frac{5}{8}}\left(Q_\psi + \frac{1}{5}Q_\chi\right). \tag{5.5}$$

• η-model: In this case the $U(1)_\eta$ charge formula takes the form

$$Q_\eta = -\frac{1}{8}\sqrt{\frac{5}{3}}\left(Q_\psi - \frac{3}{5}Q_\chi\right), \tag{5.6}$$

and motivated from string theory constructions [225].

• Finally, two trivial cases: χ-model where $\phi = 0$, and ψ-model where $\phi = \pi/2$.

The phenomenological implications of these models have recently been discussed in [226, 227, 228, 229], while an analysis with a general mixing angle, ϕ, can be found in [230, 231, 232]. The (ψ, N, η)-charges of the $SU(5)$ representations are shown in Table 5.1. Details for the χ-model are presented separately in Table 5.2 since we use a different GUT origin for the SM spectrum. (Notice that $Q_\chi = -Q_N$ and, as a result, the RGE analysis presented in the next sections is the same.)

Having described the basic features of the models, we proceed now to the derivation of the spectrum from F-theory perspective.

E_6	$SO(10)$	$SU(5)$	$\sqrt{10}Q_\chi$	SM particle content
27	10	$\bar{5}_M$	-1	d^c, L
27	16	10_M	$-\frac{1}{2}$	Q, u^c, e^c
27	1	1_ν	0	ν^c
27	10	5_H	1	D, H_u
27	16	$\bar{5}_{\bar{H}}$	$\frac{3}{2}$	$\overline{D}, H_d$
27	16	1	$-\frac{5}{2}$	S

Table 5.2: 27 of E_6 and its $SO(10)$ and $SU(5)$ decompositions and Q_χ charges.

5.3 F-theory motivated E_6 spectrum

In F-theory, the gauge symmetry is a subgroup of E_8, the latter being associated with the highest singularity of the elliptically fibred internal space. Here we assume that the internal manifold is equipped with a divisor possessing an E_6 singularity, thus

$$E_8 \supset E_6 \times SU(3)_\perp. \tag{5.7}$$

The representations of the effective theory model, arise from the decomposition of E_8 adjoint

$$248 \to (78,1) + (1,8) + (27,3) + (\overline{27},\bar{3}).$$

In the above decomposition, we are interested in the zero modes $(27,3) + (\overline{27},\bar{3})$ lying on the Riemann surfaces formed on the intersections of seven branes with the E_6 divisor. Restricting to specific cases of GUT surfaces, such as del Pezzo or Hitzebruch, one can determine the chirality $27 - \overline{27}$ in terms of a topological index, the Euler characteristic [118, 119]. We assume the breaking of E_6 to the standard $SO(10)$ model by a non-trivial flux along $U(1)_\psi$. Since $E_8 \supset E_6 \times SU(3)_\perp$, the 27's reside on three matter curves corresponding to the Cartan roots t_i of $SU(3)_\perp$, with $t_1 + t_2 + t_3 = 0$, and this implies that the only invariant Yukawa coupling is $27_{t_1}27_{t_2}27_{t_3}$. We choose to accommodate the Higgs fields in $27_{t_3} = 27_H$ and therefore the chiral families are on the t_1, t_2 curves. However, in order to achieve a rank-one mass matrix and obtain a tree-level Yukawa coupling for the third generation, two matter curves have to be identified, and this can be achieved under the action of a Z_2 monodromy such that $t_1 = t_2$. Furthermore, choosing appropriately the restrictions of the flux parameters on the matter curves, we can arrange things so that the spectrum contains three families in $16(\to 10 + \bar{5} + 1)$, and three Higgs pairs in $10(\to 5 + \bar{5})$ and several neutral singlets [220].

Indeed, if we generally assume that the topological characteristics of the chosen manifold allow M copies of 27_{t_1} and M_H copies of 27_{t_3} representations on the corresponding matter curves, turning on a suitable $U(1)_\psi$-flux of n and m units respectively, we get the splitting shown in Table 5.3.

Matter			Higgs		
$27_{t_1}/\overline{27}_{-t_1}$	$SO(10)\times U(1)_\psi$	#	$27_{t_3}/\overline{27}_{-t_3}$	$SO(10)\times U(1)_\psi$	#
	$\#(16_1-\overline{16}_{-1})$	M		$\#(16_1^H-\overline{16}_{-1}^H)$	M_H
	$\#(10_{-2}-\overline{10}_2)$	$M+n$		$\#(10_{-2}^H-\overline{10}_2^H)$	M_H+m
	$\#(1_4-\overline{1}_{-4})$	$M-n$		$\#(1_4^H-\overline{1}_{-4}^H)$	M_H-m

Table 5.3: Splitting of 27_{t_1} ($\overline{27}_{-t_1}$) and 27_{t_3} ($\overline{27}_{-t_3}$) representations by turning on a suitable $U(1)_\psi$-flux of n and m units respectively.

Matter				Higgs			
$27_{t_1}/\overline{27}_{-t_1}$	$SO(10)\times U(1)_\psi$	#1	#2	$27_{t_3}/\overline{27}_{-t_3}$	$SO(10\times U(1)_\psi$	#1	#2
	16_1	3	3		16_1	0	0
	$\overline{10}_2$	0	1		10_{-2}	3	4
	1_4	6	7		1_{-4}	3	4

Table 5.4: Two different cases of E_6 motivated models. The two cases labelled here as #1 and #2 correspond to the choice of flux parameters in equations (5.8) and (5.9) respectively.

The spectrum also includes singlets which descend from the $SU(3)_\perp$ adjoint decomposition, designated as

$$1_{t_i-t_j}\equiv\theta_{ij},\ i,j=1,2,3.$$

As an illustration, we present two cases with minimal spectra of E_6 motivated models for two specific choices of the fluxes.

1. An economical model emerges if we choose

$$M=3,\ M_H=0,\ n=-m=-3. \tag{5.8}$$

2. An alternative possibility may arise if we choose

$$M=3,\ M_H=0,\ n=-m=-4. \tag{5.9}$$

Both cases are shown in Table 5.4. The models differ with respect to the number of 10-plets and singlets; however the number of 16-plets is always three. In the first choice, all 10-plets reside on 27_{t_3} Higgs curve, while in the second case there is an additional pair descending from $\overline{27}_{-t_1}+27_{t_3}$.

Similarly, further symmetry breaking of the $SO(10)\to SU(5)\times U(1)_\chi$ will be achieved by turning on suitable $U(1)_\chi$ fluxes [220]. Thus, for the two 16's, in general, we have

$$16_1=\begin{cases}\text{Rep} & \text{flux units}\\ 10_{-1} & 3\\ \bar{5}_3 & 3+n_\chi\\ 1_{-5} & 3-n_\chi\end{cases},\quad 16_1^H=\begin{cases}\text{Rep} & \text{flux units}\\ 10_{-1} & 0\\ \bar{5}_3 & 0+m_\chi\\ 1_{-5} & 0-m_\chi\end{cases}, \tag{5.10}$$

where the integers n_χ, m_χ represent the $U(1)_\chi$ fluxes piercing the corresponding matter curves, and the superscript 16^H is used here to denote the origin from 27_{t_3}. For the number of 10's of $SO(10)$ in the second model, we find one $\overline{10}_2$ and $4\times 10^H_{-2}$, and assuming that one pair decouples (see next section) we have

$$10^H_{-2} = \begin{cases} \text{Rep} & \text{flux units} \\ 5_2 & 3+n'_\chi \\ \bar{5}_{-2} & 3+n''_\chi \end{cases} \tag{5.11}$$

Choosing $n_\chi = -m_\chi = 1$, we find $3\times 10_{-1}$ and $4\times\bar{5}_3$ emerging from $\Sigma_{16_{t_1}}$ and $1\times 5_{-3}$ from $\Sigma_{16_{t_3}}$. In addition, there are three singlet fields, $2\times 1_{-5}+1\times 1_5$. This implies a three family $SU(5)$ spectrum (supplemented by the right-handed neutrinos), accommodated in $10+\bar{5}+1$ representations, and an extra pair of $\bar{5}+5$. Furthermore, imposing $n'_\chi = n''_\chi = 0$ the three 10's of $SO(10)$ lead to three pairs of $5_{-2}+\bar{5}_2$. In a final step the breaking of $SU(5)$ is achieved by turning on hypercharge fluxes, so that the doublet-triplet spliting mechanism is realised. The spectrum is summarised in Table 5.5. In the following sections we discuss the basic features of the effective theory and the implications of the extra matter and the light boson Z' on the gauge and the Yukawa sector.

5.3.1 Yukawa couplings of the effective model

After the E_6 breaking, the tree-level superpotential at the $SO(10)$ level contains the terms

$$\mathcal{W}_1 \supset \lambda_i 16_1 16_1 10^{H_i}_{-2} + \kappa_i 10^{H_i}_{-2} 10_{-2}\, 1_4 + \mu_i \theta_{31}\, 1_4 1^{H_i}_{-4}\,. \tag{5.12}$$

The first term provides masses to fermion fields, while for $\langle 1_4\rangle \neq 0$, the second part generates a massive state of 10_{-2} through a linear combination with $10^{H_i}_{-2}$. It transpires that at tree-level these are the only mass terms for the various 10-plets. Indeed, the couplings $(\lambda'_2 10_{-2}10_{-2} + \lambda'_3 10^{H_1}_{-2}10^{H_2}_{-2})\times 1_4$, are not possible due to the t_i charges. They only appear at a non-renormalisable level when a certain number of singlets $1_{t_1-t_3}$ are inserted. Furthermore, we observe that if θ_{31} acquires a vev $\langle\theta_{31}\rangle \sim 10^{-1} M_{GUT}$, then the two pairs of $1_4 1^{H_i}_{-4}$ become massive.

Next, let us discuss in brief possible sources of proton decay. Under further breaking of $SO(10)$ to $SU(5)\times U(1)_\chi$, the decomposition of $27/\overline{27}$ give $10/\overline{10}$'s and $\bar{5}/5$'s. The relevant term for proton decay can be $U(1)_\psi$-invariant if a singlet is introduced, so that the term $\mathcal{W}\supset 10^3_{1,-1}5_{1,3}1_{-4,0}$ is gauge invariant with respect to $SU(5)\times U(1)_\chi$. However, the t_i charges emanating from $SU(3)_\perp$ spectral symmetry, do not match. In fact, two additional singlets θ_{31} are required to generate the coupling:

$$\mathcal{W}\supset 10_{1,-1}10_{1,-1}10_{1,-1}5_{1,3}1_{-4,0}\theta^2_{31}.$$

Therefore, this term is highly suppressed.

Finally, let us briefly discuss the possible contributions to the massless spectrum from the E_6 adjoint, i.e. bulk states from the decomposition of 78. As has been previously shown [118], in groups of rank 5 or higher not all bulk states are eliminated and therefore the zero mode

Spectrum	$SU(5)$	$SO(10)$
$3 \times (Q, u^c, e^c)$	10	16
$3 \times (d^c, L)$	$\overline{5}$	16
$3 \times \nu^c$	1	$16/\overline{16}$
$3 \times \overline{D}, 4 \times H_d$	$\overline{5}$	$10/16$
$3 \times D, 4 \times H_u$	5	$10/\overline{16}$
S	1	1

Table 5.5: The spectrum of the effective model and its $SO(10)$ origin used in the RGE analysis. In addition to the H_u and H_d MSSM Higgs pair, three complete $SU(5)$ multiplets in $5 + \bar{5}$ are assumed to remain in the low energy spectrum. The content of the Table refers to the N, η, ψ models.

spectrum is expected to contain components of 78. It is possible that some of these states remain at low energies. Although there are some interesting phenomenological implications of such states [218], in the present work we will assume that they become massive at some high scale and will therefore not be included in our analysis. Some details about these states are given in Appendix D.

5.4 RGE analysis for Gauge and Yukawa couplings

As we have seen, from the decomposition of the E_6 representations there are always additional fields, beyond those of the MSSM spectrum. For our RGE analysis we will consider an effective model that contains the three families embedded in three 16-plets $\in SO(10)$, where the three right-handed neutrinos decouple at a scale $\sim 10^{14}$ GeV. As shown in the previous section the exact form of the low energy spectrum and the superpotential depends on specific choices of fluxes, singlet vevs and other parameters. Here, we will focus on a single case where additional matter comprises three complete $SU(5)$ vectorlike $5 + \bar{5}$ multiplets and a singlet S, and the remaining singlets $1_4, 1_{-4}$ are assumed to decouple from the light spectrum. The MSSM Higgs fields H_u, H_d are accommodated in 5-plets arising from the $SO(10)$ tenplets 10_{-2}. We suppose that all other components are removed from the spectrum either by appealing to fluxes or due to a possible doublet-triplet splitting mechanism through couplings with the bulk states. Under these assumptions, we have the particle content presented in Table 5.5.

The computation of the 2-loop RGE's was performed with the use of the Mathematica code `SARAH-4.10.0` [221]. We consider only the Yukawa couplings of the third generation (called here as Y_t, Y_b and Y_τ) and for simplicity, we neglect the effects of $U(1)$ kinetic mixing[1]. We take $M_{SUSY} = 1$ TeV, $M_S = 8$ TeV and a Majorana scale $M_N = 10^{14}$ GeV, where the heavy right-handed neutrinos decouple from the theory, while all the other extra particles decouple at the scale M_S.

[1] An analysis of the effects of $U(1)$ mixing at the 2-loop level is presented in [233].

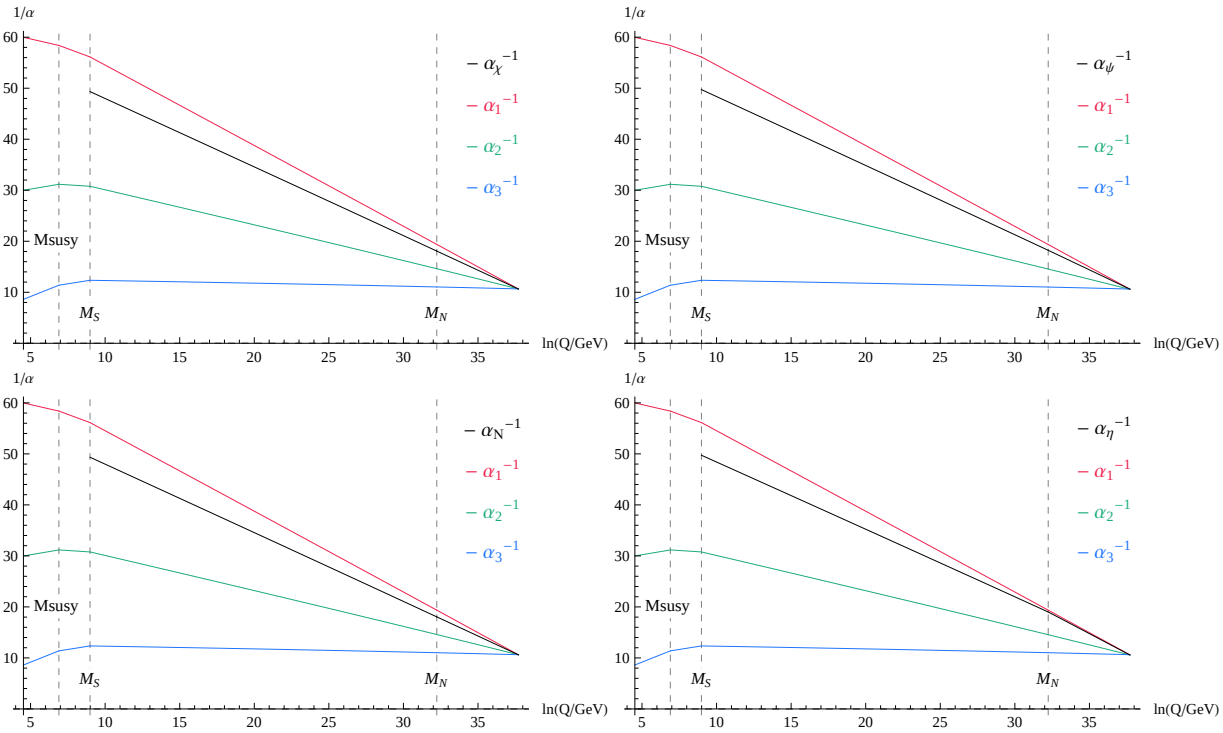

Figure 5.1: Gauge coupling unification in E_6 models. In all cases $M_{GUT} = 2.4 \times 10^{16}$ GeV with $g_U \simeq 1.09$. Here $M_{SUSY} = 10^3$ GeV, $M_S = 8 \times 10^3$ GeV and $M_N = 10^{14}$ GeV. Top: left $U(1)_\chi$, right $U(1)_\psi$. Bottom: left $U(1)_N$, right $U(1)_\eta$.

Using the mass scales and parameters as described above, we obtain values of the three SM gauge couplings within the range constrained by the experimental results. In Figure 5.1 we present their evolution together with the abelian factor corresponding to the $U(1)_\chi, U(1)_\psi, U(1)_N$, and $U(1)_\eta$ models respectively. As shown in the figure, the decoupling of $U(1)$ is assumed at the mass scale $M_S = 8$ TeV. The beta coefficient of the extra $U(1)$ gauge coupling depends on the corresponding charge as follows:

$$b_\chi = 163/20, \quad b_\psi = 25/3, \quad b_N = 163/20, \quad b_\eta = 227/30. \tag{5.13}$$

By assuming unification at $M_{GUT} = 2.4 \times 10^{16}$ GeV we obtain the following values for the extra gauge coupling at the scale $M_S = 8$ TeV :

$$g_\chi(M_S) \simeq 0.508, \quad g_\psi(M_S) \simeq 0.506, \quad g_N(M_S) \simeq 0.508, \quad g_\eta(M_S) \simeq 0.506. \tag{5.14}$$

Next we proceed with the Yukawa sector. In Figures 5.2 and 5.3 we present the evolution of the third generation Yukawa couplings for $\tan\beta = 50$. Figure 5.2 corresponds to $|\mu| = 0.5$ TeV and Figure 5.3 to $|\mu| = 0.8$ TeV. In both cases, the masses of the sfermions were taken in the range of $2 - 3$ TeV and the trilinear parameter $A_t = 2.2$ TeV. We observe that, in contrast to the minimal spectrum, in the presence of additional vectorlike matter, a moderate value of the top Yukawa coupling at the GUT-scale can reproduce the top mass at the electroweak scale.

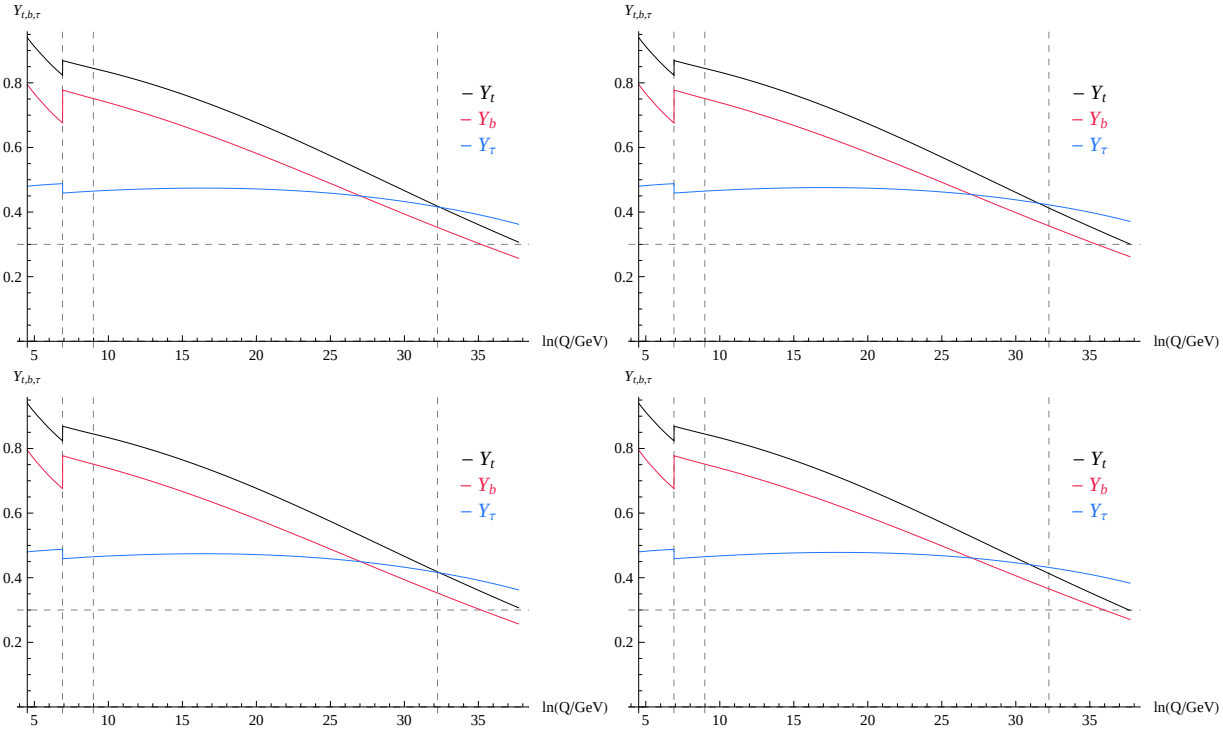

Figure 5.2: Running of t-b-τ Yukawa couplings. The horizontal dashed line corresponds to $Y = 0.3$ and is used here for guidance. Here $\tan\beta = 50$, $|\mu| = 0.5$ TeV and $A_t = 2.2$ TeV. Top: left $U(1)_\chi$, right $U(1)_\psi$. Bottom: left $U(1)_N$, right $U(1)_\eta$.

Furthermore, comparing Figures 5.2 and 5.3, we see that an increment of the SUSY threshold corrections [57], [234] and the value of $|\mu|$, implies larger GUT values of the Yukawa couplings. Some representative values for the same SUSY parameters but two different values of μ are presented in Tables 5.6 and 5.7. Our findings show that the results are the same for χ and N models. For a discussion of sparticle spectroscopy with t-b-τ Yukawa unification see [235] and references therein.

We close this section with a few observations. First, we notice that raising the scale M_S by a few TeV increases slightly the value of the Yukawa couplings. At the same time we get a lower value of the gauge coupling g_U at M_{GUT}.

E_6 model	Y_t	Y_b	Y_τ	Y_H	Y_D
$U(1)_\chi$	0.305	0.257	0.361	0.336	0.306
$U(1)_\psi$	0.300	0.262	0.370	0.330	0.300
$U(1)_N$	0.305	0.257	0.361	0.336	0.306
$U(1)_\eta$	0.297	0.270	0.380	0.345	0.324

Table 5.6: Numerical values of the Yukawa couplings at M_{GUT} for $\tan\beta = 50$ and $|\mu| = 0.5$ TeV. The last two columns refer to the Yukawa couplings of the vectorlike pairs.

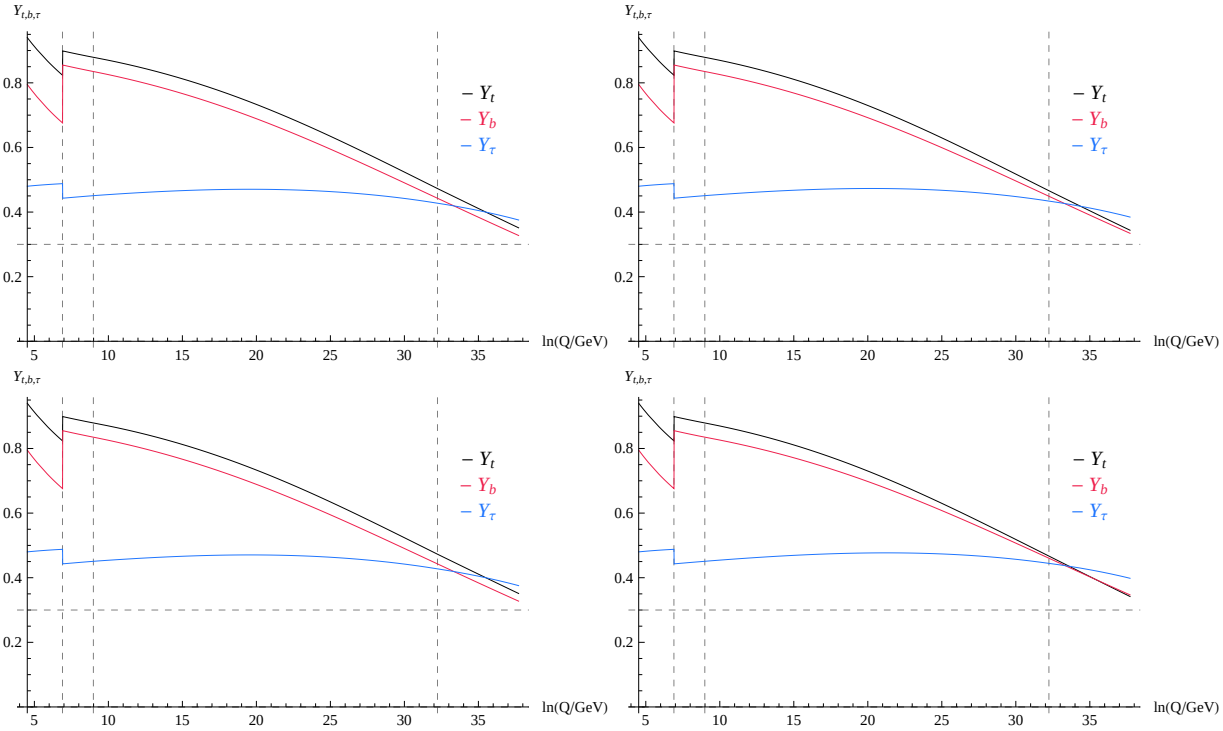

Figure 5.3: Running of t-b-τ Yukawa couplings. The horizontal dashed line corresponds to Y=0.3 and is used here for guidance. Here $tan\beta = 50$, $|\mu| = 0.8$ TeV and $A_t = 2.2$ TeV. Top: left $U(1)_\chi$, right $U(1)_\psi$. Bottom: left $U(1)_N$, right $U(1)_\eta$.

If the mass of the Z' boson is much heavier than M_Z we can neglect mixing effects and the mass of the extra neutral Z' boson is given by the following formula [116]:

$$M_{Z'} \approx g'(Q_S s^2 + Q_{H_u} v_u^2 + Q_{H_d} v_d^2)^{1/2}$$

where Q_i's are refer to the charges under the extra $U(1)$ and s is the VEV of the singlet field S. Thus, using the values 5.14 for the extra gauge coupling g', the masses for the various models discussed so far are:

$$M_{Z_\psi} \approx 4.67 \text{ TeV}, \quad M_{Z_N} \approx 4.54 \text{ TeV}, \quad M_{Z_\eta} \approx 3.70 \text{ TeV}. \tag{5.15}$$

In all cases, the predicted mass of the Z' boson lies just above the current experimental bounds given by [212, 213, 214]

$$M_{Z'}^{exp} > 3.4 - 4.1 \text{ TeV} .$$

Next we discuss the extra doublet and vectorlike color triplet fields. As an example, following [229], we assume that the Yukawa couplings, Y_H and Y_D, of one pair $H_u + H_d$ and one pair $D + \bar{D}$, unify asymptotically with the Yukawa couplings of the third generation at the GUT scale. The values of these couplings at the GUT scale are also presented in Tables 5.6 and 5.7.

E_6 model	Y_t	Y_b	Y_τ	Y_H	Y_D
$U(1)_\chi$	0.350	0.326	0.374	0.361	0.350
$U(1)_\psi$	0.342	0.333	0.383	0.372	0.358
$U(1)_N$	0.350	0.326	0.374	0.361	0.350
$U(1)_\eta$	0.340	0.345	0.396	0.372	0.371

Table 5.7: Numerical values of the Yukawa couplings at the GUT scale for $\tan\beta = 50$ and $|\mu| = 0.8$ TeV. The last two columns refer to the Yukawa couplings of the third family vectorlike pairs.

Using the RGE's we predict the value at the scale M_S. We find that the masses of $D + \bar{D}$ and the extra $H_u + H_d$ doublets are:

$$m_D \simeq 5.92 \quad \text{TeV}, \tag{5.16}$$

$$m_H \simeq 3.44 \quad \text{TeV}. \tag{5.17}$$

Finally, in our analysis we have found that in the presence of extra vectorlike pairs and singlet fields at a few TeV scale, the third generation fermion masses and in particular the top-mass can be correctly reproduced with moderate values of the Yukawa couplings at the GUT scale. As we will show, this is in agreement with the predictions from F-theory computations.

5.4.1 Yukawa Couplings in E_6 from F-Theory

In F-theory, the Yukawa couplings are realised when three Riemann surfaces accommodating matter fields intersect at a single point on the GUT surface, S. Given the specific geometry of the compact space, we can solve the appropriate equations of motion and determine the profile of the wavefunctions of the states involved. The Yukawa couplings are then obtained by computing the integral of the overlapping wavefunctions at the triple intersections. The final result of the computation depends on local flux densities permeating the matter curves. In the present study, we consider an E_8 point of enhancement (which contains both top and bottom/tau type Yukawa couplings) and follow the procedures described in a series of papers [145]-[152]. We should note that the flux units considered in Section 5.3 are integer valued as they arise from the Dirac quantisation

$$\frac{1}{2\pi}\int_{\Sigma\subset S} F = n_f\,,$$

where n_f is an integer, Σ denotes a matter curve, and F is the gauge field strength tensor, i.e., the flux. In the same section we also described how the flux units piercing different matter curves Σ determine the chiral states which are globally present in a given model. However as described in section 4.3 of the previous Chapter, while the flux units in Section 5.3 define the full spectrum of the model, the study of the trilinear couplings involve the calculation of the wavefunctions and their overlaps on a local, approximately flat patch around a point of intersection. In this local approach it is the local values of flux -and not the global quantisation constraints- that matter. The local fluxes determine the chiral states at the local point. Besides those, there can be additional chiral fermions localised in other regions of the matter curve, with the total

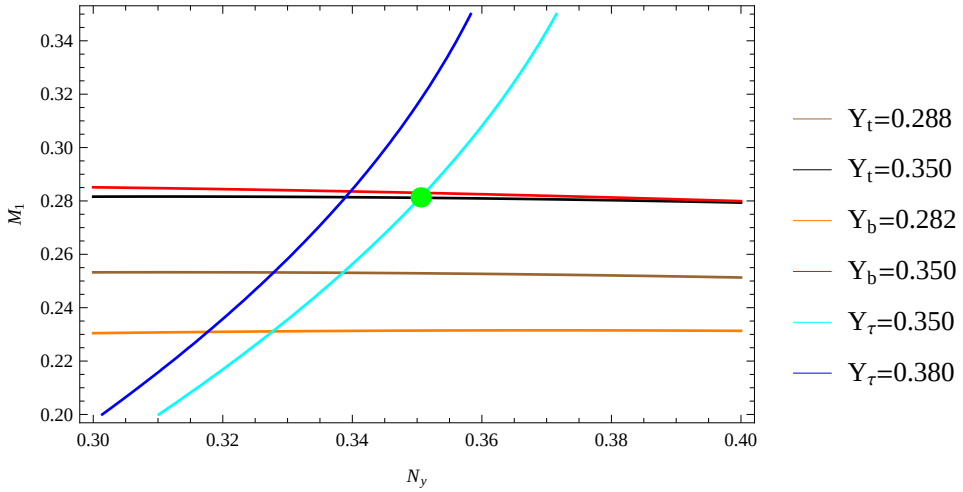

Figure 5.4: Values of the Yukawa couplings from the E_8 point in F-theory without imposing any constraint on the flux parameters. Green point corresponds to $Y_t \approx Y_b \approx Y_\tau = 0.35$.

chirality determined by the integral of the magnetic flux along the matter curve. The relation between local and global fluxes is not a clear issue since it requires a complete knowledge of the geometry of the matter curve. A more sophisticated *local vs. global* analysis is given in [149]. In our present approach, we will consider ranges of flux densities corresponding to a wide range of integer values encompassing also those flux parameters used in Section 5.3.

The procedure and the form of the wavefunctions is similar with those presented in Chapter 4. Here we follow the formulation of [152] and we deal with two types of flux density parameters. The first type is parametrised by the flux density numbers M_i, N_i where $i = 1, 2$, and descend from a worldvolume flux which is necessary to induce chirality on the matter curves accommodating the 10-plets, $\bar{5}$-plets and 5-plets of $SU(5)_{GUT}$. The second type parametrised by N_Y and $\tilde{N}_Y$, is related to the hypercharge flux which breaks the $SU(5)$ symmetry to the Standard Model and in addition generates the observed chirality of the fermion families.

In Figure 5.4 we plot the bottom, tau and top Yukawa coupling at the local flux-density parameter space M_1 and N_Y. For the remaining flux density parameters involved in the computation we consider the values $N_1 = 0.187, M_2 = 1.23, N_2 = 0.701, \tilde{N}_Y = 0.09$. For a reasonable range of the M_1 and N_Y parameters, the values of $Y_{t,b,\tau}$ lie approximately between 0.3 and 0.4. There is a single (M_1, N_Y) point (shown with green color bullet in Figure 5.4) where all Yukawa couplings of the third generation attain the same value $Y_{t,b,\tau} = 0.35$.

Before closing this Chapter, we make a few comments regarding the issues emerging from supersymmetry breaking, such as soft masses and flavour changing neutral currents (FCNC). The structure of the SUSY breaking soft terms have been studied for a large class of string and flux compactifications with a MSSM-like spectrum [236]-[240]. In many cases the presence of non-diagonal flavor dependent SUSY-breaking soft terms are generically induced. The presence of such terms can lead to dangerous FCNC effects which can create tension with other phenomenological predictions of the low energy theory. In the case of F-theory generalisations, SUSY breaking soft terms and its phenomenological implications have been extensively dis-

cussed in the past [241]-[245], [148]. Especially in [244], [245], it is shown how SUSY breaking soft terms for fields on matter curves are generated from closed string fluxes, applying the results on F-theory local models and including contributions from magnetic fluxes. In the special case of non-constant fluxes flavor dependent soft terms arise which must lie in the multi-TeV range in order to avoid FCNC effects. However, the results strongly depend on the internal geometry, the background fluxes and there is considerable uncertainty from model dependent factors. On the other hand these flavor violating effects may be suppressed if the close string fluxes vary slowly over S.

Gravity mediated SUSY breaking is also a possible source of FCNC after integrating out heavy modes. In F-theory local models this scenario has been discussed in [148] where it is shown that off-diagonal terms are not induced due to the presence of geometric $U(1)$ symmetries, while a full study of FCNC requires the study of the difference $m_{22}^2 - m_{11}^2$ of the soft scalar masses m_{ij}. We expect that this will be suppressed for a wide range of the parameter space while a detailed computation is beyond the scope of this thesis.

Chapter 6

Summary and Conclusions

String theory is currently the best-known candidate for a theory of quantum gravity, having the necessary ingredients to describe all known elementary particles and interactions. Supersymmetry, grand unified theories, discrete family symmetries and alternative symmetry breaking mechanisms arising from the additional compact dimensions. In the same direction, F-theory as a non-perturbative version of II-B string theory, provides a unified perspective on various aspects of string model building. In this thesis, we have presented a systematic analysis of F-theory models and their phenomenological implications. Below we summarize the main conclusions of this dissertation.

In Chapter 2, a class of $SU(5)$ SUSY GUT models which arise in the context of the spectral cover with Klein Group monodromy $V_4 = Z_2 \times Z_2$ was studied. By investigating the symmetry structures of the spectral cover equation and the defining equations of the matter curves it is possible to understand the F-theory geometric origin of matter parity, which so far has been just assumed in an *ad hoc* way. In particular, we have shown how the simplest Z_2 matter parities can be realised via the new geometric symmetries respected by the spectral cover. By exploiting the various ways that these symmetries can be assigned, there are a large number of possible variants. A minimal example of this kind, where the low energy effective theory below the GUT scale is just the MSSM with no exotics and standard matter parity was presented. Furthermore, by deriving general properties of the singlet sector, we were able to identify two singlets, which provide suitable candidates for a two right-handed neutrinos. We were thus able to derive the MSSM extended by a two right-handed neutrino seesaw mechanism. In addition all baryon and lepton number violating operators emerging from higher non-renormalisable operators are be forbidden. The work presented in Chapter 2 has been published in *Physical review D* (PRD) [3].

In the third Chapter an F-theory derived $SU(5)$ model was constructed, with the implications of the arising non-Abelian familiy symmetry being considered, following from work in [172] and [1]. Using the spectral cover formalism, assuming a point of E_8 enhancement descending to an $SU(5)$ GUT group, the corresponding maximal symmetry (also $SU(5)$) should reduce down to a subgroup of the Weyl group, S_5. By applying Galois theory knowledge the conditions on the coefficients of the spectral cover polynomial in the case of the non-Abelian discrete group D_4

were derived. This symmetry was assumed to play the role of a family symmetry in the low energy effective model. Similar to the model presented in Chapter 2, a geometric symmetry was also employed to produce an R-parity-like Z_2 symmetry. The combined effect of this framework on the effective field theory has been examined, and the resulting model shown to exhibit parity violation in the form of neutron-antineutron oscillations, while being free from dangerous proton decay operators. The experimental constraints on this interesting process have been calculated, using current data on the masses of supersymmetric partners. Detection of such baryon-violating processes on the oncoming experiments, without proton decay, serve as a potential smoking gun prediction for this type of model.

Due to the presence of the D_4 family symmetry, special attention was given on the neutrino sector of the model and it was shown that at lowest orders this model predicts the lightest neutrino to be massless. Correspondingly, the masses of the two other generations then equate to the mass differences from experiment, with the hierarchy being normal ordered. The mixing angles were also probed numerically, with results that are consistent with large mixing in the neutrino sector and a small but non-zero reactor mixing angle. The work presented in Chapter 3 has been published in *Journal of High Energy Physics* (JHEP), [2].

Chapter 4 provides a first dedicated study of R-parity violation (RPV) in F-theory semi-local and local constructions based on the $SU(5)$ GUT. Within this framework, the analysis presented is as general as possible, with the primary aim of making a connection between F-theory and experiment. We have focussed on semi-local and local F-theory $SU(5)$ constructions, where a non-trivial hypercharge flux breaks the GUT symmetry down to the Standard Model and in addition renders several GUT multiplets incomplete. Acting on the Higgs curves this novel mechanism can be regarded as the surrogate for the doublet-triplet splitting of conventional GUTs. However, from a general perspective, at the same time the hyperflux may work as a displacement mechanism, removing certain components of GUT multiplets while accommodating fermion generations on other matter curves.

In the first part of the Chapter we considered semi-local constructions, focussing on F-theory $SU(5)_{GUT}$ models which are classified according to the discrete symmetries – acting as identifications on the $SU(5)_\perp$ representations – and appearing as a subgroup of the maximal $SU(5)_\perp$ Weyl group S_5. Furthermore, we considered phenomenologically appealing scenarios with the three fermion generations distributed on different matter curves and showed that RPV couplings are a generic feature on this class of models. Upon introducing the flux breaking mechanism, we classified all possible cases of incomplete GUT multiplets and examined the implications of their associated RPV couplings. Then we focused on the induced MSSM plus RPV Yukawa sector which involves only part of the MSSM allowed RPV operators as a consequence of the missing components of the multiplets projected out by flux effects. Next, we tabulated all distinct cases and the type of physical process (baryon number violation, lepton number violation or proton decay) that can arise from particular operators involving different types of incomplete multiplets.

In the second part of Chapter 4 we computed the strength of the RPV Yukawa couplings, which mainly depend on the topological properties of the internal space and are more or less

independent of many details of a particular model, enabling us to study a generic local F-theory setting. Due to their physical relevance, we paid special attention to those couplings originating from the $SU(5)$ operator $10\cdot\bar{5}\cdot\bar{5}$ in the presence of general fluxes, which is realised at an $SO(12)$ point of enhancement. Then, we applied the already developed F-theory techniques for the calculation of the strengths of Yukawa couplings in the case of RPV operators. Taking into account flux restrictions, which limit the types of RPV operators that may appear simultaneously, we then calculated ratios of Yukawa couplings, from which the physical RPV couplings at the GUT scale can be determined. We have explored the possible ranges of the Yukawa coupling strengths of the $10\cdot\bar{5}\cdot\bar{5}$-type operators in a five-dimensional parameter space, corresponding to the number of the distinct flux parameters/densities associated with this superpotential term. Varying these densities over a reasonable range of values, we have observed the tendencies of the various Yukawa strengths with respect to the flux parameters and, to eliminate uncertainties from overall normalization constants, we have computed the ratios of the RPV couplings to the bottom Yukawa one. This way, using the experimentally determined mass of the bottom quark, we compared our results to limits on these couplings from experiment.

The results show firstly that, in semi-local F-theory constructions based on $SU(5)$ GUTs, RPV is a generic feature, but may occur without proton decay, due to flux effects. Secondly, our calculations based on a local F-theory approach show that the value of the RPV Yukawa couplings, at the GUT scale, may be naturally suppressed over large regions of parameter space. Furthermore, we found that the existence of LLe^c type of RPV interactions from F-Theory are expected to be within the current bounds. This implies that such lepton number violating operators could be present in the effective theory, but simply below current experimental limits, and so lepton number violation could be observed in the future. Similarly, the baryon number violating operators $c^c d_j^c d_k^c$ and $t^c d_j^c d_k^c$ could also be present, leading to $n-\bar{n}$ oscillations. Finally some QLd^c operators could be present leading to lepton number violating processes such as $K^+ \to \pi^- e^+ e^+$ and $D^+ \to K^- e^+ e^+$. In conclusion, the results suggest that RPV SUSY consistent with proton decay and current limits may be discovered future experiments, shedding light on the nature of F-theory constructions. The work presented in Chapter 3 has been published in *Journal of High Energy Physics* (JHEP) [4].

In the final Chapter of this thesis, we have presented effective field theory models embedded in E_6 with an extra neutral gauge boson (Z') and additional vectorlike fields in the low energy spectrum. The extra matter fields (beyond the MSSM spectrum), assumed to remain at the TeV region include triplets and doublets comprising three complete $5+\bar{5}$-plets of $SU(5)$, as well as neutral singlets. It is shown that this spectrum can be embedded naturally in an F-theory scenario where abelian fluxes are used to break the E_6 symmetry to $SU(5)$. Using renormalisation group analysis at two-loop level, we explore the implications of this spectrum on the running of the gauge and Yukawa couplings. We perform this analysis by assuming a Z' boson mass compatible with the LHC bounds and masses of the extra fields ~ 10 TeV, and we take into account threshold corrections of SUSY particles and a right-handed neutrino scale 10^{14} GeV. We find that moderate values at the GUT scale of the third generation Yukawa coulings in the range $Y_{t,b,\tau} \sim 0.3-0.4$ and $\tan\beta \sim 50$ can successfully reproduce their low energy masses.

Finally, based on previous detailed work on Yukawa couplings in F-theory, we compute the third generation Yukawa couplings generated by a configuration of intersecting seven-branes with the GUT divisor. We assume a configuration with a single E_8 point of enhancement and compute the relevant integral taking into account non-trivial fluxes associated with the symmetry breaking. We express the results in terms of the local flux densities and find that their values are in the same range with those found by the renormalisation group analysis using as inputs the known low energy masses of the charged fermions of the third family. We also find points in the F-theory parameter space of the flux densities where $t - b - \tau$ Yukawa couplings attain a common value. This work has been published in *Physics Letters B* [5].

Appendices

Appendix A

Topics in Galois Theory

A.1 Basic Galois Theory

According to Galois theory if $\mathcal{L}$ is the splitting field of a separable polynomial $P \in \mathcal{F}[x]$, then the Galois group $Gal(\mathcal{L}/\mathcal{F})$ is associated with the permutations of the roots of P. Let P has degree n. Then in $\mathcal{L}[x]$ we can write the P as the product

$$P(x) = c(x - t_1) \dots (x - t_n) \tag{A.1}$$

where $c \neq 0$ and the roots $t_1, \dots t_n \in \mathcal{L}$ are distinct. In this situation we get a map

$$Gal(\mathcal{L}/\mathcal{F}) \to S_n$$

which is a one-to-one group homomorphism. Important rôle in the determination of the Galois group of a polynomial plays the discriminant, which is a symmetric function of the roots t_i. The discriminant $\Delta(P) \in \mathcal{F}$ of a (monic) polynomial $P \in \mathcal{F}[x]$ with $P = (x - t_1) \dots (x - t_n)$ in a splitting field $\mathcal{L}$ of P is

$$\Delta(P) = \prod_{i<j} (t_i - t_j)^2. \tag{A.2}$$

Another useful object is the square root of the discriminant:

$$\sqrt{\Delta(P)} = \prod_{i<j} (t_i - t_j) \quad \in \mathcal{L}. \tag{A.3}$$

Note that while Δ is uniquely determined by P, the above square root depends on how the roots are labeled. It is obvious that the $\sqrt{\Delta(P)}$ controls the relation between $Gal(\mathcal{L}/\mathcal{F})$ and the alternating group $A_n \subset S_n$. More precisely, the image of $Gal(\mathcal{L}/\mathcal{F})$ lies in A_n if and only if $\sqrt{\Delta(P)} \in \mathcal{F}$ (i.e., $\Delta(P)$ is the square of an element of $\mathcal{F}$). In our case we deal with a fourth degree polynomial corresponding to the spectral surface C_4, hence our starting point is S_4 and A_4.

To reduce further the S_4/A_4 down to their subgroups (D_4, Z_4 and V_4) we need the service of the so called *resolvent cubic* of P

$\Delta(P)$	R_3 in $\mathcal{F}$	$Gal(\mathcal{L}/\mathcal{F})$
$\neq \square$	irreducible	S_4
$= \square$	irreducible	A_4
$\neq \square$	reducible	D_4 or Z_4
$= \square$	reducible	V_4

Table A.1: The Galois groups for the various cases of the discriminant and the reducibility of the cubic resolvent R_3.

$$R_3 = (x - x_1)(x - x_2)(x - x_3) \tag{A.4}$$

where now the x_i's are symmetric polynomials of the roots with

$$x_1 = t_1t_2 + t_3t_4, \quad x_2 = t_1t_3 + t_2t_4, \quad x_3 = t_3t_2 + t_1t_4. \tag{A.5}$$

A permutation of the indices carries x_1 to one of the three polynomials x_i, i=1,2,3. Since S_4 has order 24, the stabilizer of x_1 is of order 8, it is one of the three dihedral groups D_4. Also, $\Delta(R_3) = \Delta(P)$, so when P is separable so is R_3. Using the discriminant and the reducibility of the cubic resolvent we can correlate the groups S_4, D_4, Z_4, A_4 and V_4 with the Galois group of a quartic irreducible polynomial. The analysis above with respect to $\Delta(P)$ and R_3 is summarized in Table A.1.

A.2 An Alternative Cubic Resolvent

Another resolvent cubic that shares its discriminant with the quartic polynomial can be built using the following three roots:

$$z_1 = (t_1 + t_2)(t_3 + t_4), \quad z_2 = (t_1 + t_3)(t_2 + t_4), \quad z_3 = (t_1 + t_4)(t_2 + t_3) \tag{A.6}$$

with the two symmetric polynomial set-ups related as follows :

$$z_1 = x_2 + x_3, \quad z_2 = x_1 + x_3, \quad z_3 = x_1 + x_2. \tag{A.7}$$

To see that the two discriminants coincide, note that the differences for each set of symmetric polynomials are related as:

$$x_i - x_j = -(z_i - z_j) \tag{A.8}$$

and since the discriminant can be expressed as products of these difference it is trivial to see that the two must coincide:

$$\Delta = \prod_{i \neq j}(z_i - z_j) = \prod_{i \neq j}(x_i - x_j)\,. \tag{A.9}$$

In the case of $C_4 \times C_1$ spectral cover split, the cubic resolvent of C_4 has the form:

$$g(s) = a_5^{-3/2}[(a_5 s)^3 - 2a_3(a_5 s)^2 + (a_3^2 + a_2a_4 - 4a_1a_5)a_5 s + (a_2^2a_5 - a_2a_3a_4 + a_1a_4^2)]\,. \tag{A.10}$$

We can see that, by setting $g(0) = 0$ we obtain the following condition:

$$a_2^2 a_5 - a_2 a_3 a_4 + a_1 a_4^2 = 0\,. \tag{A.11}$$

Substituting the above condition in the equation of the fives the result is zero, which is not a surprising result since the three symmetric functions of the roots, z_i, can be used to rewrite the equation of the GUT fives as:

$$P_5 = \prod_{i,j}(t_i + t_j) = z_1 z_2 z_3 \prod_{i}^{4}(t_i + t_5) = -g(0)\prod_{i}^{4}(t_i + t_5). \tag{A.12}$$

If we substitute this new condition into the discriminant we find that it now reads:

$$\Delta \propto 4\left(4a_1 a_5 - a_2 a_4\right)\left(a_3^2 + a_2 a_4 - 4a_1 a_5\right)^2 \tag{A.13}$$

Combined with the constraint for tracelessness of the GUT group[1], $b_1 = 0$, the condition becomes:

$$g(0) = 0 \to a_7 a_2^2 + a_3 a_6 a_2 = a_0 a_1 a_6^2\,. \tag{A.14}$$

Correspondingly the fives of the GUT group now have an equation that factors into only two parentheses,

$$P_5 = \left(a_7 a_2^2 + a_3 a_6 a_2 - a_0 a_1 a_6^2\right)\left(a_3 a_6^2 + a_7\left(a_2 a_6 + a_1 a_7\right)\right) \to P_a P_b\,, \tag{A.15}$$

where, the first factor vanishes due to the constraint and corresponds to the roots $z_1 z_2 z_3 = 0$.

In this relation it is clear that the trivial condition $g(0) = 0$ automatically leads to $P_5 = 0$. So we need a more general factorisation for the cubic polynomial. In general a cubic is reducible if it can be factorised as a linear and a quadratic part.

[1] $\{a_4 \to a_0 a_6, a_5 \to -a_0 a_7\}$

Appendix B

Details for the $SU(5) \times D_4 \times U(1)$ model

B.1 Irreducible representations of D_4

Since we have four weights related, the representation of the 10s of the GUT group will be quadruplets of D_4: $(t_1, t_2, t_3, t_4)^{\mathrm{T}}$. Physically we may take each of these weights to represent a corner of a square (or an equivalent interpretation). These weights will transform in this representation such that the two generators required to describe all possible transformations are equivalent to a rotation about the center of the square of $\frac{\pi}{2}$ and a reflection about a line passing through the center - say the diagonal running between the top right and bottom left corners (see Figure B.1).

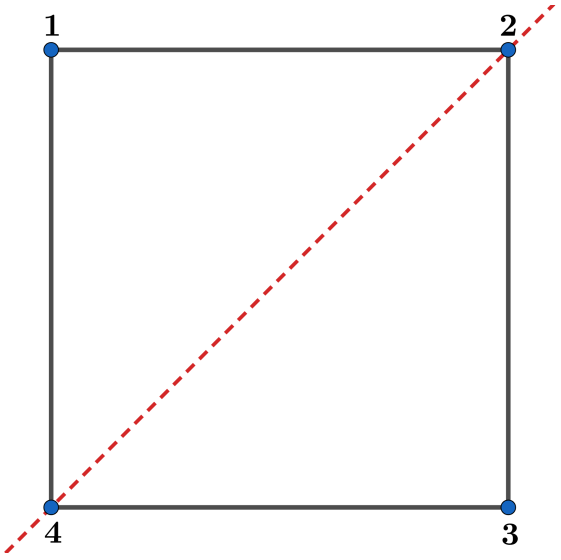

Figure B.1: The diehedral group D_4 represents the symmetries of a square. The dashed line shows a possible reflection symmetry, while it also has a rotational symmetry if rotated by $\frac{n\pi}{2}$.

The two generators are:

$$a = \begin{pmatrix} 0 & 0 & 0 & 1 \\ 1 & 0 & 0 & 0 \\ 0 & 1 & 0 & 0 \\ 0 & 0 & 1 & 0 \end{pmatrix}, \tag{B.1}$$

$$b = \begin{pmatrix} 1 & 0 & 0 & 0 \\ 0 & 0 & 0 & 1 \\ 0 & 0 & 1 & 0 \\ 0 & 1 & 0 & 0 \end{pmatrix}. \tag{B.2}$$

These generators must obey the general conditions for dihedral groups, which for D_4 are:

$$a^4 = b^2 = \mathrm{I} \tag{B.3}$$

$$b \cdot a \cdot b = a^{-1} \tag{B.4}$$

It is trivial to see that these conditions are obeyed by our generators. In order to obtain the irreducible representations we should put this basis into block-diagonal form, which is achieved by applying the appropriate unitary matrices.

Since D_4 is known to have a two-dimensional irreducible representation, we might assume that our four-dimensional case can be taken to a block diagonal form including either a doublet and two singlets or two doublets via a unitary transformation.

If we initially assume two doublets, then we may put some conditions on our unitary matrix:

$$A' = U \cdot A \cdot U^{\mathrm{T}} = \begin{pmatrix} - & - & 0 & 0 \\ - & - & 0 & 0 \\ 0 & 0 & - & - \\ 0 & 0 & - & - \end{pmatrix} \tag{B.5}$$

$$B' = U \cdot B \cdot U^{\mathrm{T}} = \begin{pmatrix} - & - & 0 & 0 \\ - & - & 0 & 0 \\ 0 & 0 & - & - \\ 0 & 0 & - & - \end{pmatrix} \tag{B.6}$$

$$\mathrm{I} = U \cdot U^{\mathrm{T}}. \tag{B.7}$$

If we make use of these conditions, there are a number of equivalent solutions for U, one of which is:

$$U = \frac{1}{\sqrt{2}} \begin{pmatrix} 1 & 0 & 1 & 0 \\ 0 & 1 & 0 & 1 \\ 1 & 0 & -1 & 0 \\ 0 & 1 & 0 & -1 \end{pmatrix}. \tag{B.8}$$

This matrix will give a block diagonal form for the generators. Explicitly this is:

$$A' = \begin{pmatrix} 0 & 1 & 0 & 0 \\ 1 & 0 & 0 & 0 \\ 0 & 0 & 0 & -1 \\ 0 & 0 & 1 & 0 \end{pmatrix}, \tag{B.9}$$

$$B' = \begin{pmatrix} 1 & 0 & 0 & 0 \\ 0 & 1 & 0 & 0 \\ 0 & 0 & 1 & 0 \\ 0 & 0 & 0 & -1 \end{pmatrix}, \tag{B.10}$$

$$\begin{pmatrix} t_1 \\ t_2 \\ t_3 \\ t_4 \end{pmatrix} \to \frac{1}{\sqrt{2}} \begin{pmatrix} t_1 + t_3 \\ t_2 + t_4 \\ t_1 - t_3 \\ t_2 - t_4 \end{pmatrix}. \tag{B.11}$$

A cursory examination reveals that the conditions for D_4 are still fulfilled by this new basis, and it would seem that at a minimum we have two doublets of the group. However we shall now examine if one of the doublets decomposes to two singlets.

The upper block of the B' generator takes the form of the identity, so we might suppose that the first of our two doublets could decompose into two singlets. Using the same conditions as for the four-dimensional starting point, which can be enforced on the two-dimensional case, we can find easily that:

$$V = \frac{1}{\sqrt{2}} \begin{pmatrix} 1 & 1 \\ 1 & -1 \end{pmatrix} \tag{B.12}$$

$$A'' = \begin{pmatrix} 1 & 0 \\ 0 & -1 \end{pmatrix} \tag{B.13}$$

$$B'' = \begin{pmatrix} 1 & 0 \\ 0 & 1 \end{pmatrix} \tag{B.14}$$

$$\frac{1}{\sqrt{2}} \begin{pmatrix} t_1 + t_3 \\ t_2 + t_4 \end{pmatrix} \to \frac{1}{2} \begin{pmatrix} t_1 + t_2 + t_3 + t_4 \\ t_1 - t_2 + t_3 - t_4 \end{pmatrix} \tag{B.15}$$

It would seem then in this case that the four-dimensional representation of D_4 can be reduced to a doublet and two singlets forming an irreducible representation. The type of the singlets can be determined by examination of the conjugacy classes of the group, which reveals that the upper singlet is of the type 1_{++}, while the lower is 1_{+-}. Table 3.2 summarising the representations of the tens.

B.1.1 D_4 representations for GUT group Fundamental representation

In F-theory the fiveplets of the $SU(5)$ GUT group are described in terms of the roots as:

$$t_i + t_j = 0 \, \forall i \neq j \, . \tag{B.16}$$

which gives a total of ten solutions, though these will be subject discrete group actions. Under the action of a D_4 symmetry, we can see trivially that since the weight t_5 is chosen to be the invariant root, all the roots corresponding to the fiveplets of the form $t_i + t_5$ will transform separately to the $i, j \neq 5$ roots. In fact, these will form a doublet and two singlets under D_4: 1_{++} and 1_{+-}.

The remaining six roots (not related with t_5) of P_5 can be studied as a sextet, say:

$$R_6 = \begin{pmatrix} t_1 + t_3 \\ t_2 + t_4 \\ t_1 + t_2 \\ t_3 + t_4 \\ t_1 + t_4 \\ t_2 + t_3 \end{pmatrix} . \tag{B.17}$$

By construction, we have arranged that the array manifestly has block diagonal generators, A and B, such that the first two lines have generators:

$$A = \begin{pmatrix} 0 & 1 \\ 1 & 0 \end{pmatrix} \quad B = \begin{pmatrix} 1 & 0 \\ 0 & 1 \end{pmatrix} . \tag{B.18}$$

We can again refer to the previous analysis for the tenplets in order to see that this reduces to two singlets: 1_{++} and 1_{+-}.

The remaining quadruplet has generators:

$$A = \begin{pmatrix} 0 & 0 & 1 & 0 \\ 0 & 0 & 0 & 1 \\ 0 & 1 & 0 & 0 \\ 1 & 0 & 0 & 0 \end{pmatrix} \quad B = \begin{pmatrix} 0 & 0 & 0 & 1 \\ 0 & 0 & 1 & 0 \\ 0 & 1 & 0 & 0 \\ 1 & 0 & 0 & 0 \end{pmatrix} , \tag{B.19}$$

which we can block diagonalise using the unitary matrix:

$$U = \frac{1}{\sqrt{2}} \begin{pmatrix} 1 & 1 & 0 & 0 \\ 0 & 0 & 1 & 1 \\ -1 & 1 & 0 & 0 \\ 0 & 0 & 1 & -1 \end{pmatrix} . \tag{B.20}$$

This gives two blocks, which are distinguished principally by their A generators:

$$A' = \begin{pmatrix} 0 & 1 & 0 & 0 \\ 1 & 0 & 0 & 0 \\ 0 & 0 & 0 & -1 \\ 0 & 0 & 1 & 0 \end{pmatrix} \quad B' = \begin{pmatrix} 0 & 1 & 0 & 0 \\ 1 & 0 & 0 & 0 \\ 0 & 0 & 0 & 1 \\ 0 & 0 & 1 & 0 \end{pmatrix} . \tag{B.21}$$

D_4 rep.	t_5	t_i	Type
1_{++}	-1	$t_1+t_2+t_3+t_4$	θ_α
1_{+-}	-1	$t_1-t_2+t_3-t_4$	θ_β
2	-1	$\begin{pmatrix} t_4-t_2 \\ t_1-t_3 \end{pmatrix}$	θ_γ
1_{++}	$+1$	$-t_1-t_2-t_3-t_4$	θ'_α
1_{+-}	$+1$	$-t_1+t_2-t_3+t_4$	θ'_β
2	$+1$	$\begin{pmatrix} t_2-t_4 \\ t_3-t_1 \end{pmatrix}$	θ'_γ
1_{++}	0	$t_1+t_2+t_3+t_4$	θ_1
1_{+-}	0	$t_1-t_2+t_3-t_4$	θ_2
1_{+-}	0	$-t_1+t_2-t_3+t_4$	θ_2
1_{--}	0	$-t_1-t_2-t_3-t_4$	θ_3
2	0	$\begin{pmatrix} t_2-t_4 \\ t_3-t_1 \end{pmatrix}$	θ_4
1_{+-}	0	$t_1-t_2+t_3-t_4$	θ_2
1_{--}	0	$t_1+t_2+t_3+t_4$	θ_3
2	0	$\begin{pmatrix} t_4-t_2 \\ t_1-t_3 \end{pmatrix}$	θ_4

Table B.1: The complete list of the irreducible representations of D_4 obtained by block diagonalizing the singlets of the GUT group. Each of these GUT singlets is labeled as θ_i to classify them, since some appear to be in some sense degenerate.

The upper block can be further diagonalised to yield two singlets, using the unitary matrix:

$$V_u = \frac{1}{\sqrt{2}} \begin{pmatrix} 1 & 1 \\ 1 & -1 \end{pmatrix}, \tag{B.22}$$

$$A''_u = B''_u = \begin{pmatrix} 1 & 0 \\ 0 & 1 \end{pmatrix}, \tag{B.23}$$

which, after consulting a character table for the group, returns two singlets of the type 1_{++}.

The lower block can be rotated into the usual doublet basis by the matrix:

$$V_d = \frac{1}{\sqrt{2}} \begin{pmatrix} 1 & 1 \\ -1 & 1 \end{pmatrix}. \tag{B.24}$$

The full set of states arising from the fiveplets is given in main text, see Table 3.3. Similar we can find the D_4 Representations for GUT Group singlet spectrum forming by the roots $t_i - t_j$. These are presented in Table B.1.

B.2 Flatness Conditions

In the construction of the D_4 model presented in Chapter 3 we used various singlet states in order to obtain a phenomenological realistic model. These singlets acquire VEV's and hence should be consistent with the supersymmetric F and D flatness conditions. Singlets spectrum in F-Theory is described by the equation

$$\prod_{i \neq j}(t_i - t_j) = 0$$

where the product is the discriminant of the spectral cover polynomial. By calculating the discriminant and enforcing the $b_1 = 0$ ansatz solution along with the splitting options we end up with the following equation

$$\begin{aligned}
&a_0 a_2^3 a_7^2 \left(-a_7^3\kappa - a_2 a_7^2 \lambda \mu^2 + 2a_0 a_2^3 \mu^4 + a_2 a_7^2 \mu\right)^2 \\
&\left(256 a_0^2 a_7^3 a_2^2 \kappa^3 + 128 a_0 a_7^4 a_2 \kappa^2 \lambda^2 + 144 a_0^2 a_7^2 a_2^3 \kappa^2 \lambda \mu^2 + 27 a_0^3 a_2^5 \kappa^2 \mu^4 + 192 a_0^2 a_7^2 a_2^3 \kappa^2 \mu + 16 a_7^5 \kappa \lambda^4 \right. \\
&+4 a_0 a_7^3 a_2^2 \kappa \lambda^3 \mu^2 - 18 a_0^2 a_7 a_2^4 \kappa \lambda \mu^3 - 144 a_0 a_7^3 a_2^2 \kappa \lambda - 6 a_0^2 a_7 a_2^4 \kappa \mu^2 - 4 a_7^4 a_2 \lambda^3 - a_0 a_7^2 a_2^3 \lambda^2 \mu^2 \\
&\left.+18 a_0 a_7^2 a_2^3 \lambda \mu - 80 a_0 a_7^3 a_2^2 \kappa \lambda^2 \mu + 4 a_0^2 a_2^5 \mu^3 + 27 a_0 a_7^2 a_2^3\right) = 0
\end{aligned} \tag{B.25}$$

As we observe we have nine factors, four of which correspond to a minus parity assignment. These are the a_0 factor, the double factor $\left(-a_7^3\kappa - a_2 a_7^2 \lambda \mu^2 + 2a_0 a_2^3 \mu^4 + a_2 a_7^2 \mu\right)$ and $256 a_0^2 a_7^3 a_2^2 \kappa^3 + \ldots$.

B.2.1 *F*-flatness

In general the Superpotential for the massless singlet fields ($\theta_{ij} \equiv \theta_{t_i - t_j}$) is

$$\mathcal{W} = \mu_{ijk} \theta_{ij} \theta_{jk} \theta_{ki} \tag{B.26}$$

while the F-flatness conditions are given by :

$$\frac{\partial \mathcal{W}}{\partial \theta_{ij}} = \mu_{ijk} \theta_{jk} \theta_{ki} = 0. \tag{B.27}$$

For the model presented in the main text, the invariant tree-level singlet operators are

$$\begin{aligned}
\mathcal{W}_\theta = &\mu_1 \theta_1 \theta_\alpha \theta'_\alpha + \mu_2 \theta_1 \theta_\beta \theta'_\beta + \mu_3 \theta_1 \theta_\gamma \theta'_\gamma + \mu_4 \theta_3 \theta_\gamma \theta'_\gamma \\
&+ \lambda_1 \theta_4 \theta_\gamma \theta'_\alpha + \lambda_2 \theta_4 \theta'_\gamma \theta_\alpha + \lambda_3 \theta'_4 \theta'_\gamma \theta_\beta + \lambda_4 \theta'_4 \theta_\gamma \theta'_\beta \\
&+ \lambda_5 \theta_2 \theta_\alpha \theta'_\beta + \lambda_6 \theta_2 \theta'_\alpha \theta_\beta + \lambda_7 \theta_2 \theta_4 \theta'_4
\end{aligned} \tag{B.28}$$

where all the singlets have positive parity except the θ_β, θ'_β, θ_2 and θ'_4. Here with θ_4 we mean the θ_a (θ'_4 which *corresponds to* right-handed neutrino states ν_R).

Minimization of the superpotential leads to the following F-flatness conditions:

$$\begin{aligned}
\frac{\partial \mathcal{W}}{\partial \theta_1} &= \mu_1 \theta_\alpha \theta'_\alpha + \mu_2 \theta_\beta \theta'_\beta + \mu_3 \theta_\gamma \theta'_\gamma = 0 \\
\frac{\partial \mathcal{W}}{\partial \theta_2} &= \lambda_5 \theta_\alpha \theta'_\beta + \lambda_5 \theta'_\alpha \theta_\beta + \lambda_7 \theta_4 \theta'_4 = 0 \\
\frac{\partial \mathcal{W}}{\partial \theta_3} &= \mu_4 \theta_\gamma \theta'_\gamma = 0 \\
\frac{\partial \mathcal{W}}{\partial \theta_4} &= \lambda_1 \theta_\gamma \theta'_\alpha + \lambda_2 \theta'_\gamma \theta'_\alpha + \lambda_7 \theta_2 \theta'_4 = 0 \\
\frac{\partial \mathcal{W}}{\partial \theta'_4} &= \lambda_3 \theta'_\gamma \theta_\beta + \lambda_4 \theta_\gamma \theta'_\beta + \lambda_7 \theta_2 \theta_4 = 0 \\
\frac{\partial \mathcal{W}}{\partial \theta_\alpha} &= \mu_1 \theta_1 \theta'_\alpha + \lambda_2 \theta_4 \theta'_\gamma + \lambda_5 \theta_2 \theta'_\beta = 0 \\
\frac{\partial \mathcal{W}}{\partial \theta'_a} &= \mu_1 \theta_1 \theta_\alpha + \lambda_1 \theta_4 \theta_\gamma + \lambda_6 \theta_\beta \theta_2 = 0 \\
\frac{\partial \mathcal{W}}{\partial \theta_\beta} &= \mu_2 \theta_1 \theta'_\beta + \lambda_3 \theta'_4 \theta'_\gamma + \lambda_6 \theta_2 \theta'_\alpha = 0 \\
\frac{\partial \mathcal{W}}{\partial \theta'_\beta} &= \mu_2 \theta_1 \theta_\beta + \lambda_4 \theta'_4 \theta_\gamma + \lambda_5 \theta_2 \theta_\alpha = 0 \\
\frac{\partial \mathcal{W}}{\partial \theta_\gamma} &= \mu_3 \theta_1 \theta'_\gamma + \mu_4 \theta_3 \theta'_\gamma + \lambda_1 \theta_4 \theta'_\alpha + \lambda_4 \theta'_4 \theta'_\beta = 0 \\
\frac{\partial \mathcal{W}}{\partial \theta'_\gamma} &= \mu_3 \theta_1 \theta_\gamma + \mu_4 \theta_3 \theta_\gamma + \lambda_2 \theta_4 \theta_\alpha + \lambda_3 \theta'_4 \theta_b = 0
\end{aligned}$$

As we can see we have a system consist of 11-equations. Solving the system with the requirements $\langle \theta'_4 \rangle = 0 \to \langle \nu_1 \rangle = \langle \nu_2 \rangle = 0$ and $\langle \theta_2 \rangle = 0$ we end up with a large number of solutions. The most palatable one gives the following relations between the VEV's,

$$\langle \theta_\alpha \rangle^2 \equiv \alpha^2 = 2 \frac{\lambda_1 \mu_3}{\lambda_2 \mu_1} \gamma_1 \gamma_2 \tag{B.29}$$

$$a_1^2 = \frac{\mu_1 \mu_3}{2 \lambda_1 \lambda_2} \frac{\gamma_1 \langle \theta_1 \rangle}{\gamma_2} \quad and \quad a_2^2 = \frac{\mu_1 \mu_3}{2 \lambda_1 \lambda_2} \frac{\gamma_2 \langle \theta_1 \rangle}{\gamma_1} \tag{B.30}$$

$$\langle \theta_3 \rangle = \frac{\mu_2}{\mu_3} \langle \theta_1 \rangle \tag{B.31}$$

with all the other singlet VEV's equal to zero, except the $\langle \theta_\beta \rangle$ which will be subject to the D-flatness condition. Notice that equation (B.29) gives $\alpha^2 = 2\gamma_1\gamma_2$ for $\lambda_1\mu_3 = \lambda_2\mu_1$. We should also observe that combining the equations in (B.30) we end up with the relation $a_1\gamma_2 = \pm a_2\gamma_1$.

B.2.2 D-flatness

In SUSY models with extra $U(1)$ factors the D-flatness condition is given by

$$\sum_{i,j} Q_{ij}^A \left(|\langle \theta_{ij} \rangle|^2 - |\langle \theta_{ji} \rangle|^2 \right) = - \frac{Tr Q^A}{192 \pi^2} g_s^2 M_s^2 \tag{B.32}$$

where Q_{ij}^A here represents the singlet $U(1)$ charges and the trace TrQ^A is over all singlet and non-singlet states. The D-flatness conditions must be checked for all the $U(1)'s$ participating in the model. In our case we have the D_4 symmetry and one $U(1)$ descending from the perpendicular $SU(5)$. The trace in the case of $SU(5)$ has the general form

$$TrQ^A = 5\sum n_{ij}(t_i - t_j) + 10\sum n_k t_k + \sum m_{ij}(t_i - t_j). \tag{B.33}$$

The coefficients n_{ij}, n_k and m_{ij} corresponds to the $M_{U(1)}$ multiplicities. Only the curves with a t_5 charge contributes to the relation since the $t_{l=1,2,3,4}$ are subject to the D_4 symmetry rules. Using this information, the computation of the trace gives:

$$TrQ = (m'_\alpha + m'_\beta + 2m'_\gamma - m_\alpha - m_\beta - 2m_\gamma - 5)t_5 \tag{B.34}$$

where the m_i, m'_i are the (unknown) multiplicities of the singlets θ_i and θ'_i, with $i = \alpha, \beta, \gamma$. Inserting the trace in the relation (B.32) we end up with the following equation

$$|\theta'_\alpha|^2 - |\theta_\alpha|^2 + |\theta'_\beta|^2 - |\theta_\beta|^2 + |\theta'_\gamma|^2 - |\theta_\gamma|^2 = (5 - \tilde{m}_\alpha - \tilde{m}_\beta - 2\tilde{m}_\gamma)\mathcal{X} \tag{B.35}$$

where $\tilde{m}_i \equiv m'_i - m_i$ and $\mathcal{X} = \frac{g_s^2 M_s^2}{192\pi^2}$. By using the results from the F-flatness analysis the we end up with the relation

$$\alpha^2 + \beta^2 + 2\gamma_1\gamma_2 = (\tilde{m}_\alpha + \tilde{m}_\beta + 2\tilde{m}_\gamma - 5)\mathcal{X} \tag{B.36}$$

which gives an estimation for the scale of β VEV ,

$$\beta^2 = \tilde{\mathcal{M}}\mathcal{X} - \left(1 + \frac{\mu_1\lambda_2}{\mu_3\lambda_1}\right)\alpha^2 \approx \tilde{\mathcal{M}}\mathcal{X} - 2\alpha^2 \tag{B.37}$$

In the above equation we make use of the equation (B.29) and the approach $\lambda_1\mu_3 \approx \lambda_2\mu_1$ in the last step. Finally for shorthand we have set $\tilde{\mathcal{M}} \equiv \tilde{m}_\alpha + \tilde{m}_\beta + 2\tilde{m}_\gamma - 5$. Observing equation (B.37) we see that $\tilde{M}$ is positive and as a result $\tilde{m}_\alpha + \tilde{m}_\beta + 2\tilde{m}_\gamma > 5$.

In summary, equations (B.29,B.30,B.31) and (B.37) show us that controlling the scale of $\gamma_{1,2}$ and $\langle\theta_1\rangle$ we can have an estimation of the scale of all the other singlets participating in the model. That way we have a freedom on the designation of the singlet VEV's scales.

B.3 Geometric Parity for the $C_5 \to C_4 \times C_1$ spectral cover split

Here we apply the geometric parity approach described in Chapter 2 for the case where the spectral cover is taken to split as $C_5 \to C_4 \times C_1$. The geometric symmetry is communicated to the matter curves by consistency with the original spectral cover equation. It is trivial to determine that the coefficients of C_5 are related to the $C_4 \times C_1$ coefficients by:

$$b_k = \sum_{n+m=12-k} a_i a_j \tag{B.38}$$

a_n	$N=2$	$N=3$	$N=4$	$N=5$
a_1	$-$	α^2	β^2	γ^2
a_2	$+$	α	β	γ
a_3	$-$	1	1	1
a_4	$+$	α^2	β^3	γ^4
a_5	$-$	α	β^2	γ^3
a_6	$+$	1	β	γ^2
a_7	$-$	α^2	1	γ

Table B.2: Z_N parities coming from geometric symmetry of the spectral cover. In the case of $C_5 \to C_4 \times C_1$, a general phase relates the parities of $a_{1,2,3,4,5}$, such that if we flip the parity of a_1 all the other a_i in this chain must also change. A similar rule applies to $a_{6,7}$.

where $i \neq j$. As such, we can directly write that if

$$a_n \to \mathrm{e}^{i\psi_n}\mathrm{e}^{i(3-n)\phi}a_n \tag{B.39}$$

so that the product $a_n a_m$ picks up a total phase:

$$a_n a_m \to \mathrm{e}^{i(\psi_n+\psi_m)}\mathrm{e}^{i(6-n-m)\phi}a_n a_m = \mathrm{e}^{i(\psi_n+\psi_m)}\mathrm{e}^{-i(6-k)\phi}a_n a_m \tag{B.40}$$

then provided the phases of the a_n coefficients satisfy $\chi = \psi_n + \psi_m$, the symmetry is handed down to the split spectral cover. This is trival to enforce since the phases are independent of the index k. It can also be demonstrated that this consistency requires the coefficients of $C_4 \times C_1$ to have phases in two cycles: $\psi_i = \psi_1 = \psi_2 = \cdots = \psi_5$ and $\psi_j = \psi_6 = \psi_7$, in order to be consistent with the C_5 phase.

Table B.2 shows some examples of possible parities we might assign to the $C_4 \times C_1$ coefficients. In most cases, the minimal $N = 2$ scenario will be the most appealing and manageable choice, though this mechanism is not confined to it.

Appendix C

Various cases of RPV in F-theory local set-ups

C.1 Spectral cover: RPV couplings for the various monodromies

In this Appendix we examine the semi-local F-theory models in detail in order to demonstrate that RPV couplings are generic or at least common. To this end we note that:

1. We are interested in models with matter being distributed on different curves. We call this class of models as multi-curve models. We note that

2. The models defined in this framework "choose" the H_u assignment for us, since a tree-level, renormalizable, perturbative top-Yukawa requires the existence of the coupling

$$\mathbf{10}_a\mathbf{10}_a\mathbf{5}_b \tag{C.1}$$

such that the perpendicular charges cancel out. As such, all the models listed above will have a definite assignment for the curve supporting H_u, and we do not assign the remaining MSSM states to curves, i.e. all the remaining $\mathbf{5}$ curves will be called $\overline{\mathbf{5}}_a$, making clear that they are either supporting some $\overline{\mathbf{5}}_M$ or H_d. Furthermore, we will refer to the $\mathbf{10}$ curve containing the top quark as $\mathbf{10}_M$.

3. The indication for existence of tree-level, renormalizable, perturbative RPV is given by the fact we can find two couplings of the form

$$\mathbf{10}_a\overline{\mathbf{5}}_b\overline{\mathbf{5}}_c \tag{C.2}$$

$$\mathbf{10}_d\overline{\mathbf{5}}_e\overline{\mathbf{5}}_f \tag{C.3}$$

for $(b,c) \neq (e,f)$, and a, d unconstrained. This happens as H_d cannot be both supported in one of the $\overline{\mathbf{5}}_b$, $\overline{\mathbf{5}}_c$ and at the same time in one of the $\overline{\mathbf{5}}_e$, $\overline{\mathbf{5}}_f$.

4. We do not make any comment on flux data. The above criteria can be evaded by switching off the fluxes such that the RPV coupling (once the assignment of H_d to a curve is realised) disappears.

With this in mind we study the possible RPV realisations in multi-curve models.

C.1.1 $2+1+1+1$

In this case the spectral cover polynomial splits into four factors, three linear terms and a quadratic one. Also, due to the quadratic factor we impose a Z_2 monodromy. The bestiary of matter curves and their perpendicular charges (t_i) is given in Table C.1.1.

Curve :	5_{H_u}	5_1	5_2	5_3	5_4	5_5	5_6	10_M	10_2	10_3	10_4
Charge :	$-2t_1$	$-t_1-t_3$	$-t_1-t_4$	$-t_1-t_5$	$-t_3-t_4$	t_3-t_5	$-t_4-t_5$	t_1	t_3	t_4	t_5

Table C.1: Matter curves and the corresponding $U(1)$ charges for the case of a $2+1+1+1$ spectral cover split. Note that because of the Z_2 monodromy we have $t_1 \longleftrightarrow t_2$.

In this model RPV is expected to be generic as we have the following terms

$$\mathbf{10}_4\overline{\mathbf{5}}_1\overline{\mathbf{5}}_2,\ \mathbf{10}_3\overline{\mathbf{5}}_1\overline{\mathbf{5}}_3,\ \mathbf{10}_M\overline{\mathbf{5}}_1\overline{\mathbf{5}}_6,\ \mathbf{10}_2\overline{\mathbf{5}}_2\overline{\mathbf{5}}_3,\ \mathbf{10}_M\overline{\mathbf{5}}_2\overline{\mathbf{5}}_5,\ \mathbf{10}_M\overline{\mathbf{5}}_3\overline{\mathbf{5}}_4 \tag{C.4}$$

C.1.2 $2+2+1$

Here the spectral cover polynomial splits into three factors, it is the product of two quadratic terms and a linear one. We can impose a $Z_2 \times Z_2$ monodromy which leads to the following identifications between the weights,$(t_1 \leftrightarrow t_2)$ and $(t_3 \leftrightarrow t_4)$. In this case there are two possible assignments for H_u (and $\mathbf{10}_M$), as we can see in Table C.1.2 below.

				case 1				
Curve	5_{H_u}	5_1	5_2	5_3	5_4	10_M	10_2	10_3
Charge	$-2t_1$	$-t_1-t_3$	$-t_1-t_5$	$-t_3-t_5$	$-2t_3$	t_1	$-t_3$	t_5
				case 2				
Curve	5_{H_u}	5_1	5_2	5_3	5_4	10_M	10_2	10_3
Charge	$-2t_3$	$-t_1-t_3$	$-t_1-t_5$	$-t_3-t_5$	$-2t_1$	t_3	$-t_1$	t_5

Table C.2: The scenario of a $2+2+1$ spectral cover split with the corresponding matter curves and $U(1)$ charges. Note that we have two possible cases.

$2+2+1$ **case 1**

The bestiary of matter curves and their perp charges is given in the upper half table of Table C.1.2.

In this model RPV is expected to be generic as we have the following terms

$$\mathbf{10}_2\overline{\mathbf{5}}_1\overline{\mathbf{5}}_2,\ \mathbf{10}_M\overline{\mathbf{5}}_1\overline{\mathbf{5}}_3,\ \mathbf{10}_M\overline{\mathbf{5}}_2\overline{\mathbf{5}}_4,\ \mathbf{10}_3\overline{\mathbf{5}}_1\overline{\mathbf{5}}_1 \tag{C.5}$$

Notice that if $\overline{\mathbf{5}}_1$ contains only one state, then the last coupling is absent due to anti-symmetry of SU(5) contraction.

$2+2+1$ **case 2**

The bestiary of matter curves and their perp charges is given in the lower half table of Table C.1.2.

In this model RPV is expected to be generic as we have the following terms

$$\mathbf{10}_M\overline{\mathbf{5}}_1\overline{\mathbf{5}}_2,\ \mathbf{10}_2\overline{\mathbf{5}}_1\overline{\mathbf{5}}_3,\ \mathbf{10}_M\overline{\mathbf{5}}_3\overline{\mathbf{5}}_4,\ \mathbf{10}_3\overline{\mathbf{5}}_1\overline{\mathbf{5}}_1 \tag{C.6}$$

Notice that if $\overline{\mathbf{5}}_1$ contains only one state, then the last coupling is absent due to anti-symmetry of SU(5) contraction.

C.1.3 $3+1+1$

In this case spectral cover factorisation leads to a cubic and two linear factors. We can impose a Z_3 monodromy for the roots of the cubic part. The bestiary of matter curves and their perpendicular charges is given in Table **??**:

Curve	5_{H_u}	5_1	5_2	5_3	10_M	10_2	10_3
Charge	$-2t_1$	$-t_1-t_4$	$-t_1-t_5$	$-t_4-t_5$	t_1	t_4	t_5

Table C.3: Matter curves and the corresponding $U(1)$ charges for the case of a $3+1+1$ spectral cover split. Note that we have impose a Z_3 monodromy.

In this model R-parity violation is not immediately generic as we only have

$$\mathbf{10}_2\overline{\mathbf{5}}_1\overline{\mathbf{5}}_2,\ \mathbf{10}_M\overline{\mathbf{5}}_1\overline{\mathbf{5}}_3 \tag{C.7}$$

and as such assigning H_d to $\overline{\mathbf{5}}_1$ avoids tree-level, renormalizable, perturbative RPV.

C.1.4 $3+2$

These type of models are in general very constrained because of the large monodromies which leads to a low number of matter curves.

In this case there are two possible assignments for H_u (and $\mathbf{10}_M$), as described in Table C.1.4.

		case 1			
Curve	5_{H_u}	5_2	5_3	10_M	10_2
Charge	$-2t_1$	$-t_1-t_3$	$-2t_3$	t_1	t_3
		case 2			
Curve	5_{H_u}	5_2	5_3	10_M	10_2
Charge	$-2t_3$	$-t_1-t_3$	$-2t_1$	t_3	t_1

Table C.4: The two possible cases in the scenario of a $3+2$ spectral cover split, the matter curves and the corresponding $U(1)$ charges.

$3+2$ case 1

The matter curves content is given in the upper half of Table C.1.4 (case 1).

Possible RPV couplings are

$$\mathbf{10}_M\overline{\mathbf{5}}_2\overline{\mathbf{5}}_3\,,\ \mathbf{10}_2\overline{\mathbf{5}}_2\overline{\mathbf{5}}_2 \tag{C.8}$$

Notice that if $\overline{\mathbf{5}}_2$ contains only one state, then the last coupling is absent due to anti-symmetry of SU(5) contraction.

$3+2$ case 2

This second scenario is referred as case 2 in the lower half of Table C.1.4.

Only one coupling

$$\mathbf{10}_M\overline{\mathbf{5}}_2\overline{\mathbf{5}}_2 \tag{C.9}$$

which is either RPV or is absent. Notice that if $\overline{\mathbf{5}}_2$ contains only one state, then the last coupling is absent due to anti-symmetry of SU(5) contraction.

C.2 Local chirality constraints on flux densities and RPV operators

The chiral spectrum of a matter curve is locally sensitive to the flux data. This is happens as there is a notion of local chirality due to local index theorems [149, 151]. The presence of a chiral state in a sector with root ρ is given if the matrix

$$m_\rho = \begin{pmatrix} -q_P & q_S & im^2 q_{z_1} \\ q_S & q_P & im^2 q_{z_2} \\ -im^2 q_{z_1} & -im^2 q_{z_2} & 0 \end{pmatrix}$$

with q_i presented in Table 4.4, has positive determinant

$$\det m_\rho > 0. \tag{C.10}$$

As such, if we want a certain RPV coupling to be present, then the above condition has to be satisfied for the three states involved in the respective interaction at the $SO(12)$ enhancement point. For example, in order for the emergence of an QLd^c type of RPV interaction, locally the spectrum has to support a Q, a L, and a d^c states. The requirement that at a single point Equation (C.10) hold for each of these states imposes constraints on the values of the flux density parameters.

Therefore, while RPV effects in general include all three operators - QLd^c, $u^cd^cd^c$, LLe^c - there are regions of the parameter space that allow for the elimination of some or all of the couplings. These are in principle divided into four regions, depending on the sign of the parameters $\tilde{N}_Y$ and N_Y. In the appendix we present the resulting regions of the parameter space and which operators are allowed in each.

C.2.1 $\tilde{N}_Y \leq 0$

For $\tilde{N}_Y \leq 0$, the conditions on the flux density parameters for which each RPV interaction is turned on are

$$\begin{aligned} QLd^c: \; & M > \frac{-\tilde{N}_Y}{6} \\ & N_a - N_b > \frac{-N_Y}{2} \\ u^c d^c d^c: \; & M > \frac{\tilde{N}_Y}{3} \\ & N_a - N_b > -\frac{N_Y}{3} \\ LLe^c: \; & M > -\tilde{N}_Y \\ & N_a - N_b > \frac{-N_Y}{2} \end{aligned}$$

Depending on the sign of N_Y, the above conditions define different regions of the flux density parameter space. These are presented in Tables C.5 and C.6.

–	$M < \frac{\tilde{N}_Y}{3}$	$\frac{\tilde{N}_Y}{3} < M < \frac{-\tilde{N}_Y}{6}$	$\frac{-\tilde{N}_Y}{6} < M < -\tilde{N}_Y$	$-\tilde{N}_Y < M$
$(N_a - N_b) < \frac{-N_Y}{2}$	None	None	None	None
$\frac{-N_Y}{2} < (N_a - N_b) < \frac{N_Y}{3}$	None	None	QLd^c	QLd^c, LLe^c
$\frac{N_Y}{3} < (N_a - N_b)$	None	$u^c d^c d^c$	QLd^c, $u^c d^c d^c$	All

Table C.5: Regions of the parameter space and the respective RPV operators supported for $\tilde{N}_Y \leq 0$, $N_Y > 0$

–	$M < \frac{\tilde{N}_Y}{3}$	$\frac{\tilde{N}_Y}{3} < M < \frac{-\tilde{N}_Y}{6}$	$\frac{-\tilde{N}_Y}{6} < M < -\tilde{N}_Y$	$-\tilde{N}_Y < M$
$(N_a - N_b) < \frac{N_Y}{3}$	None	None	None	None
$\frac{N_Y}{3} < (N_a - N_b) < \frac{-N_Y}{2}$	None	$u^c d^c d^c$	$u^c d^c d^c$	$u^c d^c d^c$
$\frac{-N_Y}{2} < (N_a - N_b)$	None	$u^c d^c d^c$	QLd^c, $u^c d^c d^c$	All

Table C.6: Regions of the parameter space and the respective RPV operators supported for $\tilde{N}_Y \leq 0$, $N_Y < 0$

C.2.2 $\tilde{N}_Y > 0$

For $\tilde{N}_Y > 0$, the conditions on the flux density parameters for which each RPV interaction is turned on are

$$\begin{aligned} QLd^c: \; M &> \frac{\tilde{N}_Y}{3} \\ N_a - N_b &> \frac{-N_Y}{2} \\ u^c d^c d^c: \; M &> \frac{2\tilde{N}_Y}{3} \\ N_a - N_b &> -\frac{N_Y}{3} \\ LLe^c: \; M &> \frac{-\tilde{N}_Y}{2} \\ N_a - N_b &> \frac{-N_Y}{2} \end{aligned}$$

Depending on the sign of N_Y, the above conditions define different regions of the flux density parameter space. These are presented in Tables C.7 and C.8.

–	$M < -\frac{-\tilde{N}_Y}{2}$	$-\frac{-\tilde{N}_Y}{2} < M < \frac{\tilde{N}_Y}{3}$	$\frac{\tilde{N}_Y}{3} < M < \frac{2\tilde{N}_Y}{3}$	$\frac{2\tilde{N}_Y}{3} < M$
$(N_a - N_b) < \frac{-N_Y}{2}$	None	None	None	None
$\frac{-N_Y}{2} < (N_a - N_b) < \frac{N_Y}{3}$	None	LLe^c	QLd^c, LLe^c	QLd^c, LLe^c
$\frac{N_Y}{3} < (N_a - N_b)$	None	LLe^c	QLd^c, LLe^c	All

Table C.7: Regions of the parameter space and the respective RPV operators supported for $\tilde{N}_Y > 0$, $N_Y > 0$

–	$M < -\frac{-\tilde{N}_Y}{2}$	$-\frac{-\tilde{N}_Y}{2} < M < \frac{\tilde{N}_Y}{3}$	$\frac{\tilde{N}_Y}{3} < M < \frac{2\tilde{N}_Y}{3}$	$\frac{2\tilde{N}_Y}{3} < M$
$(N_a - N_b) < \frac{N_Y}{3}$	None	None	None	None
$\frac{N_Y}{3} < (N_a - N_b) < \frac{-N_Y}{2}$	None	None	None	$u^c d^c d^c$
$\frac{-N_Y}{2} < (N_a - N_b)$	None	LLe^c	QLd^c, LLe^c	All

Table C.8: Regions of the parameter space and the respective RPV operators supported for $\tilde{N}_Y > 0$, $N_Y < 0$

Appendix D

Matter from the E_6 bulk

Up to now, we have assumed that the chiral fields of the effective theory originate from the $27, \overline{27}$ matter curves. In this appendix we would like to examine the posibility of obtaining the MSSM spectrum from the bulk, i.e., the E_6 adjoint. To ensure that there are no chiral states from 27's we may impose the condition $(3c_1(S) - t) \cdot \mathcal{F}_{U(1)} = 0$ [216] where $\mathcal{F}_{U(1)}$ is the flux along the $U(1) \in SU(3)_\perp$ of (5.7), $c_1(S)$ is the first Chern class of the GUT surface and $-t$ that of the normal bundle.

We recall that the E_6 GUT is broken to the Standard Model, with the use of instanton configurations which take values along $U(1)$ factors with respect to the particular symmetry breaking. Under the breaking pattern

$$E_6 \to SU(3) \times SU(2) \times U(1)_Y \times U(1)_\chi \times U(1)_\psi$$

the decomposition of 78 reads as follows:

$$\begin{aligned} 78 \to\ & (1,1)_{0,0,0} + \{(1,1)_{0,0,0} + [(1,1)_{0,0,0} + (3,1)_{0,0,0} + (8,1)_{0,0,0} + (3,2)_{-5,0,0} + (\bar{3},2)_{5,0,0}] \\ & + [(1,1)_{6,4,0} + (\bar{3},1)_{-4,4,0} + (3,2)_{1,4,0}] + [(1,1)_{-6,-4,0} + (3,1)_{4,-4,0} + (\bar{3},2)_{-1,-4,0}]\} \\ & + \{(1,1)_{0,-5,-3} + [(1,2)_{-3,3,-3} + (\bar{3},1)_{2,3,-3}] + [(1,1)_{6,-1,-3} + (\bar{3},1)_{-4,-1-3} + (3,2)_{1,-1,-3}]\} \\ & + \{(1,1)_{0,5,3} + [(1,2)_{3,-3,3} + (3,1)_{-2,-3,3}] + [(1,1)_{-6,1,3} + (3,1)_{4,1,3} + (\bar{3},2)_{-1,1,3}]\}. \end{aligned} \tag{D.1}$$

Matter arising from E_6 bulk is subject to topological constraints. For a line bundle $\mathcal{L}_j$ over a del Pezzo S, the number of states n_j is given in terms of the Euler character $\chi(\mathcal{L}_j) = -n_j$, where

$$\chi(S, \mathcal{L}) = 1 + \frac{1}{2} c_1(\mathcal{L}_j) \cdot c_1(\mathcal{L}_j) + \frac{1}{2} c_1(\mathcal{L}_j) \cdot c_1(S) \tag{D.2}$$

In (D.2), $c_1(\mathcal{L})$ denotes the first Chern number of the line bundle and $c_1(S) = -K_S$, where K_S is the canonical class of S. For the conjugate fields

$$-n_j^* = \chi(S, \mathcal{L}_j^{-1}) = 1 + \frac{1}{2} c_1(\mathcal{L}_j) \cdot c_1(\mathcal{L}_j) - \frac{1}{2} c_1(\mathcal{L}_j) \cdot c_1(S) \tag{D.3}$$

so the net number of chiral minus anti-chiral states is

$$n_j - n_j^* = -c_1(\mathcal{L}_j) \cdot c_1(S) \tag{D.4}$$

Exotic (SM)	E_6 Origin	$SO(10)$ Origin	$SU(5)$ Origin	Multiplicity n_j
$Q_R = (\overline{3},2)_{\frac{5}{6}}$	78	45	24	$n_1 = -\chi(\mathcal{L}_1, S)$
$Q = (3,2)_{\frac{1}{6}}$	78	45	10	$n_2 = -\chi(\mathcal{L}_2, S)$
$U^c = (\overline{3},1)_{-\frac{2}{3}}$	78	45	10	$n_3 = -\chi(\mathcal{L}_1^{-1} \otimes \mathcal{L}_2, S)$
$E^c = (1,1)_1$	78	45	10	$n_4 = -\chi(\mathcal{L}_1 \otimes \mathcal{L}_2, S)$
$S = (1,1)_0$	78	16	1	$n_5 = -\chi(\mathcal{L}_2^{-1} \otimes \mathcal{L}_3, S)$
$\bar{D} = (\overline{3},1)_{\frac{1}{3}}$	78	16	$\overline{5}$	$n_6 = -\chi(\mathcal{L}_2 \otimes \mathcal{L}_3, S)$
$L = (1,2)_{-\frac{1}{2}}$	78	16	$\overline{5}$	$n_7 = -\chi(\mathcal{L}_1^{-1} \otimes \mathcal{L}_2 \otimes \mathcal{L}_3, S)$
$\mathcal{E}^c = (1,1)_1$	78	16	10	$n_8 = -\chi(\mathcal{L}_1 \otimes \mathcal{L}_3, S)$
$\mathcal{Q} = (3,2)_{\frac{1}{6}}$	78	16	10	$n_9 = -\chi(\mathcal{L}_3, S)$
$\mathcal{U}^c = (\overline{3},1)_{-\frac{2}{3}}$	78	16	10	$n_{10} = -\chi(\mathcal{L}_1^{-1} \otimes \mathcal{L}_3, S)$

Table D.1: E_6 bulk states and their multiplicities

Next, we define the following three line bundles:

$$\mathcal{L}_1 = (5,0,0), \quad \mathcal{L}_2 = (1,4,0), \quad \mathcal{L}_3 = (1,-1,-3) \tag{D.5}$$

and express all the $U(1)$ charges in (D.1) as linear combinations

$$(Y,\chi,\psi) = \kappa\mathcal{L}_1 + \lambda\mathcal{L}_2 + \mu\mathcal{L}_3 = (5\kappa+\lambda+\mu, 4\lambda-\mu, -3\mu) \tag{D.6}$$

Then, the multiplicity of the fields is given in terms of Euler characteristic:

$$n_j = -\chi(\mathcal{L}_j, S) \qquad \text{where} \qquad \mathcal{L}_j \to \mathcal{L}_1^{\kappa} \otimes \mathcal{L}_2^{\lambda} \otimes \mathcal{L}_3^{\mu} \tag{D.7}$$

Table D.1 summarises all possible MSSM states, their origin with repsect to the E_6 and $SO(10)$ as well as their multiplicities in terms of the corresponding Euler characters. The multiplicities of the conjugate fields are: $n_j^* = (n_j)^* = \chi(\mathcal{L}_j^{-1}, S)$. In order to impose the appropriate constraints to obtain the MSSM spectrum, we define

$$A = c_1(\mathcal{L}_1)^2 \qquad A_1 = c_1(\mathcal{L}_1)\cdot c_1(\mathcal{S}) \tag{D.8}$$

$$B = c_1(\mathcal{L}_2)^2 \qquad A_2 = c_1(\mathcal{L}_2)\cdot c_1(\mathcal{S}) \tag{D.9}$$

$$C = c_1(\mathcal{L}_3)^2 \qquad A_3 = c_1(\mathcal{L}_3)\cdot c_1(\mathcal{S}) \tag{D.10}$$

First, we would like to eliminate the $Q_R/\overline{Q}_R$ exotics arising from the adjoint **24**. This requires $n_1 = n_1^* = 0$ which lead to the following two conditions

$$A_1 = c_1(\mathcal{L}_1)\cdot c_1(S) = -c_1(\mathcal{L}_1)\cdot K_S = 0 \tag{D.11}$$

$$A = c_1(\mathcal{L}_1)\cdot c_1(\mathcal{L}_1) = -2 \tag{D.12}$$

Since $c_1(\mathcal{L}_1)$ belongs to the second homology group $\mathcal{H}_2(S,Z)$, the orthogonality condition (D.11) implies that it is a vector in the orthogonal compliment of the canonical class, while the second

one implies that $c_1(\mathcal{L}_Y)$ corresponds to a root of the exceptional symmetry associated with the del Pezzo surface.

The multiplicities of the remaining bulk states given in Table D.1 are easily expressed in terms of the $A_{2,3}, B, C$ quantities. We note that there are MSSM states emerging from different $SO(10)$ representations, but their total number can be expressed only in terms of two quantities, namely

$$\alpha = A_2 + A_3,\ \beta = -(B + C) \tag{D.13}$$

Then,

$$n_Q = \frac{\beta - \alpha}{2} - 2 \qquad n_{\bar{Q}} = \frac{\beta + \alpha}{2} - 2 \tag{D.14}$$

$$n_{d^c} = \frac{\beta - \alpha}{2} - 1 \qquad n_{\bar{d}^c} = \frac{\beta + \alpha}{2} - 1 \tag{D.15}$$

$$n_{u^c} = n_{e^c} = n_l = \frac{\beta - \alpha}{2} \qquad n_{\bar{u}^c} = n_{\bar{e}^c} = n_{\bar{l}} = \frac{\beta + \alpha}{2} \tag{D.16}$$

From the above, it is easy now to determine the chiral states, since

$$\delta n_a = -\alpha,\ a = Q, u^c, e^c, e, d^c$$

There are two characteristic cases that we now examine. First, choosing $\alpha = -3$ we obtain exactly the content of three chiral families. The second possibility arises for $\alpha = 0$ where there are only vectorlike states from the E_6 adjoint. In this case we have the following content

$$n_Q = n_{d^c} - 1 = \frac{\beta}{2} - 2,\ n_{u^c} = n_{e^c} = n_l = \frac{\beta}{2} \tag{D.17}$$

while an equal number of conjugate fields is assumed.

From the requirement $n_Q \geq 0$, we infer that $\beta \geq 4$. Then, the minimal scenario would be $\beta = 4$, $a = 0$, which can be realised for

$$c_1(\mathcal{L}_2)^2 + c_1(\mathcal{L}_3)^2 = -4,\ \ (c_1(\mathcal{L}_2) + c_1(\mathcal{L}_3)) \cdot K_S = 0$$

which implies $n_Q = 0, n_{d^c} = 1$ and $n_{u^c} = n_{e^c} = n_l = 2$ and similarly for their complex conjugates.

Possible model building and phenomenological implications of the spectrum requires further analysis.

Bibliography

[1] A. Karozas, S. F. King, G. K. Leontaris and A. Meadowcroft, "Discrete Family Symmetry from F-Theory GUTs," JHEP **1409** (2014) 107 [arXiv:1406.6290].

[2] A. Karozas, S. F. King, G. K. Leontaris and A. K. Meadowcroft, "Phenomenological implications of a minimal F-theory GUT with discrete symmetry," JHEP **1510** (2015) 041 doi:10.1007/JHEP10(2015)041 [arXiv:1505.00937 [hep-ph]].

[3] M. Crispim Romão, A. Karozas, S. F. King, G. K. Leontaris and A. K. Meadowcroft, "MSSM from F-theory SU(5) with Klein Monodromy," Phys. Rev. D **93** (2016) no.12, 126007 doi:10.1103/PhysRevD.93.126007 [arXiv:1512.09148 [hep-ph]].

[4] M. Crispim Romão, A. Karozas, S. F. King, G. K. Leontaris and A. K. Meadowcroft, "R-Parity violation in F-Theory," JHEP **1611** (2016) 081 doi:10.1007/JHEP11(2016)081 [arXiv:1608.04746 [hep-ph]].

[5] A. Karozas, G. K. Leontaris and Q. Shafi, "Vectorlike particles, Z' and Yukawa unification in F-theory inspired E_6," Phys. Lett. B **778** (2018) 213 doi:10.1016/j.physletb.2018.01.032 [arXiv:1710.00929 [hep-ph]].

[6] A. Karozas, S. F. King, G. K. Leontaris and A. K. Meadowcroft, "750 GeV diphoton excess from E_6 in F-theory GUTs," Phys. Lett. B **757** (2016) 73 doi:10.1016/j.physletb.2016.03.054 [arXiv:1601.00640 [hep-ph]].

[7] W. Ahmed and A. Karozas, "Inflation from a no-scale supersymmetric $SU(4)_c \times SU(2)_L \times SU(2)_R$ model," Phys. Rev. D **98** (2018) no.2, 023538 doi:10.1103/PhysRevD.98.023538 [arXiv:1804.04822 [hep-ph]].

[8] S. L. Glashow, "Partial Symmetries of Weak Interactions," Nucl. Phys. **22** (1961) 579. doi:10.1016/0029-5582(61)90469-2

[9] S. Weinberg, "A Model of Leptons," Phys. Rev. Lett. **19** (1967) 1264. doi:10.1103/PhysRevLett.19.1264

[10] A. Salam, "Weak and Electromagnetic Interactions," Conf. Proc. C **680519** (1968) 367.

[11] P. W. Higgs, "Broken symmetries, massless particles and gauge fields," Phys. Lett. **12** (1964) 132. doi:10.1016/0031-9163(64)91136-9

[12] P. W. Higgs, "Broken Symmetries and the Masses of Gauge Bosons," Phys. Rev. Lett. **13** (1964) 508. doi:10.1103/PhysRevLett.13.508

[13] F. Englert and R. Brout, "Broken Symmetry and the Mass of Gauge Vector Mesons," Phys. Rev. Lett. **13** (1964) 321. doi:10.1103/PhysRevLett.13.321

[14] G. S. Guralnik, C. R. Hagen and T. W. B. Kibble, "Global Conservation Laws and Massless Particles," Phys. Rev. Lett. **13** (1964) 585. doi:10.1103/PhysRevLett.13.585

[15] Y. Nambu, "Quasiparticles and Gauge Invariance in the Theory of Superconductivity," Phys. Rev. **117** (1960) 648. doi:10.1103/PhysRev.117.648;

[16] J. Goldstone, "Field Theories with Superconductor Solutions," Nuovo Cim. **19** (1961) 154. doi:10.1007/BF02812722

[17] N. Cabibbo, "Unitary Symmetry and Leptonic Decays," Phys. Rev. Lett. **10** (1963) 531. doi:10.1103/PhysRevLett.10.531 ; M. Kobayashi and T. Maskawa, "CP Violation in the Renormalizable Theory of Weak Interaction," Prog. Theor. Phys. **49** (1973) 652. doi:10.1143/PTP.49.652

[18] A. M. Sirunyan *et al.* [CMS Collaboration], "Observation of $t\bar{t}H$ production," Phys. Rev. Lett. **120** (2018) no.23, 231801 doi:10.1103/PhysRevLett.120.231801, 10.1130/PhysRevLett.120.231801 [arXiv:1804.02610 [hep-ex]].

[19] M. Aaboud *et al.* [ATLAS Collaboration], "Observation of Higgs boson production in association with a top quark pair at the LHC with the ATLAS detector," Phys. Lett. B **784** (2018) 173 doi:10.1016/j.physletb.2018.07.035 [arXiv:1806.00425 [hep-ex]].

[20] A. Bilal, "Lectures on Anomalies," arXiv:0802.0634 [hep-th].

[21] S. L. Glashow, J. Iliopoulos and L. Maiani, "Weak Interactions with Lepton-Hadron Symmetry," Phys. Rev. D **2** (1970) 1285. doi:10.1103/PhysRevD.2.1285

[22] G. Aad *et al.* [ATLAS Collaboration], "Observation of a new particle in the search for the Standard Model Higgs boson with the ATLAS detector at the LHC," Phys. Lett. B **716** (2012) 1 doi:10.1016/j.physletb.2012.08.020 [arXiv:1207.7214 [hep-ex]].

[23] G. Aad *et al.* [ATLAS Collaboration], "Evidence for the spin-0 nature of the Higgs boson using ATLAS data," Phys. Lett. B **726** (2013) 120 doi:10.1016/j.physletb.2013.08.026 [arXiv:1307.1432 [hep-ex]].

[24] S. Chatrchyan *et al.* [CMS Collaboration], Phys. Lett. B **716** (2012) 30 doi:10.1016/j.physletb.2012.08.021 [arXiv:1207.7235 [hep-ex]].

[25] S. Chatrchyan *et al.* [CMS Collaboration], JHEP **1306** (2013) 081 doi:10.1007/JHEP06(2013)081 [arXiv:1303.4571 [hep-ex]].

[26] D. Buttazzo, G. Degrassi, P. P. Giardino, G. F. Giudice, F. Sala, A. Salvio and A. Strumia, JHEP **1312** (2013) 089 doi:10.1007/JHEP12(2013)089 [arXiv:1307.3536 [hep-ph]].

[27] Y. Fukuda *et al.* [Super-Kamiokande Collaboration], Phys. Rev. Lett. **81** (1998) 1562 doi:10.1103/PhysRevLett.81.1562 [hep-ex/9807003], Y. Ashie *et al.* [Super-Kamiokande Collaboration], Phys. Rev. Lett. **93** (2004) 101801 doi:10.1103/PhysRevLett.93.101801 [hep-ex/0404034], K. Eguchi *et al.* [KamLAND Collaboration], Phys. Rev. Lett. **90** (2003) 021802 doi:10.1103/PhysRevLett.90.021802 [hep-ex/0212021], P. Adamson *et al.* [MINOS Collaboration], Phys. Rev. Lett. **101** (2008) 131802 doi:10.1103/PhysRevLett.101.131802

[28] Neutrino Oscillations: Celebrating the Nobel Prize in Physics 2015-2016. Special Issue on Edited by Tommy Ohlsson. Nucl. Phys. **B908**,1. http://www.sciencedirect.com/science/journal/05503213/908/supp/C

[29] C. Patrignani *et al.* [Particle Data Group], "Review of Particle Physics," Chin. Phys. C **40** (2016) no.10, 100001. doi:10.1088/1674-1137/40/10/100001

[30] N. Aghanim *et al.* [Planck Collaboration], arXiv:1807.06209 [astro-ph.CO].

[31] S. Weinberg, "Baryon and Lepton Nonconserving Processes," Phys. Rev. Lett. **43** (1979) 1566. doi:10.1103/PhysRevLett.43.1566

[32] P. Minkowski, Phys. Lett. **67B** (1977) 421. doi:10.1016/0370-2693(77)90435-X; T. Yanagida, Conf. Proc. C **7902131** (1979) 95. M. Gell-Mann, P. Ramond and R. Slansky, Conf. Proc. C **790927** (1979) 315 [arXiv:1306.4669 [hep-th]]; R. N. Mohapatra and G. Senjanovic, Phys. Rev. Lett. **44** (1980) 912. doi:10.1103/PhysRevLett.44.912

[33] M. Magg and C. Wetterich, Phys. Lett. **94B** (1980) 61. doi:10.1016/0370-2693(80)90825-4; J. Schechter and J. W. F. Valle, Phys. Rev. D **22** (1980) 2227. doi:10.1103/PhysRevD.22.2227; G. Lazarides, Q. Shafi and C. Wetterich, Nucl. Phys. B **181** (1981) 287. doi:10.1016/0550-3213(81)90354-0; R. N. Mohapatra and G. Senjanovic, Phys. Rev. D **23** (1981) 165. doi:10.1103/PhysRevD.23.165; T. P. Cheng and L. F. Li, Phys. Rev. D **22** (1980) 2860. doi:10.1103/PhysRevD.22.2860

[34] R. Foot, H. Lew, X. G. He and G. C. Joshi, Z. Phys. C **44** (1989) 441. doi:10.1007/BF01415558

[35] R. N. Mohapatra *et al.*, Rept. Prog. Phys. **70** (2007) 1757 doi:10.1088/0034-4885/70/11/R02 [hep-ph/0510213].

[36] R. Massey, T. Kitching and J. Richard, Rept. Prog. Phys. **73** (2010) 086901 doi:10.1088/0034-4885/73/8/086901 [arXiv:1001.1739 [astro-ph.CO]].

[37] D. Clowe, A. Gonzalez and M. Markevitch, Astrophys. J. **604** (2004) 596 doi:10.1086/381970 [astro-ph/0312273].

[38] D. Clowe, M. Bradac, A. H. Gonzalez, M. Markevitch, S. W. Randall, C. Jones and D. Zaritsky, Astrophys. J. **648** (2006) L109 doi:10.1086/508162 [astro-ph/0608407].

[39] L. Canetti, M. Drewes and M. Shaposhnikov, "Matter and Antimatter in the Universe," New J. Phys. **14** (2012) 095012 doi:10.1088/1367-2630/14/9/095012 [arXiv:1204.4186 [hep-ph]].

[40] S. Weinberg, "The Cosmological Constant Problem," Rev. Mod. Phys. **61** (1989) 1. doi:10.1103/RevModPhys.61.1

[41] H. Miyazawa, Prog. Theor. Phys. **36** (1966) no.6, 1266. doi:10.1143/PTP.36.1266

[42] S. R. Coleman and J. Mandula, Phys. Rev. **159** (1967) 1251. doi:10.1103/PhysRev.159.1251

[43] A. Neveu and J. H. Schwarz, Nucl. Phys. B **31** (1971) 86. doi:10.1016/0550-3213(71)90448-2

[44] P. Ramond, Phys. Rev. D **3** (1971) 2415. doi:10.1103/PhysRevD.3.2415

[45] Y. A. Golfand and E. P. Likhtman, JETP Lett. **13** (1971) 323 [Pisma Zh. Eksp. Teor. Fiz. **13** (1971) 452].

[46] J. L. Gervais and B. Sakita, Nucl. Phys. B **34** (1971) 632. doi:10.1016/0550-3213(71)90351-8

[47] D. V. Volkov and V. P. Akulov, JETP Lett. **16** (1972) 438 [Pisma Zh. Eksp. Teor. Fiz. **16** (1972) 621].

[48] J. Wess and B. Zumino, Phys. Lett. **49B** (1974) 52. doi:10.1016/0370-2693(74)90578-4

[49] R. Haag, J. T. Lopuszanski and M. Sohnius, Nucl. Phys. B **88** (1975) 257. doi:10.1016/0550-3213(75)90279-5

[50] P. Fayet and S. Ferrara, "Supersymmetry," Phys. Rept. **32** (1977) 249. doi:10.1016/0370-1573(77)90066-7

[51] J. G. Taylor, "A Review of Supersymmetry and Supergravity," Prog. Part. Nucl. Phys. **12** (1984) 1. doi:10.1016/0146-6410(84)90002-4

[52] S. P. Martin, "A Supersymmetry primer," Adv. Ser. Direct. High Energy Phys. **21** (2010) 1 [Adv. Ser. Direct. High Energy Phys. **18** (1998) 1] doi:10.1142/9789812839657$_0$001, 10.1142/9789814307505$_0$001 [hep-ph/9709356].

[53] P. C. West, "Introduction to supersymmetry and supergravity," Singapore, Singapore: World Scientific (1990) 425 p

[54] J. Wess and J. Bagger, "Supersymmetry and supergravity," Princeton, USA: Univ. Pr. (1992) 259 p

[55] S. Weinberg, "The quantum theory of fields. Vol. 3: Supersymmetry,"

[56] J. Terning, "Modern supersymmetry: Dynamics and duality," (International series of monographs on physics. 132) doi:10.1093/acprof:oso/9780198567639.001.0001

[57] A. Djouadi, "The Anatomy of electro-weak symmetry breaking. II. The Higgs bosons in the minimal supersymmetric model," Phys. Rept. **459** (2008) 1 doi:10.1016/j.physrep.2007.10.005 [hep-ph/0503173].

[58] P. Fayet, "Supergauge Invariant Extension of the Higgs Mechanism and a Model for the electron and Its Neutrino," Nucl. Phys. B **90** (1975) 104. doi:10.1016/0550-3213(75)90636-7

[59] E. Witten, "Dynamical Breaking of Supersymmetry," Nucl. Phys. B **188** (1981) 513. doi:10.1016/0550-3213(81)90006-7

[60] A. B. Lahanas and D. V. Nanopoulos, "The Road to No Scale Supergravity," Phys. Rept. **145** (1987) 1. doi:10.1016/0370-1573(87)90034-2

[61] G. F. Giudice and R. Rattazzi, "Theories with gauge mediated supersymmetry breaking," Phys. Rept. **322** (1999) 419 doi:10.1016/S0370-1573(99)00042-3 [hep-ph/9801271].

[62] L. Randall and R. Sundrum, "Out of this world supersymmetry breaking," Nucl. Phys. B **557** (1999) 79 doi:10.1016/S0550-3213(99)00359-4 [hep-th/9810155].

[63] G. F. Giudice, M. A. Luty, H. Murayama and R. Rattazzi, "Gaugino mass without singlets," JHEP **9812** (1998) 027 doi:10.1088/1126-6708/1998/12/027 [hep-ph/9810442].

[64] M. A. Luty, "2004 TASI lectures on supersymmetry breaking," hep-th/0509029.

[65] S. Dimopoulos and H. Georgi, "Softly Broken Supersymmetry and SU(5)," Nucl. Phys. B **193** (1981) 150. doi:10.1016/0550-3213(81)90522-8

[66] H. P. Nilles, "Supersymmetry, Supergravity and Particle Physics," Phys. Rept. **110** (1984) 1. doi:10.1016/0370-1573(84)90008-5

[67] S. Dimopoulos, S. Raby and F. Wilczek, "Supersymmetry and the Scale of Unification," Phys. Rev. D **24** (1981) 1681. doi:10.1103/PhysRevD.24.1681

[68] J. R. Ellis, S. Kelley and D. V. Nanopoulos, "Probing the desert using gauge coupling unification," Phys. Lett. B **260** (1991) 131. doi:10.1016/0370-2693(91)90980-5 ; P. Langacker and M. x. Luo, "Implications of precision electroweak experiments for M_t, ρ_0, $\sin^2\theta_W$ and grand unification," Phys. Rev. D **44** (1991) 817. doi:10.1103/PhysRevD.44.817

[69] J. E. Kim and H. P. Nilles, "The mu Problem and the Strong CP Problem," Phys. Lett. **138B** (1984) 150. doi:10.1016/0370-2693(84)91890-2

[70] U. Ellwanger, C. Hugonie and A. M. Teixeira, "The Next-to-Minimal Supersymmetric Standard Model," Phys. Rept. **496** (2010) 1 doi:10.1016/j.physrep.2010.07.001 [arXiv:0910.1785 [hep-ph]].

[71] C. Panagiotakopoulos and K. Tamvakis, "New minimal extension of MSSM," Phys. Lett. B **469** (1999) 145 doi:10.1016/S0370-2693(99)01247-2 [hep-ph/9908351].

[72] G. R. Farrar and P. Fayet, "Phenomenology of the Production, Decay, and Detection of New Hadronic States Associated with Supersymmetry," Phys. Lett. **76B** (1978) 575. doi:10.1016/0370-2693(78)90858-4

[73] H. K. Dreiner, "An Introduction to explicit R-parity violation," Adv. Ser. Direct. High Energy Phys. **21** (2010) 565 doi:10.1142/9789814307505$_0$017 [hep-ph/9707435].

[74] R. Barbier *et al.*, "R-parity violating supersymmetry," Phys. Rept. **420** (2005) 1 doi:10.1016/j.physrep.2005.08.006 [hep-ph/0406039].

[75] F. Takayama and M. Yamaguchi, "Gravitino dark matter without R-parity," Phys. Lett. B **485** (2000) 388 doi:10.1016/S0370-2693(00)00726-7 [hep-ph/0005214].

[76] K. Abe *et al.* [Super-Kamiokande Collaboration], Phys. Rev. D **95** (2017) no.1, 012004 doi:10.1103/PhysRevD.95.012004 [arXiv:1610.03597 [hep-ex]].

[77] S. Dimopoulos and L. J. Hall, "Lepton and Baryon Number Violating Collider Signatures from Supersymmetry," Phys. Lett. B **207** (1988) 210. doi:10.1016/0370-2693(88)91418-9

[78] J. C. Pati and A. Salam, "Lepton Number as the Fourth Color," Phys. Rev. D **10** (1974) 275 Erratum: [Phys. Rev. D **11** (1975) 703]. doi:10.1103/PhysRevD.10.275, 10.1103/PhysRevD.11.703.2

[79] J. C. Pati, "Advantages of Unity With SU(4)-Color: Reflections Through Neutrino Oscillations, Baryogenesis and Proton Decay," Int. J. Mod. Phys. A **32** (2017) no.09, 1741013 doi:10.1142/S0217751X17410135 [arXiv:1706.09531 [hep-ph]].

[80] I. Antoniadis and G. K. Leontaris, "A SUPERSYMMETRIC SU(4) x O(4) MODEL," Phys. Lett. B **216** (1989) 333. doi:10.1016/0370-2693(89)91125-8

[81] G. K. Leontaris and J. Rizos, "A Pati-Salam model from branes," Phys. Lett. B **510** (2001) 295 doi:10.1016/S0370-2693(01)00592-5 [hep-ph/0012255].

[82] M. Cvetic, T. Li and T. Liu, "Supersymmetric Pati-Salam models from intersecting D6-branes: A Road to the standard model," Nucl. Phys. B **698** (2004) 163 doi:10.1016/j.nuclphysb.2004.07.036 [hep-th/0403061].

[83] B. Assel, K. Christodoulides, A. E. Faraggi, C. Kounnas and J. Rizos, "Classification of Heterotic Pati-Salam Models," Nucl. Phys. B **844** (2011) 365 doi:10.1016/j.nuclphysb.2010.11.011 [arXiv:1007.2268 [hep-th]].

[84] P. Anastasopoulos, G. K. Leontaris and N. D. Vlachos, "Phenomenological Analysis of D-Brane Pati-Salam Vacua," JHEP **1005** (2010) 011 doi:10.1007/JHEP05(2010)011 [arXiv:1002.2937 [hep-th]].

[85] H. Georgi and S. L. Glashow, "Unity of All Elementary Particle Forces," Phys. Rev. Lett. **32** (1974) 438. doi:10.1103/PhysRevLett.32.438

[86] H. Georgi and C. Jarlskog, "A New Lepton - Quark Mass Relation in a Unified Theory," Phys. Lett. **86B** (1979) 297. doi:10.1016/0370-2693(79)90842-6

[87] P. Langacker, "Grand Unified Theories and Proton Decay," Phys. Rept. **72** (1981) 185. doi:10.1016/0370-1573(81)90059-4

[88] G. Senjanovic, "Proton decay and grand unification," AIP Conf. Proc. **1200** (2010) 131 doi:10.1063/1.3327552 [arXiv:0912.5375 [hep-ph]].

[89] N. Sakai and T. Yanagida, "Proton Decay in a Class of Supersymmetric Grand Unified Models," Nucl. Phys. B **197** (1982) 533. doi:10.1016/0550-3213(82)90457-6

[90] S. Weinberg, "Supersymmetry at Ordinary Energies. 1. Masses and Conservation Laws," Phys. Rev. D **26** (1982) 287. doi:10.1103/PhysRevD.26.287

[91] J. Hisano, H. Murayama and T. Yanagida, "Nucleon decay in the minimal supersymmetric SU(5) grand unification," Nucl. Phys. B **402** (1993) 46 doi:10.1016/0550-3213(93)90636-4 [hep-ph/9207279].

[92] T. Goto and T. Nihei, "Effect of RRRR dimension five operator on the proton decay in the minimal SU(5) SUGRA GUT model," Phys. Rev. D **59** (1999) 115009 doi:10.1103/PhysRevD.59.115009 [hep-ph/9808255].

[93] B. Bajc, P. Fileviez Perez and G. Senjanovic, "Minimal supersymmetric SU(5) theory and proton decay: Where do we stand?," hep-ph/0210374.

[94] E. Ma, "Pathways to naturally small neutrino masses," Phys. Rev. Lett. **81** (1998) 1171 doi:10.1103/PhysRevLett.81.1171 [hep-ph/9805219].

[95] M. Paraskevas and K. Tamvakis, "Hierarchical neutrino masses and mixing in non minimal-SU(5)," Phys. Rev. D **84** (2011) 013010 doi:10.1103/PhysRevD.84.013010 [arXiv:1104.1901 [hep-ph]].

[96] S. M. Barr, "A New Symmetry Breaking Pattern for SO(10) and Proton Decay," Phys. Lett. **112B** (1982) 219. doi:10.1016/0370-2693(82)90966-2

[97] J. P. Derendinger, J. E. Kim and D. V. Nanopoulos, "Anti-SU(5)," Phys. Lett. **139B** (1984) 170. doi:10.1016/0370-2693(84)91238-3

[98] I. Antoniadis, J. R. Ellis, J. S. Hagelin and D. V. Nanopoulos, "GUT Model Building with Fermionic Four-Dimensional Strings," Phys. Lett. B **205** (1988) 459. doi:10.1016/0370-2693(88)90978-1

[99] H. Fritzsch and P. Minkowski, "Unified Interactions of Leptons and Hadrons," Annals Phys. **93** (1975) 193. doi:10.1016/0003-4916(75)90211-0 CITATION = doi:10.1016/0003-4916(75)90211-0;1645 citations counted in INSPIRE as of 22 May 2018

[100] B. Ananthanarayan, G. Lazarides and Q. Shafi, "Top mass prediction from supersymmetric guts," Phys. Rev. D **44** (1991) 1613. doi:10.1103/PhysRevD.44.1613

[101] I. Gogoladze, Q. Shafi and C. S. Ün, "SO(10) Yukawa unification with $\mu < 0$," Phys. Lett. B **704** (2011) 201 doi:10.1016/j.physletb.2011.09.006 [arXiv:1107.1228 [hep-ph]].

[102] M. Badziak, "Yukawa unification in SUSY SO(10) in light of the LHC Higgs data," Mod. Phys. Lett. A **27** (2012) 1230020 doi:10.1142/S0217732312300200 [arXiv:1205.6232 [hep-ph]]; M. Badziak, M. Olechowski and S. Pokorski, "Yukawa unification in SO(10) with light sparticle spectrum," JHEP **1108** (2011) 147 doi:10.1007/JHEP08(2011)147 [arXiv:1107.2764 [hep-ph]].

[103] A. Anandakrishnan, B. C. Bryant, S. Raby and A. Wingerter, "LHC Phenomenology of SO(10) Models with Yukawa Unification," Phys. Rev. D **88** (2013) 075002 doi:10.1103/PhysRevD.88.075002 [arXiv:1307.7723 [hep-ph]].

[104] Z. Poh and S. Raby, "Yukawa Unification in an SO(10) SUSY GUT: SUSY on the Edge," Phys. Rev. D **92** (2015) no.1, 015017 doi:10.1103/PhysRevD.92.015017 [arXiv:1505.00264 [hep-ph]].

[105] S. F. King, "Unified Models of Neutrinos, Flavour and CP Violation," Prog. Part. Nucl. Phys. **94** (2017) 217 doi:10.1016/j.ppnp.2017.01.003 [arXiv:1701.04413 [hep-ph]].

[106] F. Gursey, P. Ramond and P. Sikivie, "A Universal Gauge Theory Model Based on E6," Phys. Lett. **60B** (1976) 177. doi:10.1016/0370-2693(76)90417-2

[107] Y. Achiman and B. Stech, "Quark Lepton Symmetry and Mass Scales in an E6 Unified Gauge Model," Phys. Lett. **77B** (1978) 389. doi:10.1016/0370-2693(78)90584-1

[108] Q. Shafi, "E(6) as a Unifying Gauge Symmetry," Phys. Lett. **79B** (1978) 301. doi:10.1016/0370-2693(78)90248-4

[109] P. Candelas, G. T. Horowitz, A. Strominger and E. Witten, "Vacuum Configurations for Superstrings," Nucl. Phys. B **258** (1985) 46. doi:10.1016/0550-3213(85)90602-9

[110] M. B. Green, J. H. Schwarz and E. Witten, "Superstring Theory. Vol. 1: Introduction," Cambridge, Uk: Univ. Pr. (1987) 469 P. (Cambridge Monographs On Mathematical Physics)

[111] S. P. Martin, "Extra vector-like matter and the lightest Higgs scalar boson mass in low-energy supersymmetry," Phys. Rev. D **81** (2010) 035004 doi:10.1103/PhysRevD.81.035004 [arXiv:0910.2732 [hep-ph]].

[112] K. S. Babu, B. Bajc and V. Susič, "A minimal supersymmetric E_6 unified theory," JHEP **1505** (2015) 108 doi:10.1007/JHEP05(2015)108 [arXiv:1504.00904 [hep-ph]].

[113] P. Langacker and J. Wang, "U(1)-prime symmetry breaking in supersymmetric E(6) models," Phys. Rev. D **58** (1998) 115010 doi:10.1103/PhysRevD.58.115010 [hep-ph/9804428].

[114] Y. Hosotani, "Dynamical Mass Generation by Compact Extra Dimensions," Phys. Lett. **126B** (1983) 309. doi:10.1016/0370-2693(83)90170-3

[115] Y. Hosotani, "Dynamical Gauge Symmetry Breaking as the Casimir Effect," Phys. Lett. **129B** (1983) 193. doi:10.1016/0370-2693(83)90841-9

[116] P. Langacker, "The Physics of Heavy Z' Gauge Bosons," Rev. Mod. Phys. **81** (2009) 1199 doi:10.1103/RevModPhys.81.1199 [arXiv:0801.1345 [hep-ph]].

[117] C. Vafa, "Evidence for F theory," Nucl. Phys. B **469** (1996) 403 [hep-th/9602022].

[118] C. Beasley, J. J. Heckman and C. Vafa, "GUTs and Exceptional Branes in F-theory - I," JHEP **0901** (2009) 058 [arXiv:0802.3391].

[119] C. Beasley, J. J. Heckman and C. Vafa, "GUTs and Exceptional Branes in F-theory - II: Experimental Predictions," JHEP **0901**, 059 (2009) [arXiv:0806.0102].

[120] R. Donagi and M. Wijnholt, "Breaking GUT Groups in F-Theory," arXiv:0808.2223 [hep-th].

[121] R. Donagi and M. Wijnholt, "Higgs Bundles and UV Completion in F-Theory," Commun. Math. Phys. **326** (2014) 287 [arXiv:0904.1218].

[122] F. Denef, "Les Houches Lectures on Constructing String Vacua," arXiv:0803.1194 [hep-th].

[123] J. J. Heckman, "Particle Physics Implications of F-theory," Ann. Rev. Nucl. Part. Sci. **60** (2010) 237 [arXiv:1001.0577 [hep-th]].

[124] T. Weigand, "Lectures on F-theory compactifications and model building," Class. Quant. Grav. **27** (2010) 214004 [arXiv:1009.3497 [hep-th]].

[125] G. K. Leontaris, "Aspects of F-Theory GUTs," PoS CORFU **2011** (2011) 095 doi:10.22323/1.155.0095 [arXiv:1203.6277 [hep-th]].

[126] A. Maharana and E. Palti, "Models of Particle Physics from Type IIB String Theory and F-theory: A Review," Int. J. Mod. Phys. A **28** (2013) 1330005 [arXiv:1212.0555 [hep-th]].

[127] G. K. Leontaris, "F-Theory GUT's," PoS CORFU **2014** (2015) 046. doi:10.22323/1.231.0046

[128] T. Weigand, "F-theory," PoS TASI **2017** (2018) 016. doi:10.22323/1.305.0016

[129] Katrin Becker, Melanie Becker, John H. Schwarz, "String Theory and M-Theory: A Modern Introduction," Cambridge University Press

[130] J. H. Schwarz, "An SL(2,Z) multiplet of type IIB superstrings," Phys. Lett. B **360** (1995) 13 Erratum: [Phys. Lett. B **364** (1995) 252] doi:10.1016/0370-2693(95)01405-5, 10.1016/0370-2693(95)01138-G [hep-th/9508143].

[131] A. Sen, "Orientifold limit of F theory vacua," Phys. Rev. D **55** (1997) R7345 doi:10.1103/PhysRevD.55.R7345 [hep-th/9702165].

[132] D. R. Morrison and C. Vafa, "Compactifications of F theory on Calabi-Yau threefolds. 2.," Nucl. Phys. B **476** (1996) 437 [hep-th/9603161].

[133] K. Kodaira, "On compact Analytic surfaces", Annals of Math. 77(1963)563.

[134] M. Bershadsky, K. A. Intriligator, S. Kachru, D. R. Morrison, V. Sadov and C. Vafa, Nucl. Phys. B **481** (1996) 215 doi:10.1016/S0550-3213(96)90131-5 [hep-th/9605200].

[135] D. R. Morrison and W. Taylor, "Matter and singularities," JHEP **1201** (2012) 022 [arXiv:1106.3563 [hep-th]].

[136] R. Blumenhagen, T. W. Grimm, B. Jurke and T. Weigand, "Global F-theory GUTs," Nucl. Phys. B **829** (2010) 325 doi:10.1016/j.nuclphysb.2009.12.013 [arXiv:0908.1784 [hep-th]].

[137] M. Esole and S. -T. Yau, "Small resolutions of SU(5)-models in F-theory," arXiv:1107.0733 [hep-th].

[138] J. Tate, "Algorithm for Determining the Type of a Singular Fiber in an Elliptic Pencil," in Modular Functions of One Variable IV, Lecture Notes in Math. vol. 476, Springer-Verlag, Berlin (1975).

[139] J. J. Heckman and C. Vafa, "Flavor Hierarchy From F-theory," Nucl. Phys. B **837** (2010) 137 [arXiv:0811.2417 [hep-th]].

[140] A. Font and L. E. Ibanez, JHEP **0902** (2009) 016 doi:10.1088/1126-6708/2009/02/016 [arXiv:0811.2157 [hep-th]].

[141] S. Cecotti, M. C. N. Cheng, J. J. Heckman and C. Vafa, "Yukawa Couplings in F-theory and Non-Commutative Geometry," arXiv:0910.0477.

[142] H. Hayashi, T. Kawano, R. Tatar and T. Watari, "Codimension-3 Singularities and Yukawa Couplings in F-theory," Nucl. Phys. B **823** (2009) 47 doi:10.1016/j.nuclphysb.2009.07.021 [arXiv:0901.4941 [hep-th]].

[143] H. Hayashi, T. Kawano, Y. Tsuchiya and T. Watari, "Flavor Structure in F-theory Compactifications," JHEP **1008** (2010) 036 [arXiv:0910.2762].

[144] A. Font and L. E. Ibanez, "Matter wave functions and Yukawa couplings in F-theory Grand Unification," JHEP **0909** (2009) 036 [arXiv:0907.4895].

[145] S. Cecotti, C. Cordova, J. J. Heckman and C. Vafa, "T-Branes and Monodromy," JHEP **1107** (2011) 030 [arXiv:1010.5780 [hep-th]].

[146] G. K. Leontaris and G. G. Ross, "Yukawa couplings and fermion mass structure in F-theory GUTs," JHEP **1102** (2011) 108 [arXiv:1009.6000].

[147] L. Aparicio, A. Font, L. E. Ibanez and F. Marchesano, "Flux and Instanton Effects in Local F-theory Models and Hierarchical Fermion Masses," JHEP **1108**, 152 (2011) [arXiv:1104.2609].

[148] P. G. Camara, E. Dudas and E. Palti, "Massive wavefunctions, proton decay and FCNCs in local F-theory GUTs," JHEP **1112** (2011) 112 [arXiv:1110.2206 [hep-th]].

[149] E. Palti, JHEP **1207** (2012) 065 doi:10.1007/JHEP07(2012)065 [arXiv:1203.4490 [hep-th]].

[150] A. Font, L. E. Ibanez, F. Marchesano and D. Regalado, "Non-perturbative effects and Yukawa hierarchies in F-theory SU(5) Unification," JHEP **1303** (2013) 140 [JHEP **1307** (2013) 036] [arXiv:1211.6529].

[151] A. Font, F. Marchesano, D. Regalado and G. Zoccarato, JHEP **1311** (2013) 125 doi:10.1007/JHEP11(2013)125 [arXiv:1307.8089 [hep-th]].

[152] F. Marchesano, D. Regalado and G. Zoccarato, "Yukawa hierarchies at the point of E_8 in F-theory," JHEP **1504** (2015) 179 [arXiv:1503.02683].

[153] F. Carta, F. Marchesano and G. Zoccarato, "Fitting fermion masses and mixings in F-theory GUTs," JHEP **1603** (2016) 126 doi:10.1007/JHEP03(2016)126 [arXiv:1512.04846 [hep-th]].

[154] A. Hebecker and J. Unwin, "Precision Unification and Proton Decay in F-Theory GUTs with High Scale Supersymmetry," JHEP **1409** (2014) 125 [arXiv:1405.2930].

[155] R. Donagi and M. Wijnholt, "Model Building with F-Theory," Adv. Theor. Math. Phys. **15** (2011) no.5, 1237 doi:10.4310/ATMP.2011.v15.n5.a2 [arXiv:0802.2969 [hep-th]].

[156] J. J. Heckman, A. Tavanfar and C. Vafa, "The Point of E(8) in F-theory GUTs," JHEP **1008** (2010) 040 [arXiv:0906.0581 [hep-th]].

[157] E. Dudas and E. Palti, "On hypercharge flux and exotics in F-theory GUTs," JHEP **1009** (2010) 013 [arXiv:1007.1297].

[158] J. Marsano and S. Schafer-Nameki, "Yukawas, G-flux, and Spectral Covers from Resolved Calabi-Yau's," JHEP **1111** (2011) 098 [arXiv:1108.1794].

[159] H. Hayashi, T. Kawano, Y. Tsuchiya and T. Watari, Nucl. Phys. B **840** (2010) 304 doi:10.1016/j.nuclphysb.2010.07.011 [arXiv:1004.3870 [hep-th]].

[160] T. W. Grimm and T. Weigand, Phys. Rev. D **82** (2010) 086009 doi:10.1103/PhysRevD.82.086009 [arXiv:1006.0226 [hep-th]].

[161] J. Marsano, Phys. Rev. Lett. **106** (2011) 081601 doi:10.1103/PhysRevLett.106.081601 [arXiv:1011.2212 [hep-th]].

[162] I. Antoniadis and G. K. Leontaris, "Building SO(10) models from F-theory," JHEP **1208** (2012) 001 [arXiv:1205.6930].

[163] C. M. Chen and Y. C. Chung, "Flipped $SU(5)$ GUTs from E_8 Singularities in F-theory," JHEP **1103**, 049 (2011) [arXiv:1005.5728].

[164] C. Mayrhofer, E. Palti, O. Till and T. Weigand, "On Discrete Symmetries and Torsion Homology in F-Theory," JHEP **1506** (2015) 029 [arXiv:1410.7814].

[165] F. Baume, E. Palti and S. Schwieger, "On E_8 and F-Theory GUTs," JHEP **1506** (2015) 039 [arXiv:1502.03878].

[166] M. Cvetic, D. Klevers, D. K. M. Peña, P. K. Oehlmann and J. Reuter, "Three-Family Particle Physics Models from Global F-theory Compactifications," JHEP **1508** (2015) 087 [arXiv:1503.02068].

[167] S. Krippendorf, D. K. Mayorga Pena, P. K. Oehlmann and F. Ruehle, "Rational F-Theory GUTs without exotics," JHEP **1407** (2014) 013 [arXiv:1401.5084].

[168] S. Krippendorf, S. Schafer-Nameki and J. M. Wong, "Froggatt-Nielsen meets Mordell-Weil: A Phenomenological Survey of Global F-theory GUTs with U(1)s," JHEP **1511** (2015) 008 [arXiv:1507.05961].

[169] N. C. Bizet, A. Klemm and D. V. Lopes, "Landscaping with fluxes and the E8 Yukawa Point in F-theory," arXiv:1404.7645

[170] K. S. Choi, "On the Standard Model Group in F-theory," Eur. Phys. J. C **74** (2014) 2939 [arXiv:1309.7297].

[171] J. Marsano, N. Saulina and S. Schafer-Nameki, "Monodromies, Fluxes, and Compact Three-Generation F-theory GUTs," JHEP **0908** (2009) 046 [arXiv:0906.4672].

[172] I. Antoniadis and G. K. Leontaris, "Neutrino mass textures from F-theory," Eur. Phys. J. C **73** (2013) 2670 [arXiv:1308.1581 [hep-th]].

[173] S. F. King, G. K. Leontaris and G. G. Ross, "Family symmetries in F-theory GUTs," Nucl. Phys. B **838** (2010) 119 doi:10.1016/j.nuclphysb.2010.05.014 [arXiv:1005.1025 [hep-ph]].

[174] G. K. Leontaris and N. D. Tracas, "Gauge coupling flux thresholds, exotic matter and the unification scale in F-SU(5) GUT," Eur. Phys. J. C **67** (2010) 489 doi:10.1140/epjc/s10052-010-1298-2 [arXiv:0912.1557 [hep-ph]].

[175] G. K. Leontaris, N. D. Tracas and G. Tsamis, "Unification, KK-thresholds and the top Yukawa coupling in F-theory GUTs," Eur. Phys. J. C **71** (2011) 1768 doi:10.1140/epjc/s10052-011-1768-1 [arXiv:1102.5244 [hep-ph]].

[176] G. K. Leontaris and N. D. Vlachos, "On the GUT scale of F-Theory SU(5)," Phys. Lett. B **704** (2011) 620 doi:10.1016/j.physletb.2011.09.060 [arXiv:1105.1858 [hep-th]].

[177] R. Ahl Laamara, M. Miskaoui and E. H. Saidi, "Building SO 10 -models with D4 symmetry," Nucl. Phys. B **901** (2015) 59 [arXiv:1511.03166].

[178] D. R. Morrison and D. S. Park, "F-Theory and the Mordell-Weil Group of Elliptically-Fibered Calabi-Yau Threefolds," JHEP **1210** (2012) 128 [arXiv:1208.2695].

[179] R. M. Fonseca, Comput. Phys. Commun. **183** (2012) 2298 doi:10.1016/j.cpc.2012.05.017 [arXiv:1106.5016 [hep-ph]].

[180] S. F. King, "Littlest Seesaw," JHEP **1602** (2016) 085 doi:10.1007/JHEP02(2016)085 [arXiv:1512.07531 [hep-ph]].

[181] S. F. King, "Large mixing angle MSW and atmospheric neutrinos from single right-handed neutrino dominance and U(1) family symmetry," Nucl. Phys. B **576** (2000) 85 [hep-ph/9912492]. S. F. King, "Constructing the large mixing angle MNS matrix in seesaw models with right-handed neutrino dominance," JHEP **0209** (2002) 011 [hep-ph/0204360].

[182] M. Berasaluce-Gonzalez, L. E. Ibanez, P. Soler and A. M. Uranga, "Discrete gauge symmetries in D-brane models," JHEP **1112** (2011) 113 [arXiv:1106.4169 [hep-th]].

[183] L. E. Ibanez, A. N. Schellekens and A. M. Uranga, "Discrete Gauge Symmetries in Discrete MSSM-like Orientifolds," Nucl. Phys. B **865** (2012) 509 [arXiv:1205.5364 [hep-th]].

[184] M. Berasaluce-Gonzalez, P. G. Camara, F. Marchesano, D. Regalado and A. M. Uranga, "Non-Abelian discrete gauge symmetries in 4d string models," JHEP **1209** (2012) 059 [arXiv:1206.2383 [hep-th]].

[185] V. Braun and D. R. Morrison, "F-theory on Genus-One Fibrations," JHEP **1408** (2014) 132 [arXiv:1401.7844 [hep-th]].

[186] P. Anastasopoulos, M. Cvetic, R. Richter and P. K. S. Vaudrevange, "String Constraints on Discrete Symmetries in MSSM Type II Quivers," JHEP **1303** (2013) 011 [arXiv:1211.1017 [hep-th]].

[187] I. Antoniadis and G. K. Leontaris, "F-GUTs with Mordell-Weil U(1)'s," Phys. Lett. B **735** (2014) 226 [arXiv:1404.6720]

[188] C. Mayrhofer, E. Palti, O. Till and T. Weigand, "Discrete Gauge Symmetries by Higgsing in four-dimensional F-Theory Compactifications," JHEP **1412** (2014) 068 [arXiv:1408.6831 [hep-th]].

[189] G. Honecker and W. Staessens, "To Tilt or Not To Tilt: Discrete Gauge Symmetries in Global Intersecting D-Brane Models," JHEP **1310** (2013) 146 [arXiv:1303.4415 [hep-th]].

[190] P. Anastasopoulos, R. Richter and A. N. Schellekens, "Discrete symmetries from hidden sectors," JHEP **1506** (2015) 189 doi:10.1007/JHEP06(2015)189 [arXiv:1502.02686 [hep-th]].

[191] G. Honecker and W. Staessens, "Discrete Abelian gauge symmetries and axions," J. Phys. Conf. Ser. **631** (2015) no.1, 012080 doi:10.1088/1742-6596/631/1/012080 [arXiv:1502.00985 [hep-th]].

[192] D. Klevers, D. K. Mayorga Pena, P. K. Oehlmann, H. Piragua and J. Reuter, "F-Theory on all Toric Hypersurface Fibrations and its Higgs Branches," JHEP **1501** (2015) 142 [arXiv:1408.4808 [hep-th]].

[193] M. Cvetic, R. Donagi, D. Klevers, H. Piragua and M. Poretschkin, "F-Theory Vacua with Z_3 Gauge Symmetry," arXiv:1502.06953 [hep-th].

[194] G. Altarelli and F. Feruglio, "Discrete Flavor Symmetries and Models of Neutrino Mixing," Rev. Mod. Phys. **82** (2010) 2701 [arXiv:1002.0211 [hep-ph]].

[195] H. Ishimori, T. Kobayashi, H. Ohki, Y. Shimizu, and M. Tanimoto, *An Introduction to Non-Abelian Discrete Symmetries for Particle Physicists*, Springer, 2012.

[196] S. F. King and C. Luhn, "Neutrino Mass and Mixing with Discrete Symmetry," Rept. Prog. Phys. **76** (2013) 056201 [arXiv:1301.1340 [hep-ph]].

[197] S. F. King, A. Merle, S. Morisi, Y. Shimizu and M. Tanimoto, "Neutrino Mass and Mixing: from Theory to Experiment," New J. Phys. **16** (2014) 045018 [arXiv:1402.4271 [hep-ph]].

[198] R. N. Mohapatra and R. E. Marshak, "Local B-L Symmetry of Electroweak Interactions, Majorana Neutrinos and Neutron Oscillations," Phys. Rev. Lett. **44** (1980) 1316 [Phys. Rev. Lett. **44** (1980) 1643].

[199] J. L. Goity and M. Sher, "Bounds on delta B = 1 couplings in the supersymmetric standard model," Phys. Lett. B **346** (1995) 69 [Erratum-ibid. B **385** (1996) 500] [hep-ph/9412208].

[200] D. G. Phillips II *et al.*, "Neutron-Antineutron Oscillations: Theoretical Status and Experimental Prospects", Phys.Rept. (2014) , arXiv:1410.1100 [hep-ex].

[201] G. Ross and M. Serna, "Unification and fermion mass structure," Phys. Lett. B **664** (2008) 97 doi:10.1016/j.physletb.2008.05.014 [arXiv:0704.1248 [hep-ph]].

[202] B. C. Allanach, A. Dedes and H. K. Dreiner, "Bounds on R-parity violating couplings at the weak scale and at the GUT scale," Phys. Rev. D **60** (1999) 075014 doi:10.1103/PhysRevD.60.075014 [hep-ph/9906209].

[203] B. C. Allanach, A. Dedes and H. K. Dreiner, "R parity violating minimal supergravity model," Phys. Rev. D **69** (2004) 115002 Erratum: [Phys. Rev. D **72** (2005) 079902] doi:10.1103/PhysRevD.69.115002, 10.1103/PhysRevD.72.079902 [hep-ph/0309196].

[204] E. J. Chun, S. Jung, H. M. Lee and S. C. Park, "Stop and Sbottom LSP with R-parity Violation," Phys. Rev. D **90** (2014) 115023 [arXiv:1408.4508 [hep-ph]].

[205] F. F. Deppisch, M. Hirsch and H. Pas, "Neutrinoless Double Beta Decay and Physics Beyond the Standard Model," J. Phys. G **39** (2012) 124007 [arXiv:1208.0727 [hep-ph]].

[206] H. K. Dreiner, M. Hanussek and S. Grab, "Bounds on R-parity Violating Couplings at the Grand Unification Scale from Neutrino Masses," Phys. Rev. D **82** (2010) 055027 [arXiv:1005.3309 [hep-ph]].

[207] V. Khachatryan *et al.* [CMS Collaboration], "Searches for R-parity-violating supersymmetry in pp collisions at sqrt(s)=8 TeV in final states with 0-4 leptons," arXiv:1606.08076 [hep-ex].

[208] G. Aad *et al.* [ATLAS Collaboration], "Summary of the searches for squarks and gluinos using $\sqrt{s} = 8$ TeV pp collisions with the ATLAS experiment at the LHC," JHEP **1510** (2015) 054 doi:10.1007/JHEP10(2015)054 [arXiv:1507.05525 [hep-ex]].

[209] G. Aad *et al.* [ATLAS Collaboration], "ATLAS Run 1 searches for direct pair production of third-generation squarks at the Large Hadron Collider," Eur. Phys. J. C **75** (2015) no.10, 510 Erratum: [Eur. Phys. J. C **76** (2016) no.3, 153] doi:10.1140/epjc/s10052-015-3726-9, 10.1140/epjc/s10052-016-3935-x [arXiv:1506.08616 [hep-ex]].

[210] M. Cvetic, D. A. Demir, J. R. Espinosa, L. L. Everett and P. Langacker, "Electroweak breaking and the mu problem in supergravity models with an additional U(1)," Phys. Rev. D **56** (1997) 2861 Erratum: [Phys. Rev. D **58** (1998) 119905] doi:10.1103/PhysRevD.56.2861, 10.1103/PhysRevD.58.119905 [hep-ph/9703317].

[211] M. Cvetic, J. Halverson and P. Langacker, "Implications of String Constraints for Exotic Matter and Z' s Beyond the Standard Model," JHEP **1111** (2011) 058 doi:10.1007/JHEP11(2011)058 [arXiv:1108.5187 [hep-ph]].

[212] V. Khachatryan *et al.* [CMS Collaboration], "Search for leptophobic Z' bosons decaying into four-lepton final states in proton-proton collisions at $\sqrt{s} = 8$ TeV," Phys. Lett. B **773** (2017) 563 doi:10.1016/j.physletb.2017.08.069 [arXiv:1701.01345 [hep-ex]].

[213] M. Aaboud *et al.* [ATLAS Collaboration], arXiv:1703.09127 [hep-ex].

[214] The ATLAS collaboration [ATLAS Collaboration], ATLAS-CONF-2017-027.

[215] C. M. Chen and Y. C. Chung, "On F-theory E_6 GUTs," JHEP **1103**, 129 (2011) doi:10.1007/JHEP03(2011)129 [arXiv:1010.5536 [hep-th]].

[216] J. C. Callaghan, S. F. King, G. K. Leontaris and G. G. Ross, "Towards a Realistic F-theory GUT," JHEP **1204** (2012) 094 [arXiv:1109.1399 [hep-ph]].

[217] J. C. Callaghan and S. F. King, "E6 Models from F-theory," JHEP **1304** (2013) 034 [arXiv:1210.6913 [hep-ph]].

[218] J. C. Callaghan, S. F. King and G. K. Leontaris, "Gauge coupling unification in E_6 F-theory GUTs with matter and bulk exotics from flux breaking," JHEP **1312** (2013) 037 [arXiv:1307.4593 [hep-ph]].

[219] M. Cvetic, R. Donagi, J. Halverson and J. Marsano, "On Seven-Brane Dependent Instanton Prefactors in F-theory," JHEP **1211** (2012) 004 doi:10.1007/JHEP11(2012)004 [arXiv:1209.4906 [hep-th]].

[220] G. K. Leontaris and Q. Shafi, "Diphoton resonance in F-theory inspired flipped SO(10)," Eur. Phys. J. C **76** (2016) no.10, 574 doi:10.1140/epjc/s10052-016-4432-y [arXiv:1603.06962 [hep-ph]].

[221] F. Staub, "SARAH 4 : A tool for (not only SUSY) model builders," Comput. Phys. Commun. **185** (2014) 1773 doi:10.1016/j.cpc.2014.02.018 [arXiv:1309.7223 [hep-ph]].
F. Staub, "Exploring new models in all detail with SARAH," Adv. High Energy Phys. **2015** (2015) 840780 doi:10.1155/2015/840780 [arXiv:1503.04200 [hep-ph]].

[222] L. E. Ibanez and J. Mas, "Low-energy Supergravity and Superstring Inspired Models," Nucl. Phys. B **286** (1987) 107. doi:10.1016/0550-3213(87)90434-2

[223] E. Ma, "Neutrino masses in an extended gauge model with E(6) particle content," Phys. Lett. B **380** (1996) 286 doi:10.1016/0370-2693(96)00524-2 [hep-ph/9507348].

[224] S. F. King, S. Moretti and R. Nevzorov, "Theory and phenomenology of an exceptional supersymmetric standard model," Phys. Rev. D **73** (2006) 035009 doi:10.1103/PhysRevD.73.035009 [hep-ph/0510419].

[225] E. Witten, "Symmetry Breaking Patterns in Superstring Models," Nucl. Phys. B **258** (1985) 75. doi:10.1016/0550-3213(85)90603-0

[226] P. Athron, D. Harries, R. Nevzorov and A. G. Williams, "E_6 Inspired SUSY benchmarks, dark matter relic density and a 125 GeV Higgs," Phys. Lett. B **760** (2016) 19 doi:10.1016/j.physletb.2016.06.040 [arXiv:1512.07040 [hep-ph]].

[227] P. Athron, A. W. Thomas, S. J. Underwood and M. J. White, "Dark matter candidates in the constrained Exceptional Supersymmetric Standard Model," Phys. Rev. D **95** (2017) no.3, 035023 doi:10.1103/PhysRevD.95.035023 [arXiv:1611.05966 [hep-ph]].

[228] Y. Hicyilmaz, M. Ceylan, A. Altas, L. Solmaz and C. S. Un, "Quasi Yukawa Unification and Fine-Tuning in U(1) Extended SSM," Phys. Rev. D **94** (2016) no.9, 095001 doi:10.1103/PhysRevD.94.095001 [arXiv:1604.06430 [hep-ph]].

[229] A. Hebbar, G. K. Leontaris and Q. Shafi, "Masses of Third Family Vector-like Quarks and Leptons in Yukawa-Unified E_6," Phys. Rev. D **93** (2016) no.11, 111701 doi:10.1103/PhysRevD.93.111701 [arXiv:1604.08328 [hep-ph]].

[230] Belangér, Geneviève, J. Da Silva and H. M. Tran, "Dark matter in U(1) extensions of the MSSM with gauge kinetic mixing," Phys. Rev. D **95** (2017) no.11, 115017 doi:10.1103/PhysRevD.95.115017 [arXiv:1703.03275 [hep-ph]].

[231] J. Y. Araz, M. Frank and B. Fuks, "Differentiating $U(1)'$ supersymmetric models with right sneutrino and neutralino dark matter," Phys. Rev. D **96** (2017) no.1, 015017 doi:10.1103/PhysRevD.96.015017 [arXiv:1705.01063 [hep-ph]].

[232] Y. Hiçyılmaz, L. Solmaz, Ş. H. Tanyıldızı and C. S. Ün, Nucl. Phys. B **933** (2018) 275 doi:10.1016/j.nuclphysb.2018.05.025 [arXiv:1706.04561 [hep-ph]].

[233] G. C. Cho, N. Maru and K. Yotsutani, "Perturbative unification of gauge couplings in supersymmetric E_6 models," Mod. Phys. Lett. A **31** (2016) no.22, 1650130 doi:10.1142/S0217732316501303 [arXiv:1602.04271 [hep-ph]].

[234] S. Antusch and M. Spinrath, "Quark and lepton masses at the GUT scale including SUSY threshold corrections," Phys. Rev. D **78** (2008) 075020 doi:10.1103/PhysRevD.78.075020 [arXiv:0804.0717 [hep-ph]].

[235] M. A. Ajaib, I. Gogoladze, Q. Shafi and C. S. Ün "Split sfermion families, Yukawa unification and muon $g-2$," JHEP **1405** (2014) 079 doi:10.1007/JHEP05(2014)079 [arXiv:1402.4918 [hep-ph]].

[236] A. Brignole, L. E. Ibanez and C. Munoz, "Towards a theory of soft terms for the supersymmetric Standard Model," Nucl. Phys. B **422** (1994) 125 Erratum: [Nucl. Phys. B **436** (1995) 747] doi:10.1016/0550-3213(94)00600-J, 10.1016/0550-3213(94)00068-9 [hep-ph/9308271].

[237] M. Grana, T. W. Grimm, H. Jockers and J. Louis, "Soft supersymmetry breaking in Calabi-Yau orientifolds with D-branes and fluxes," Nucl. Phys. B **690** (2004) 21 doi:10.1016/j.nuclphysb.2004.04.021 [hep-th/0312232].

[238] P. G. Camara, L. E. Ibanez and A. M. Uranga, "Flux induced SUSY breaking soft terms," Nucl. Phys. B **689** (2004) 195 doi:10.1016/j.nuclphysb.2004.04.013 [hep-th/0311241].; P. G. Camara, L. E. Ibanez and A. M. Uranga, "Flux-induced SUSY-breaking soft terms on D7-D3 brane systems," Nucl. Phys. B **708** (2005) 268 doi:10.1016/j.nuclphysb.2004.11.035 [hep-th/0408036].

[239] D. Lust, S. Reffert and S. Stieberger, Nucl. Phys. B **706** (2005) 3 doi:10.1016/j.nuclphysb.2004.11.030 [hep-th/0406092].

[240] K. Choi, K. S. Jeong and K. I. Okumura, JHEP **0807** (2008) 047 doi:10.1088/1126-6708/2008/07/047 [arXiv:0804.4283 [hep-ph]].

[241] L. Aparicio, D. G. Cerdeno and L. E. Ibanez, JHEP **0807** (2008) 099 doi:10.1088/1126-6708/2008/07/099 [arXiv:0805.2943 [hep-ph]].

[242] J. J. Heckman and C. Vafa, "F-theory, GUTs, and the Weak Scale," JHEP **0909** (2009) 079 doi:10.1088/1126-6708/2009/09/079 [arXiv:0809.1098 [hep-th]].

[243] R. Blumenhagen, J. P. Conlon, S. Krippendorf, S. Moster and F. Quevedo, "SUSY Breaking in Local String/F-Theory Models," JHEP **0909** (2009) 007 doi:10.1088/1126-6708/2009/09/007 [arXiv:0906.3297 [hep-th]].

[244] P. G. Camara, L. E. Ibanez and I. Valenzuela, "The String Origin of SUSY Flavor Violation," JHEP **1310** (2013) 092 doi:10.1007/JHEP10(2013)092 [arXiv:1307.3104 [hep-th]].

[245] P. G. Camara, L. E. Ibanez and I. Valenzuela, "Flux-induced Soft Terms on Type IIB/F-theory Matter Curves and Hypercharge Dependent Scalar Masses," JHEP **1406** (2014) 119 doi:10.1007/JHEP06(2014)119 [arXiv:1404.0817 [hep-th]].